

Measurements of directivity of the pressure field near rifles with and without flash suppressor

Morten Huseby and Haakon Fykse

Norwegian Defence Research Establishment (FFI)

2 April 2012

FFI-rapport 2008/01483

3533

P: ISBN 978-82-464-2171-1

E: ISBN 978-82-464-2172-8

Keywords

måling

rifle

HK 416

AG3

trykk

Approved by

Eirik Svinsås

Project manager

Jan Ivar Botnan

Director

English summary

We have measured the time series of the pressure, with and without flash suppressors. The measurements were done 84 cm from the muzzle of four rifles, in 159 directions between 3 and 161 degrees to the firing direction. The four rifles are HK 416 N, Diemaco C8 SFW, HK 417 and AG3. The measurements are documented and the results plotted with the intention of being used as reference for other publications.

Investigations of the directivity of pressure waves close to weapons are motivated by numerous applications, such as potential damage to personnel firing the weapons, risk of detection of snipers and annoyance perceived by neighbors to training ranges because of noise from military activity. We discuss each of these topics in some detail.

We also discuss the concept of angular horizontal acoustic energy density and its importance for noise engineers. While the total emitted energy is more or less independent of the geometry of the muzzle device, a change of geometry may lead to emission of less sound in front of the weapon. This results in more noise emitted upwards, thus reducing the total noise emission to the neighbors to a training range.

Sammendrag

Vi har målt tidsseriene til trykket med og uten flammedemper. Målingene ble utført 84 cm fra munningen for fire rifler, i 159 retninger mellom 3 og 161 grader på skyteretningen. De fire riflene er HK 416 N, Diemaco C8 SFW, HK 417 og AG3. Målingene er dokumentert og resultatene er plottet med hensikt å benyttes som referanse for andre publikasjoner.

Forskning på direktiviteten til trykkbølgene nær våpen er motivert av anvendelser som potensiell fare for personell som avfyrer våpnene, fare for deteksjon av skarpskyttere og støyplager for naboer til Forsvarets skyte- og øvingsfelt. Vi går gjennom alle disse temaene.

Vi diskuterer også konseptet angular horizontal acoustic energy density og dens betydning for ingeniører som driver med støyreducerende tiltak. Mens den totale utstrålte akustiske energien er ganske ufølsom for geometrien til en flammedemper, så vil en slik forandring kunne føre til mindre støy foran våpenet og mer til siden. Resultatet er mer støy oppover. Vi viser at dette reduserer den totale støyen rundt et skytefelt.

Contents

1	Introduction	7
2	blue Motivation	8
2.1	Hearing damage	8
2.2	Risk of detection	8
2.3	Pressure waves on the brain	9
2.4	Noise from training ranges	10
3	Weapons and ammunition	10
4	Measurement setup	10
4.1	Data acquisition	11
5	Muzzle devices and directivity	12
5.1	Spherical acoustic energy	14
5.2	Horizontal acoustic energy	15
5.3	Spherical vs. horizontal acoustic energy	15
6	Summary	16
7	Timeseries of the pressure	17
Appendix A	Pictures of the measurement setup	176
Appendix B	Pictures of flas suppressors	185

1 Introduction

Firing a weapon will produce a pressure wave, often referred to as a blast wave. As this pressure wave travels away from the weapon it decreases in amplitude and changes shape until it is usually referred to as sound or noise. Whether it is called pressure wave, blast wave or sound, it refers in all cases to the pressure field propagating out from the weapon, and not different physical entities.

In this work we consider the pressure field close to rifles, 80 cm from the muzzle (Figure 1.1). We perform measurements on 4 rifles with and without flash suppressors. The measurements are documented and the results plotted with the intention of being used as reference for other publications (some already published [1, 2, 3, 4]).

The measurements were conducted at the proving ground at FFI (Dompa) at 26 June, 2008 and 22 June, 2009. The pressure was measured for four rifles: HK 416 N (Heckler & Koch, Figure 2.1), Diemaco C8 (Figure 2.2), HK 417 (Figure 3.1) and AG3 (Figure 3.2).

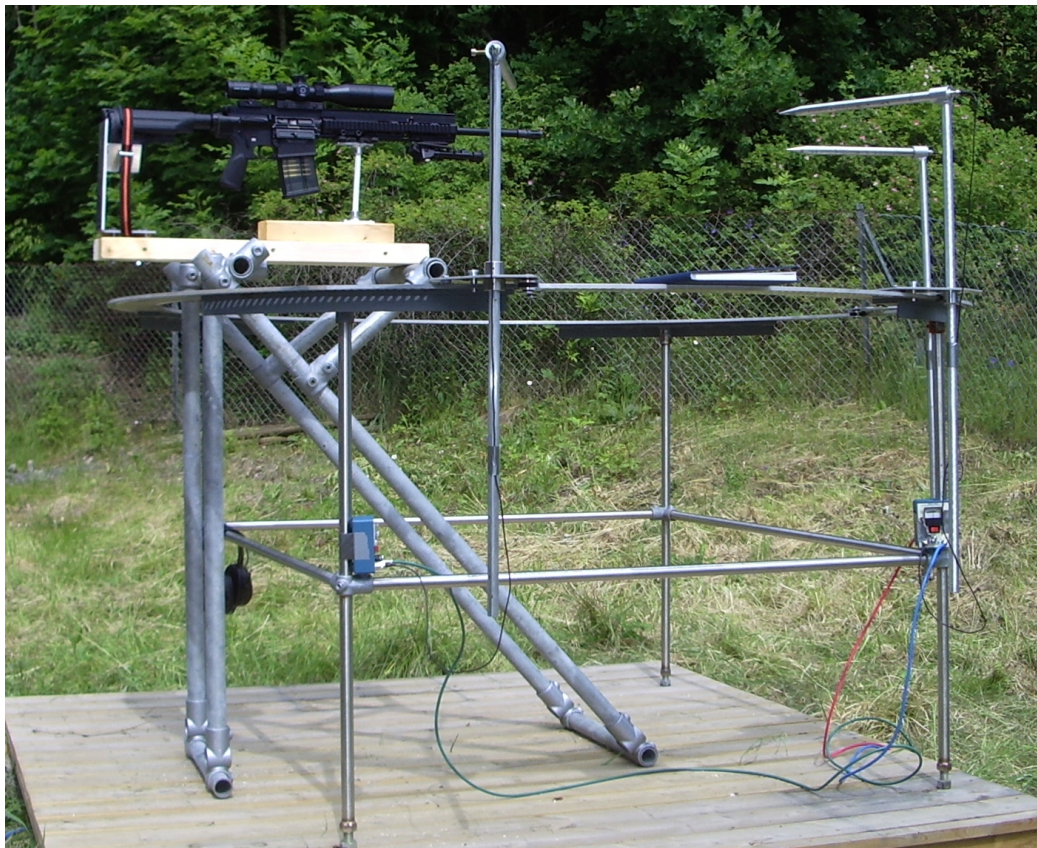


Figure 1.1 Measurement arrangement

2 Motivation

Investigations of the directivity of pressure waves close to weapons are motivated by numerous applications, such as potential damage to personnel firing the weapons, risk of detection of snipers and annoyance perceived by neighbors to training ranges because of noise from military activity.

2.1 Hearing damage

Traditionally soldiers would fire rifles standing on a line facing enemy soldiers on a well defined front. Today's scenarios calls for more advanced operations, where soldiers advance inside buildings with their colleagues more in front of or close to the side of the muzzle of the rifle. The noise from a rifle is highly directive, meaning that the noise level is about 20 dB higher in front of the weapon than behind it. Thus the noise level for a shooter may be lower than the noise level for a soldier close by.

Reflections from walls and ceilings will further increase the noise level during operations inside buildings. Additionally, weapons used in such operations will have a shorter barrel than more traditional weapons. This brings the muzzle closer to the head of the soldier, and increases the noise level. This motivates a study to increase the knowledge of the noise levels in different directions around rifles with and without flash suppressors.



Figure 2.1 HK416 N

2.2 Risk of detection

It has become more usual to fit weapons with different types of flash suppressors and silencers. The effect of these on the noise is critical for an enemy's ability to pinpoint the location from where a shot has been fired, and fire back. To be able to have the right equipment for the right situation, an assessment needs to be done of the noise levels in different directions.



Figure 2.2 *Diemaco C8 SFW*

2.3 Pressure waves on the brain

During the last years conflicts in Iraq and Afghanistan IED's (Improvised Explosive Device) accounts for a significant part of casualties. Large resources has been used to deal with blast-induced TBI (Traumatic Brain Injury) inflicted from IED's. It is found that blast-induced TBI shares clinical features with post-traumatic stress disorder (PTSD), suggesting that the blast waves injures the central nervous system in a more complex way than initially assumed [5].

Recently one has become aware that moderate pressure waves from weapons may inflict damage on the brain [6, 3] in a similar but less harmful way, compared to TBI. The skull does not significantly shield the brain from pressure waves [7, 8, 9]. The pressure waves will stretch and compress brain tissue when passing through it. The mechanics of the brain tissue has similarities to that of a football player or boxer that experiences a blow to the head, even though the mechanism for creating the pressure wave in the brain is different (non-contact vs. contact).

When exposing pigs to pressure waves similar to those experienced by soldiers firing bazookas, artillery and heavy rifles, subarachnoidal and parenchymal hemorrhages were found in the brain [9]. Rats exposed to blasts with peak pressures of 10-60 kPa experience temporary reduced cognitive function [10]. It is difficult to establish whether repeated exposure to blast waves of this kind will lead to permanent reduction of cognitive function in humans.

Since artillery and rifles have a directional noise pattern, it is important to understand the mechanisms that lead to more noise (blast waves) in specific directions, as a result of altering recoil dampeners, flash suppressors and silencers. These mechanisms are the same that governs the behavior of the noise patters measured in this work.

2.4 Noise from training ranges

Another motivation for this work is to help reduce weapon noise experienced by neighbors to military training ranges, in order to sustain the possibility for quality training. Over the last years we have considered many different aspects of this problem [11, 12]. One aspect is to determine the noise level for all the weapons used on the range. E.g. the noise level may be found by measurements at 10 m from the muzzle of a rifle or 250 m for a 155 mm Howitzer [13]. To reduce the need for time consuming and expensive measurements a numerical procedure was designed to calculate this emission level close to the weapon [14, 15, 16, 17]. First the burning gun powder is modeled inside the barrel. Then shock waves of the gun powder gas escaping from the muzzle are calculated with Autodyn (hydrocode), out to 80 cm for a rifle. Then a non-linear semi-empirical formulation may be applied to calculate the pressure at 10 m [14]. We then wanted to verify the Autodyn computations with measurements at 80 cm [18, 19, 20]. The measurements reported here may also serve as input data for verifying the non-linear noise propagation calculation from 80 cm to 10 m.

3 Weapons and ammunition

HK 416 and C8 use 5.56x45 mm ammo (NM229), while AG3 and HK 417 use 7.62x51 mm (NM231). NM231 and NM229 are regular (lead free) ammunition for these calibers in the Norwegian army. The muzzle velocity is between 800 and 900 m/s (Table 3.1).



Figure 3.1 HK 417

4 Measurement setup

To facilitate precise measurements at one degree intervals from the firing direction we built a measurement rig (Figure 1.1). The sensors can be moved as little as one degree to the side between each measurement, and may be moved without much effort. Using three sensors the range from 3 degrees to 161 degrees required 53 shots for each weapon. This



Figure 3.2 AG3

Weapon	Ammo	Barrel length mm	V_0 m/s	Weapon number
AG3	NM231 7.62 x 51 mm	450	804	1,2
HK 417	NM231 7.62 x 51 mm	508	834	3,4
C8 SFW	NM229 5.56 x 45 mm	368	875	5,6
HK 416 N	NM229 5.56 x 45 mm	406	895	7,8

Table 3.1 Properties of weapons and ammunition

results in a measurement time of about 15 minutes for each weapon. Additional pictures of the measurement setup can be seen in Appendix A.

4.1 Data acquisition

We use three pressure sensors of type PCB 137A23. The sensors are connected to PCB 480E09 signal transformers, the gain was set to 10. The output of the signal transformers was connected to a NI-PCI 4462 National Instruments data acquisition card installed in a PC. The PC runs a program in LabView 8.2. We acquired 24-bits data, at 204.8 kS/s per channel.

Parameter/Ammo	NM231	NM229
Caliber (mm)	7.62 x 51	5.56 x 45
Projektile weight (g)	8.95	3.99
Gunpowder weight (g)	2.78	1.70
Cartridge case volume (mm ³)	3516	1555

Table 3.2 Ammunisjon parameters



Figure 5.1 Flash suppressors. From the left: HK 416 N, AG3, HK 417, C8 SFW.

5 Muzzle devices and directivity

Most rifles have a muzzle device (Figure 5.1) connected to the end of the barrel, which is designed to reduce muzzle flash, sound or recoil. These muzzle devices may drastically change both the directivity and the perceived noise level of the weapon [21].

In 2005 we conducted a measurement campaign to capture sound emission data from rifles [18]. One of the rifles (FN MAG 7.62 mm) had two different barrels, one with a flash suppressor, and one with a muzzle that opens up in a conic shape. The measured pressure was much larger in front of the weapon with the conic muzzle than with the flash suppressor (Figure 5.2). However, at 70 degrees angle to the firing direction the time series of the pressure was more or less identical. This raises an interesting question. Since the amount of gun powder and bullet speed are practically identical, it seems intuitive that the total emission of acoustic energy should be the same. I.e. if the pressure is much larger in front of the weapon, it should be much smaller to the sides and backwards.

In earlier measurements we only had sensors at 3–7 different angles to the shooting direction. However, it seems that the fluid flow close to the muzzle changes on a smaller scale between 0 and 20 degrees from the firing direction. This motivated us to construct a measurement apparatus to perform measurements at 1 degree intervals from the firing direction, 80 cm from the muzzle.

The measurements were conducted at the proving ground at FFI (Dompna) at 26 June, 2008 and 22 June, 2009 (Figure 1.1). Again we observed the same phenomena. The pressure with muzzle suppressor mounted was much larger straight forward than with the clean barrel without muzzle suppressor (Figure 5.3). To the side there was not much difference. In Figure 5.4 this phenomenon is highlighted by plots of max pressure and

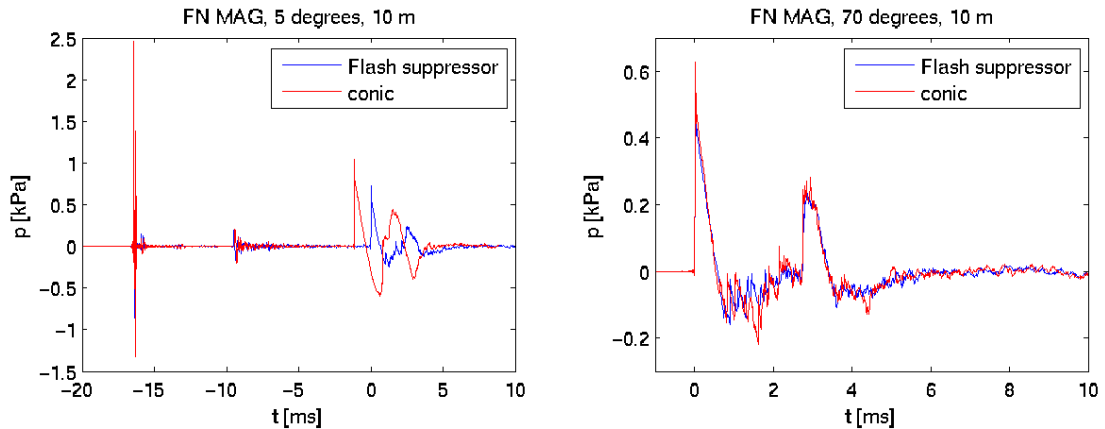


Figure 5.2 Measured time series of the pressure for FN MAG 7.62 mm at two different directions from the shooting direction

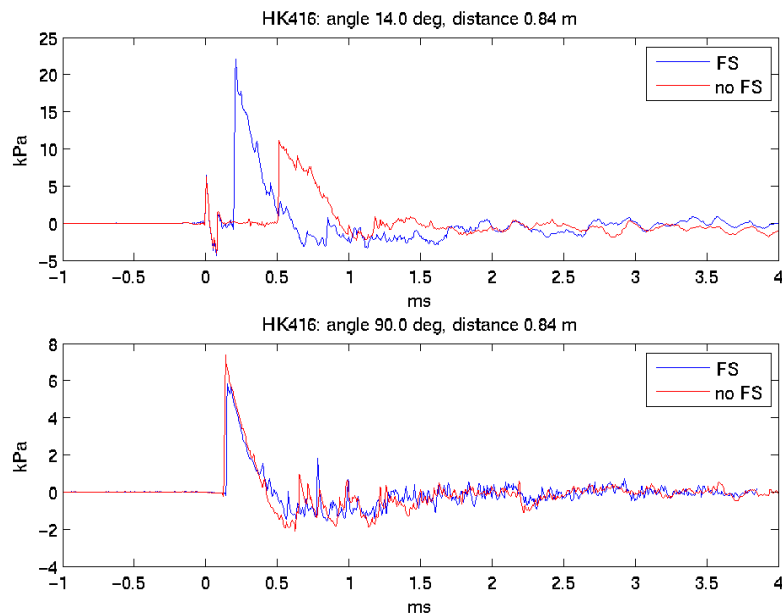


Figure 5.3 Measured time series of the pressure for HK 416 N at two different directions from the shooting direction, with and without flash suppressor, at 84 cm from the muzzle

sound exposure (SE) as function of angle from the firing direction. SE is define to be [22]

$$SE(\theta, r) = \int_0^{\infty} p^2 dt \quad (5.1)$$

Looking at Figure 5.2 with conic muzzle and flash suppressor, and Figure 5.3 with flash suppressor and clean muzzle (i.e. cylindrical muzzle) it might seem that these figures are conflicting. However, the conic muzzle has much the same shape as the flash suppressor, except that it lacks the venting holes. It seems that the conic muzzle is even more

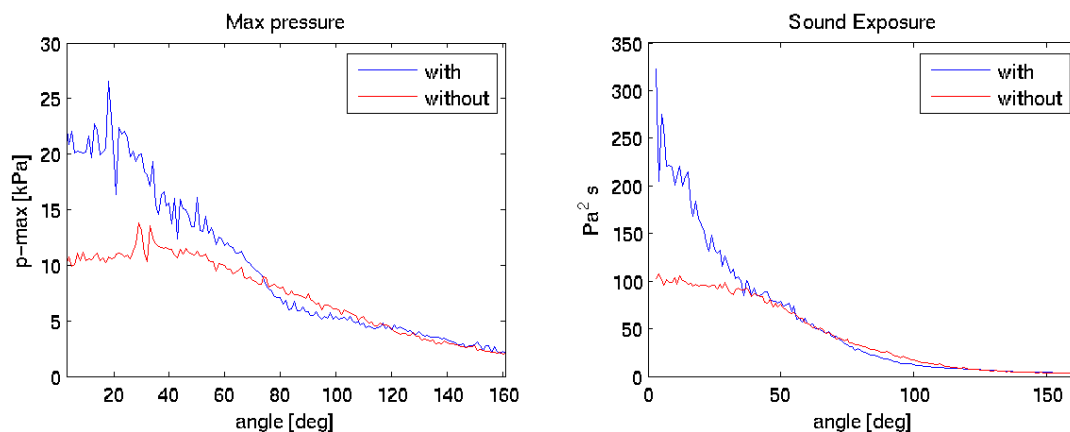


Figure 5.4 Measured time series of the pressure for HK 416 N at two different directions from the shooting direction, with and without flash suppressor, at 84 cm from the muzzle

effective that the flash suppressor in directing the energy forwards.

Since the acoustic energy emitted from the weapon is closely related to the energy of the escaping gun powder gas, it initially appears as a mystery that the shape of the muzzle device may change the total noise level of the weapon. Even if the directivity is changed, one would expect that the emitted energy is the same.

At Internoise 2011 in Osaka we introduced the concept of angular horizontal acoustic energy density (i.e. not spherical) for sound emission from directive noise sources [1]. When looking at noise from a weapon in the context of neighbor annoyance, we consider the noise in the horizontal plane. However, the noise from the weapon propagates in all directions, including upwards in the atmosphere.

5.1 Spherical acoustic energy

The total energy emitted from the weapon has to be calculated over a surface enclosing the weapon, typically a sphere. The energy propagating out of a spherical boundary (S) of radius r around the source is

$$Q_s = \int_0^\infty \int_S p \mathbf{v} \cdot \mathbf{n} dS dt = \int_0^\infty \int_0^\pi \int_0^{2\pi} p \mathbf{v} \cdot \mathbf{n} r^2 \sin \theta dt d\phi d\theta, \quad (5.2)$$

where p is the pressure, \mathbf{v} is the fluid velocity, t is time and \mathbf{n} is the normal unit vector pointing out of the domain. When the pressure waves are close to plane waves

$$p \mathbf{v} = \mathbf{n} \frac{p^2}{\rho c}, \quad (5.3)$$

where c is the speed of sound and ρ is the air density. The assumption that we have plane waves seems dubious. The validity depends on the number of wavelengths from the

source, which may be sufficient in our case, considering the high frequency nature of this phenomenon. Now Q_s can be expressed by SE given in (5.1).

$$Q_s = \frac{2\pi r^2}{\rho c} \int_0^\pi SE(\theta, r) \sin \theta d\theta. \quad (5.4)$$

If we define the angular spherical acoustic energy density

$$\tilde{w}_s(\theta) = \frac{2\pi r^2}{\rho c} SE(\theta, r) \sin \theta, \quad (5.5)$$

we get

$$Q_s = \int_0^\pi \tilde{w}_s d\theta. \quad (5.6)$$

5.2 Horizontal acoustic energy

When measuring noise emission data for use in noise propagation codes, it is of interest to calculate some sort of total energy in the horizontal plane. One such energy measure is the total energy emitted through a circle around the weapon (of unity height), i.e. a “fence” of 1 m height. Following the same steps as above, this horizontal acoustic energy is

$$Q_h(r) = \frac{2\pi r(1\text{m})}{\rho c} \int_0^\pi SE(\theta, r) d\theta. \quad (5.7)$$

Defining the angular horizontal acoustic energy density

$$\tilde{w}_h(\theta) = \frac{2\pi r}{\rho c} SE(\theta, r), \quad (5.8)$$

we get

$$Q_h = (1\text{m}) \int_0^\pi \tilde{w}_h d\theta. \quad (5.9)$$

5.3 Spherical vs. horizontal acoustic energy

In Figure 5.5 we plot the energy density as function of angle from the firing direction. We see that horizontal acoustic energy density is much larger from 0 to 30 degrees with flash suppressor, while only slightly smaller from 75 to 115 degrees. The spherical acoustic energy density is a bit larger from 0 to 30 degrees with flash suppressor, and a bit smaller from 75 to 115 degrees. If we integrate the energy densities, i.e. sum up the area under the graphs in Figure 5.5, we get the total acoustic energy emitted from the weapon. For the spherical acoustic energy we get 0.020 J with suppressor and 0.018 J without. For the horizontal acoustic energy we get 0.049 J/m with suppressor and 0.037 J/m without. Thus we see that spherical acoustic energy seems to be conserved, while horizontal acoustic energy is not.

While this mechanism now seems obvious from a physical standpoint, awareness of the concept of angular horizontal acoustic energy density may nonetheless be of help for

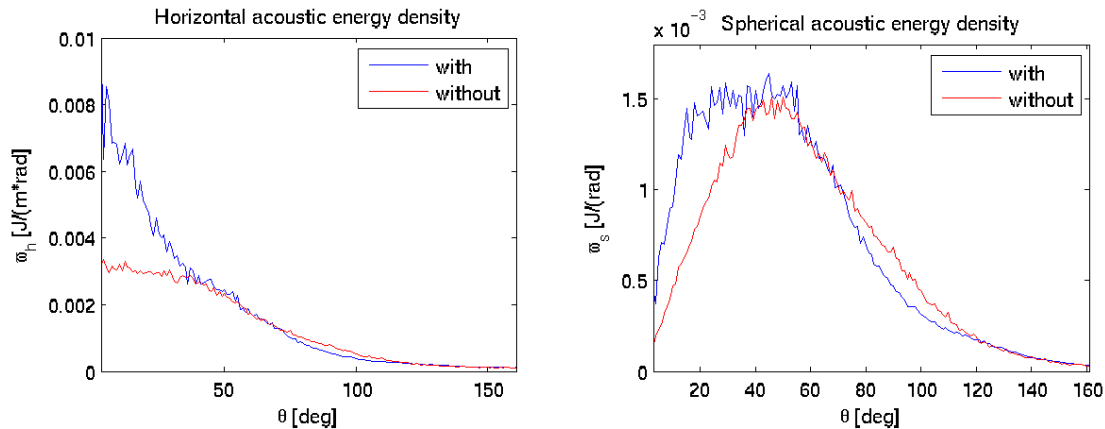


Figure 5.5 Horizontal and spherical angular acoustic energy density for HK 416 N, with and without flash suppressor

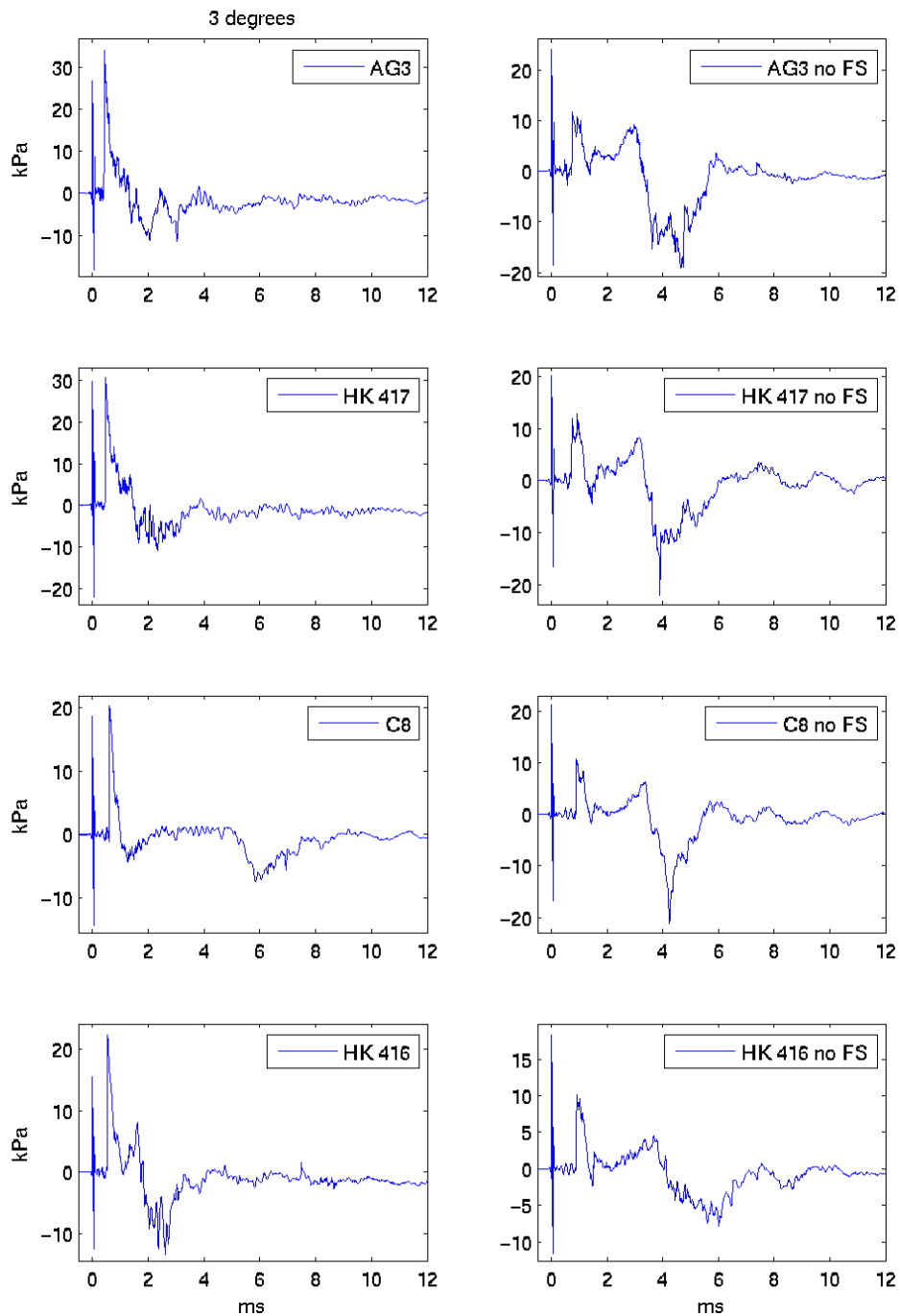
sound engineers working with noise abatement near military training fields, or any other installations that have a problem with noise from directive sources. As we see changing the geometry of the muzzle device may solve a problem in one direction without creating one in another. I.e. a weapon creating a problem at a neighbor in a specific direction close to the firing direction may change flash suppressor to avoid the problem, without significantly increasing the noise to the sides.

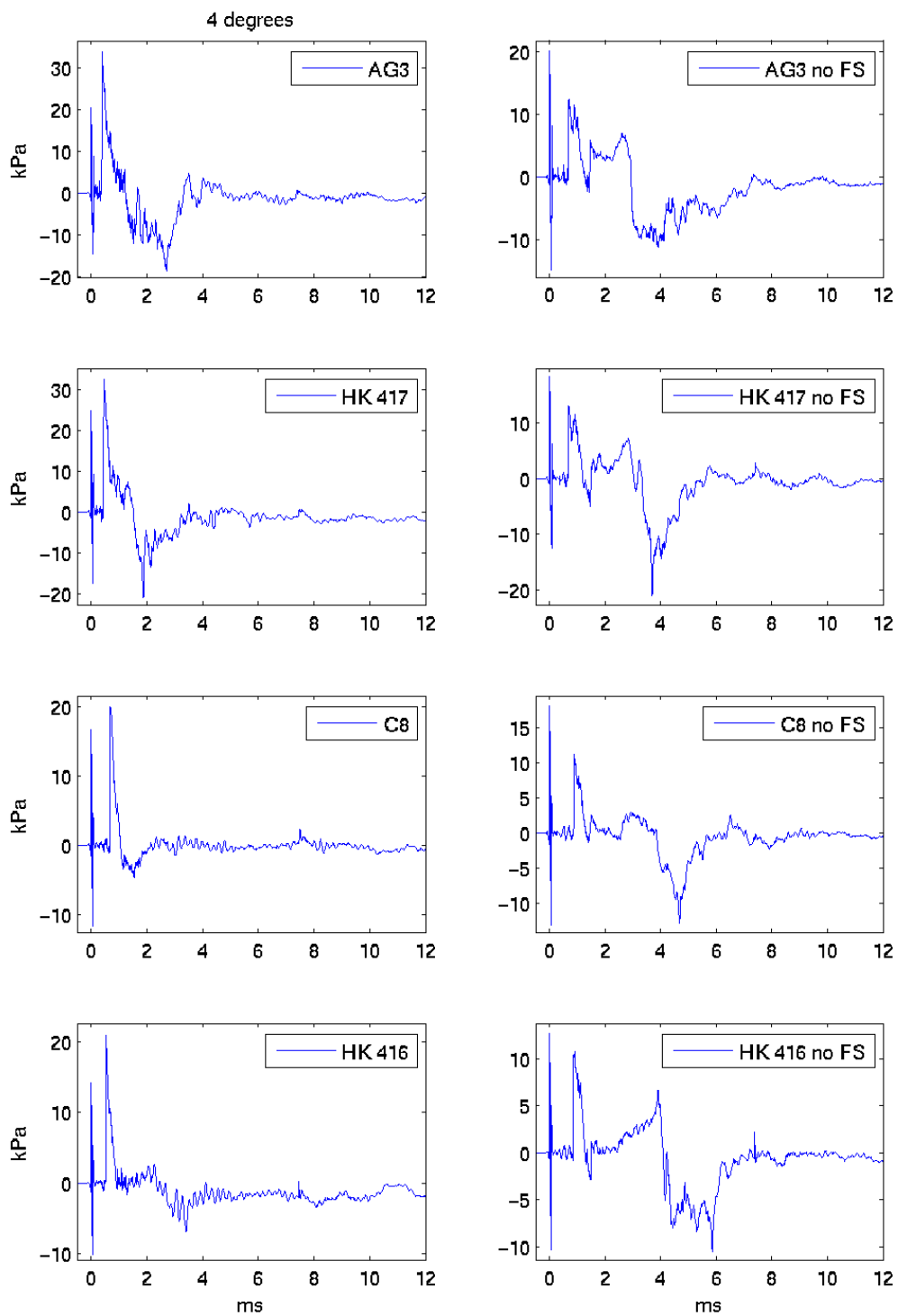
6 Summary

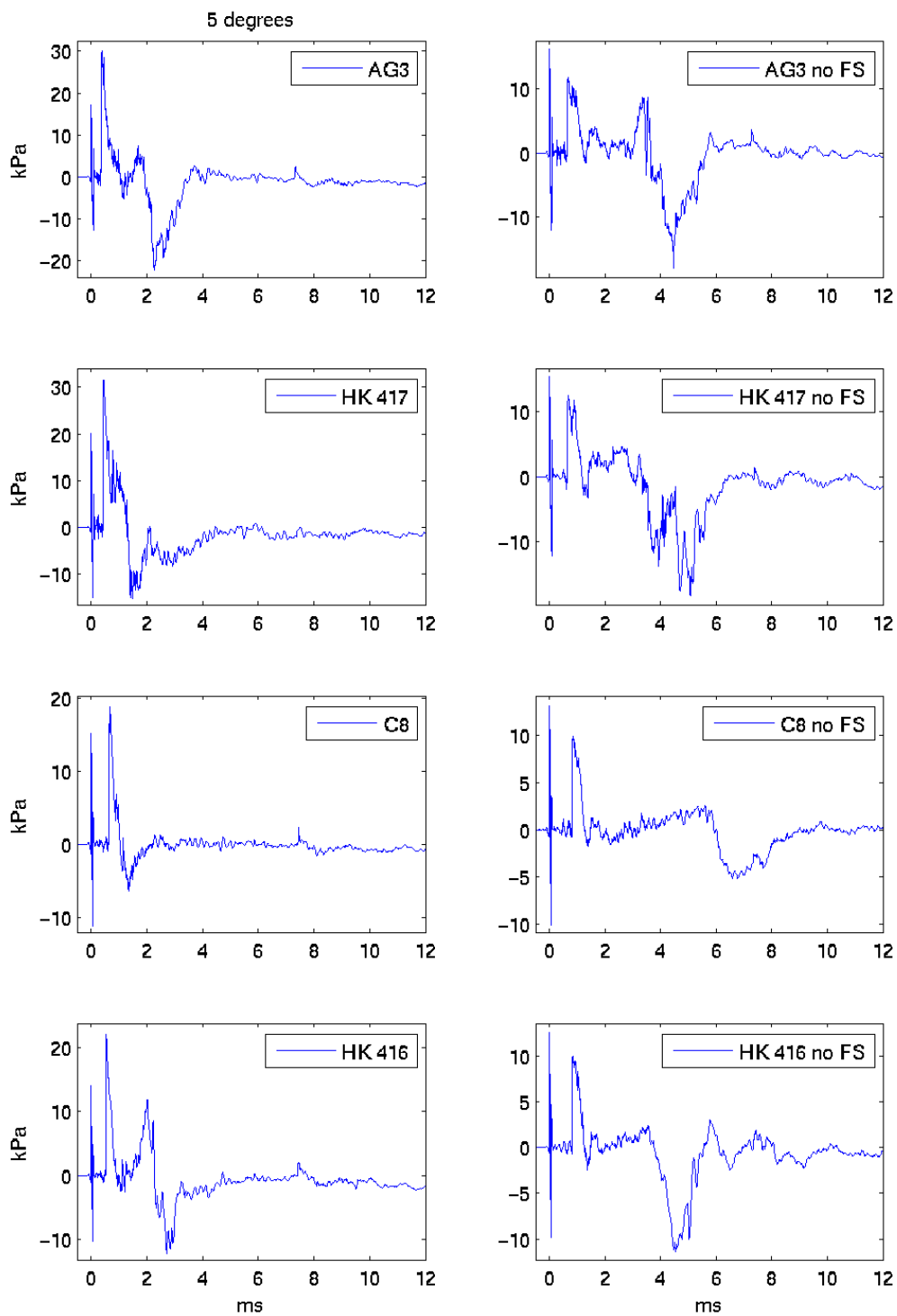
The main contribution of this report is the printed time series of the pressure for rifles with and without flash suppressors (Section 7). In addition we discussed the concept of angular horizontal acoustic energy density and its importance for noise engineers.

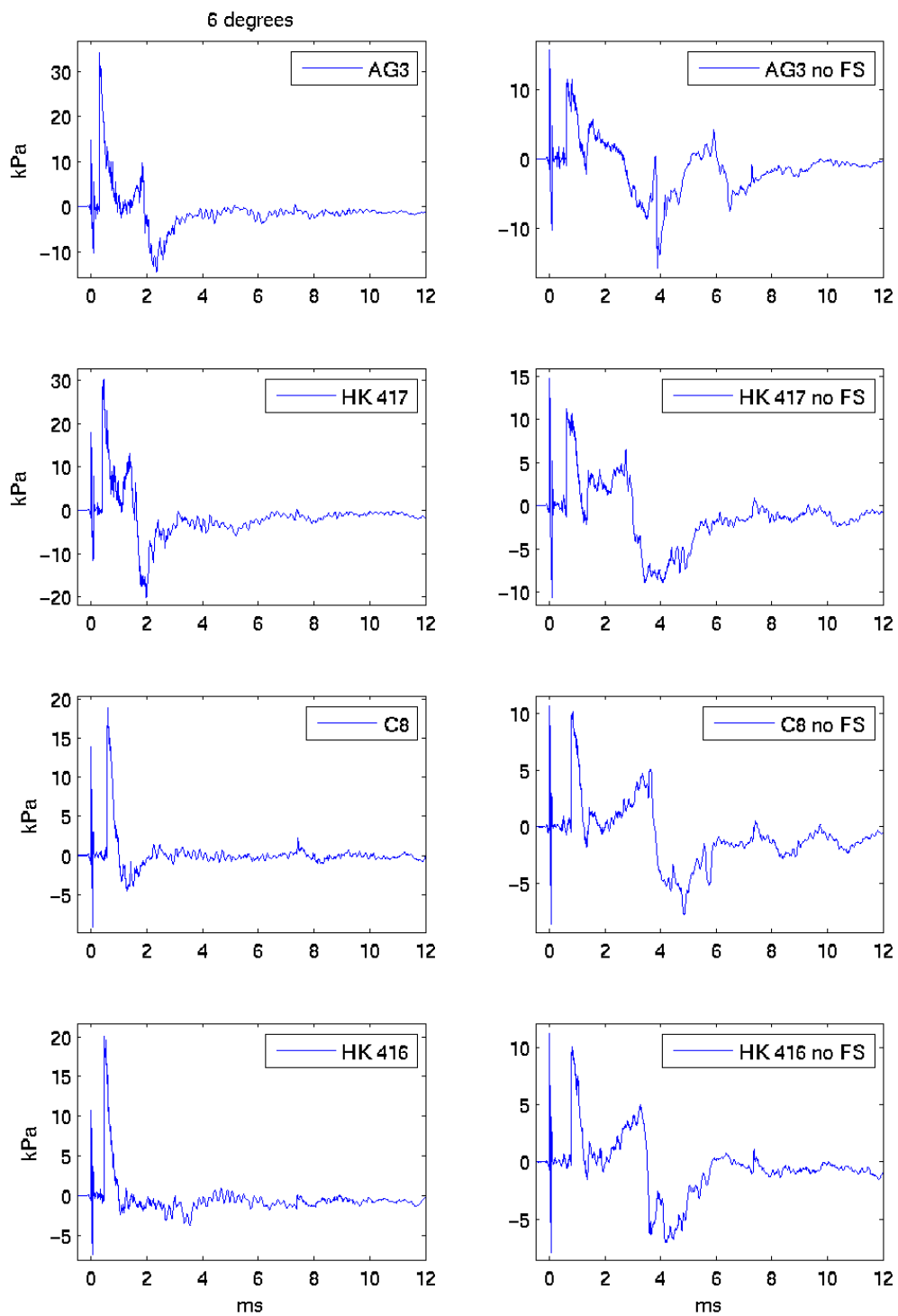
Without the muzzle device we see a large negative pressure some time after the muzzle blast. This is probably a vortex of gunpowder gas that has reached the sensor. The gunpowder gas will typically expand until it retracts and stays pretty close to the weapon. It seems however, that this vortex is dissolved more effectively by the muzzle device. It would be of interest to repeat the measurements described in this report with sensors 2 m from the muzzle, where the gun powder gas would not be present.

7 Timeseries of the pressure

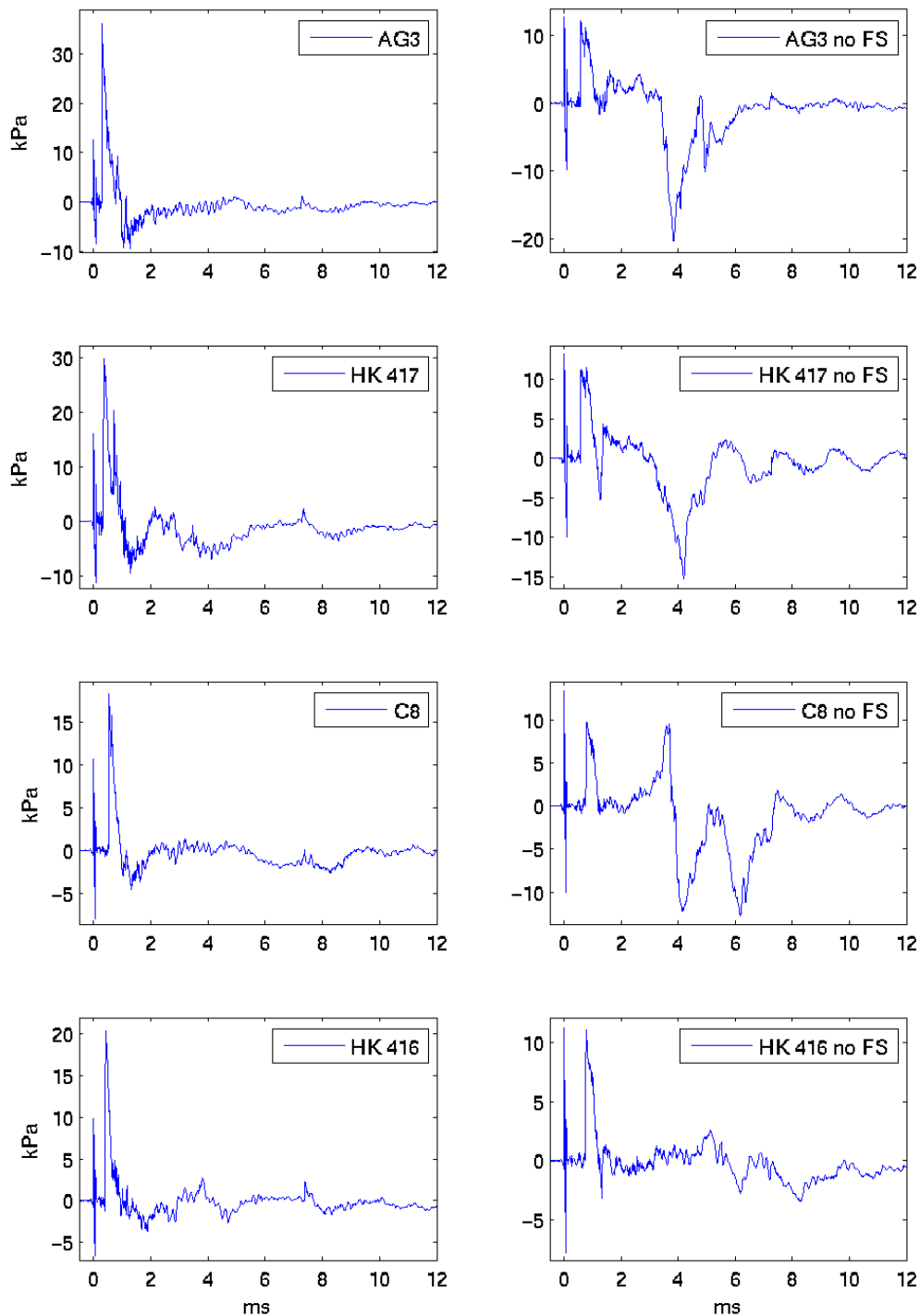


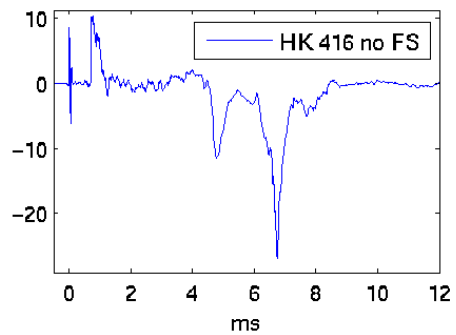
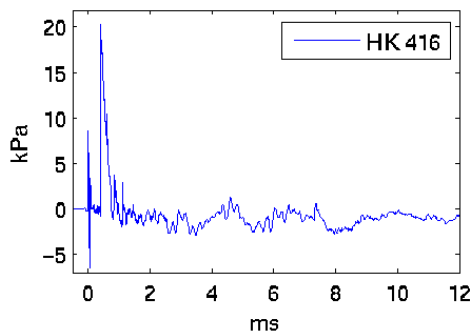
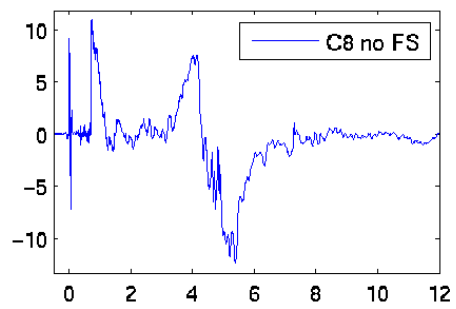
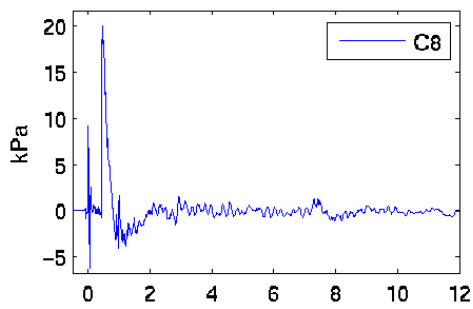
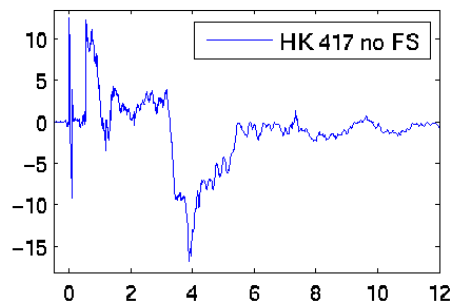
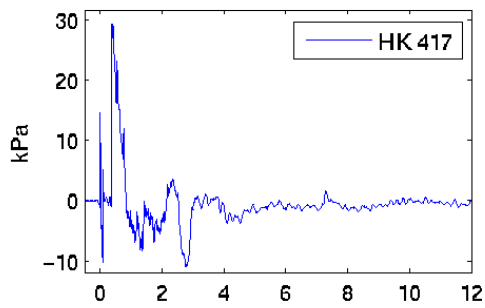
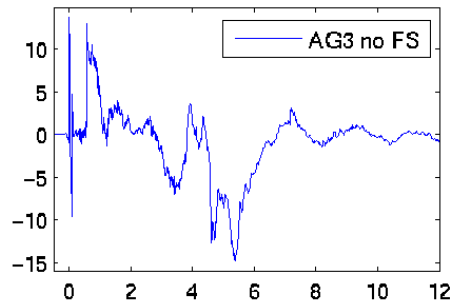
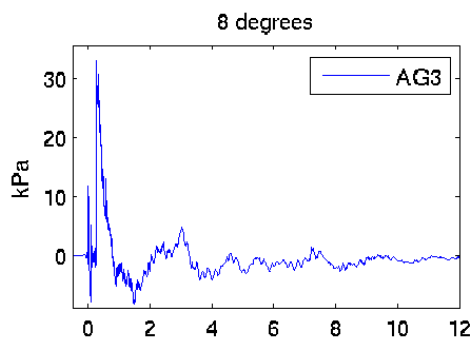




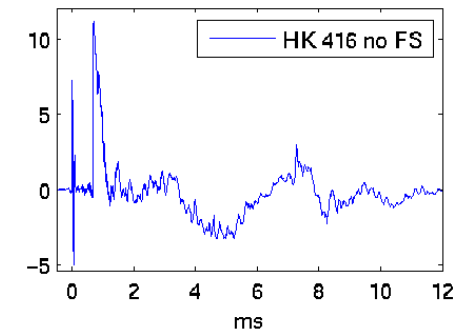
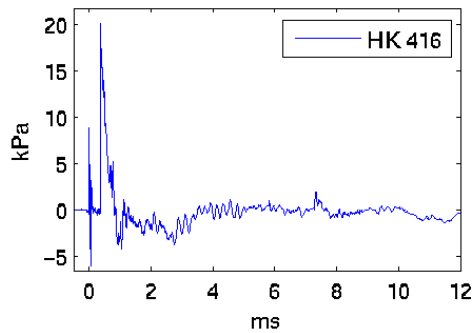
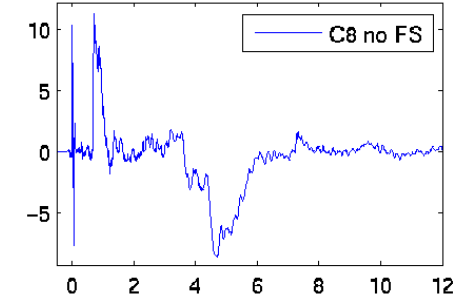
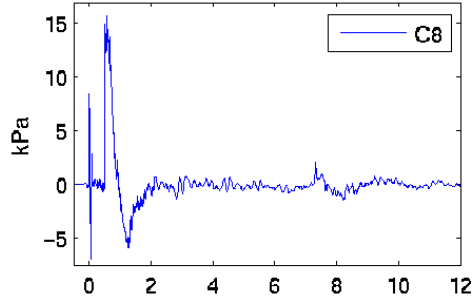
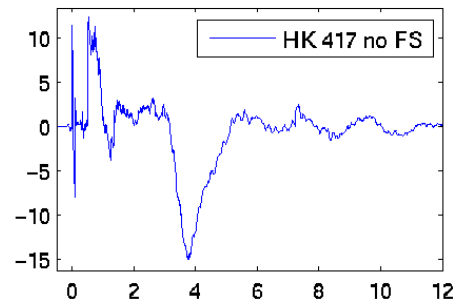
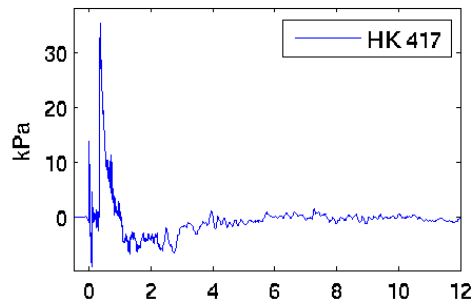
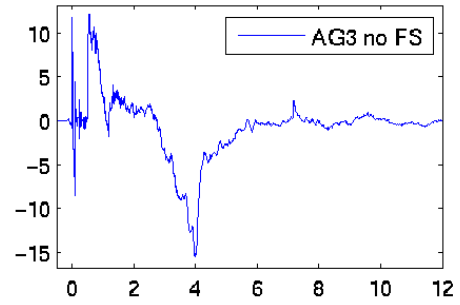
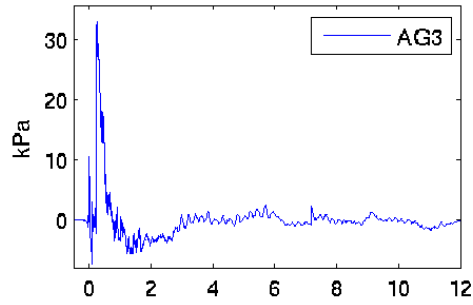


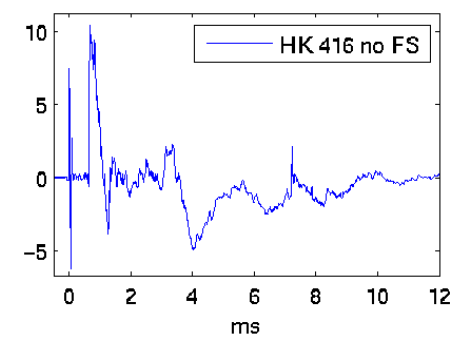
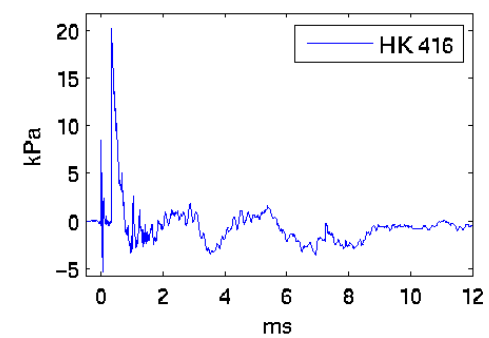
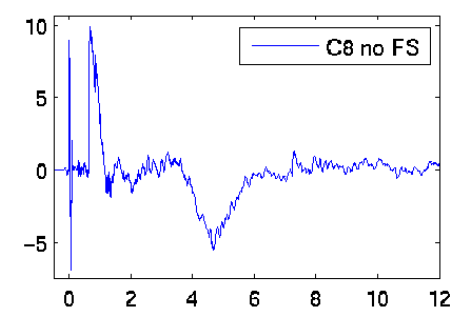
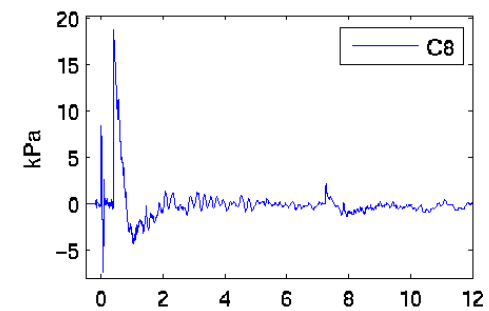
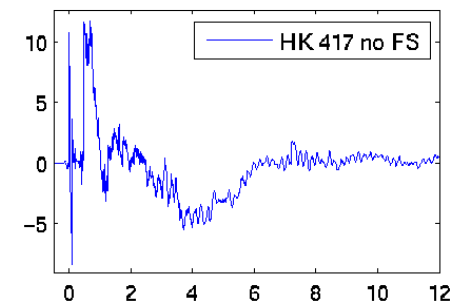
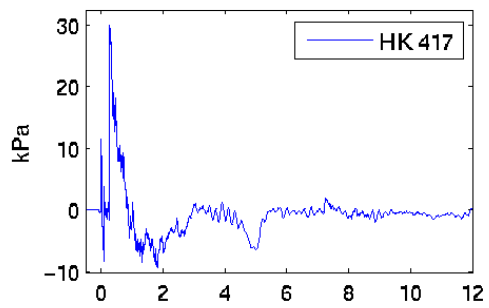
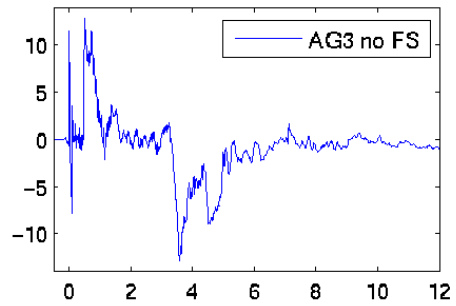
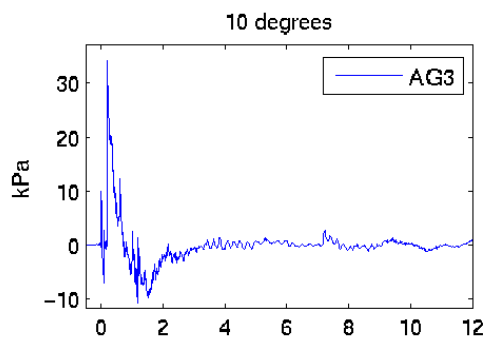
7 degrees



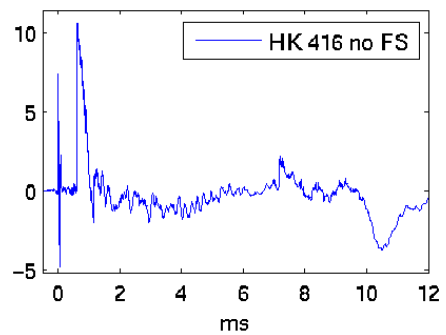
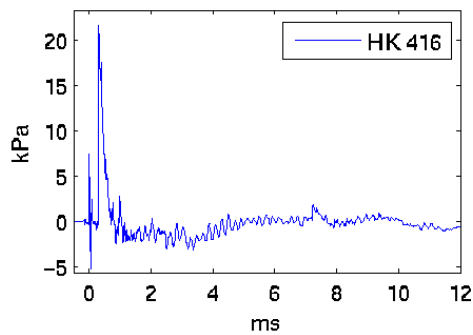
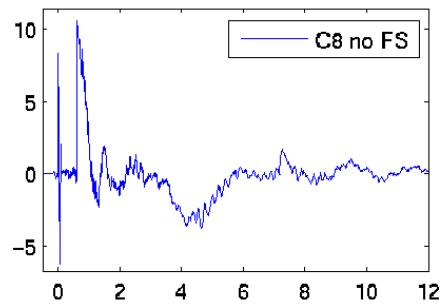
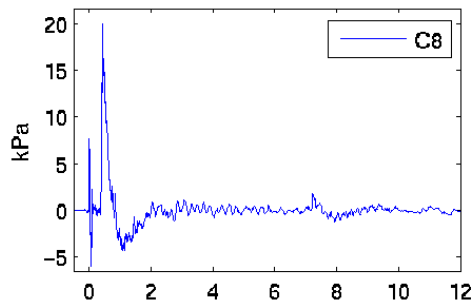
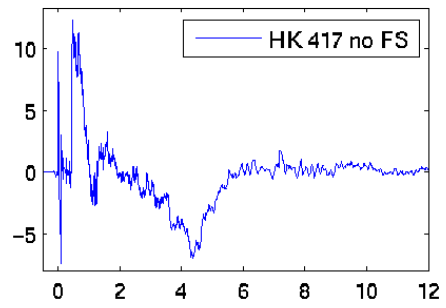
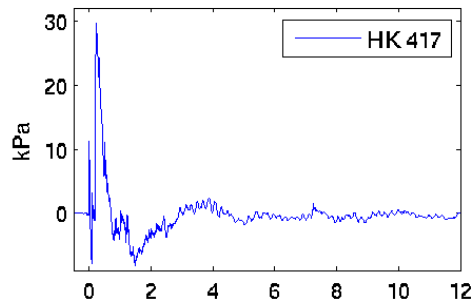
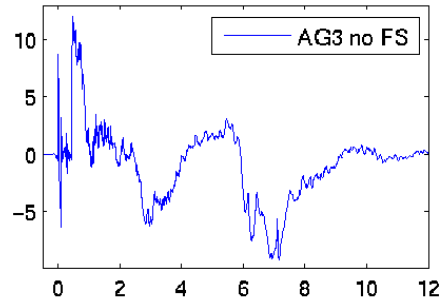
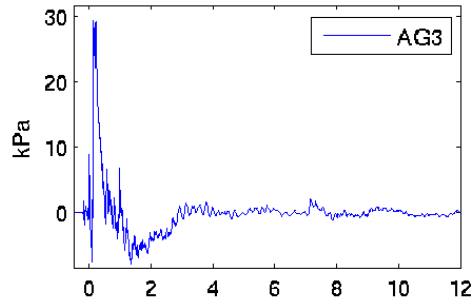


9 degrees

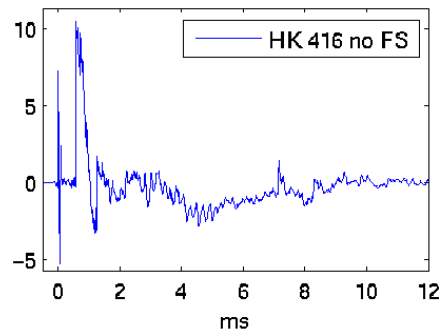
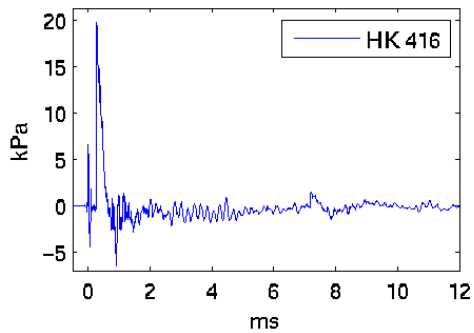
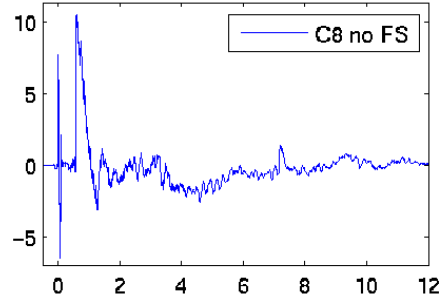
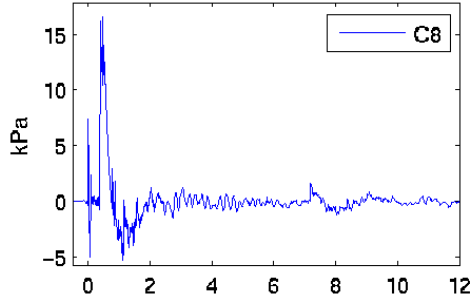
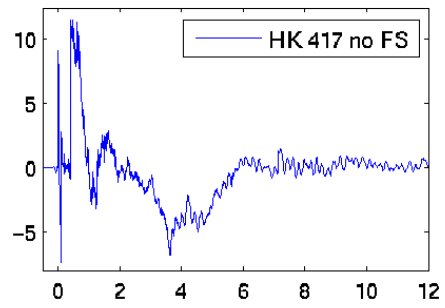
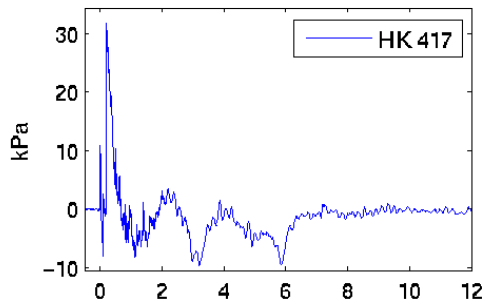
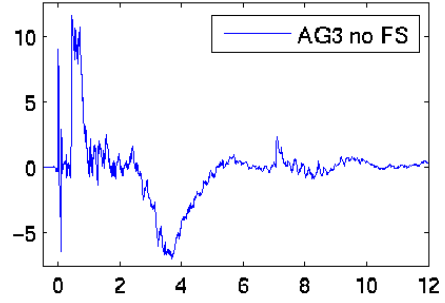
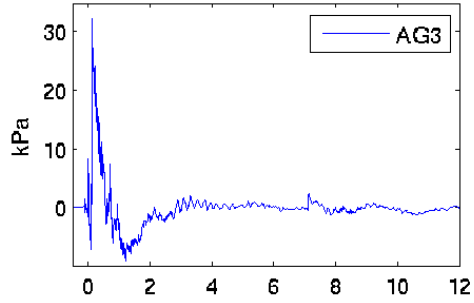




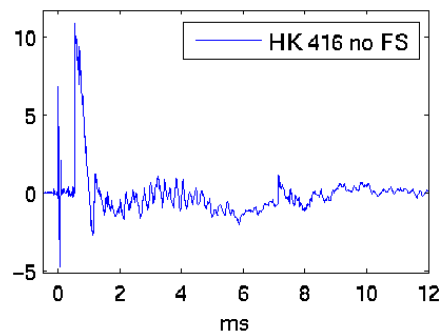
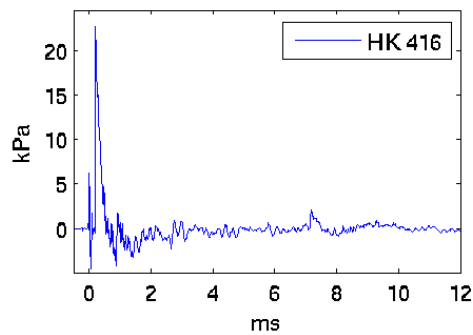
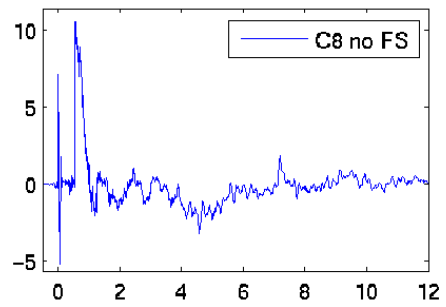
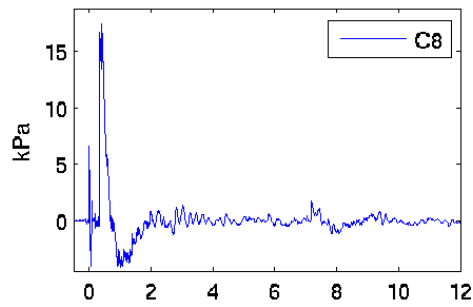
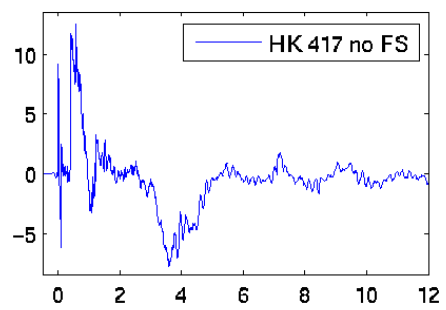
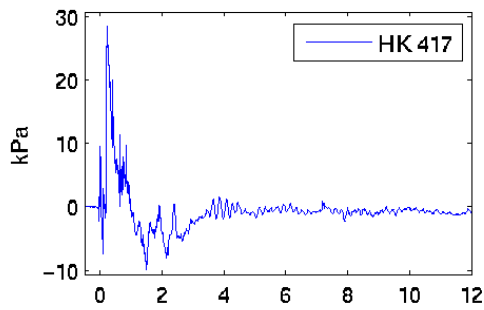
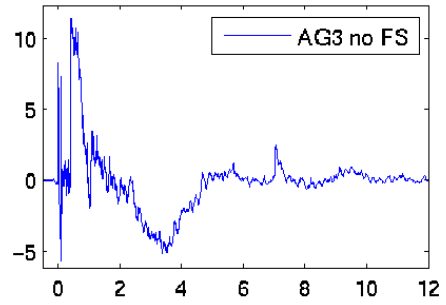
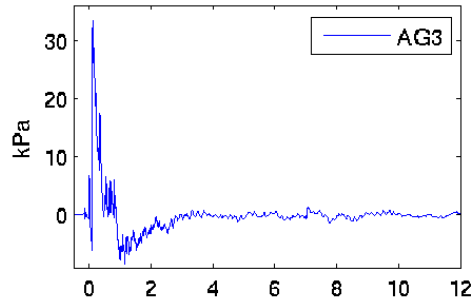
11 degrees

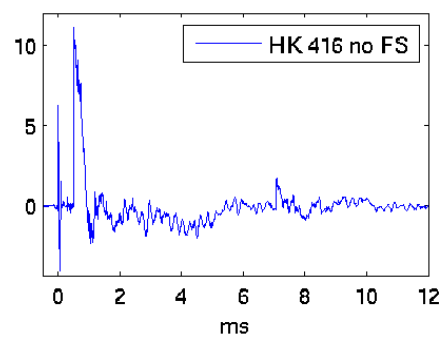
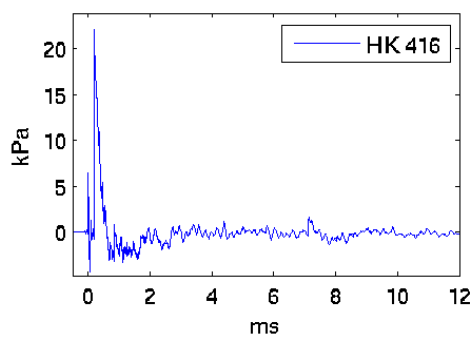
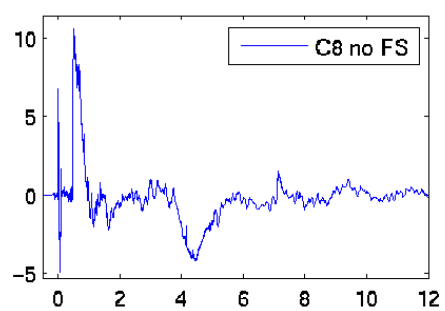
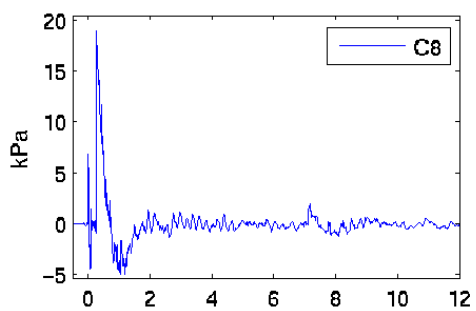
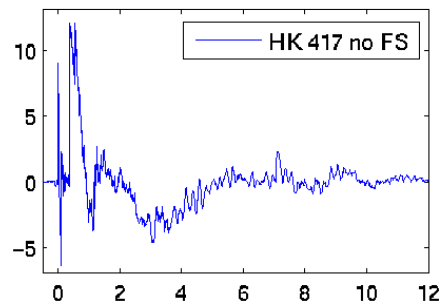
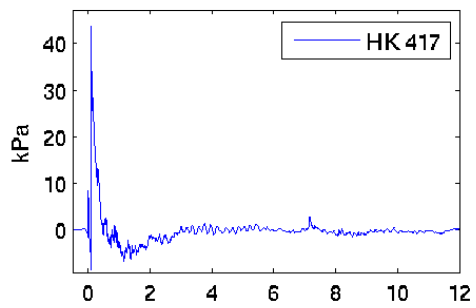
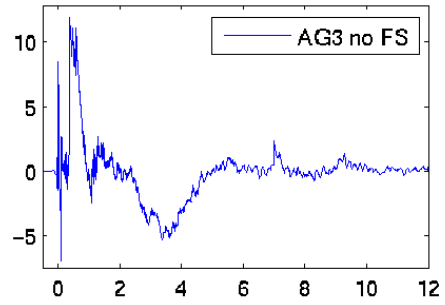
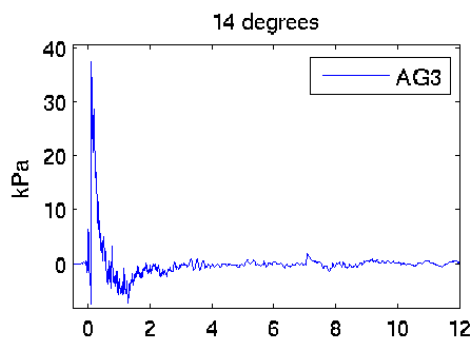


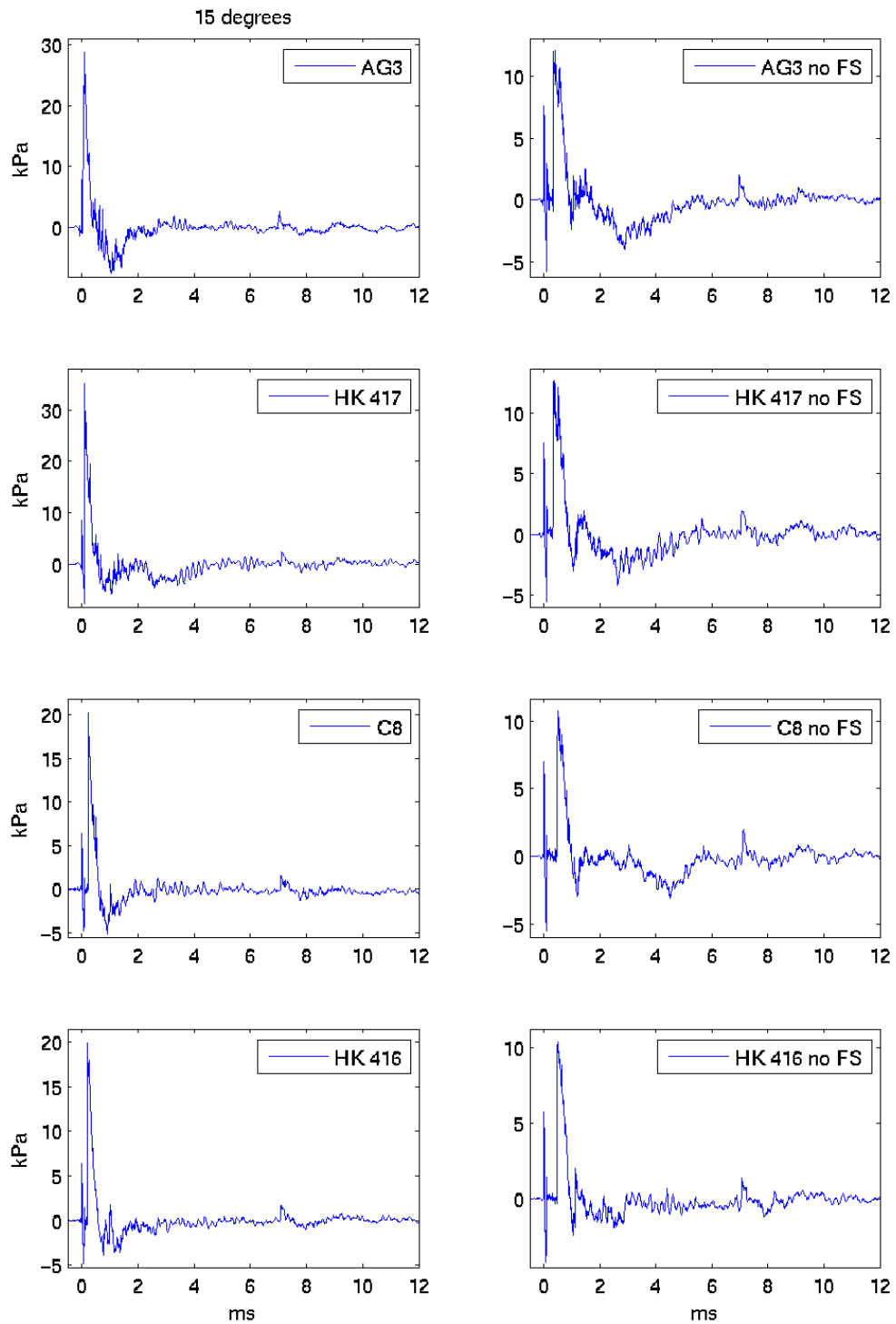
12 degrees



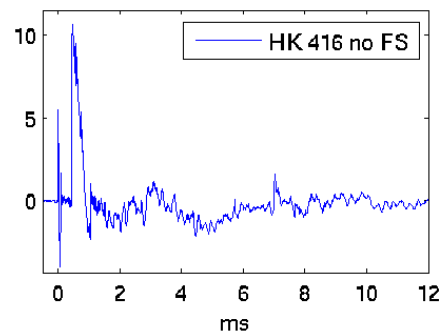
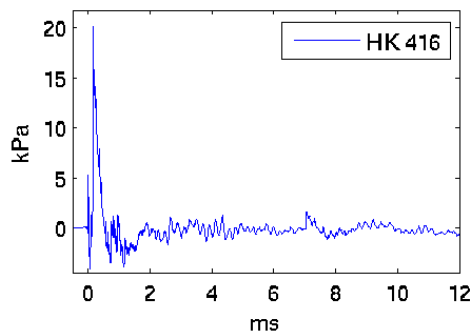
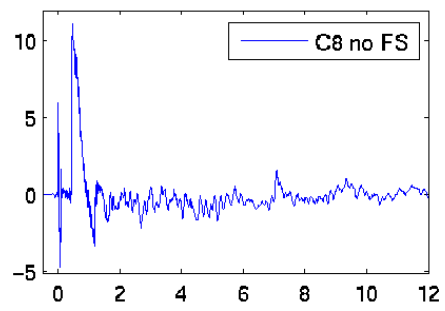
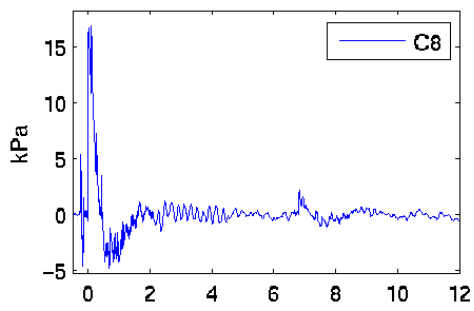
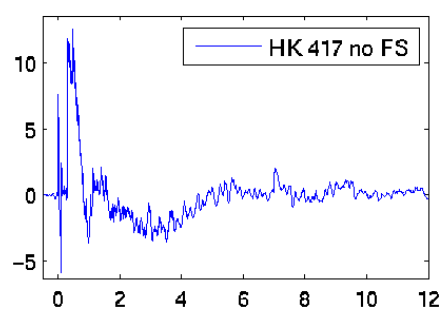
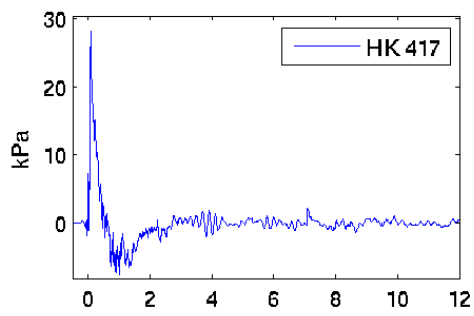
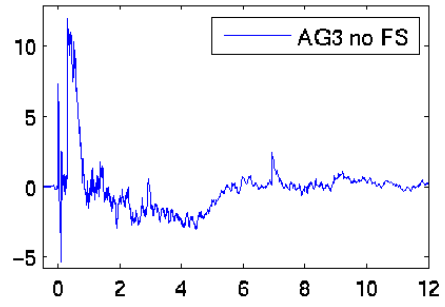
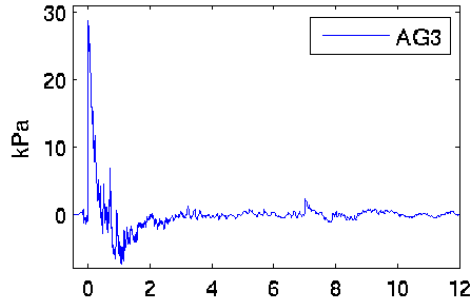
13 degrees



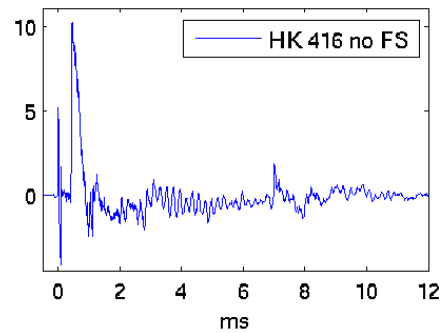
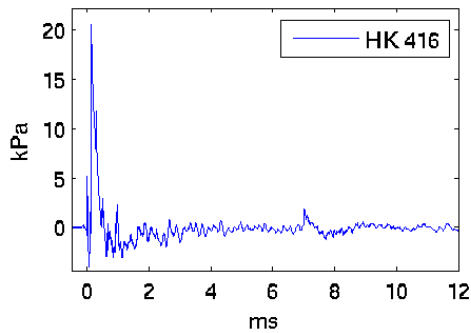
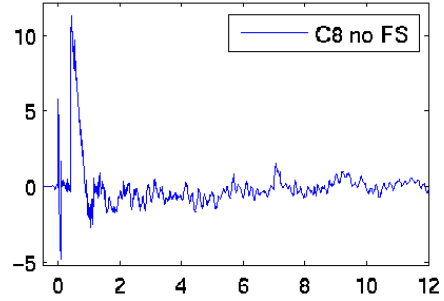
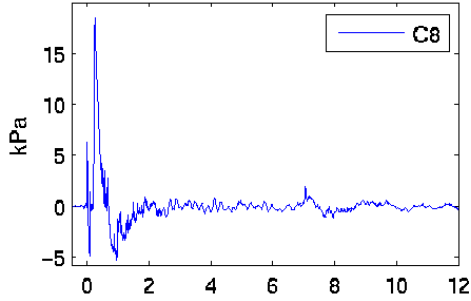
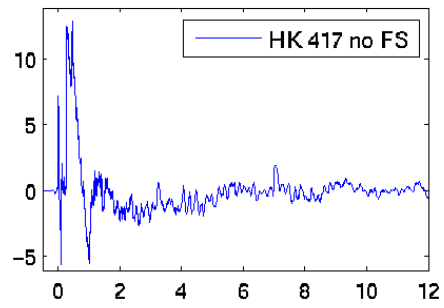
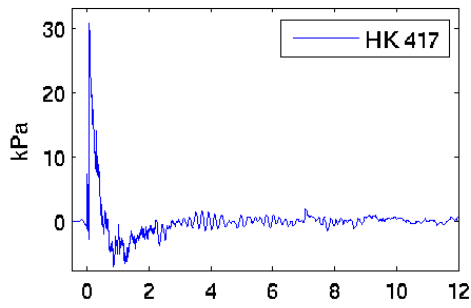
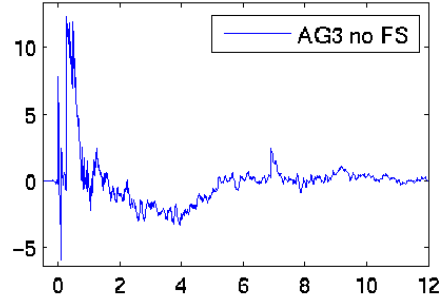
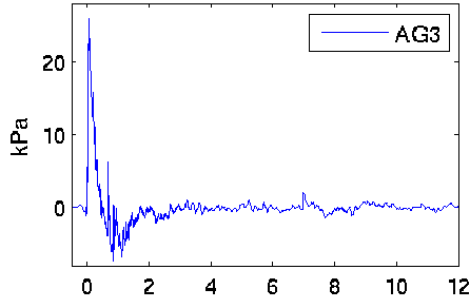




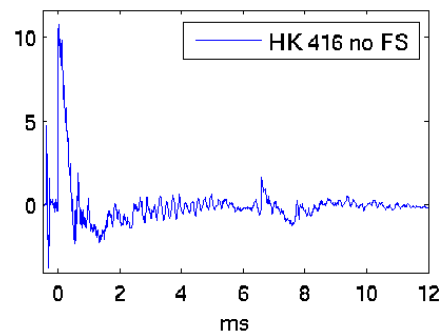
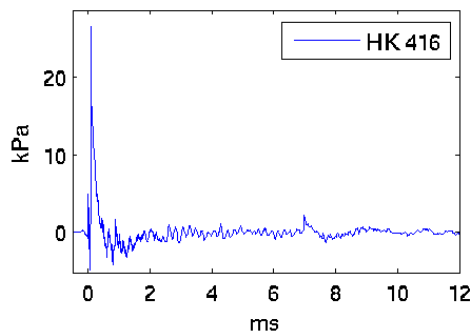
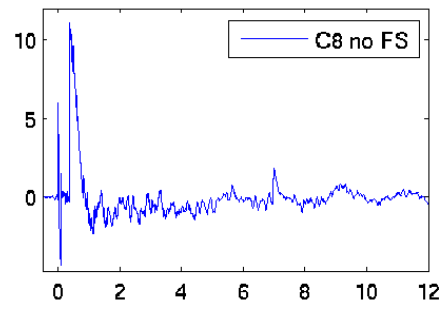
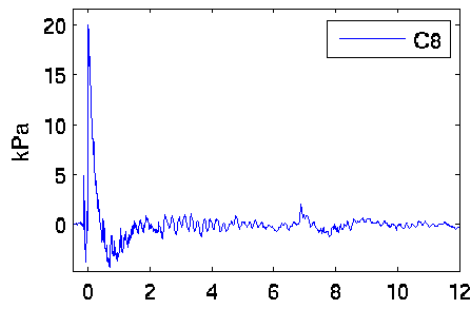
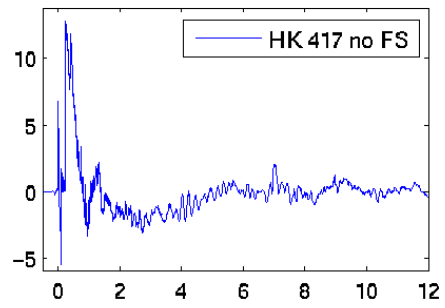
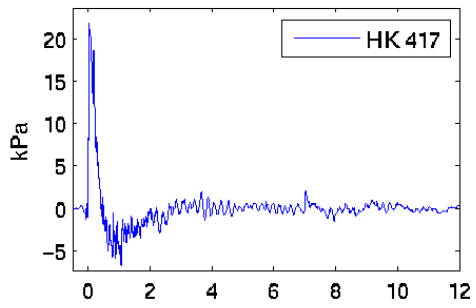
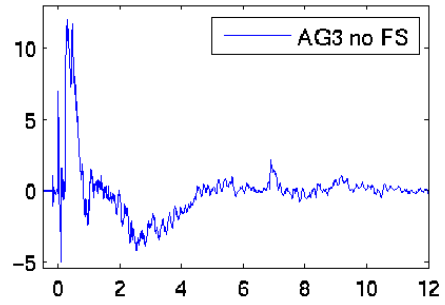
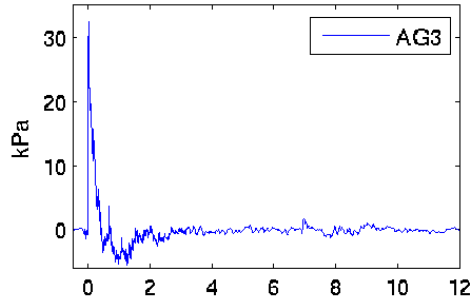
16 degrees



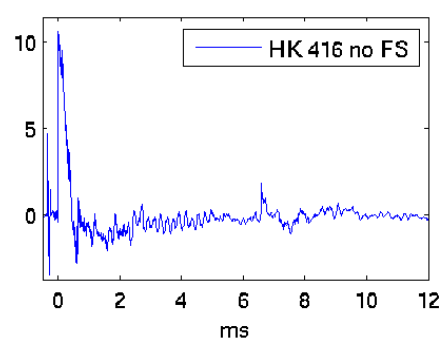
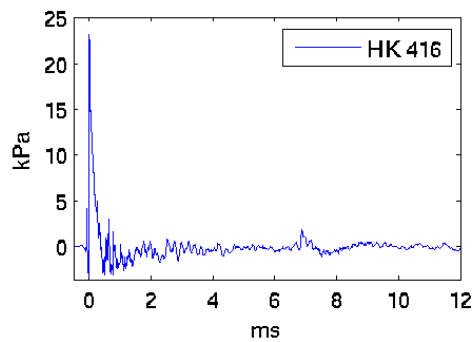
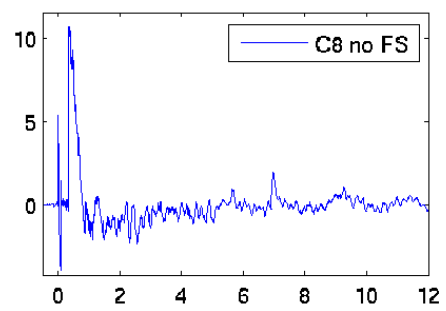
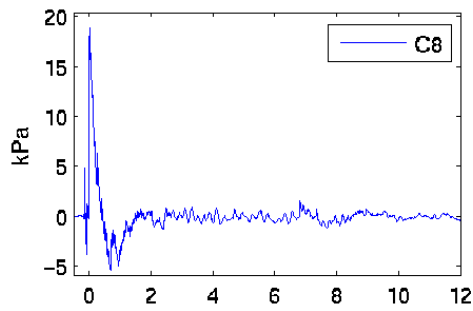
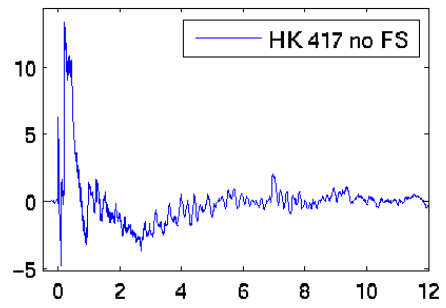
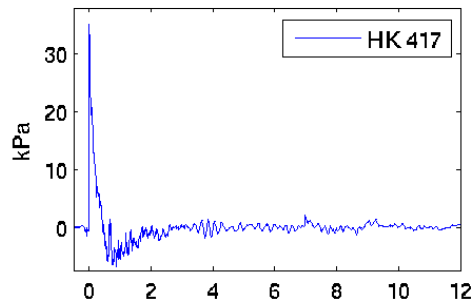
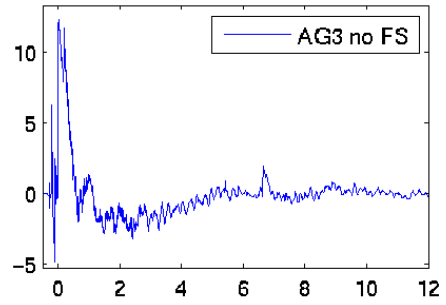
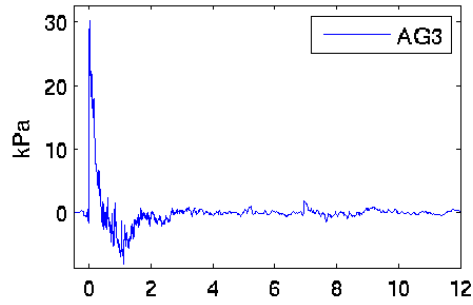
17 degrees



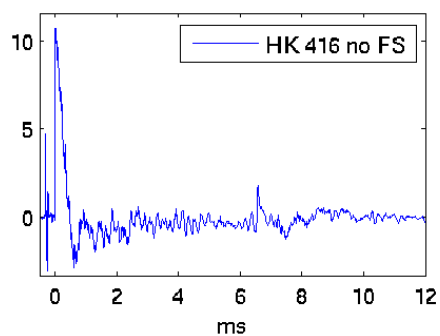
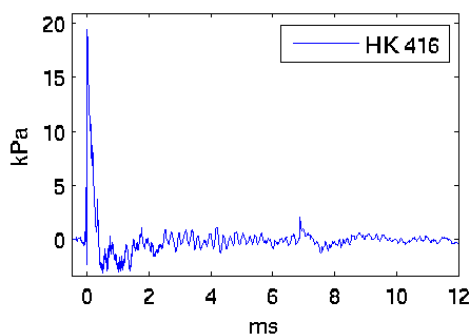
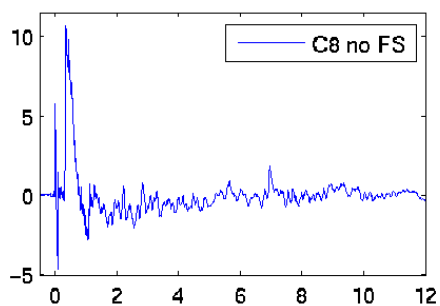
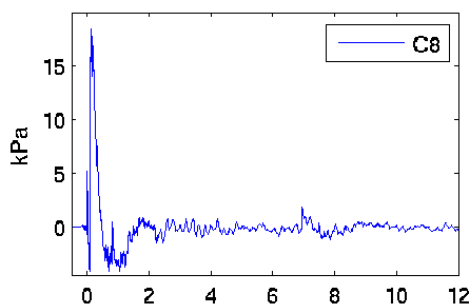
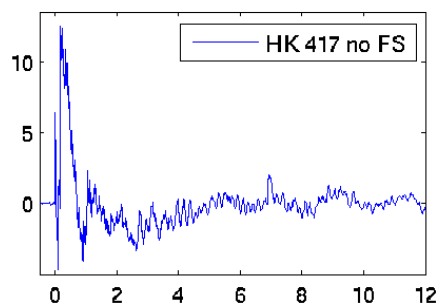
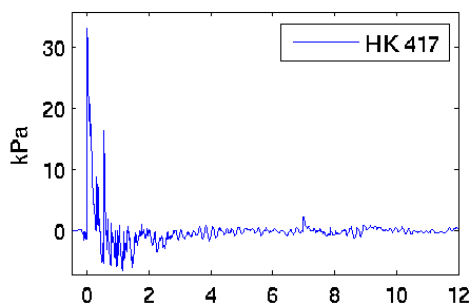
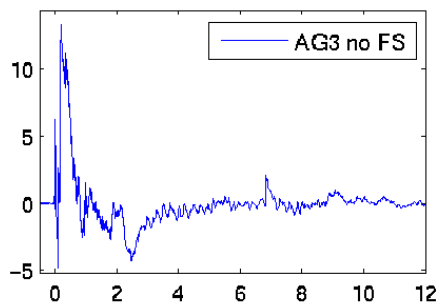
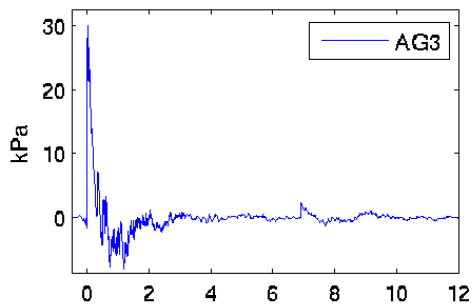
18 degrees



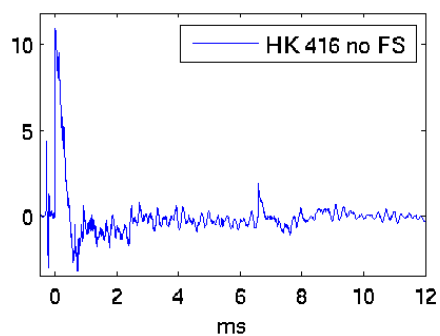
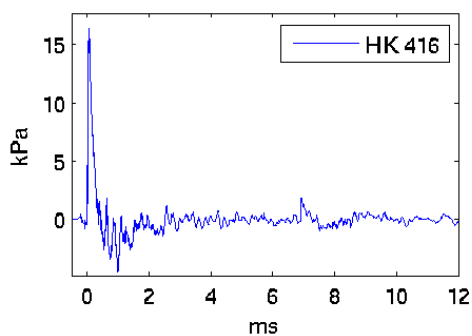
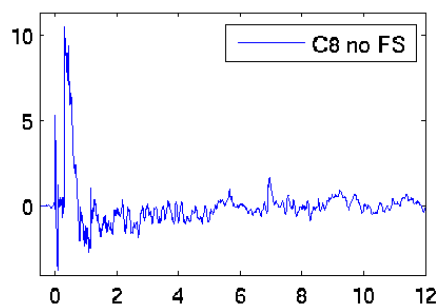
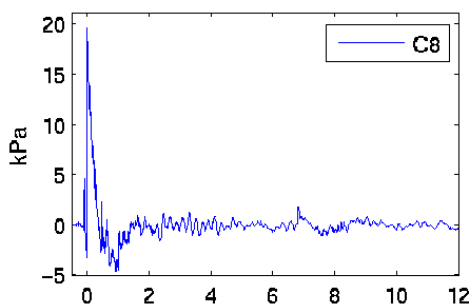
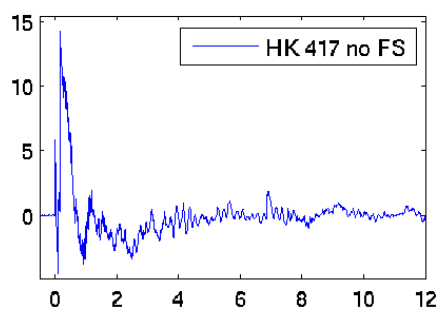
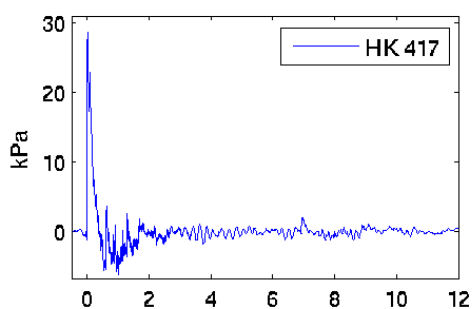
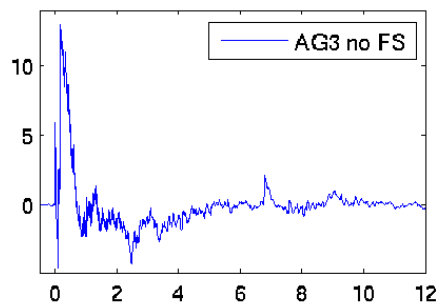
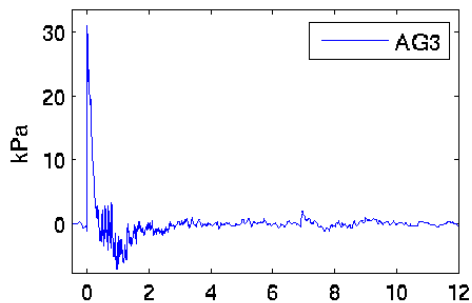
19 degrees



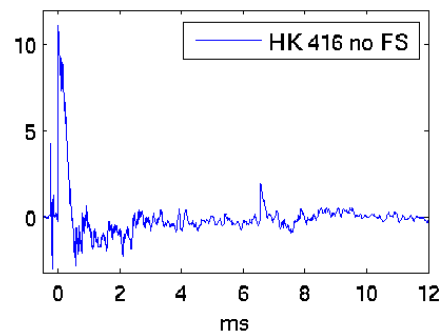
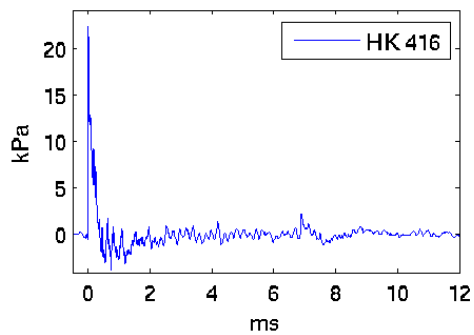
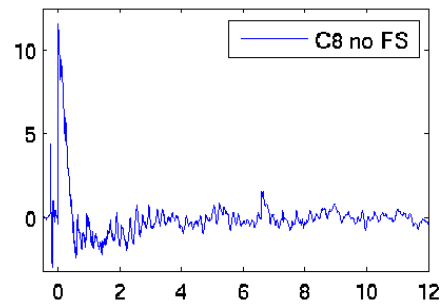
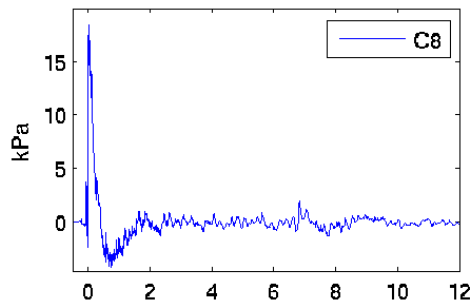
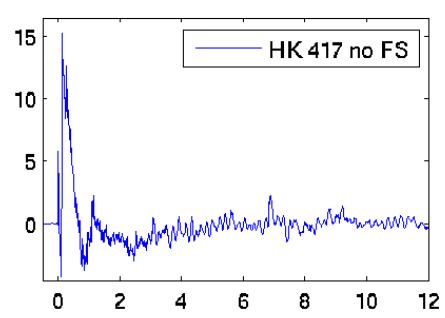
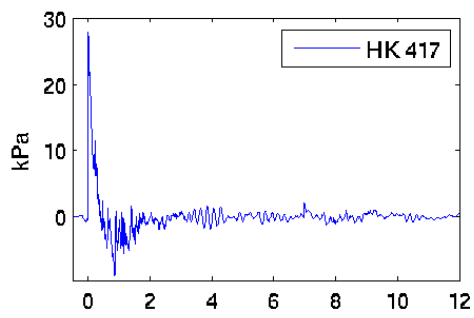
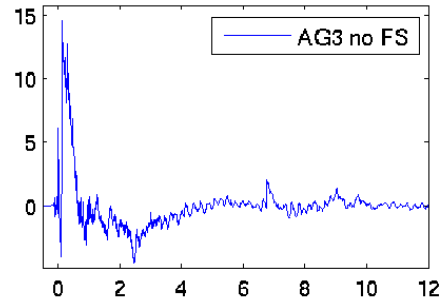
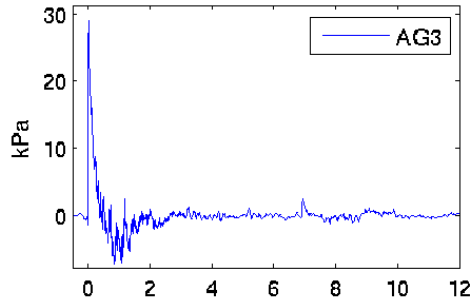
20 degrees



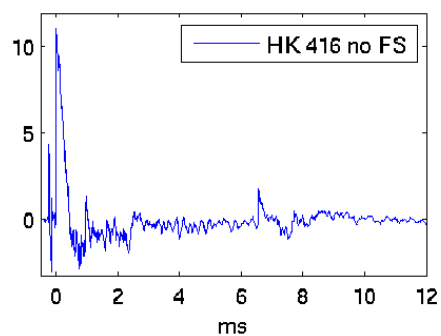
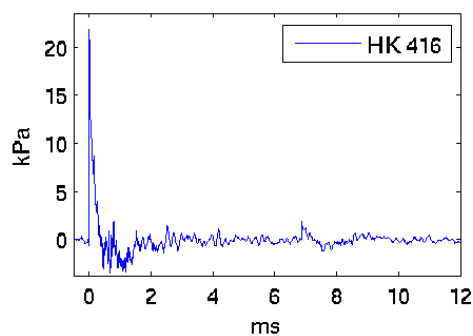
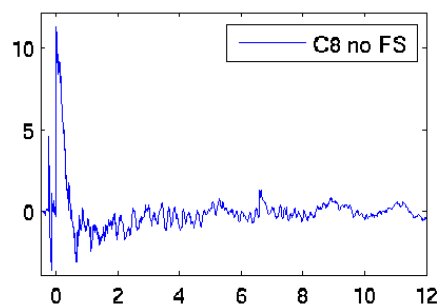
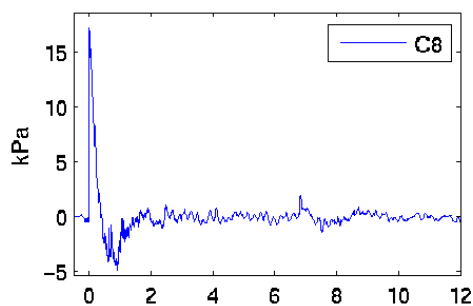
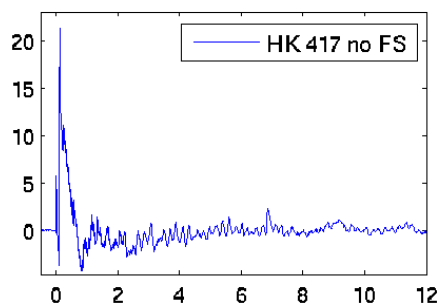
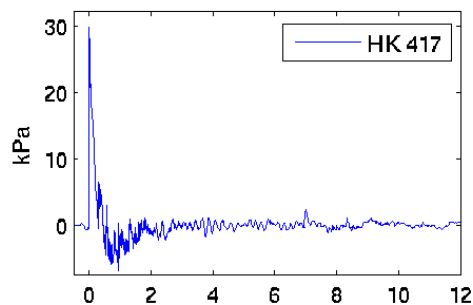
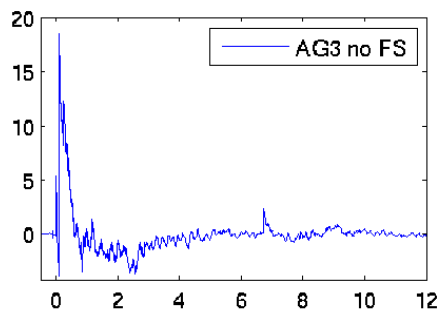
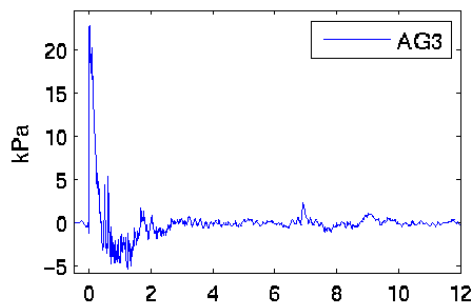
21 degrees



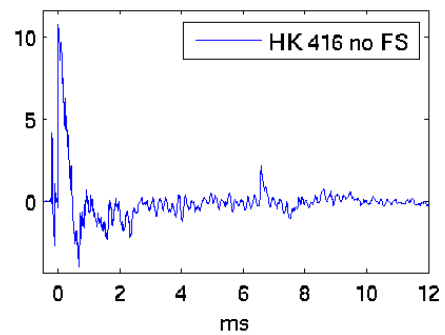
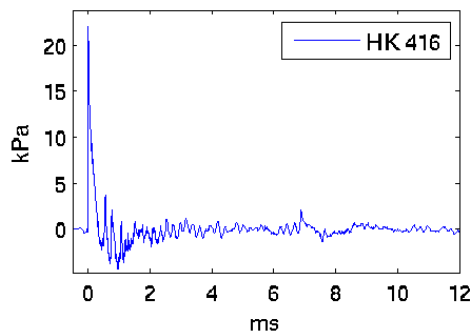
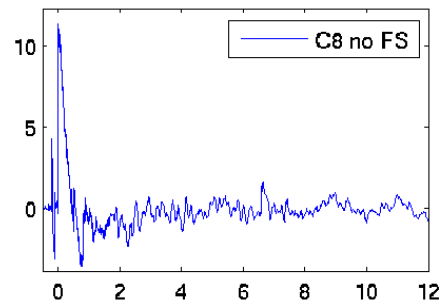
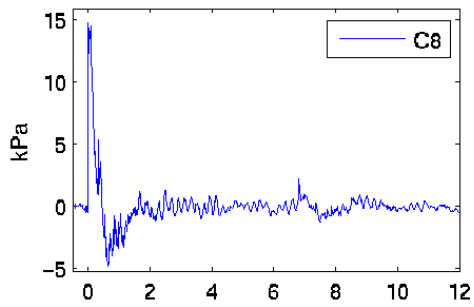
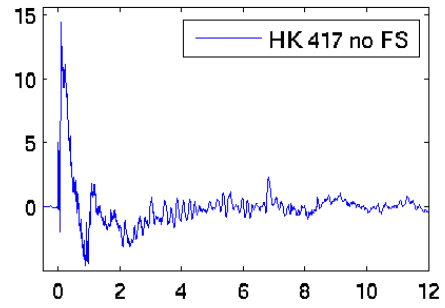
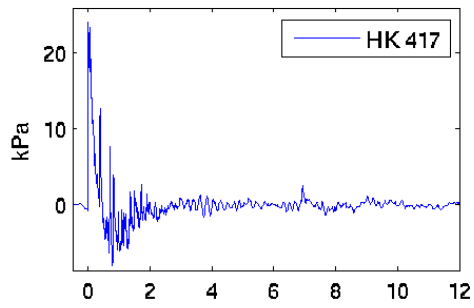
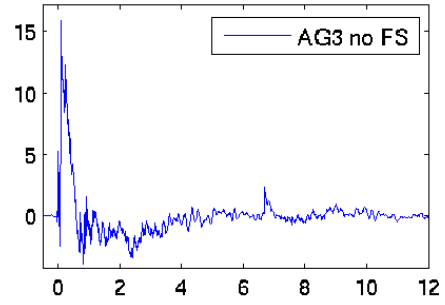
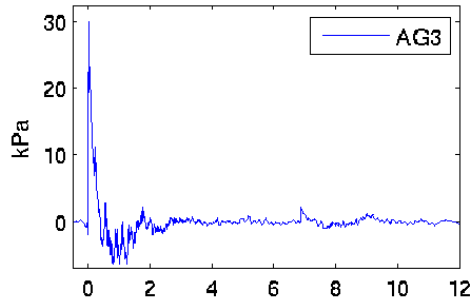
22 degrees



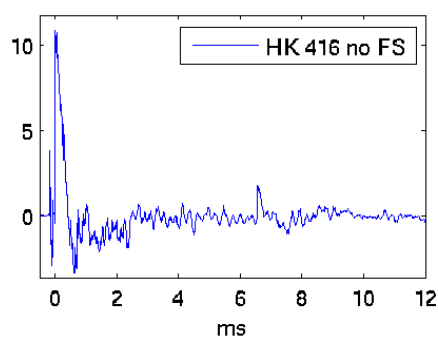
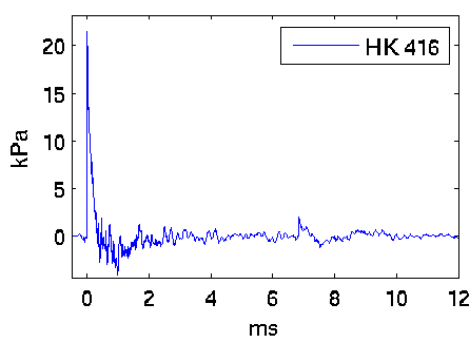
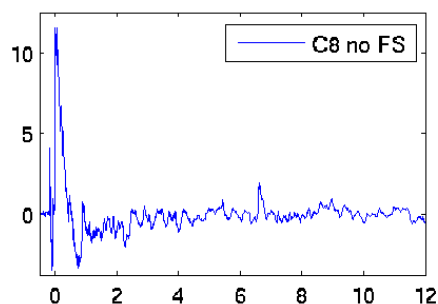
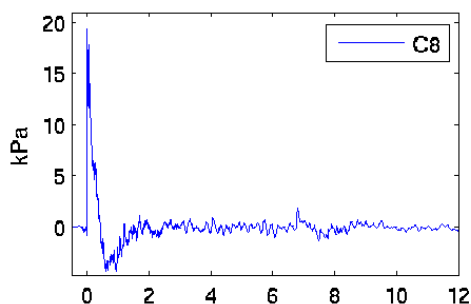
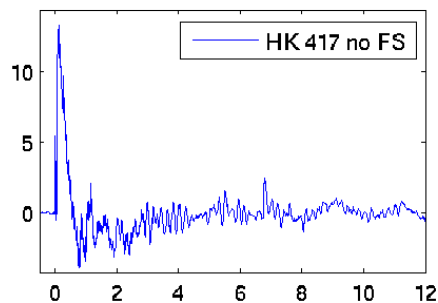
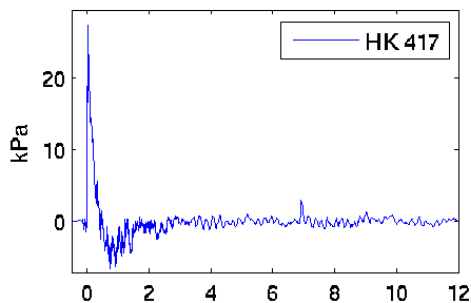
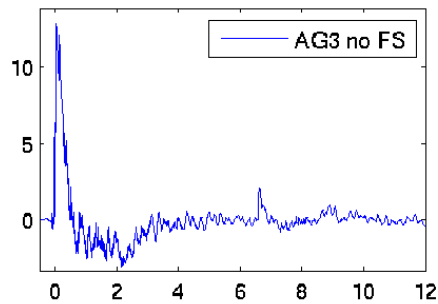
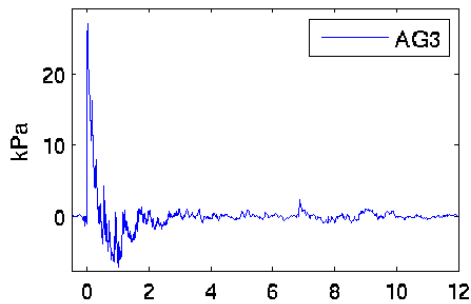
23 degrees



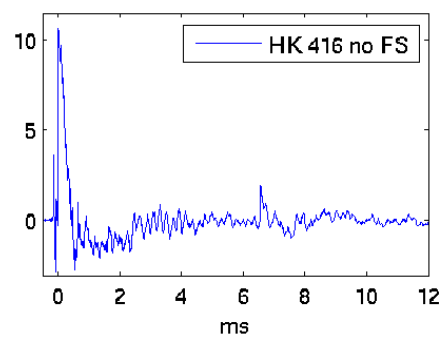
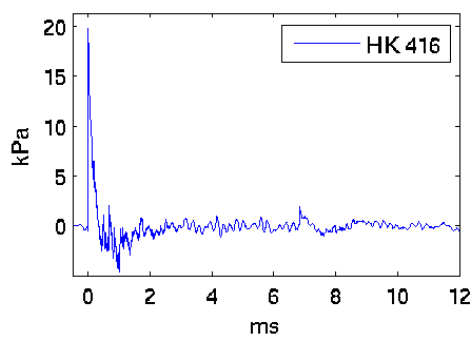
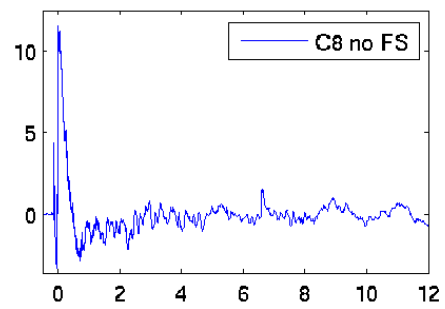
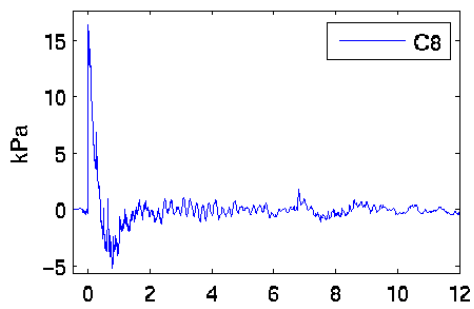
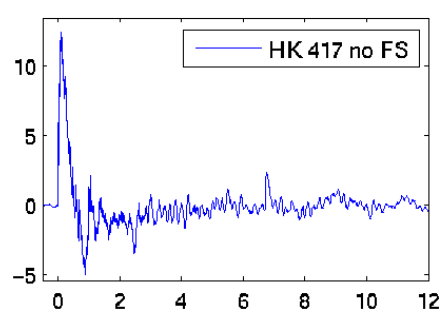
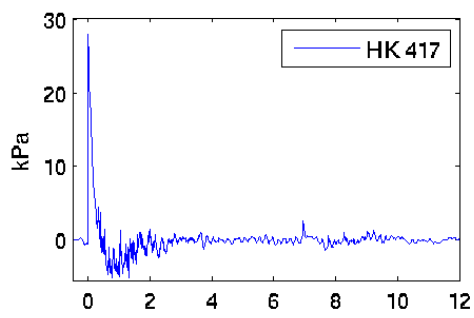
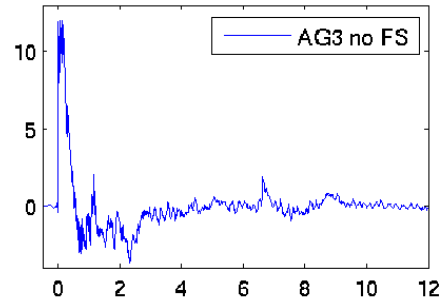
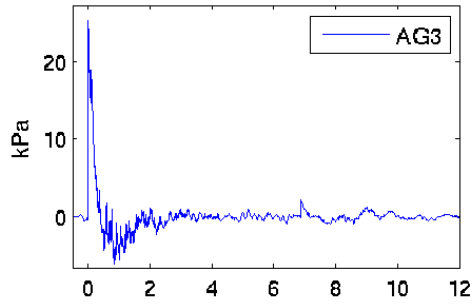
24 degrees



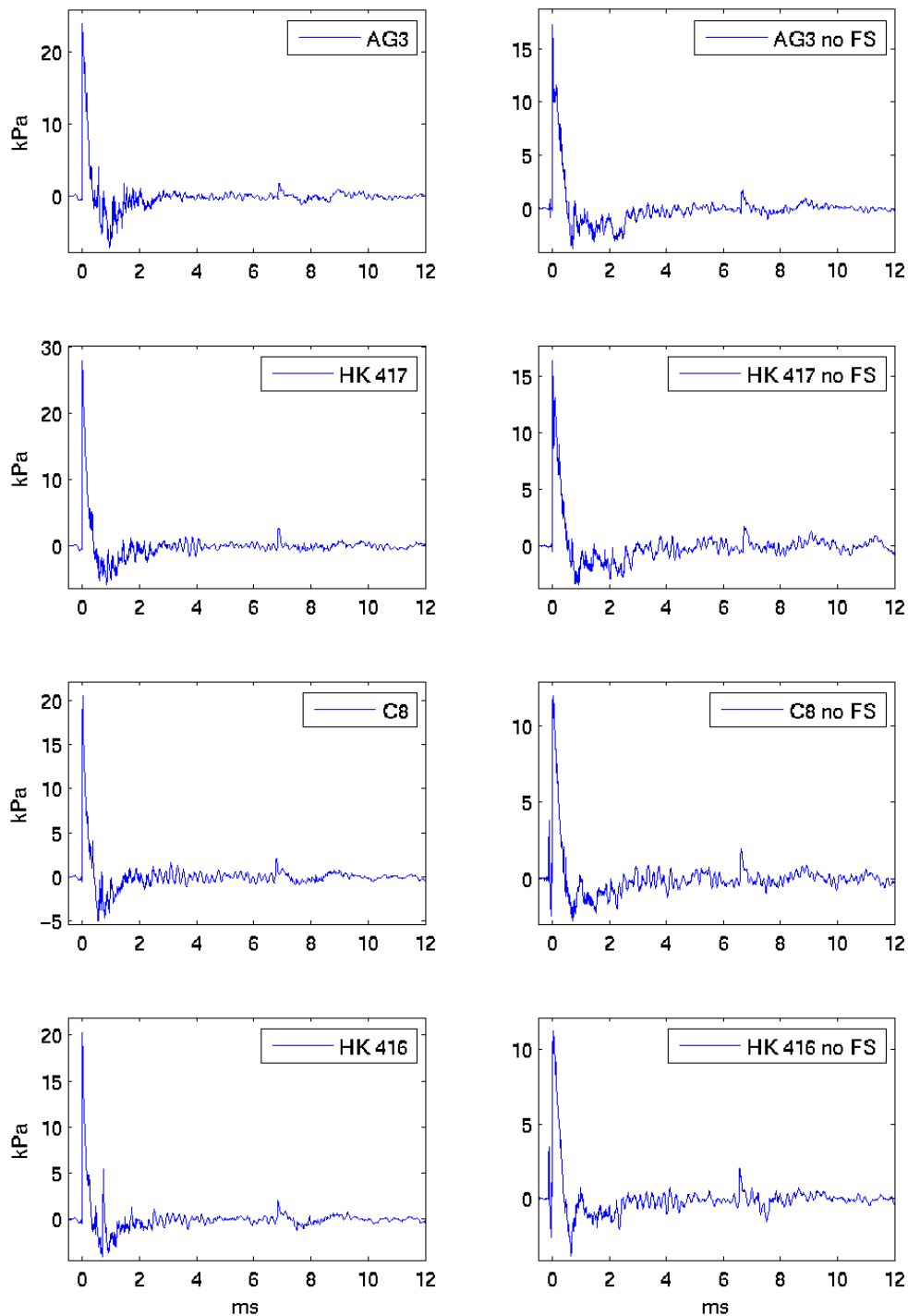
25 degrees



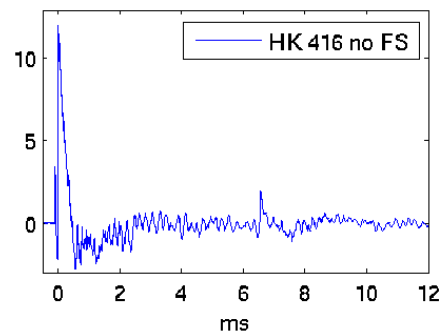
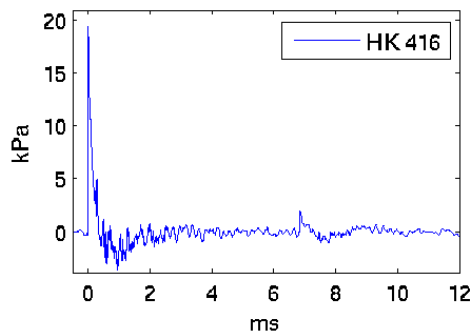
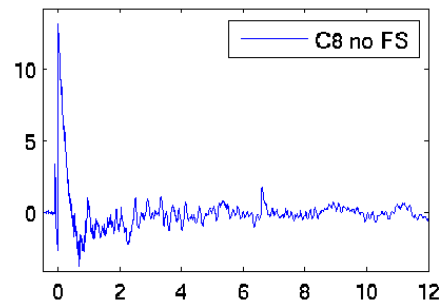
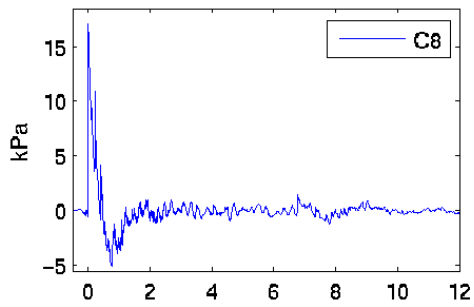
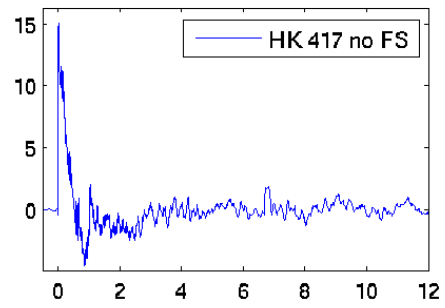
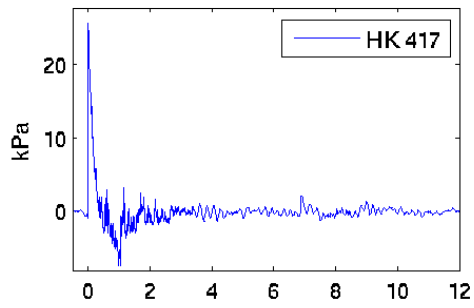
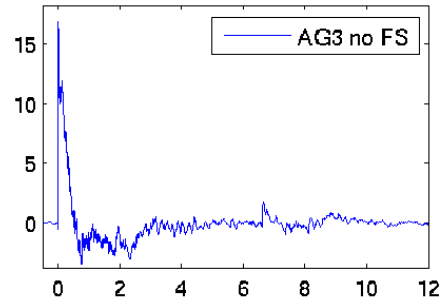
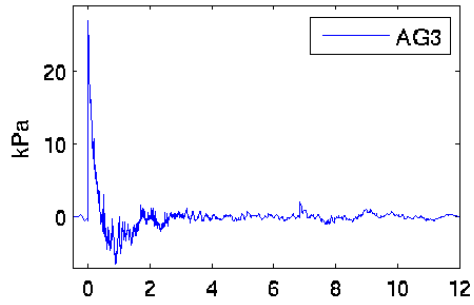
26 degrees



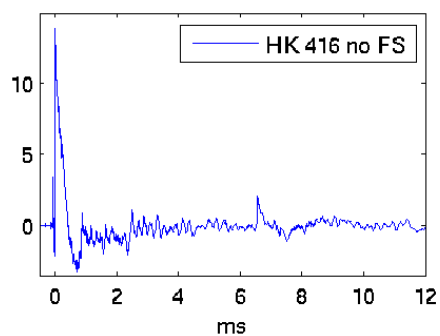
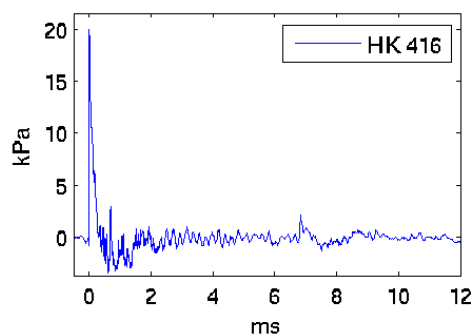
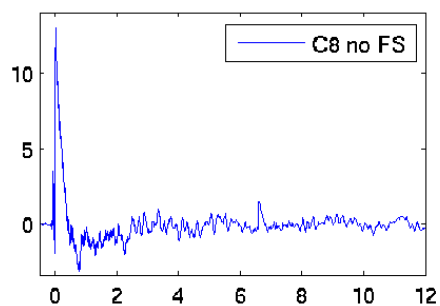
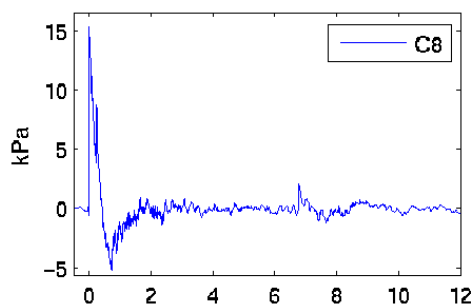
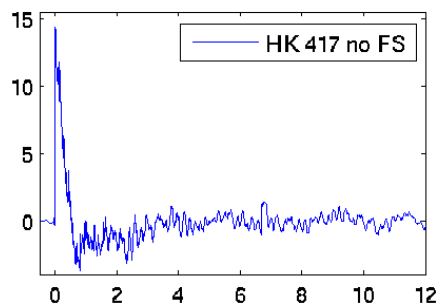
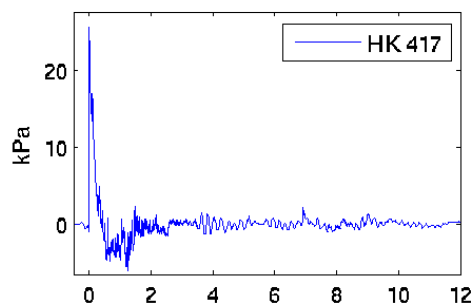
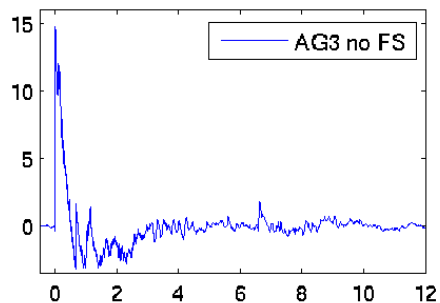
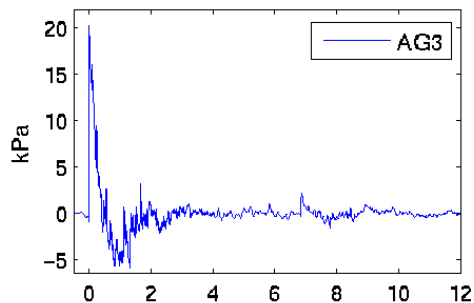
27 degrees



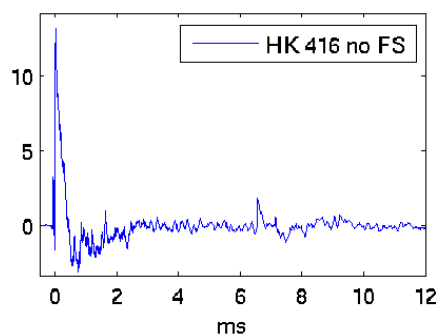
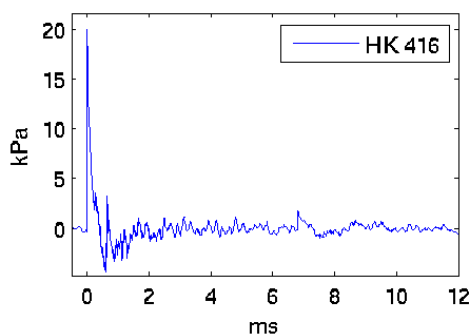
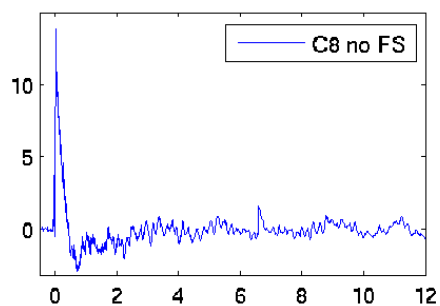
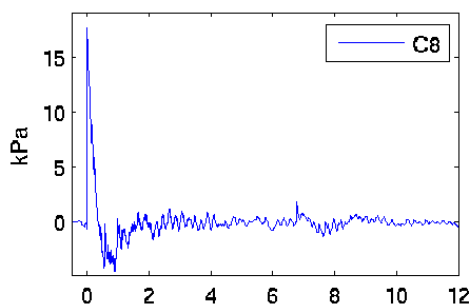
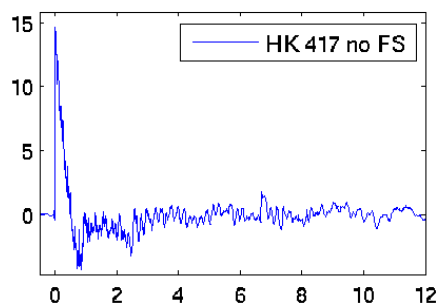
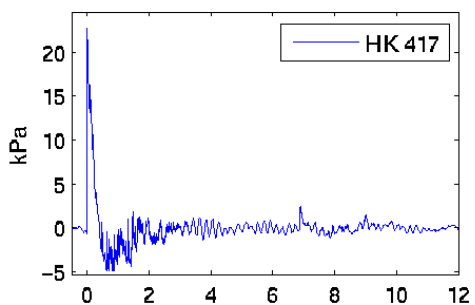
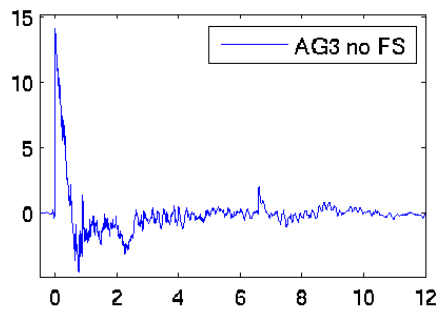
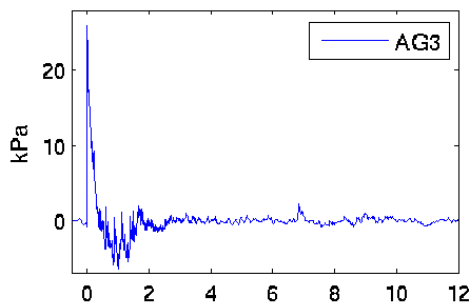
28 degrees



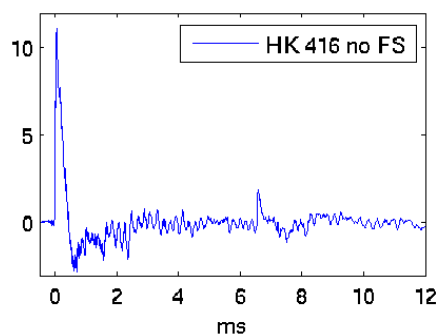
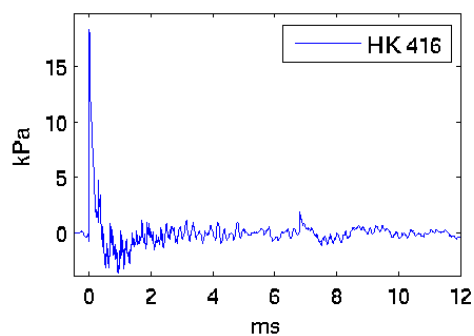
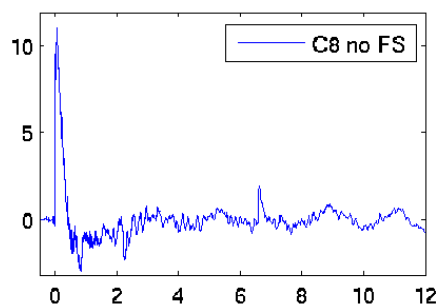
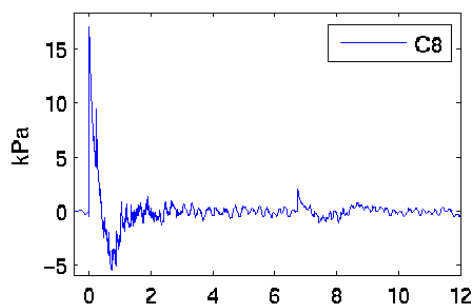
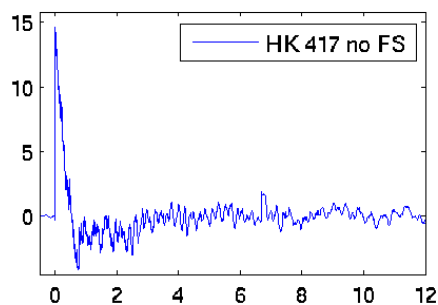
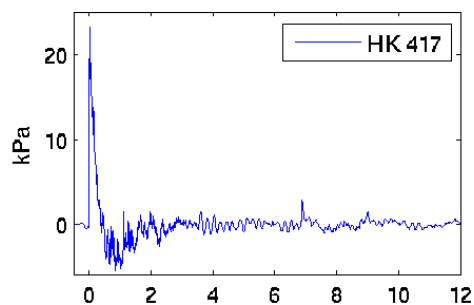
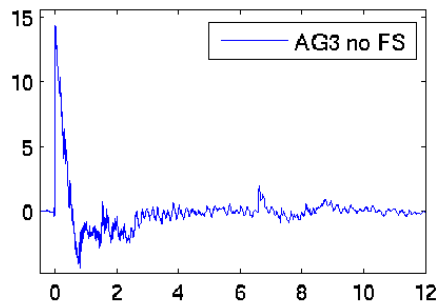
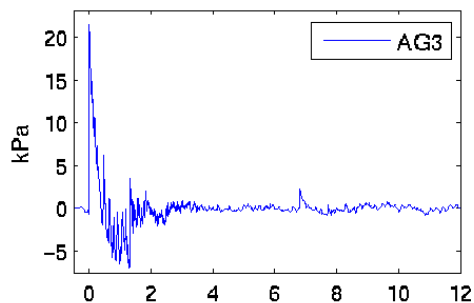
29 degrees



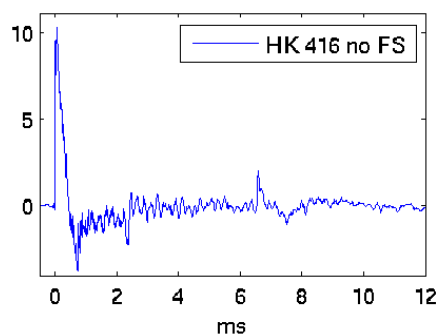
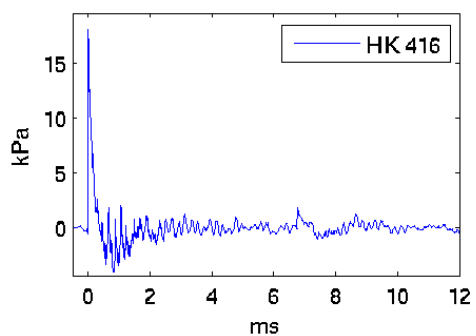
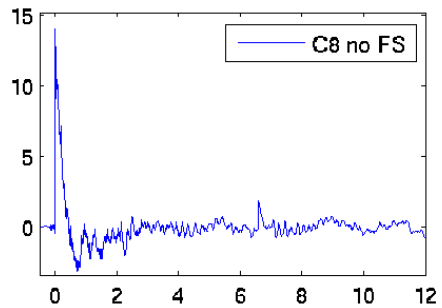
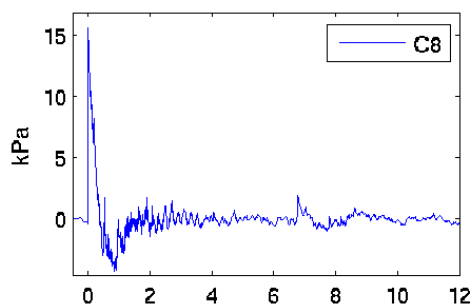
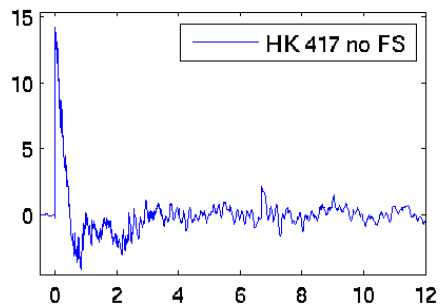
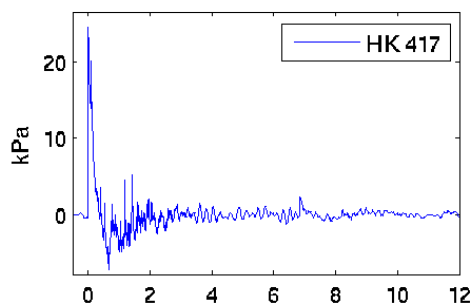
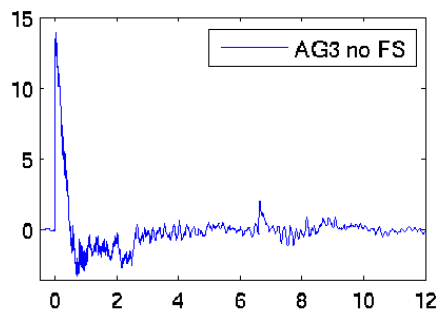
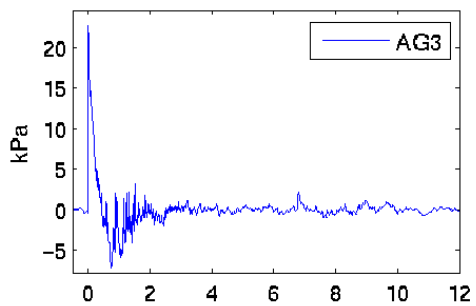
30 degrees



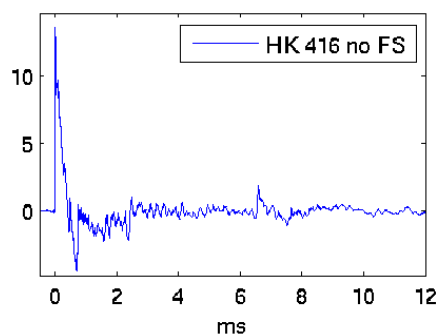
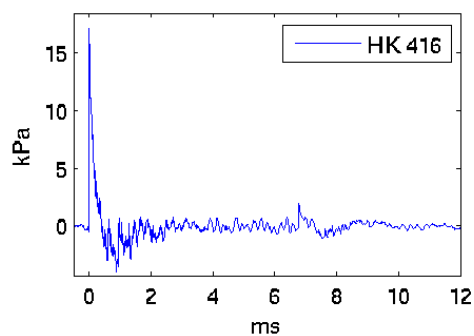
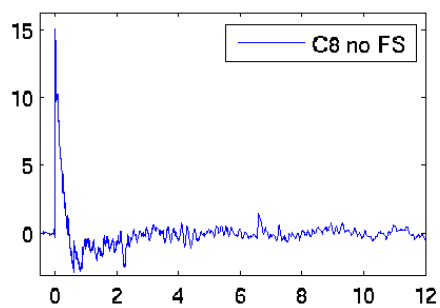
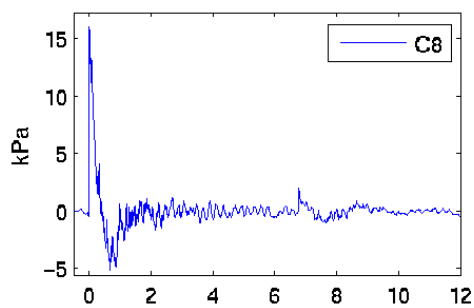
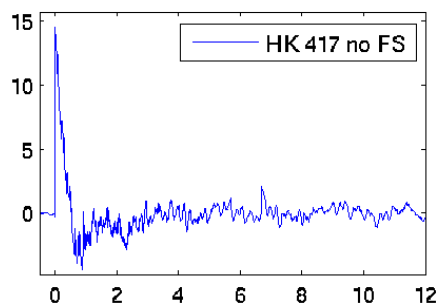
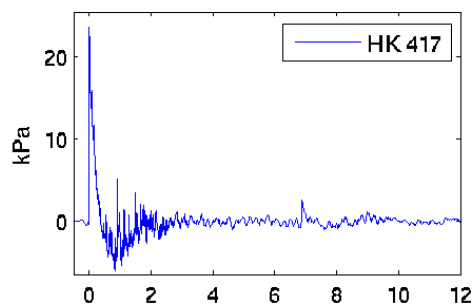
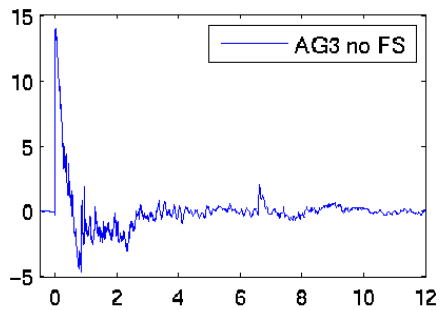
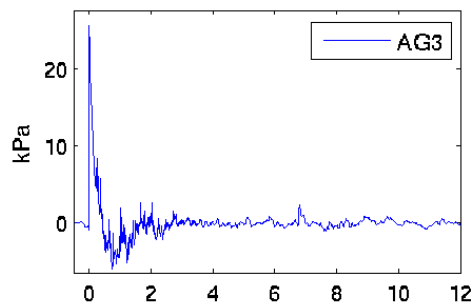
31 degrees



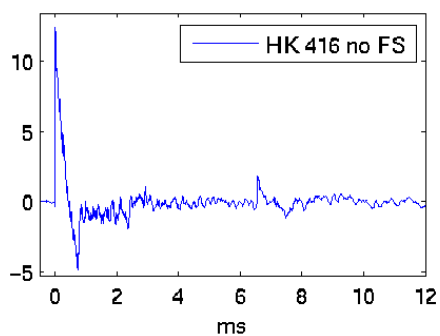
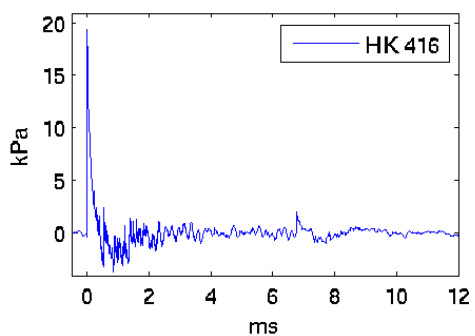
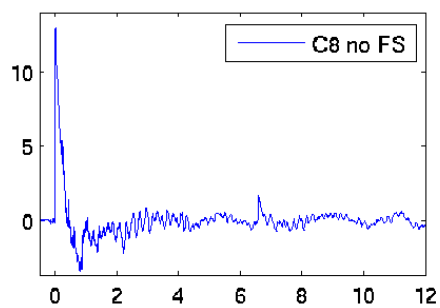
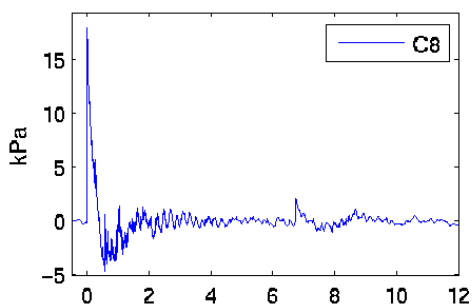
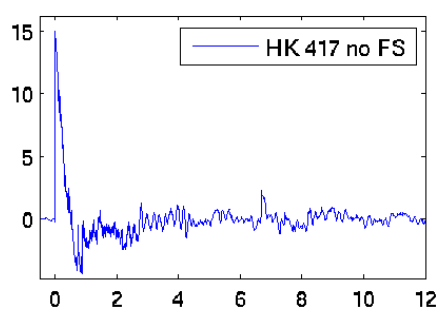
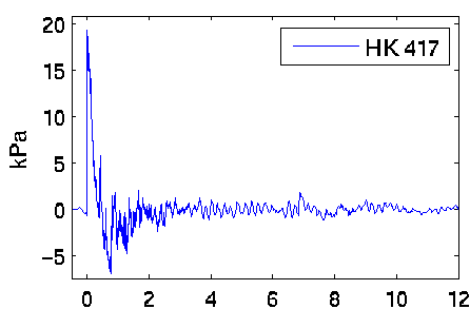
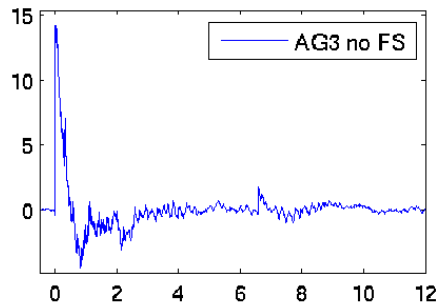
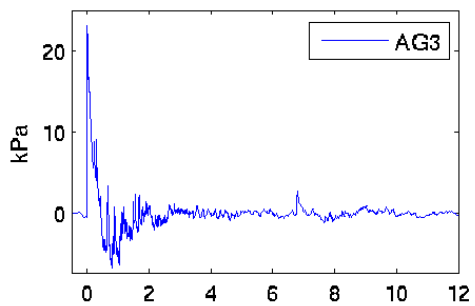
32 degrees



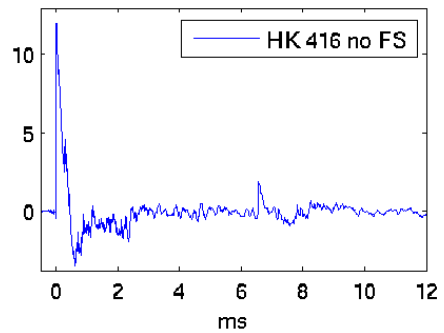
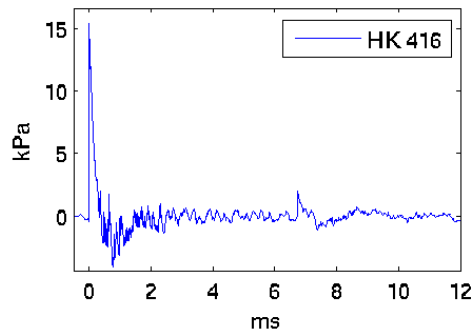
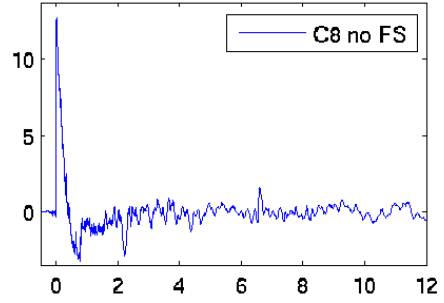
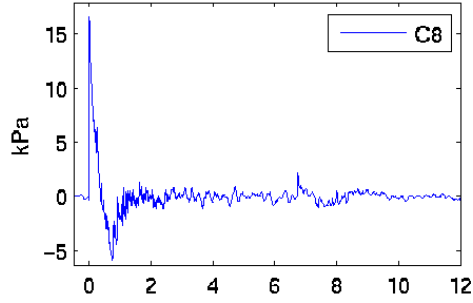
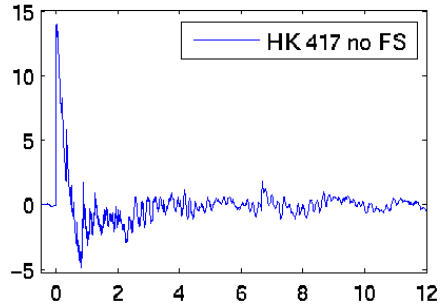
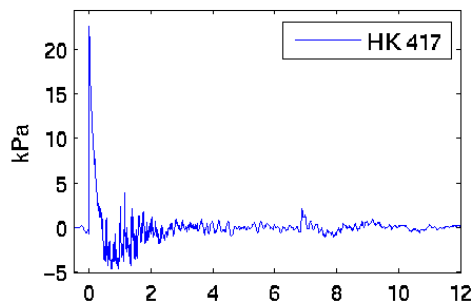
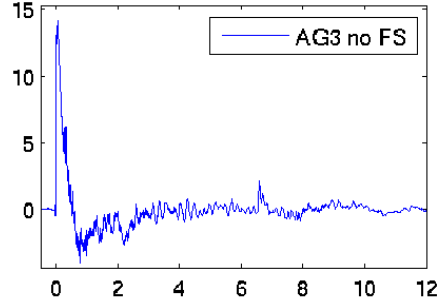
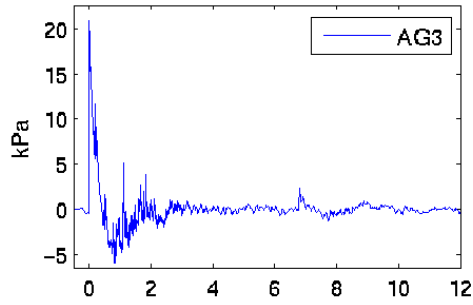
33 degrees



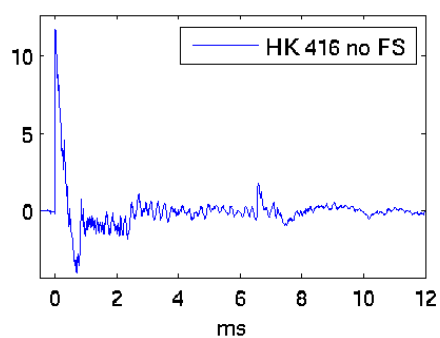
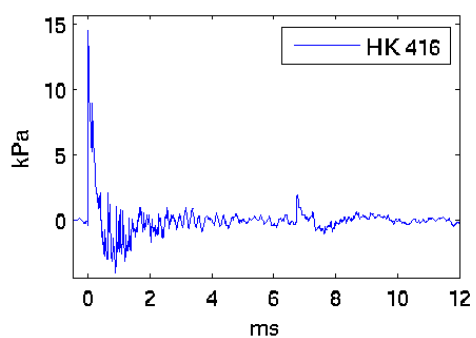
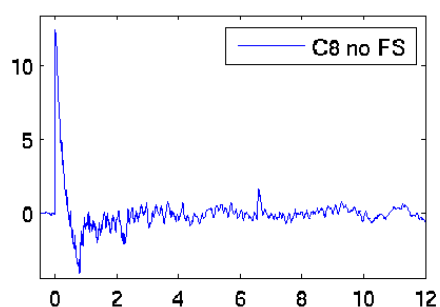
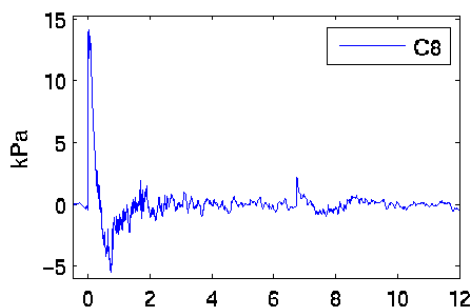
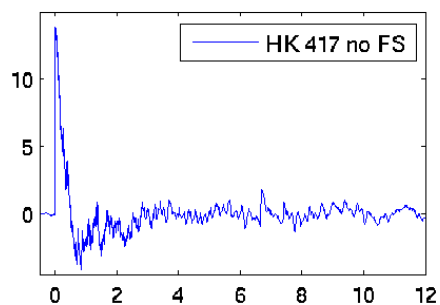
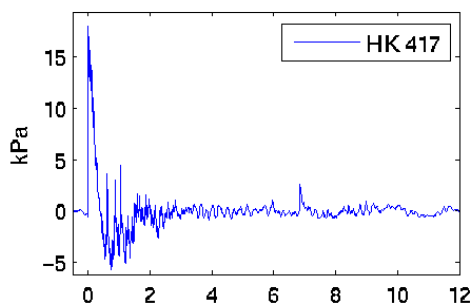
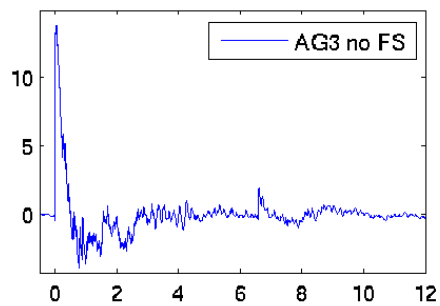
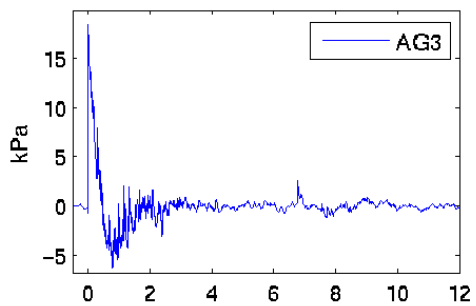
34 degrees



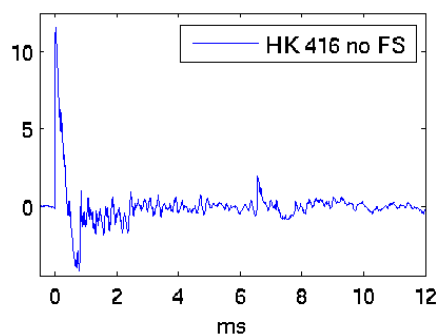
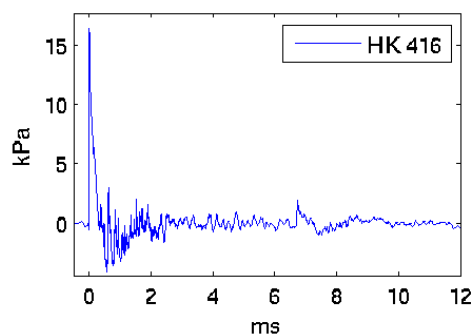
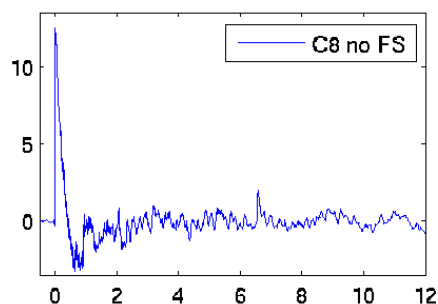
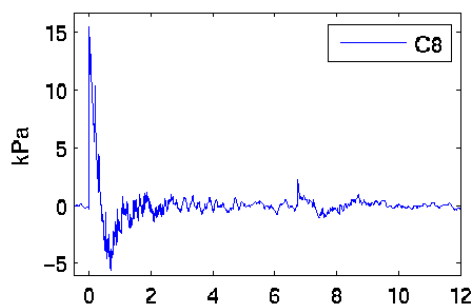
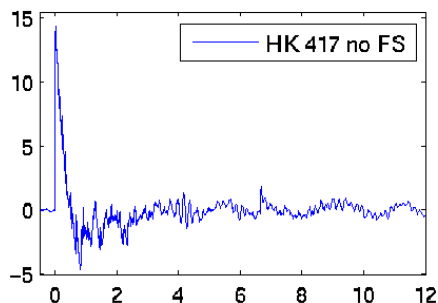
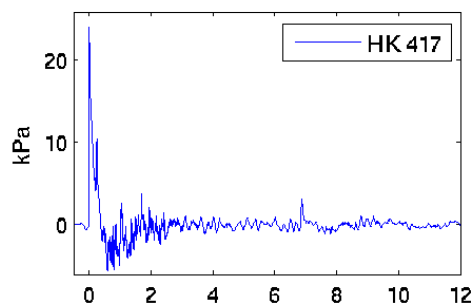
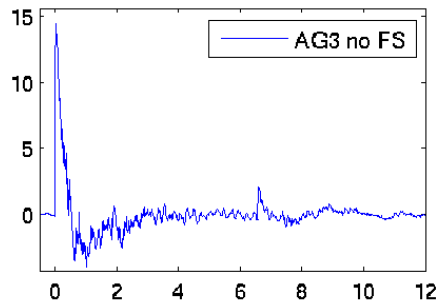
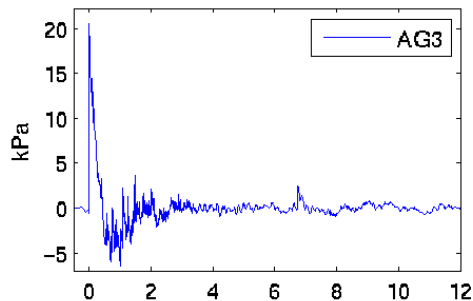
35 degrees



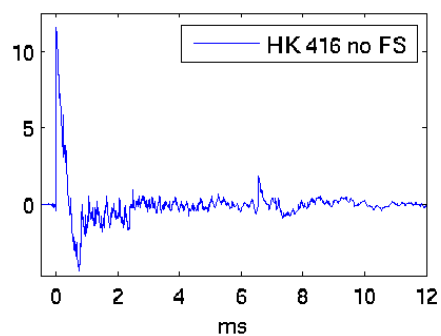
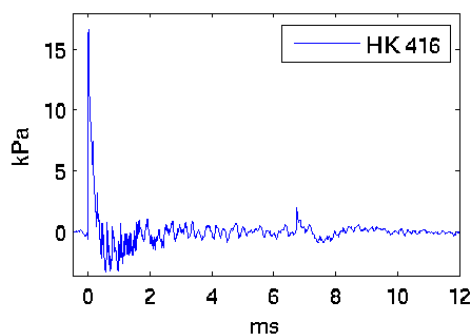
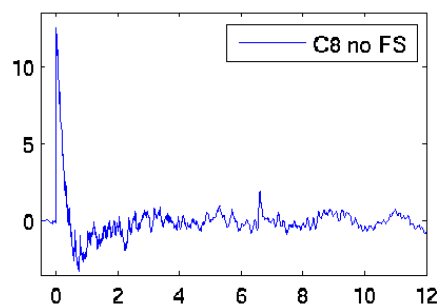
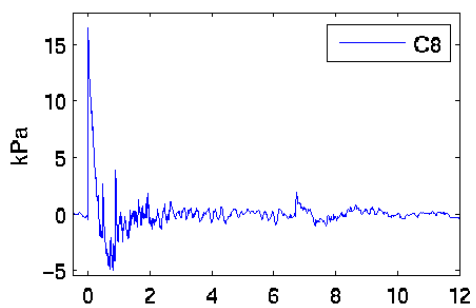
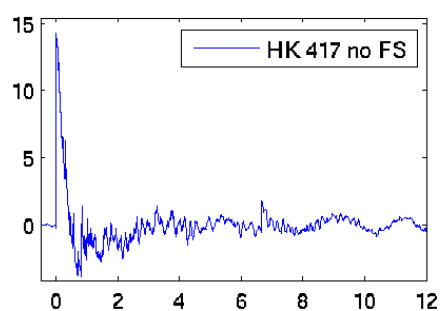
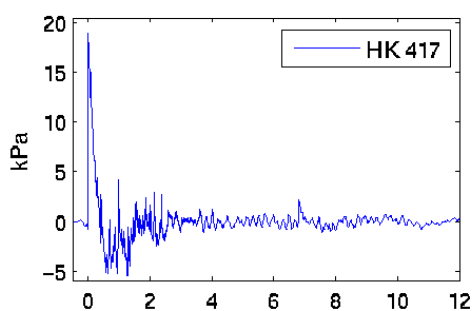
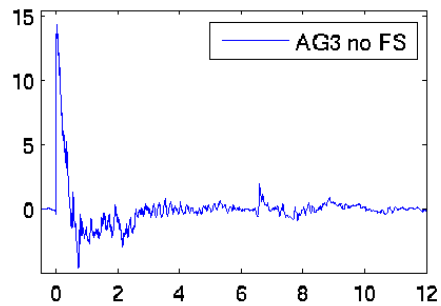
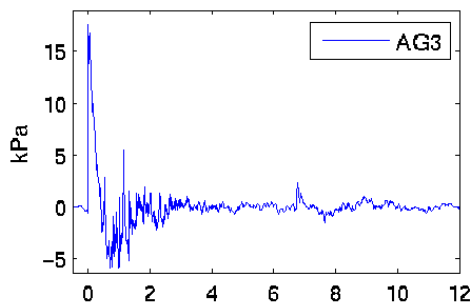
36 degrees



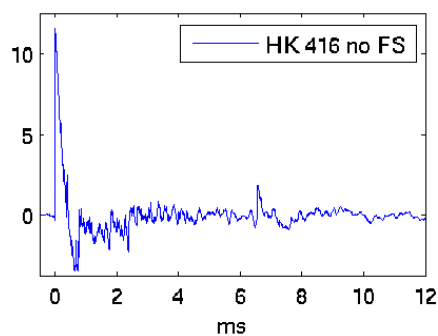
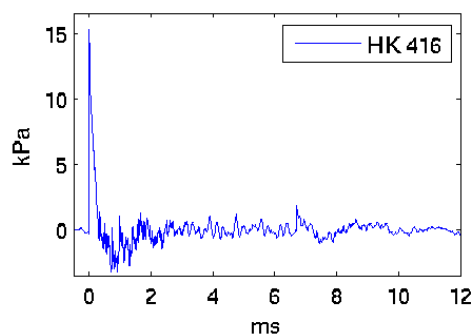
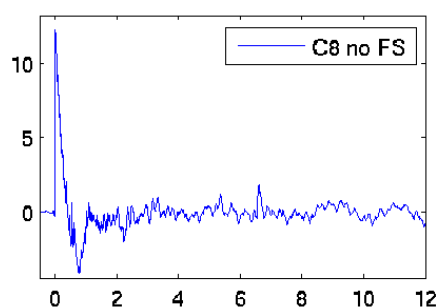
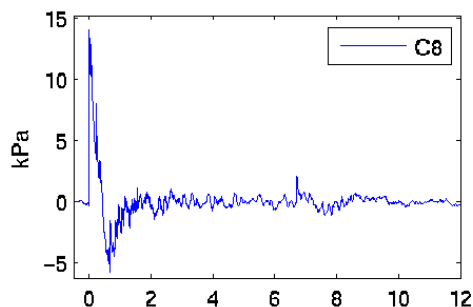
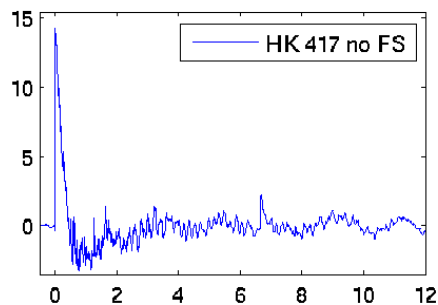
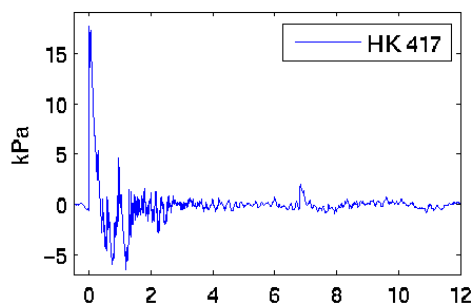
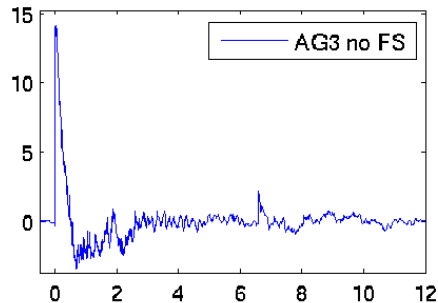
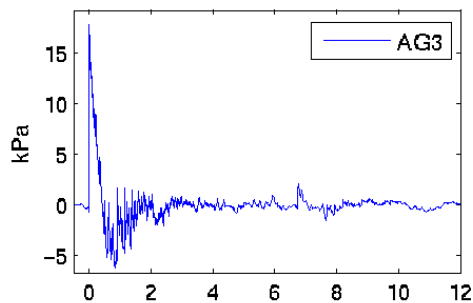
37 degrees



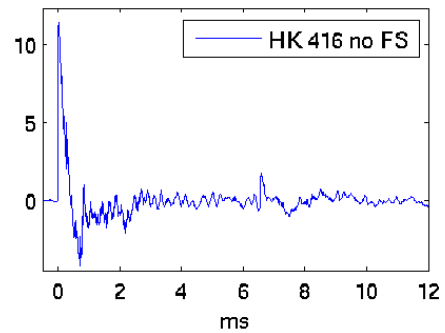
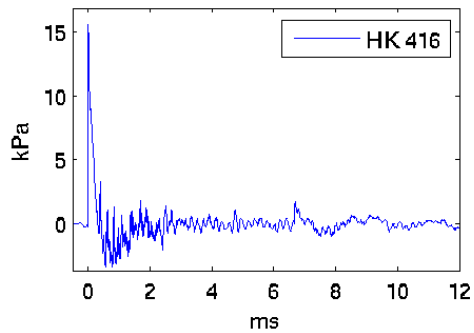
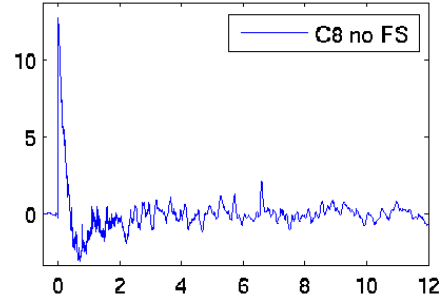
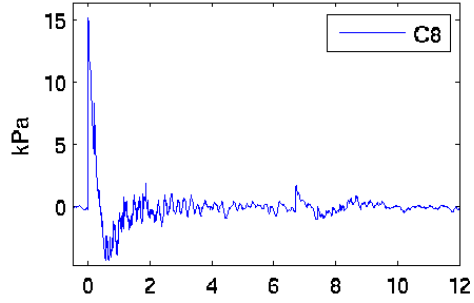
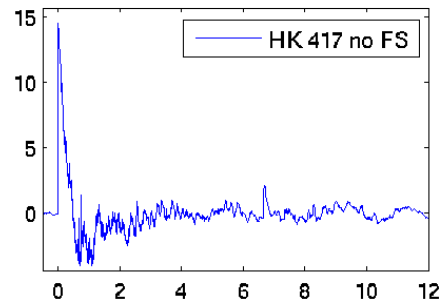
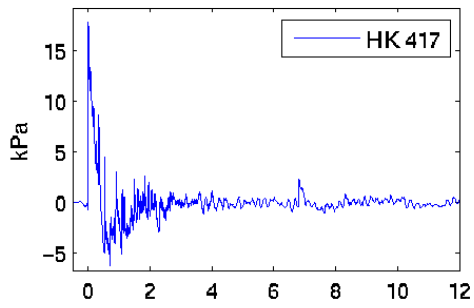
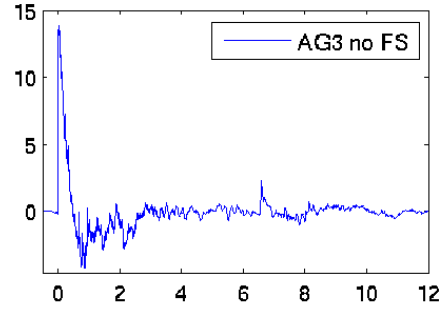
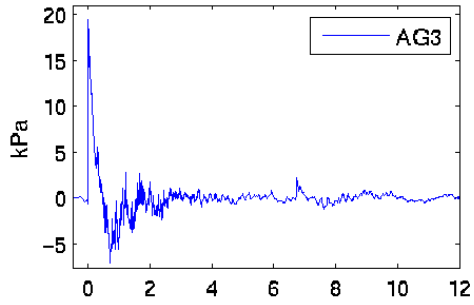
38 degrees



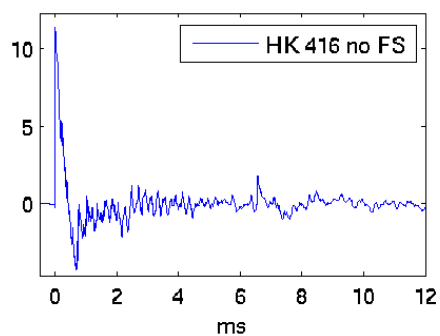
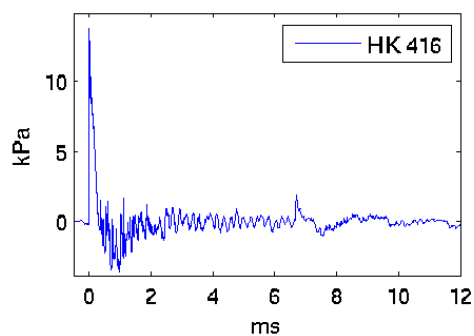
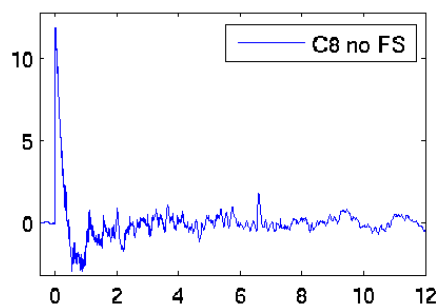
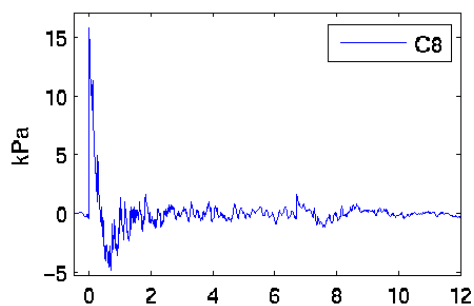
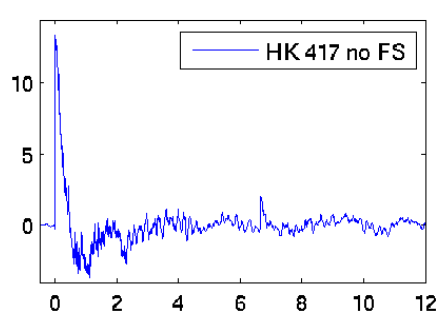
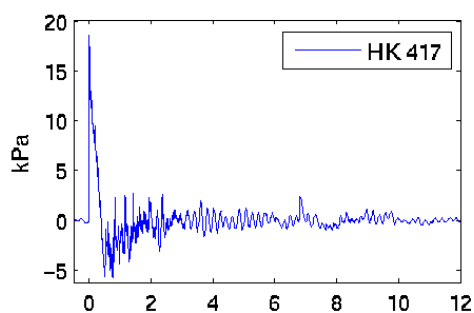
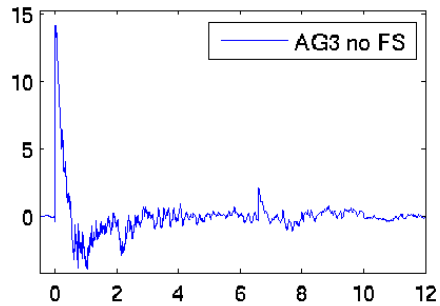
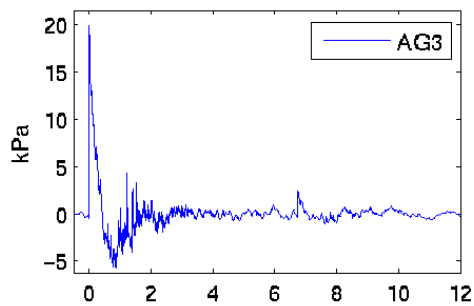
39 degrees



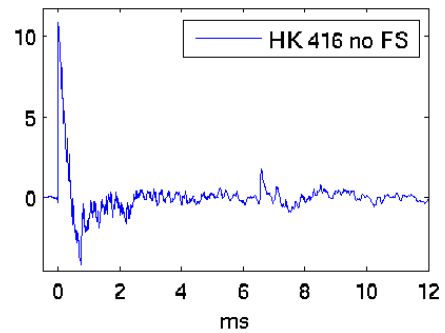
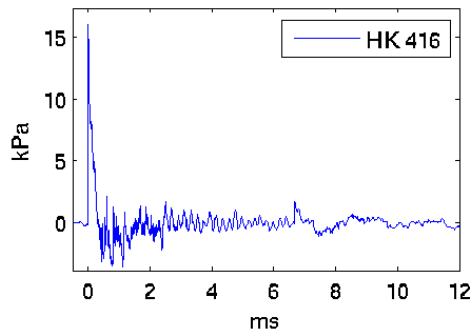
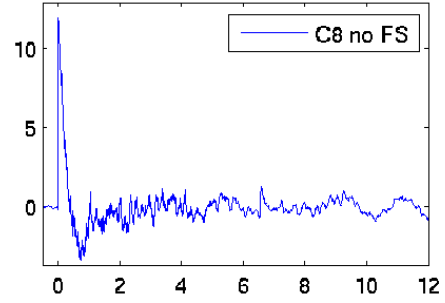
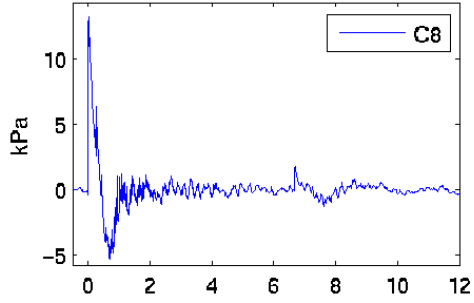
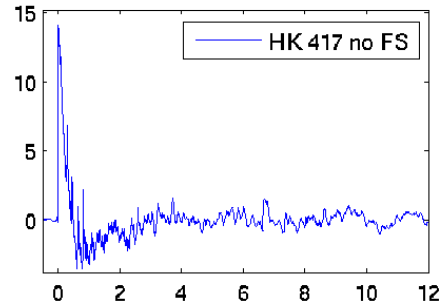
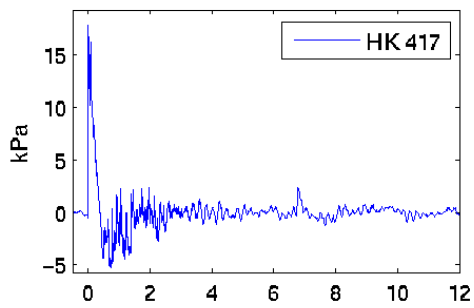
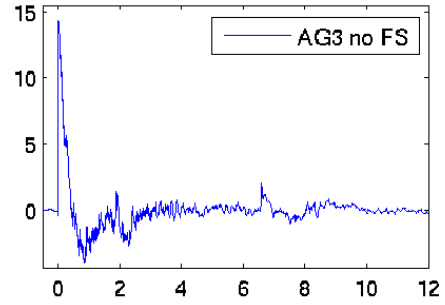
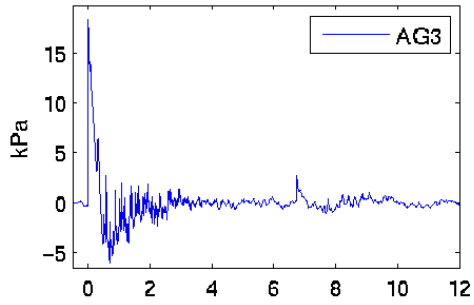
40 degrees



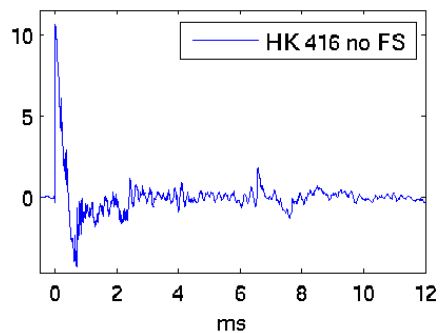
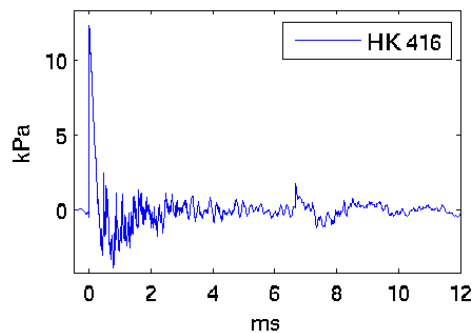
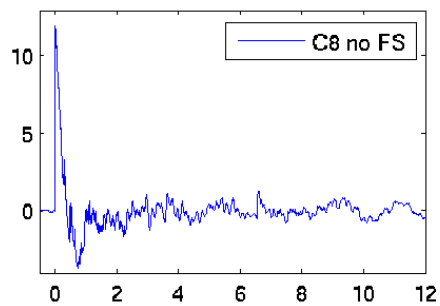
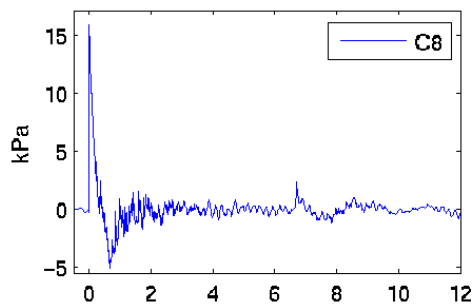
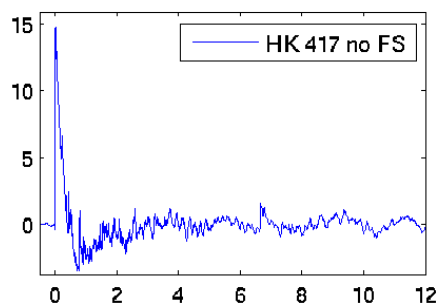
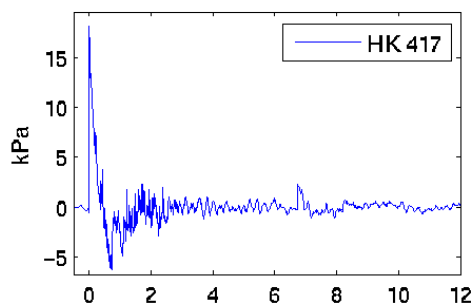
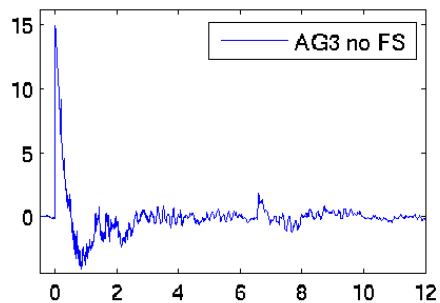
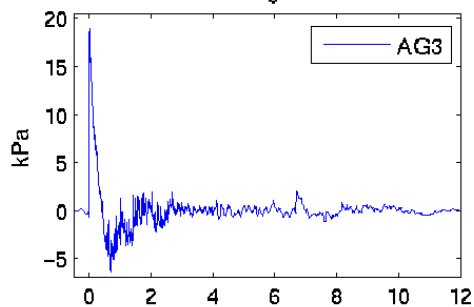
41 degrees



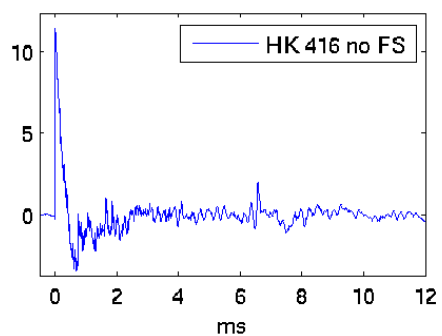
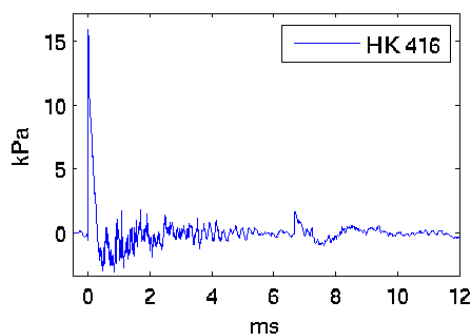
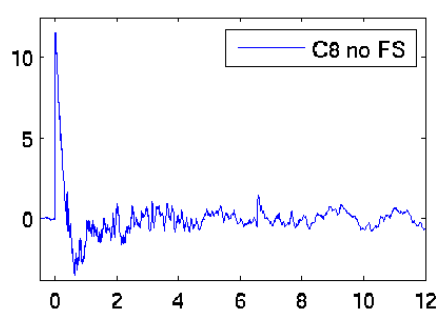
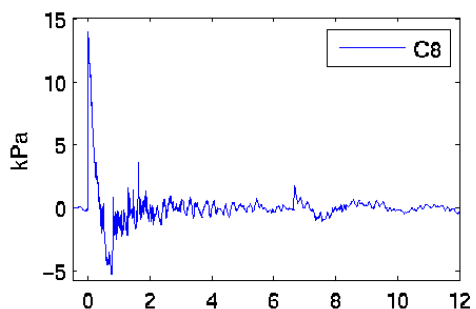
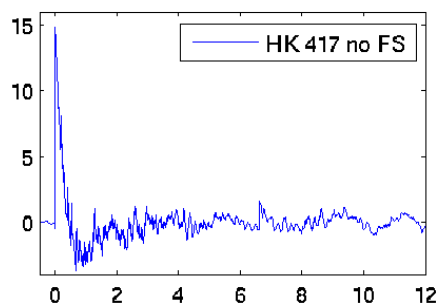
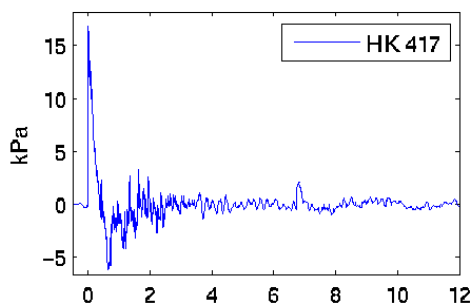
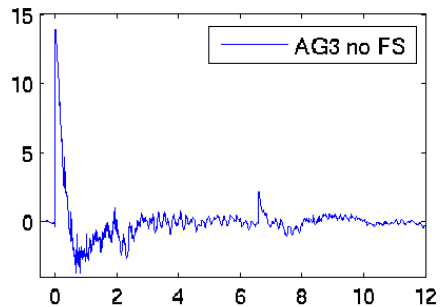
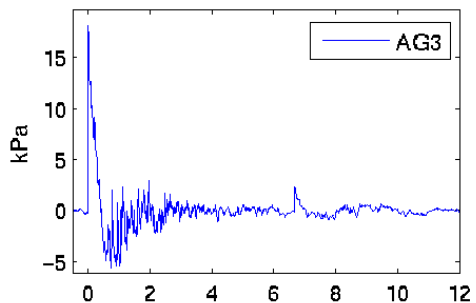
42 degrees



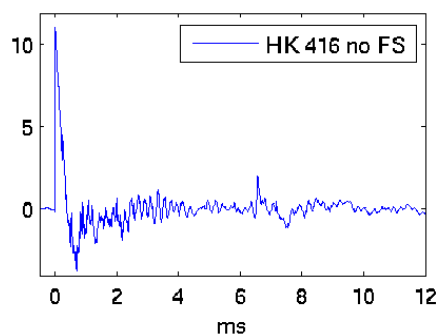
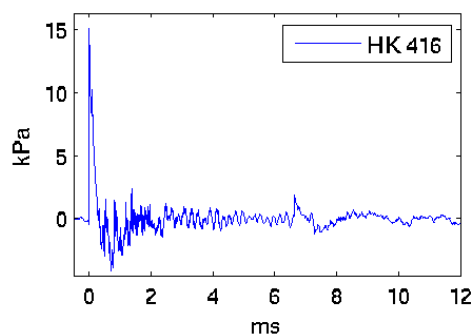
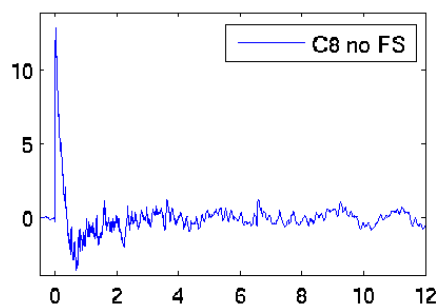
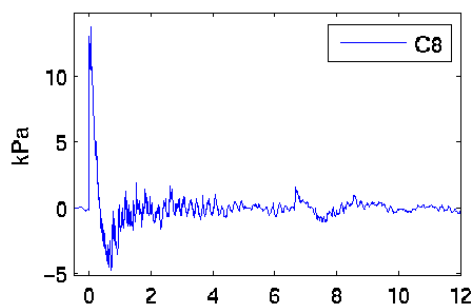
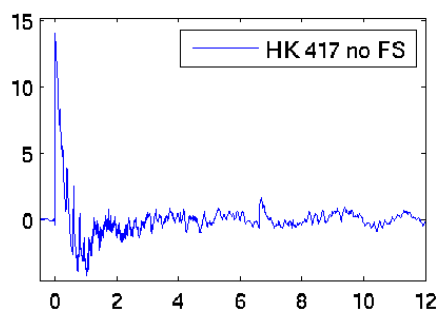
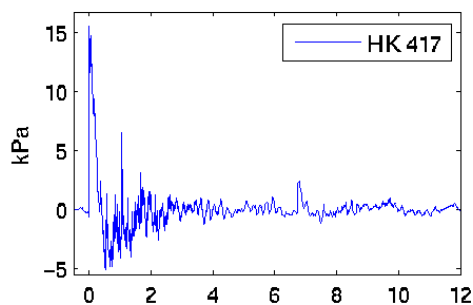
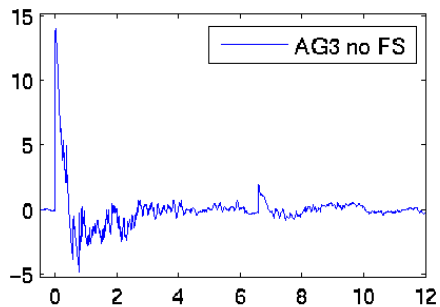
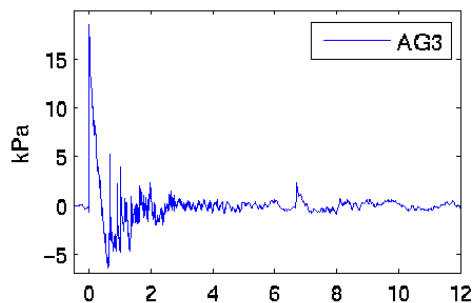
43 degrees



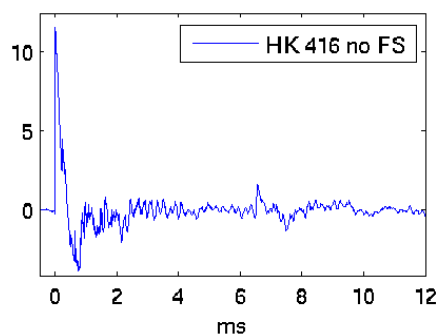
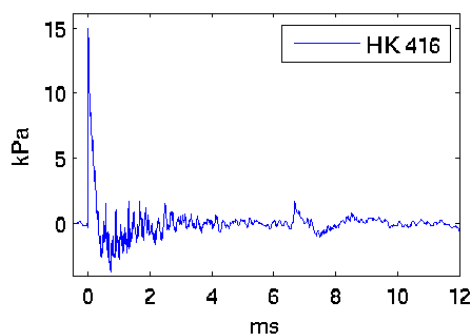
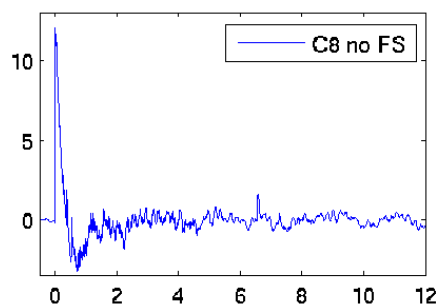
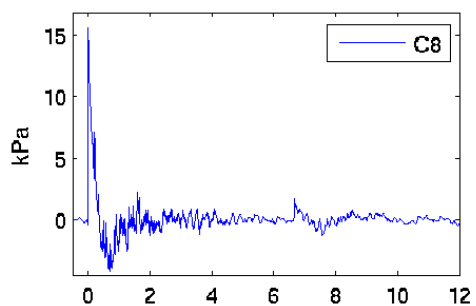
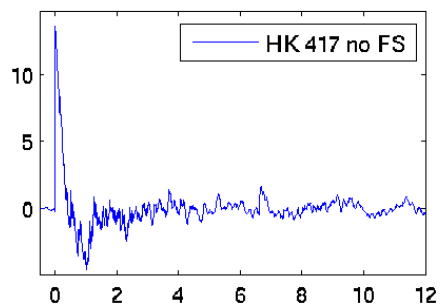
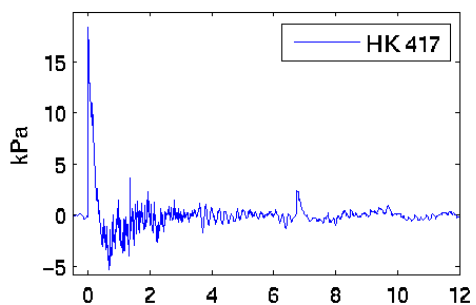
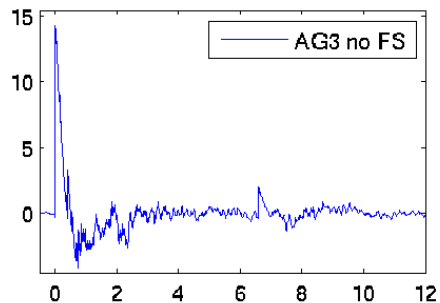
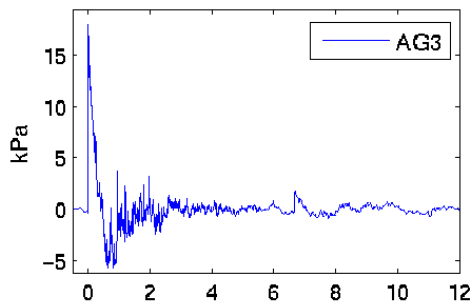
44 degrees



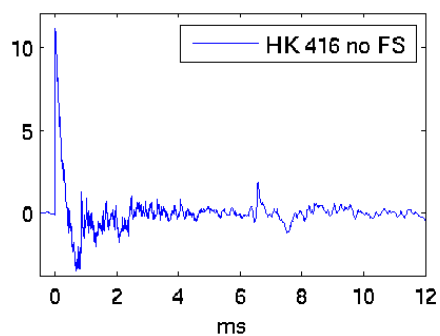
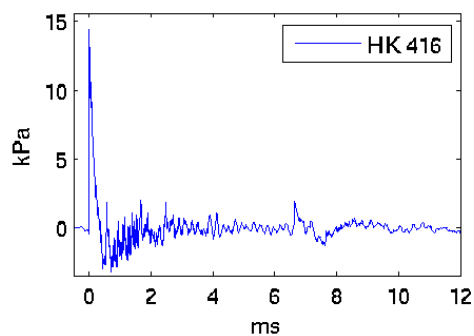
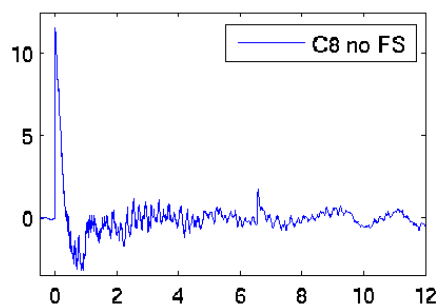
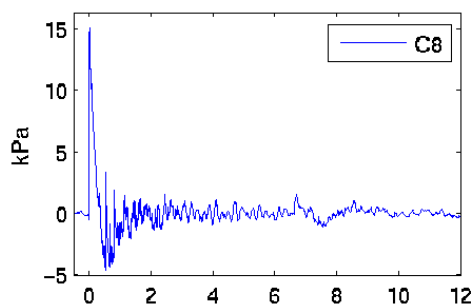
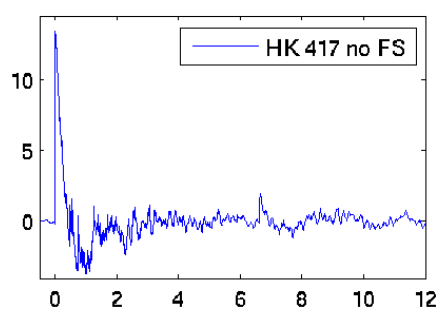
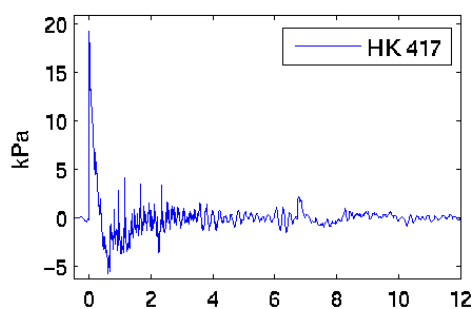
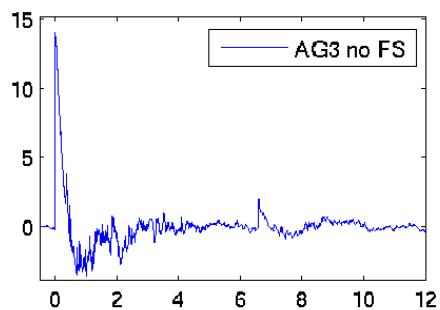
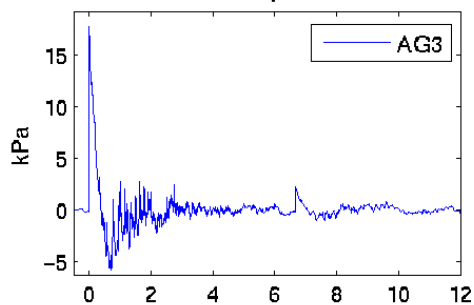
45 degrees



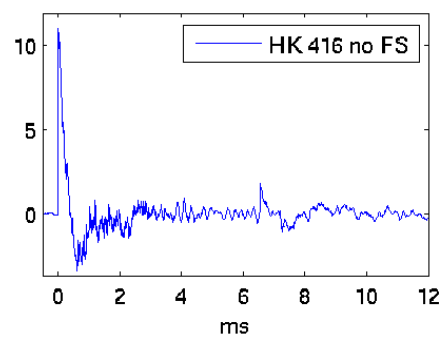
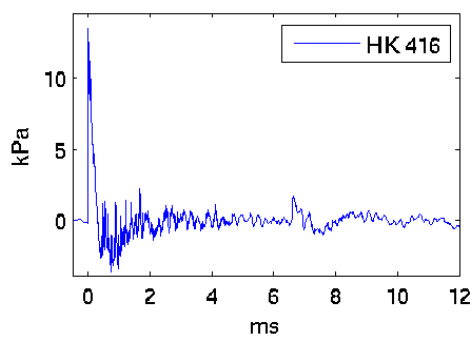
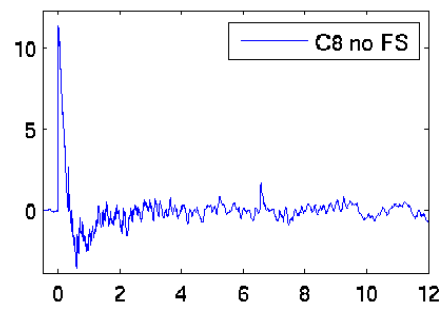
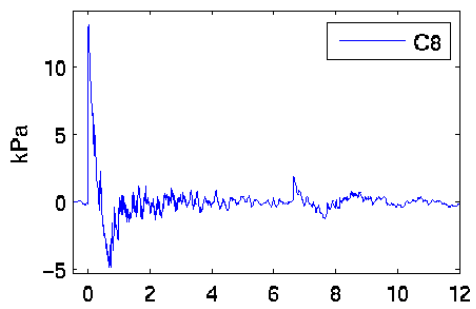
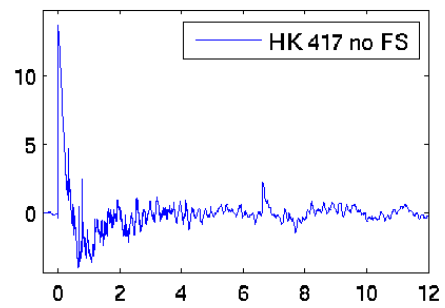
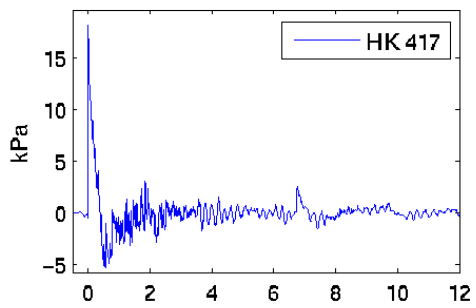
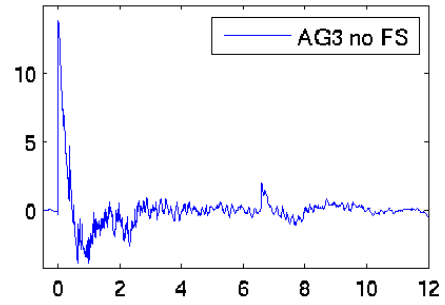
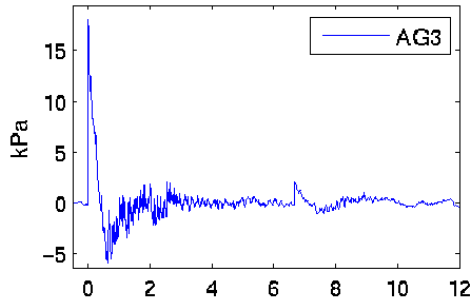
46 degrees



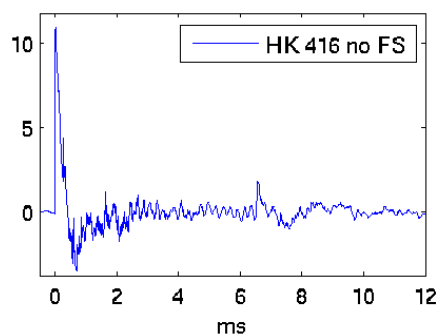
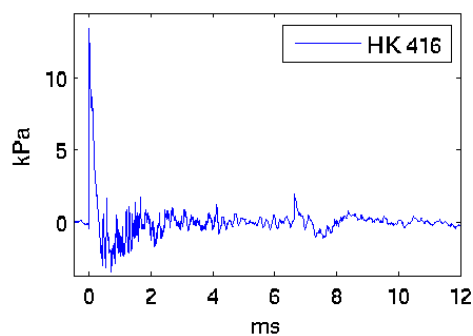
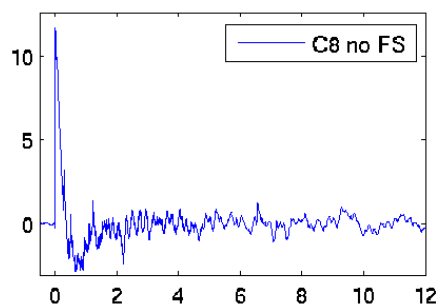
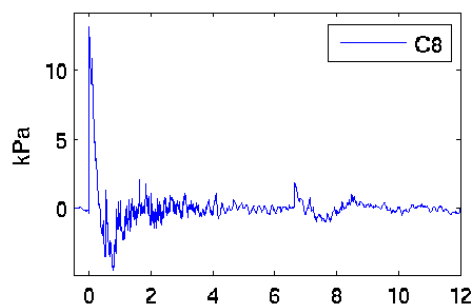
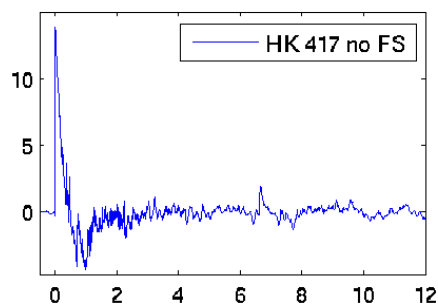
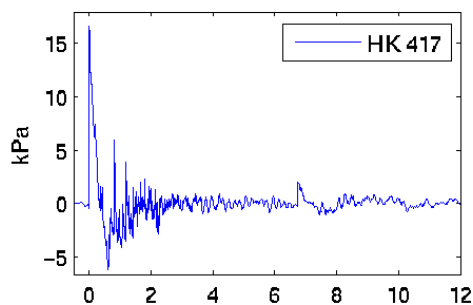
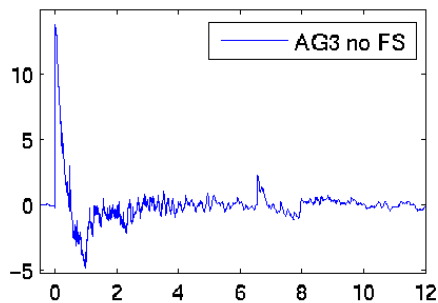
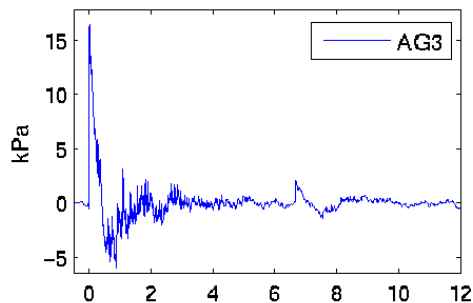
47 degrees

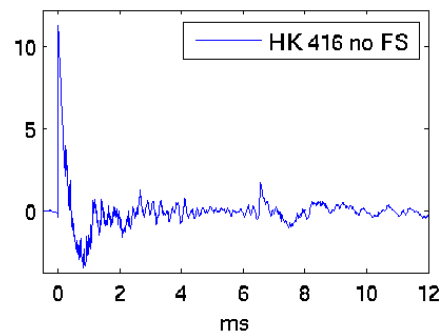
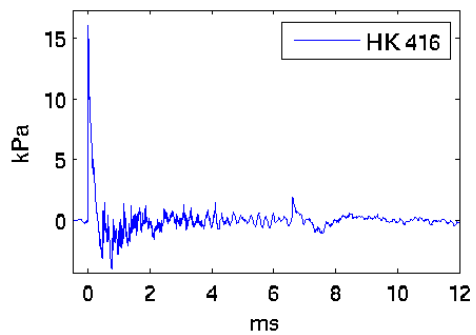
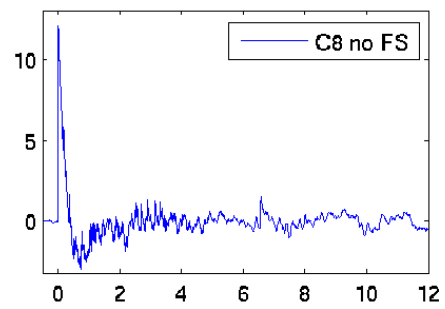
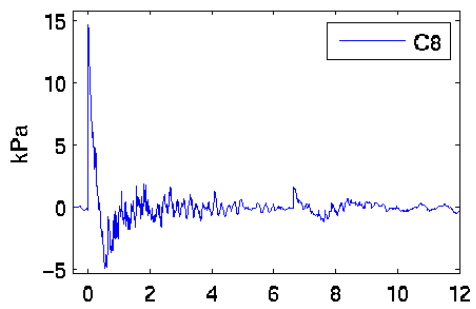
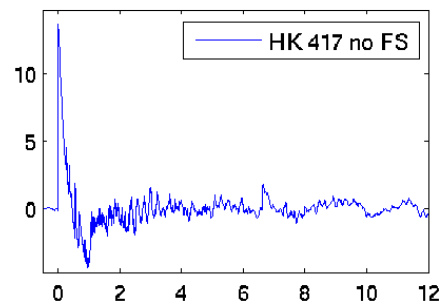
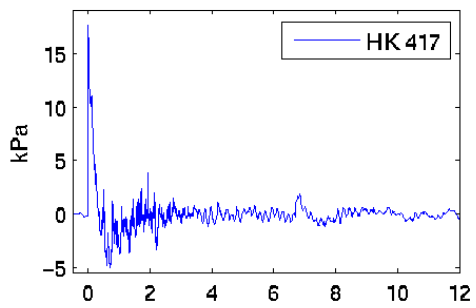
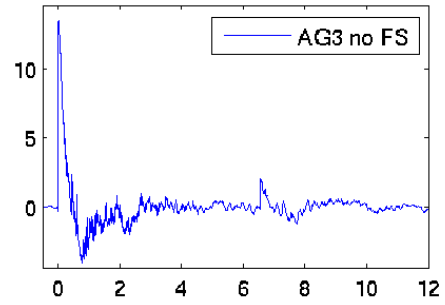
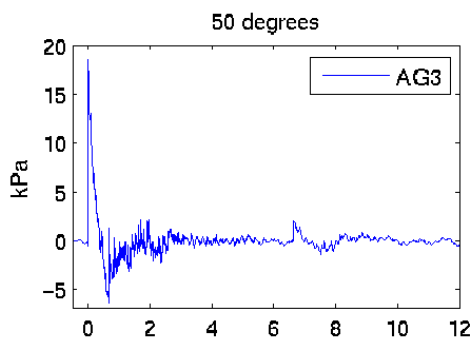


48 degrees

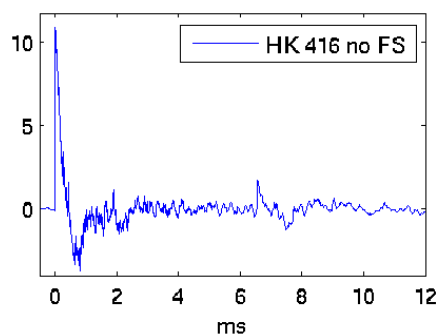
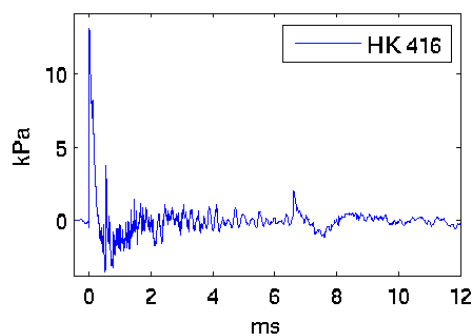
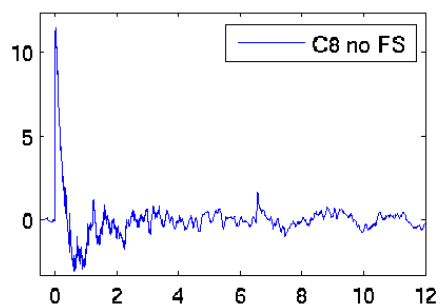
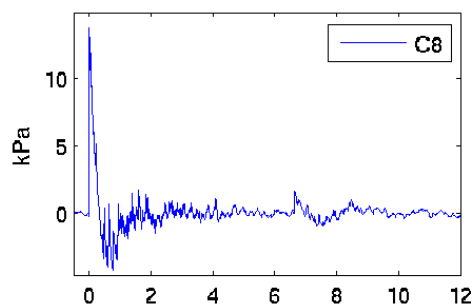
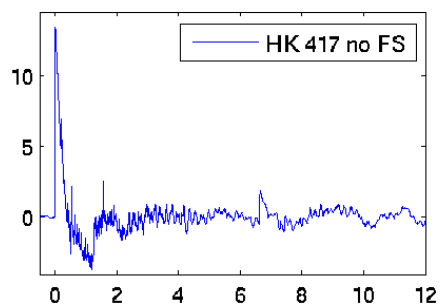
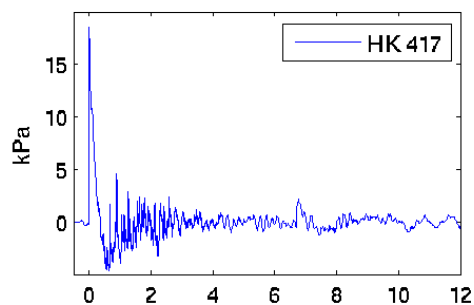
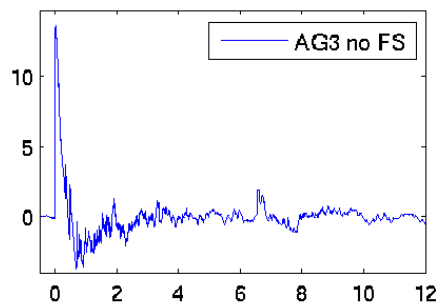
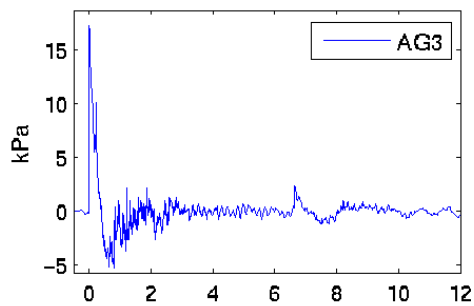


49 degrees

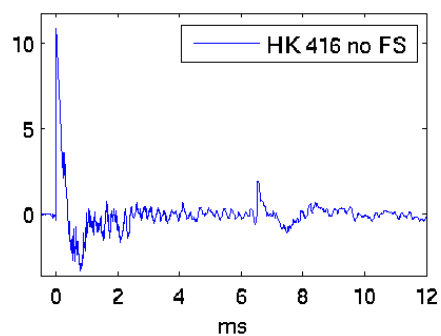
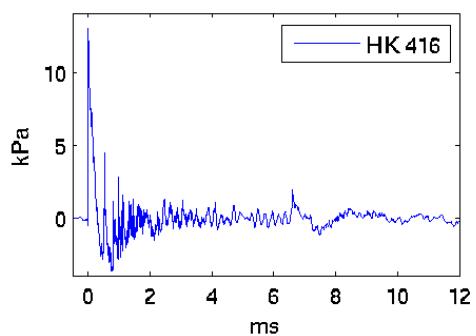
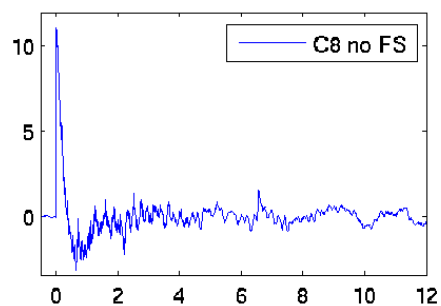
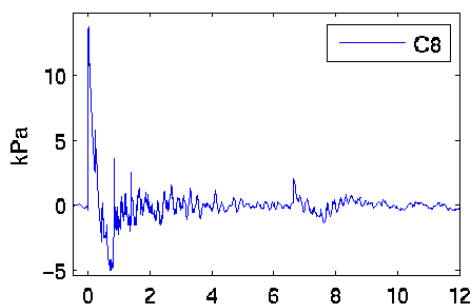
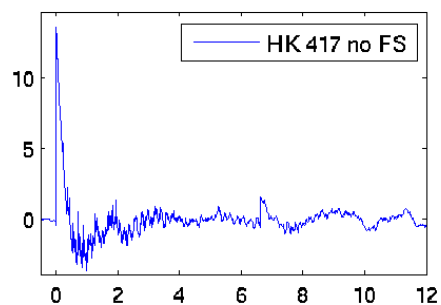
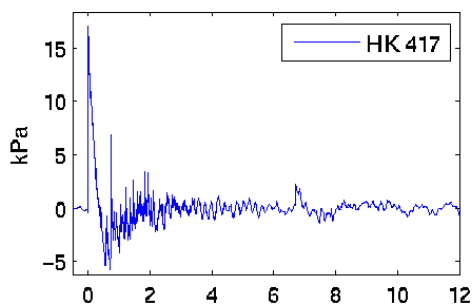
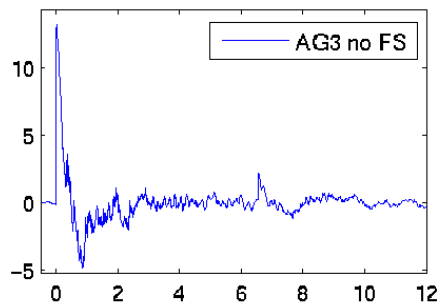
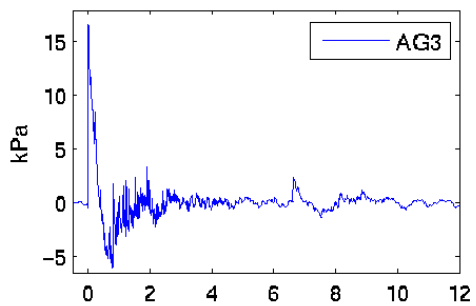




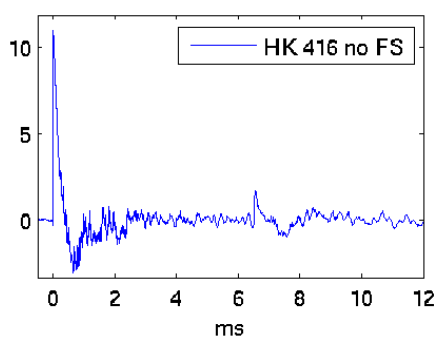
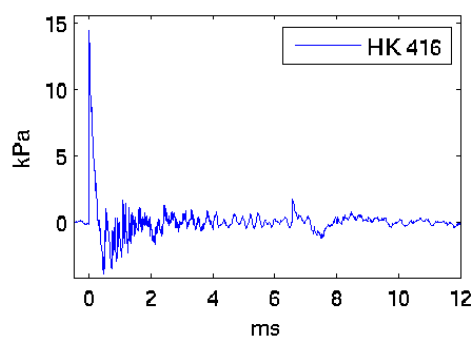
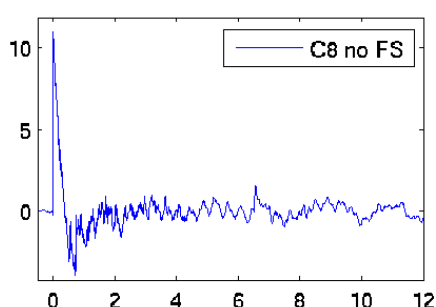
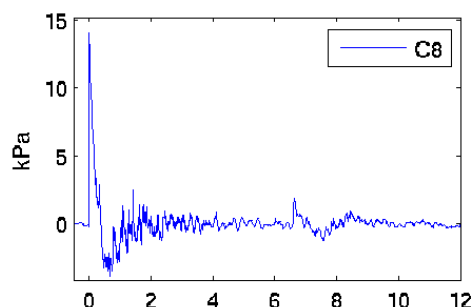
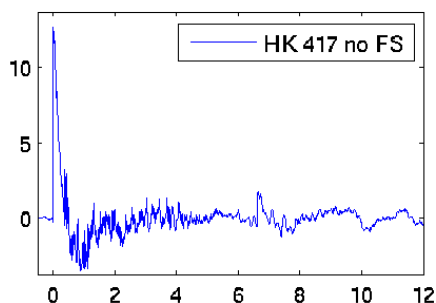
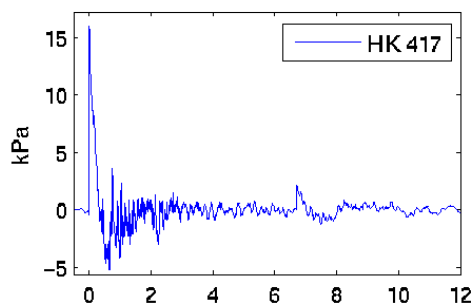
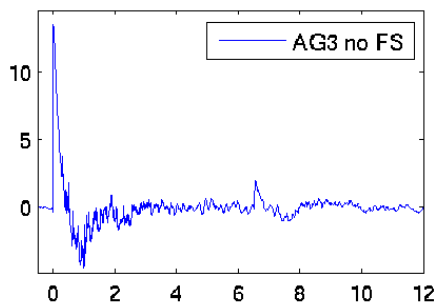
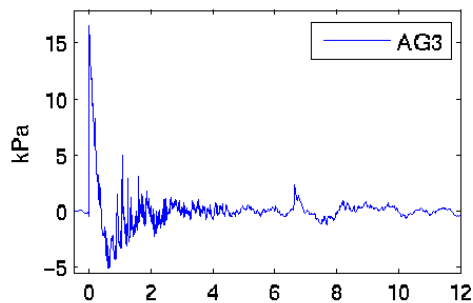
51 degrees



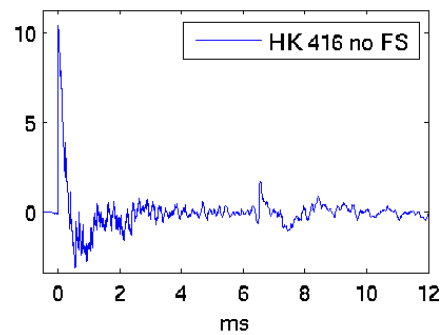
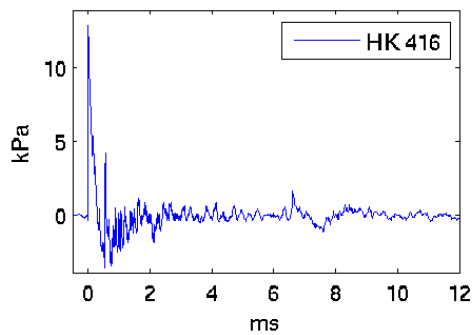
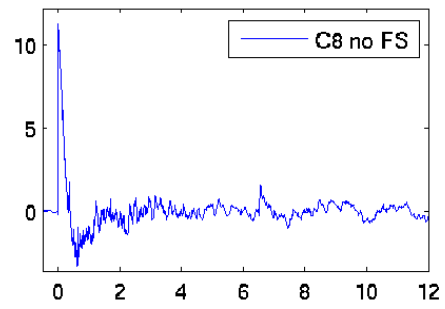
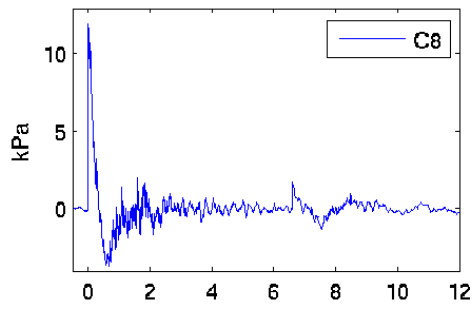
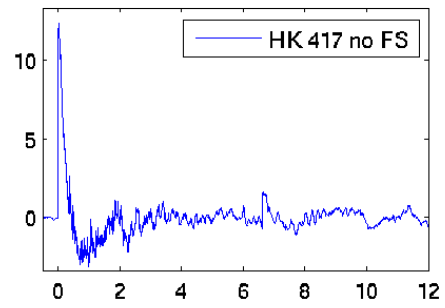
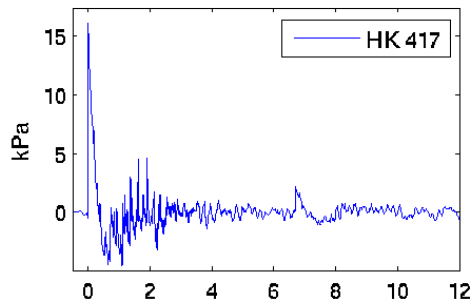
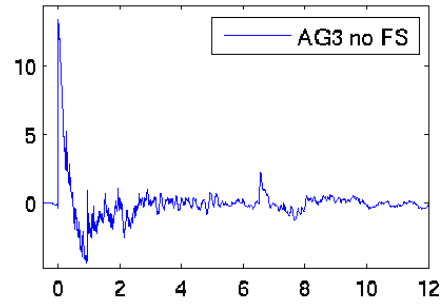
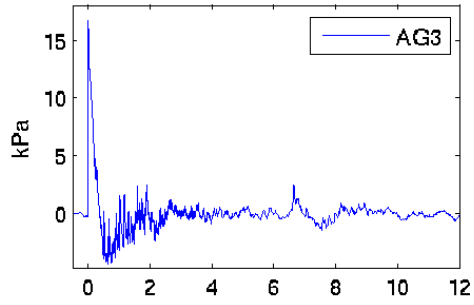
52 degrees



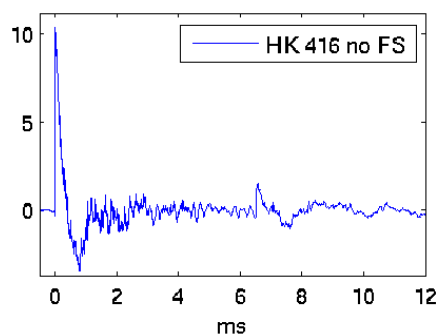
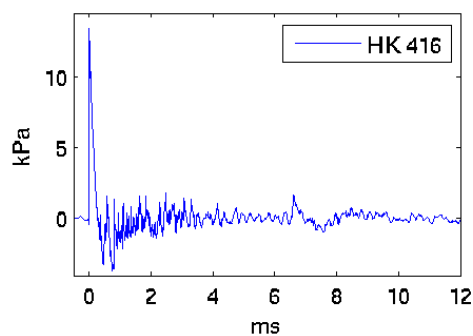
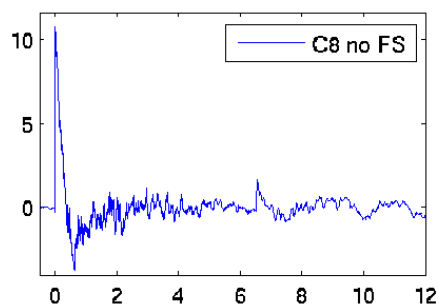
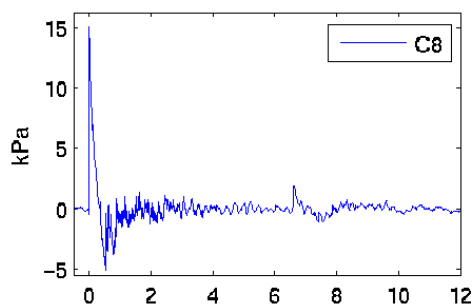
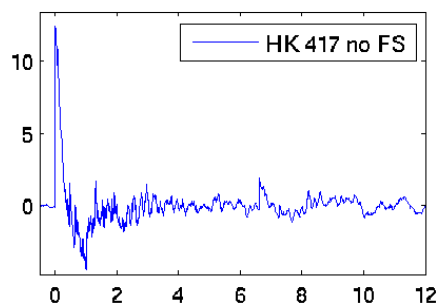
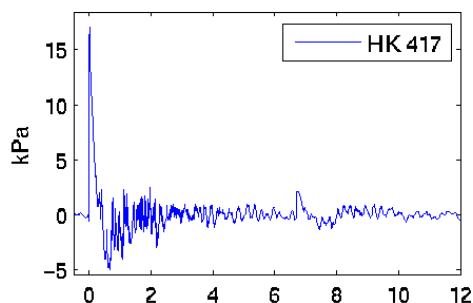
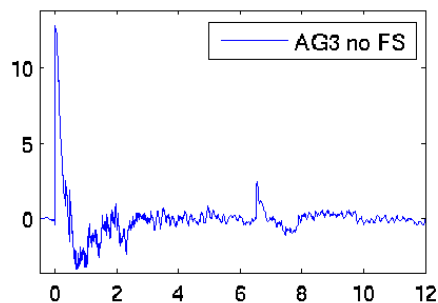
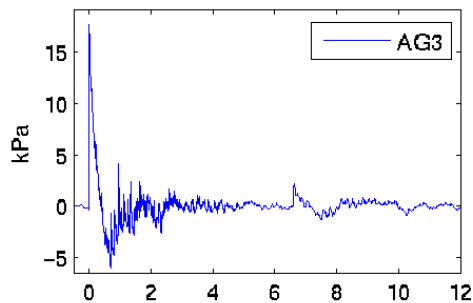
53 degrees



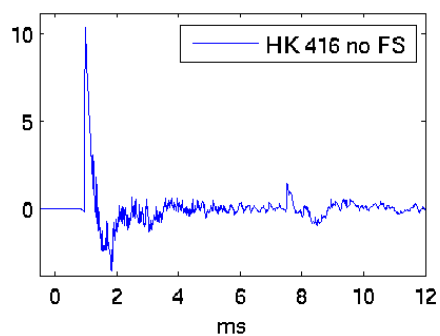
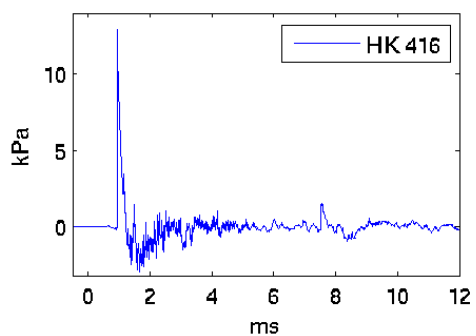
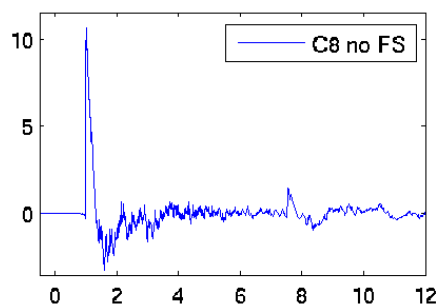
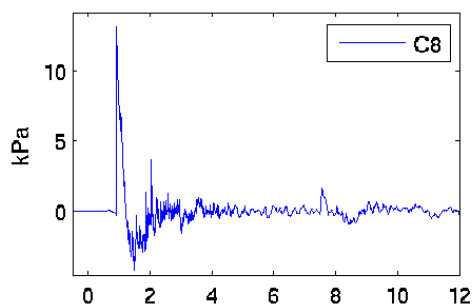
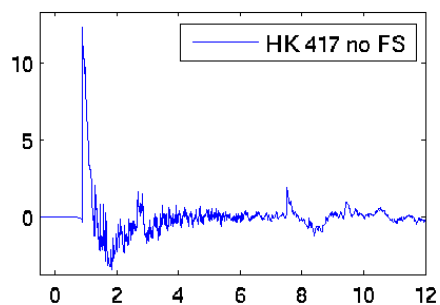
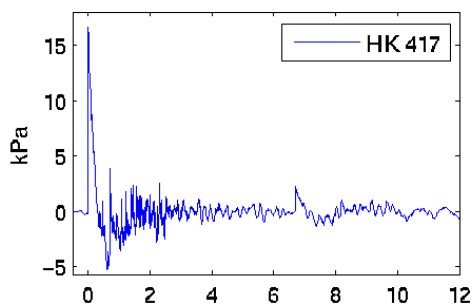
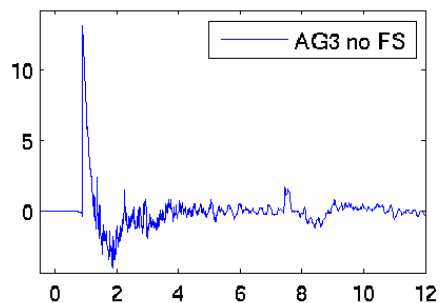
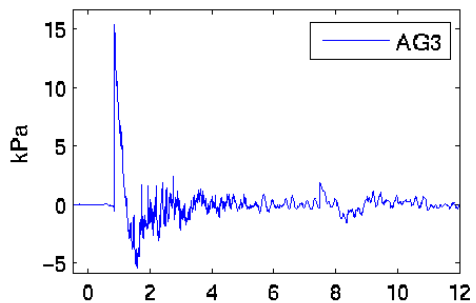
54 degrees



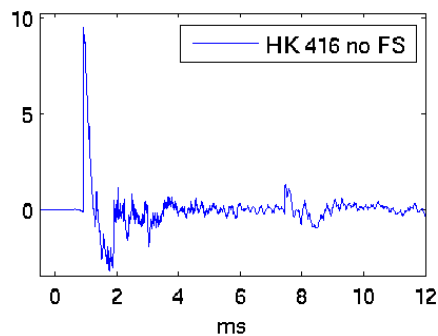
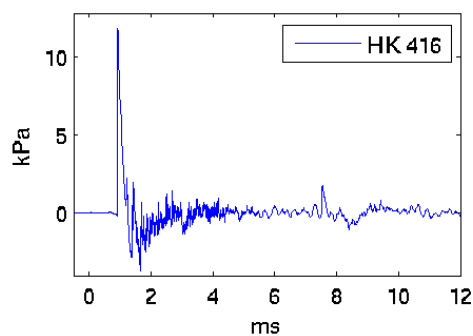
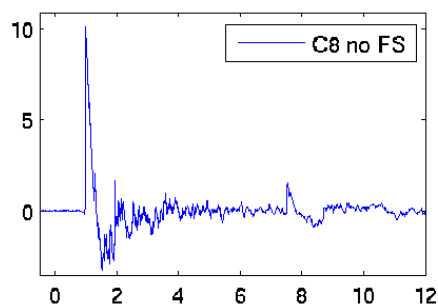
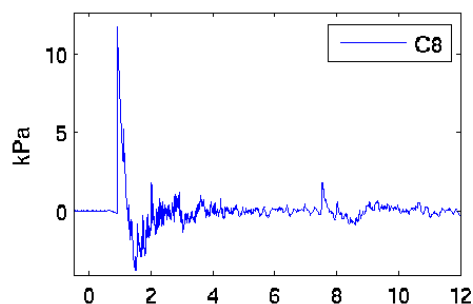
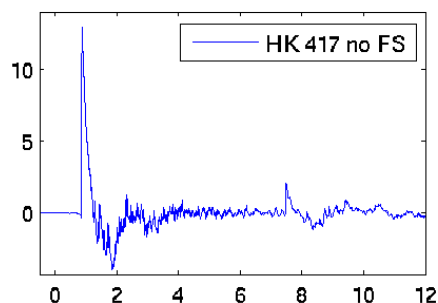
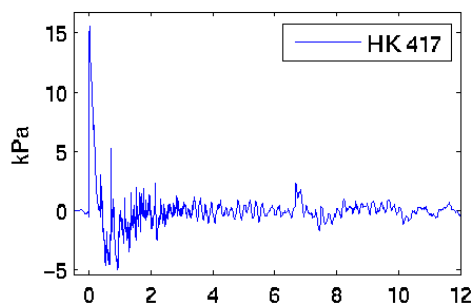
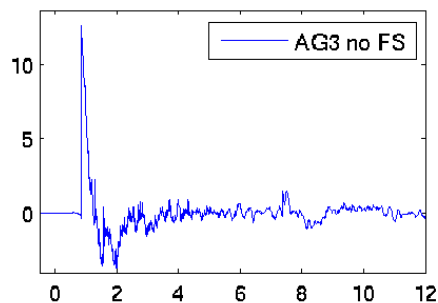
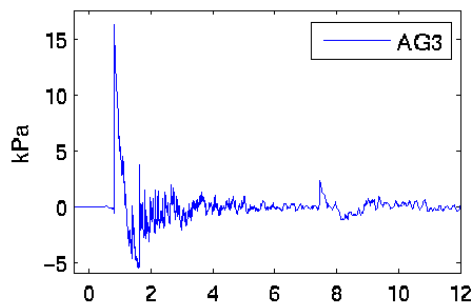
55 degrees



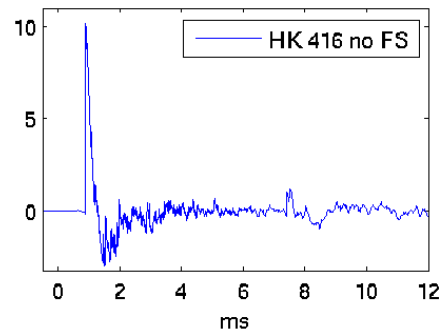
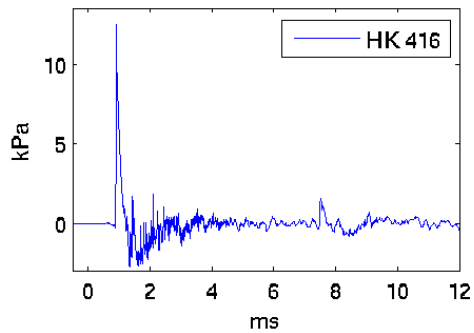
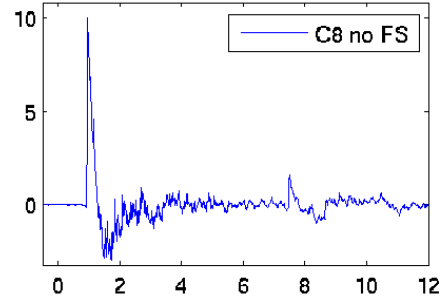
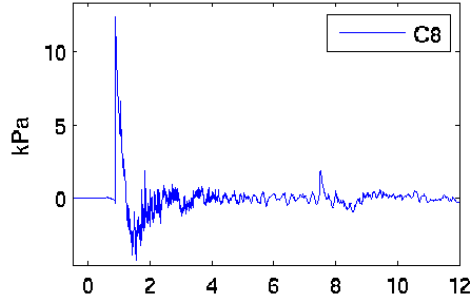
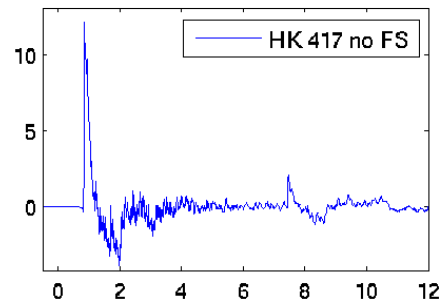
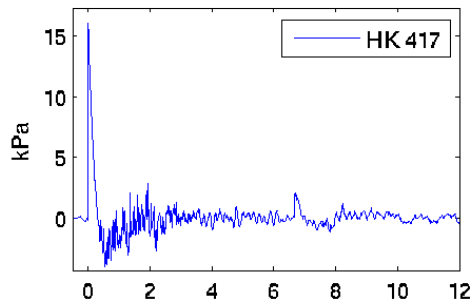
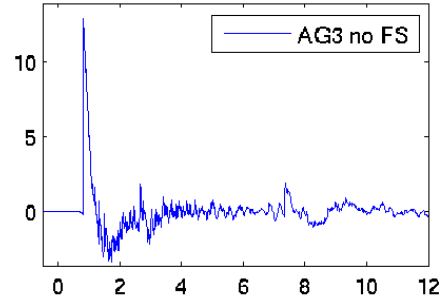
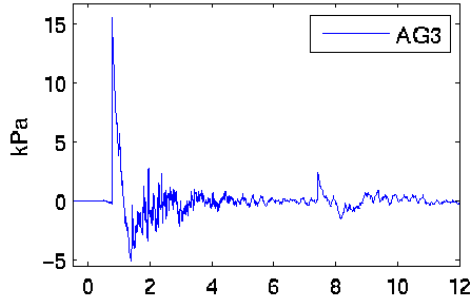
56 degrees



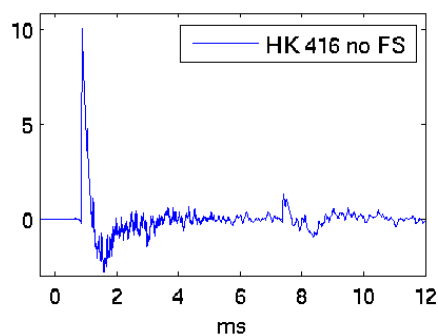
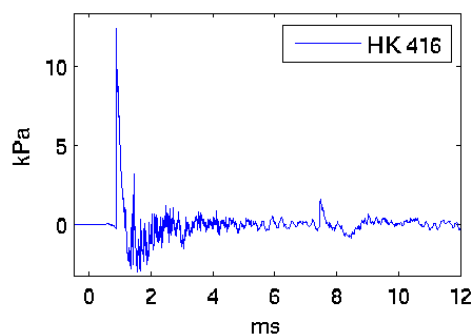
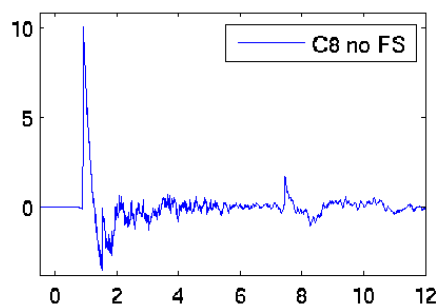
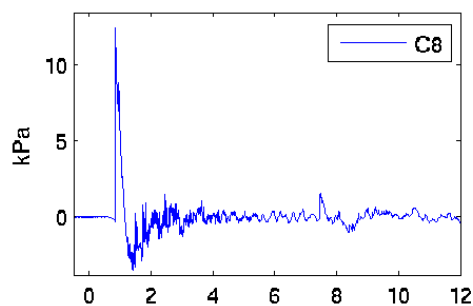
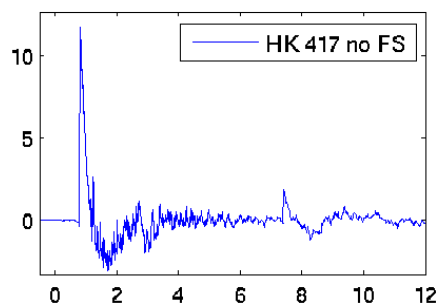
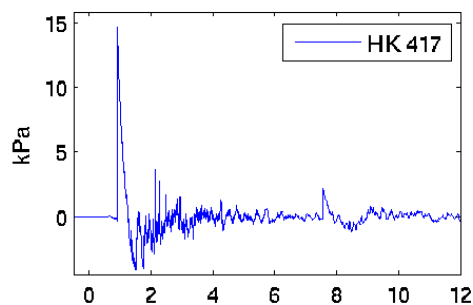
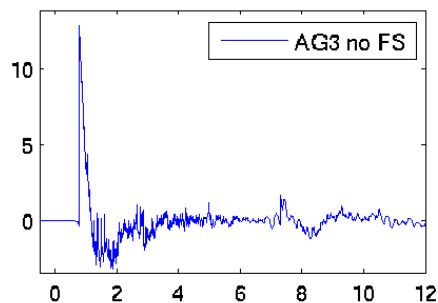
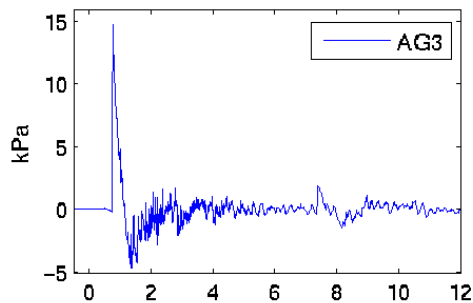
57 degrees



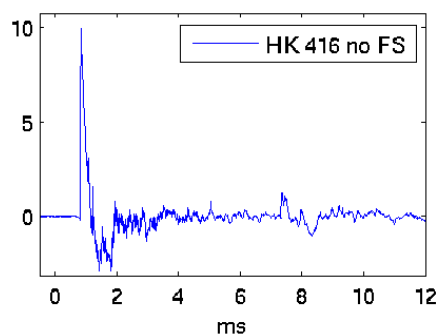
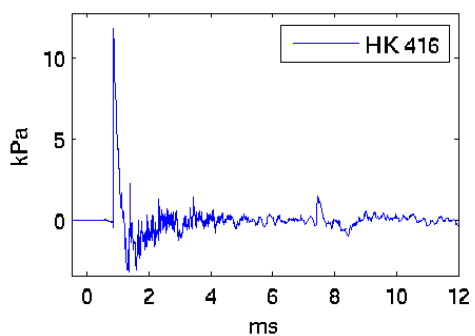
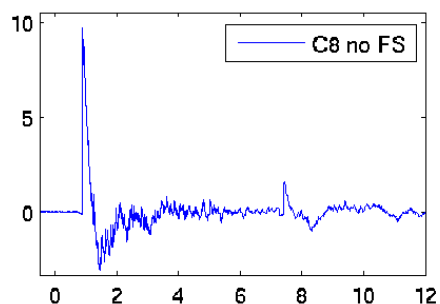
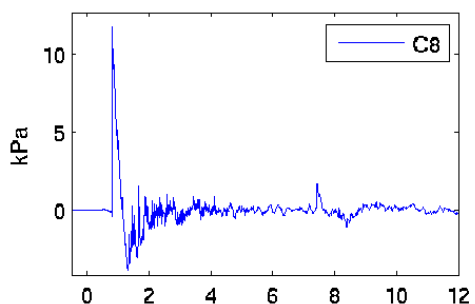
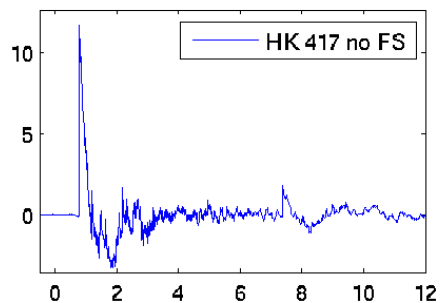
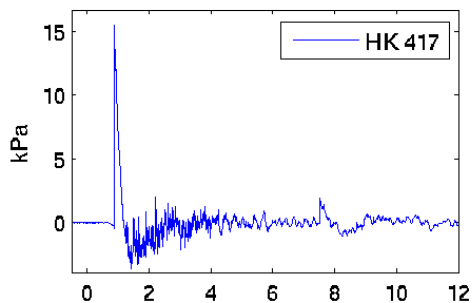
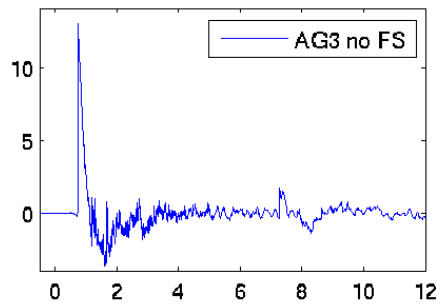
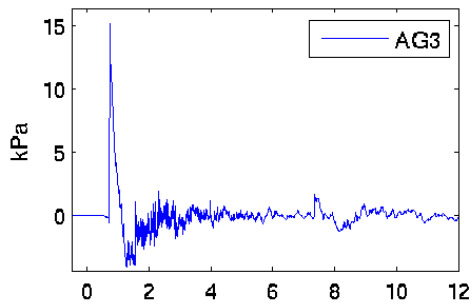
58 degrees



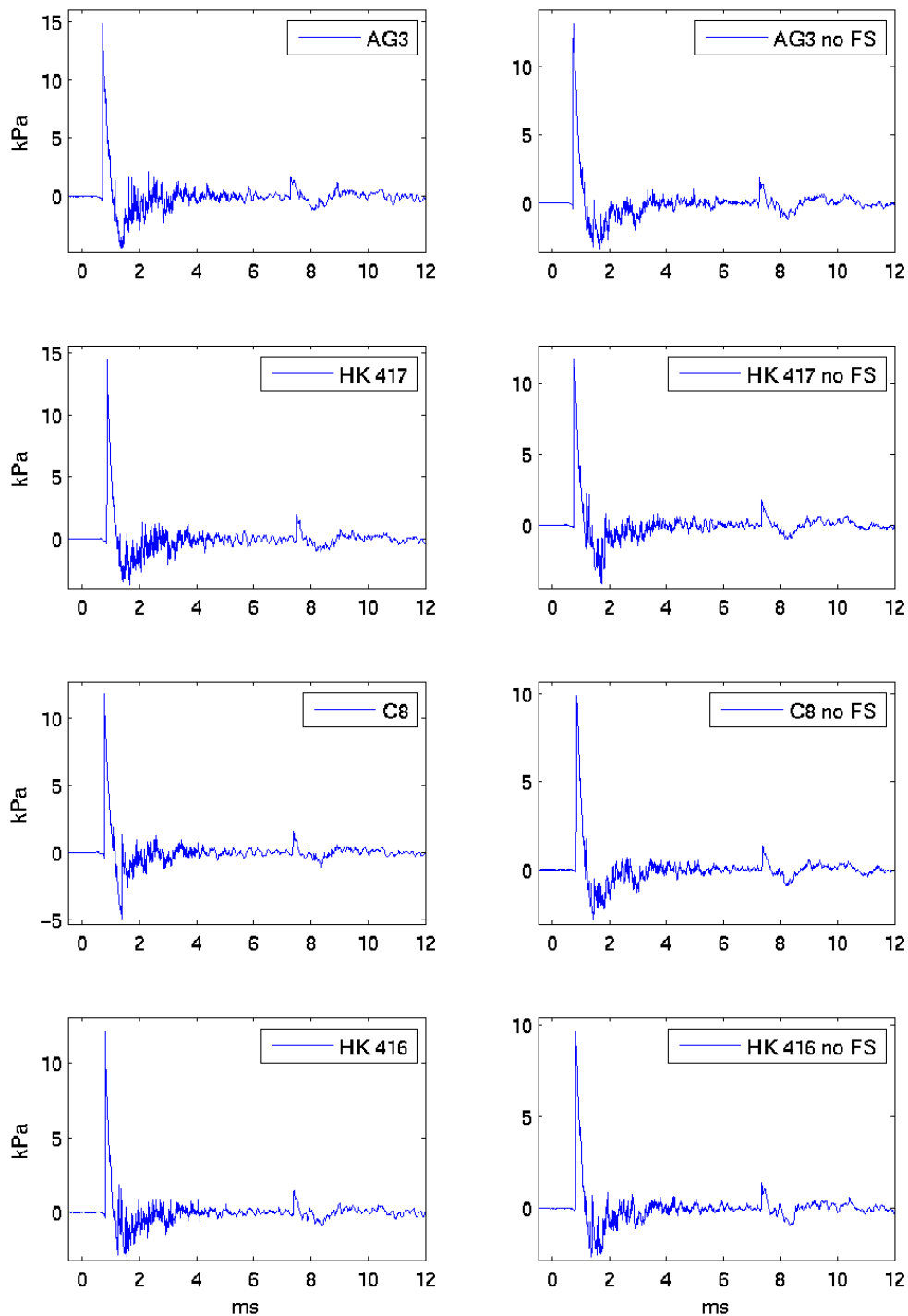
59 degrees



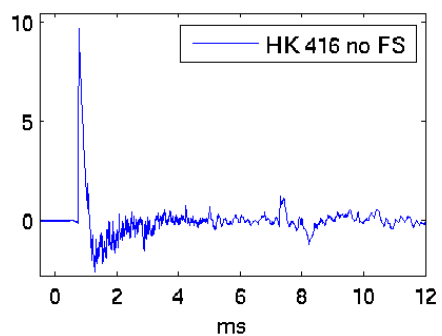
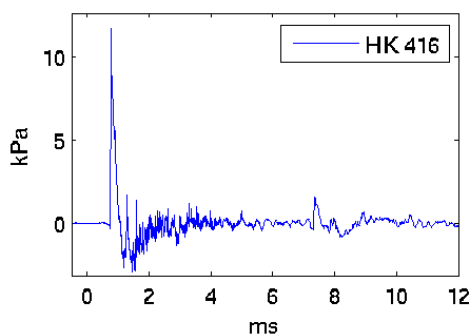
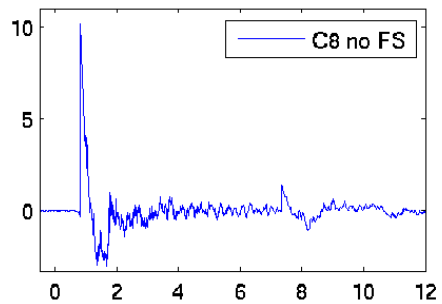
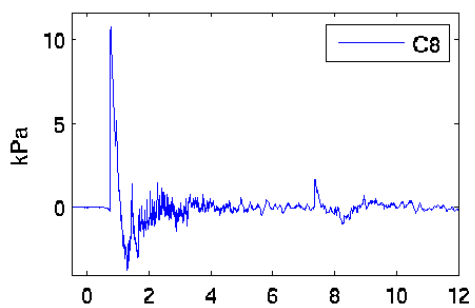
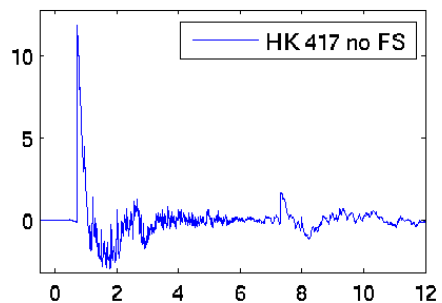
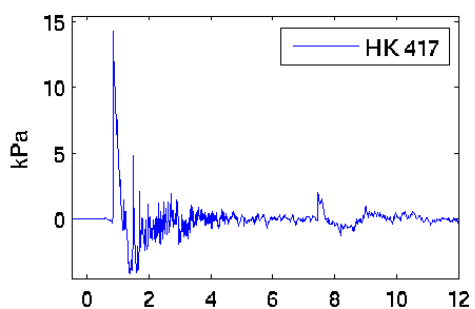
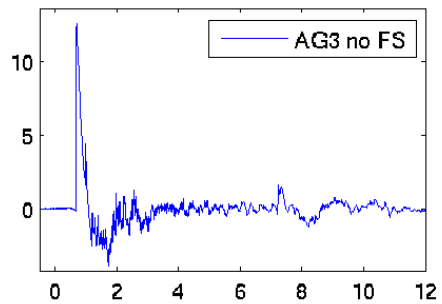
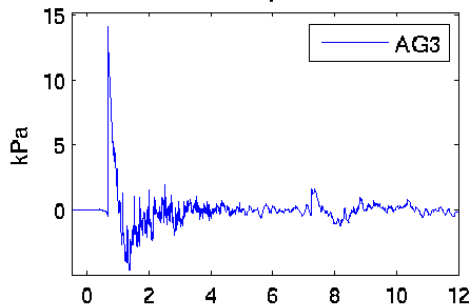
60 degrees



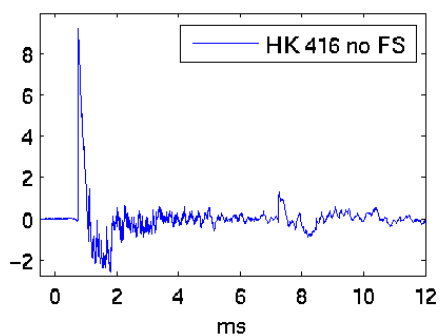
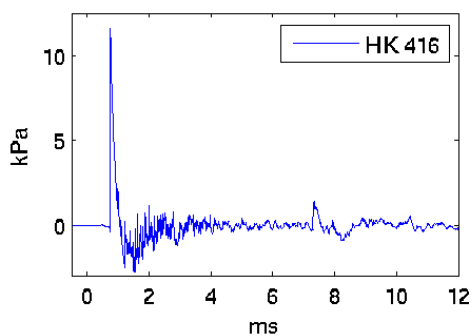
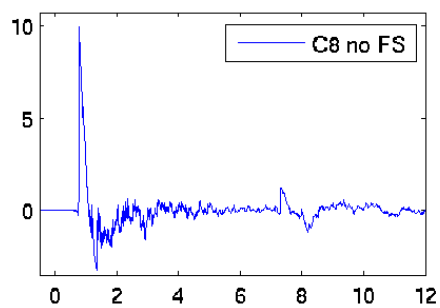
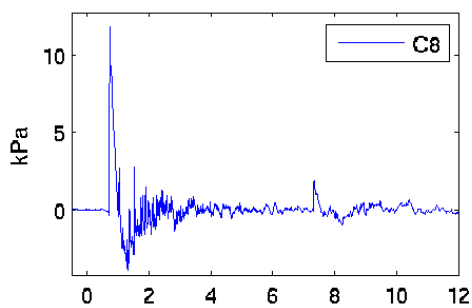
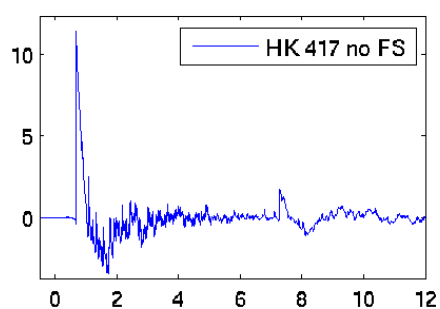
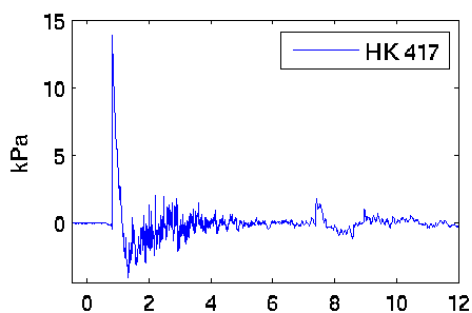
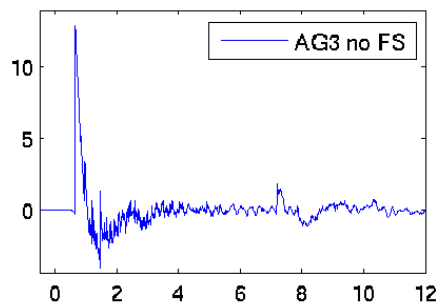
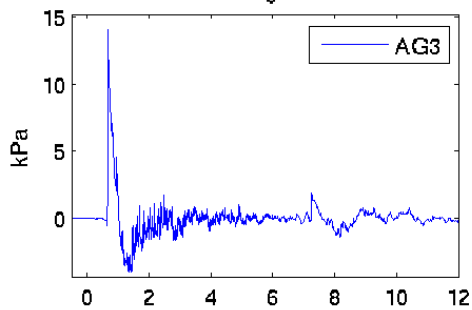
61 degrees



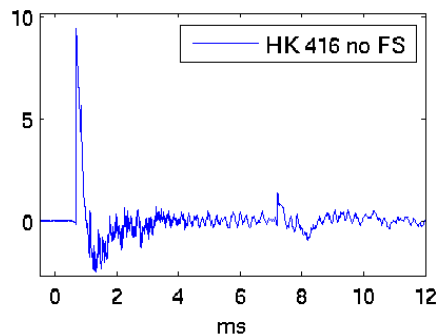
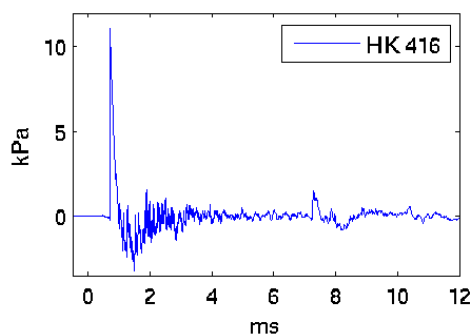
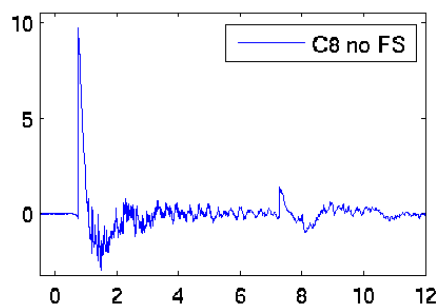
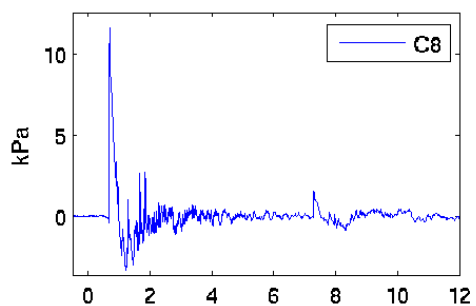
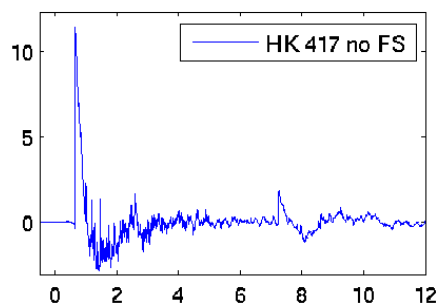
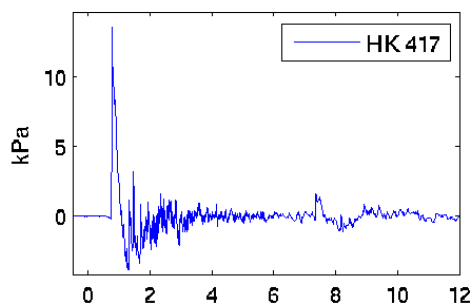
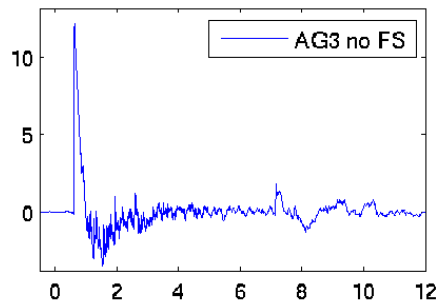
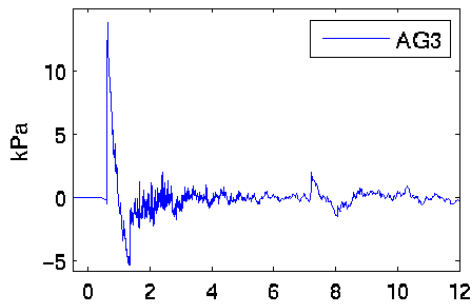
62 degrees



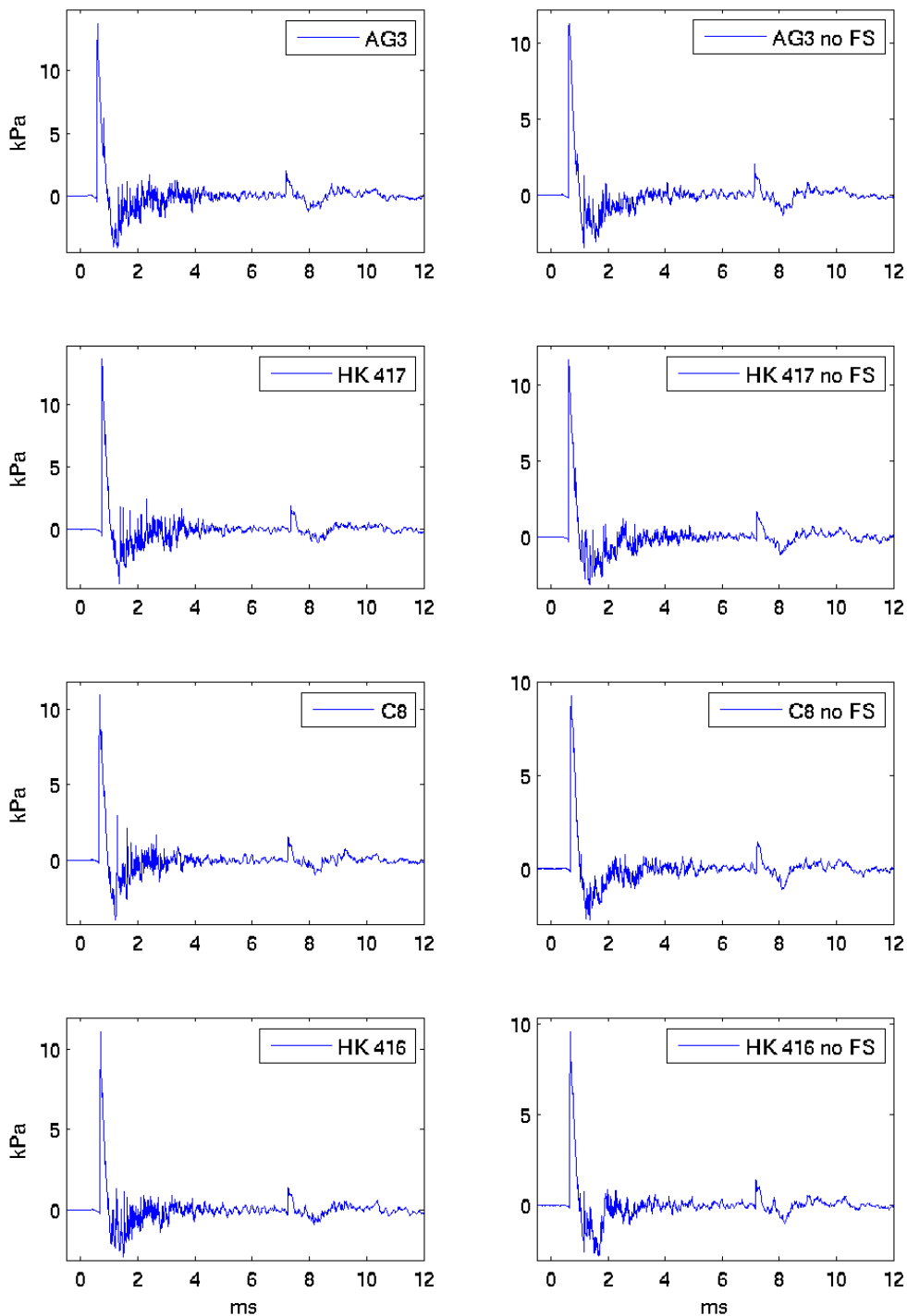
63 degrees



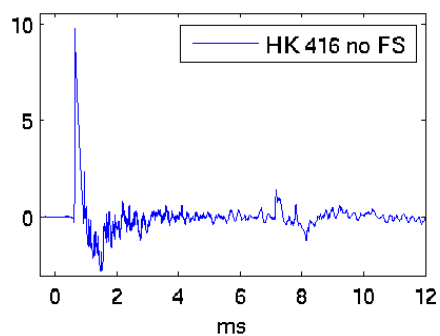
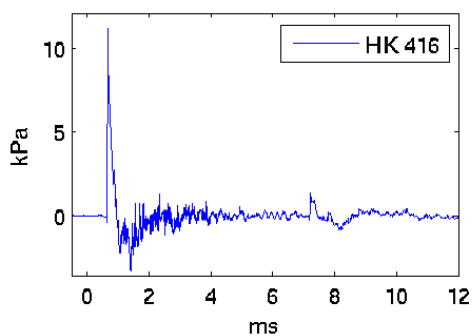
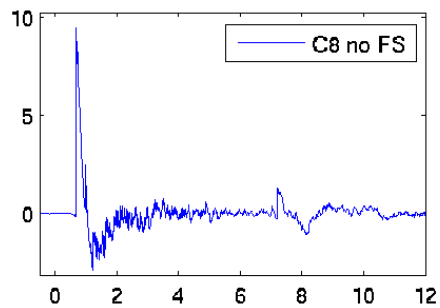
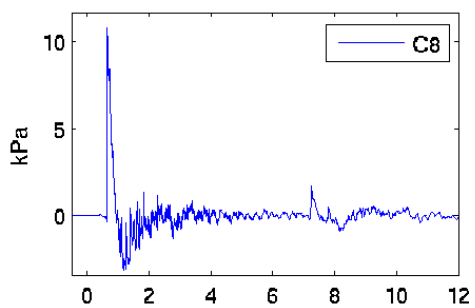
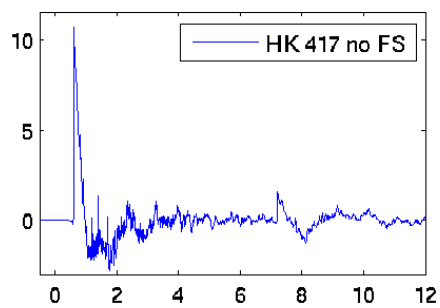
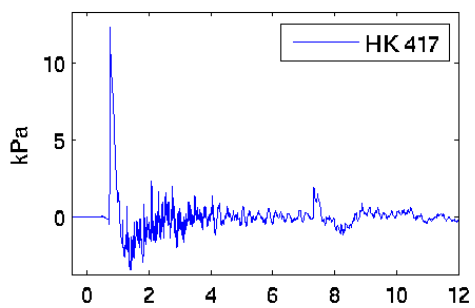
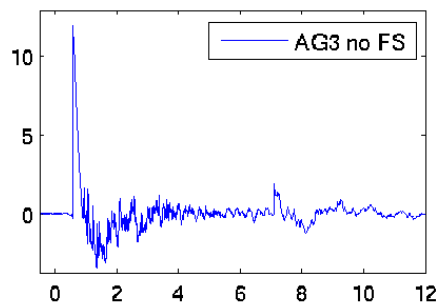
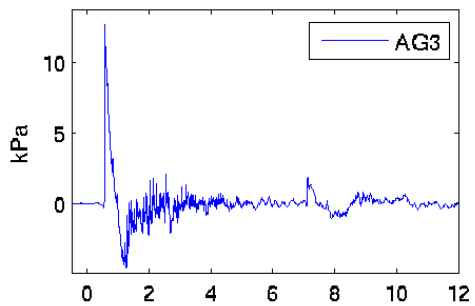
64 degrees



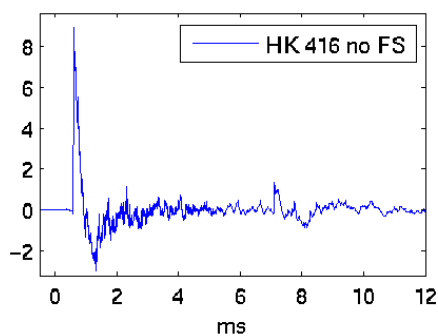
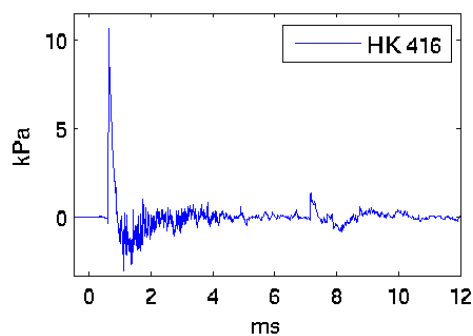
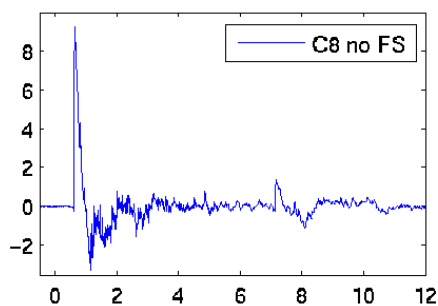
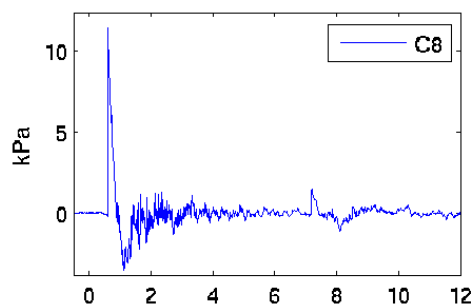
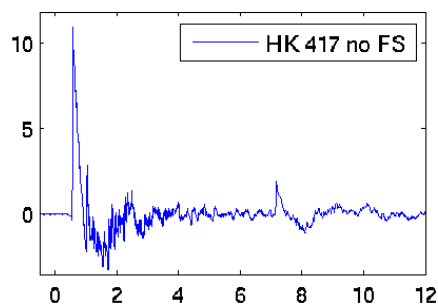
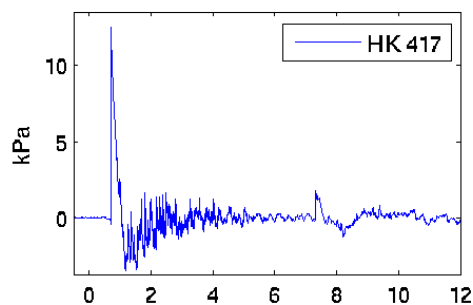
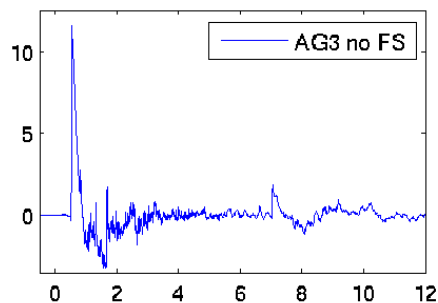
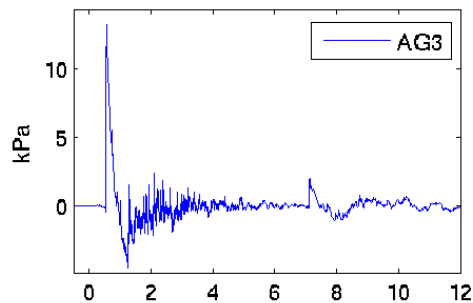
65 degrees



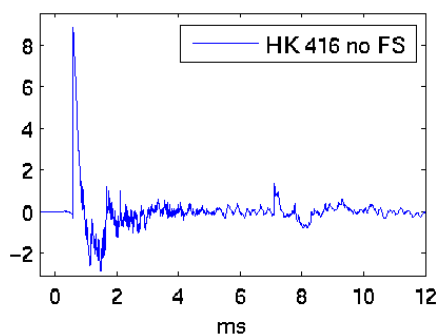
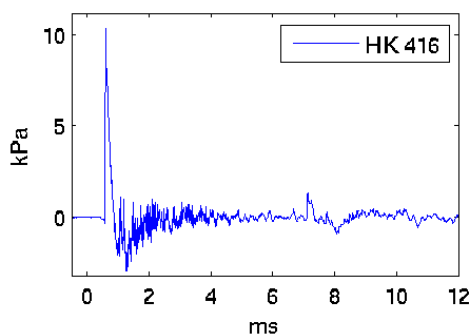
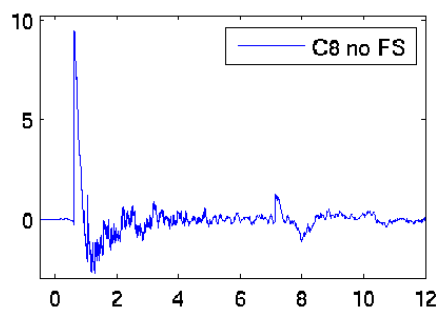
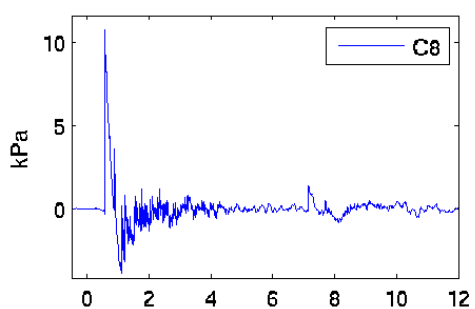
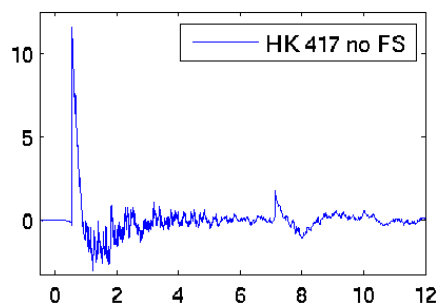
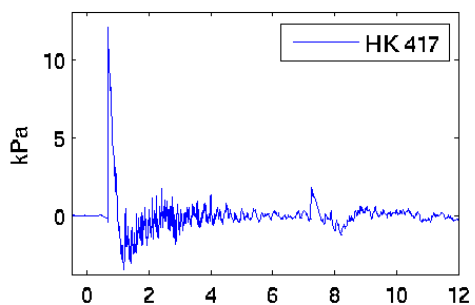
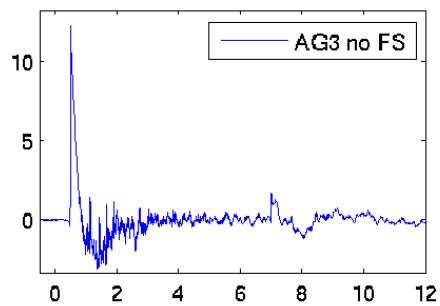
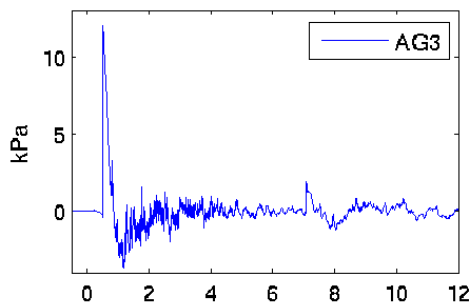
66 degrees



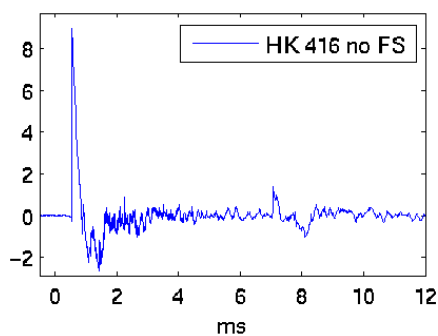
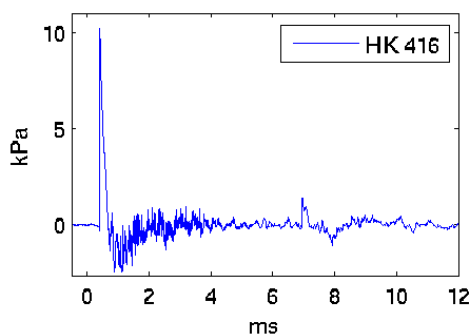
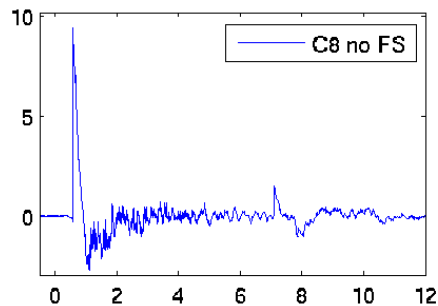
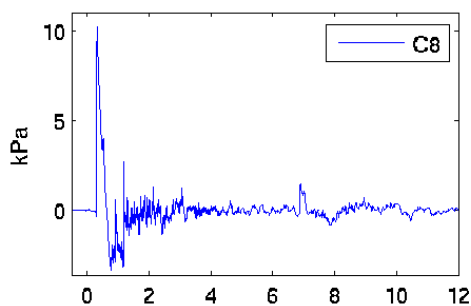
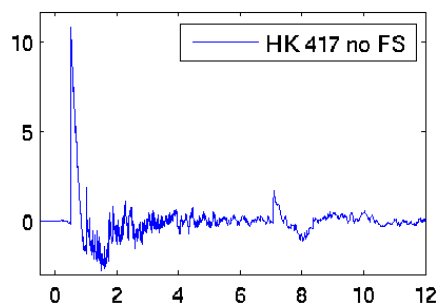
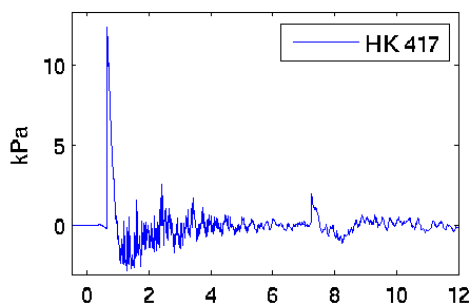
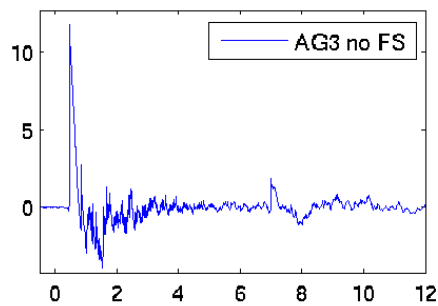
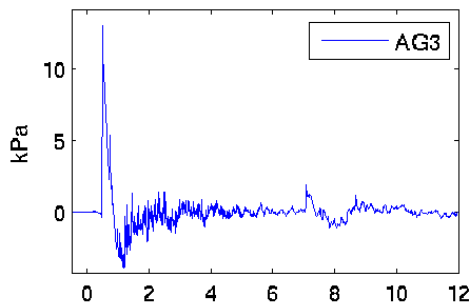
67 degrees



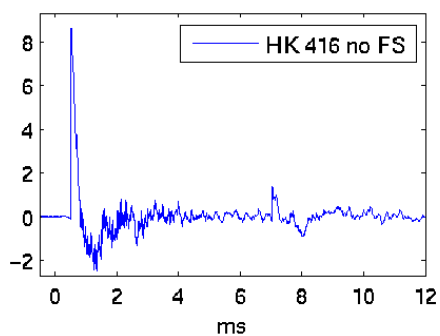
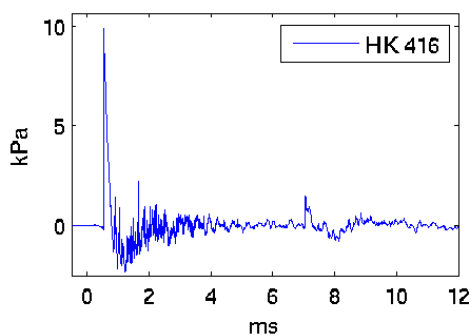
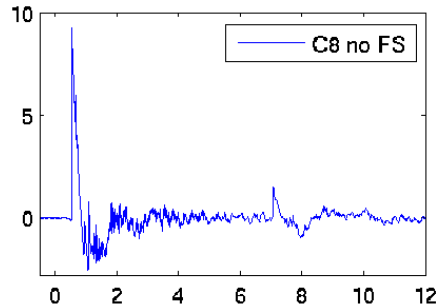
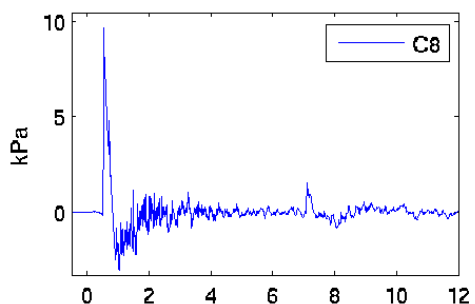
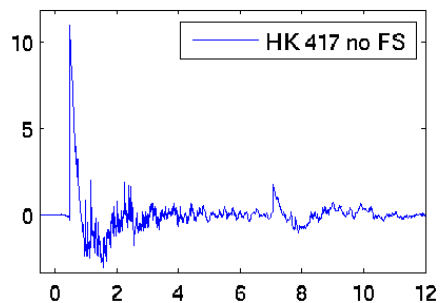
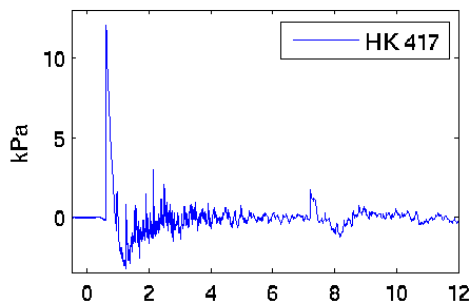
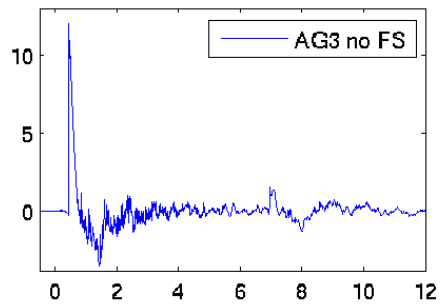
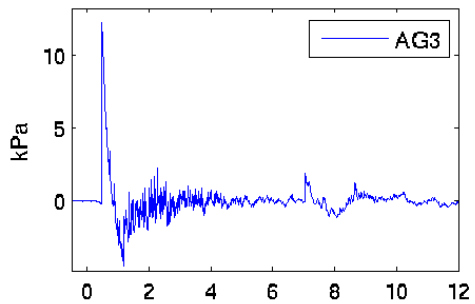
68 degrees



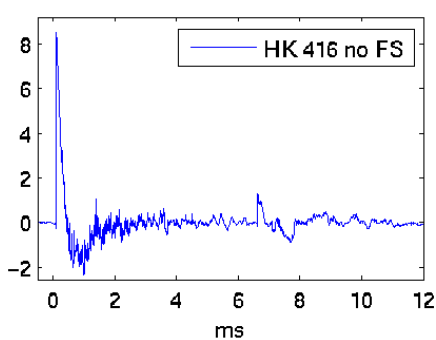
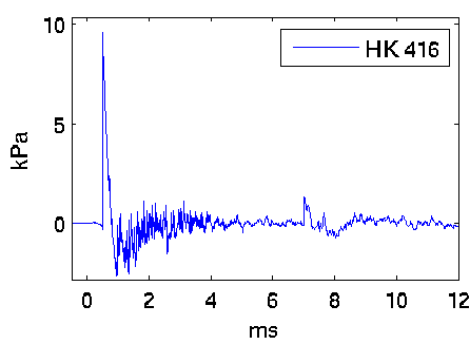
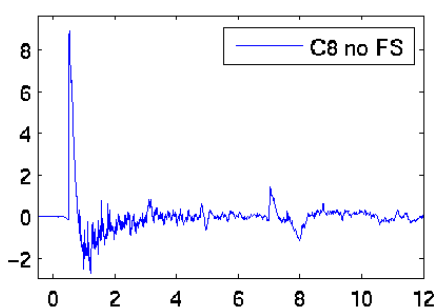
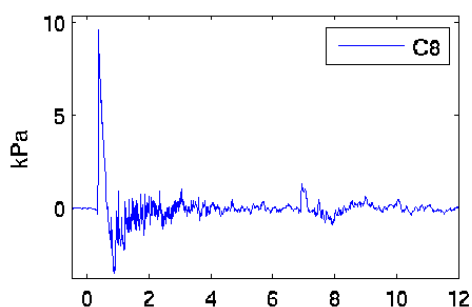
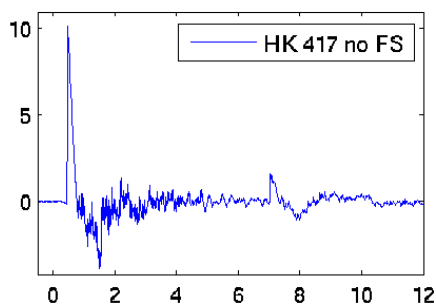
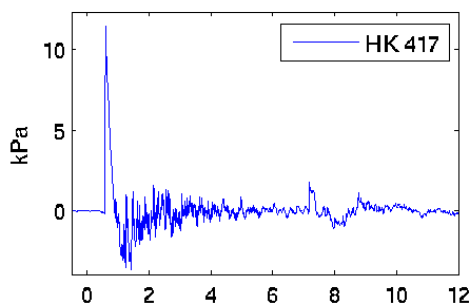
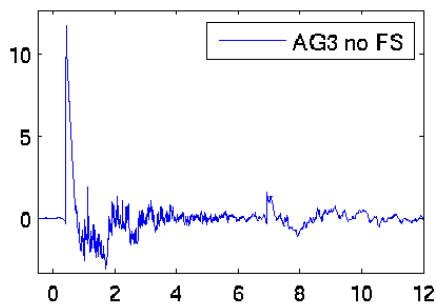
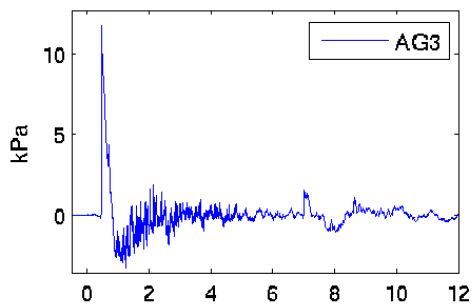
69 degrees



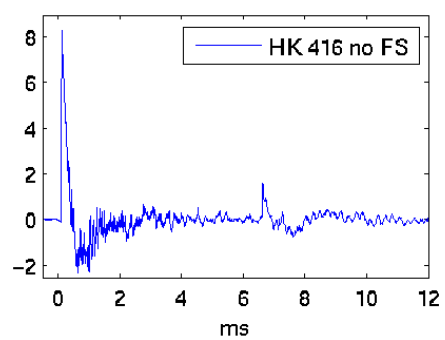
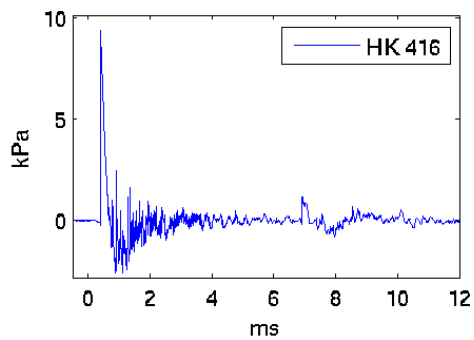
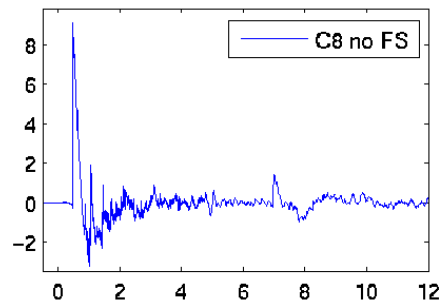
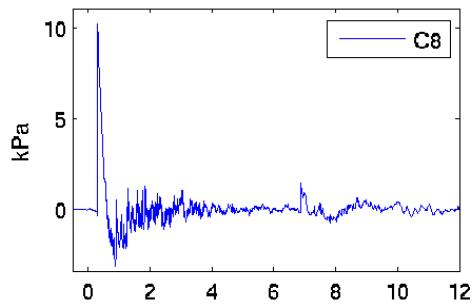
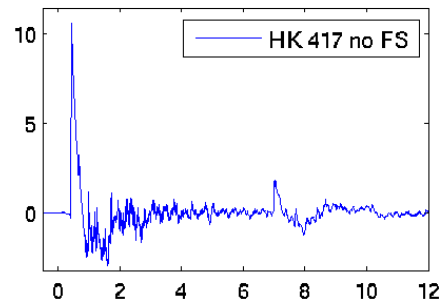
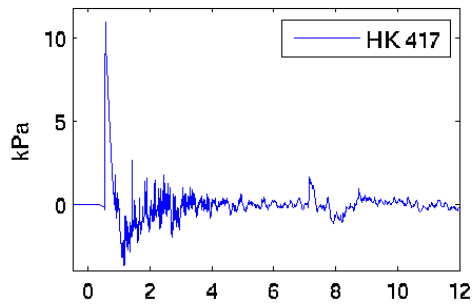
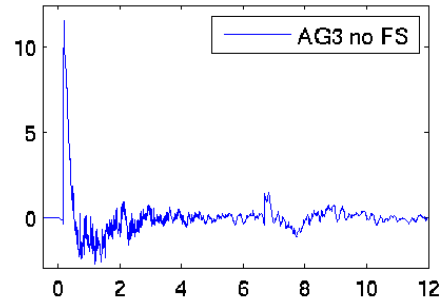
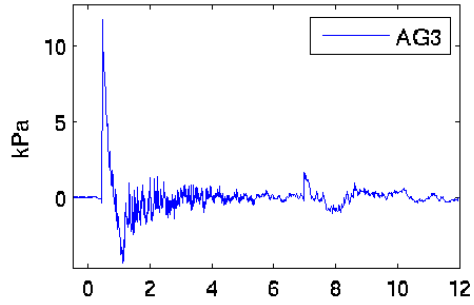
70 degrees



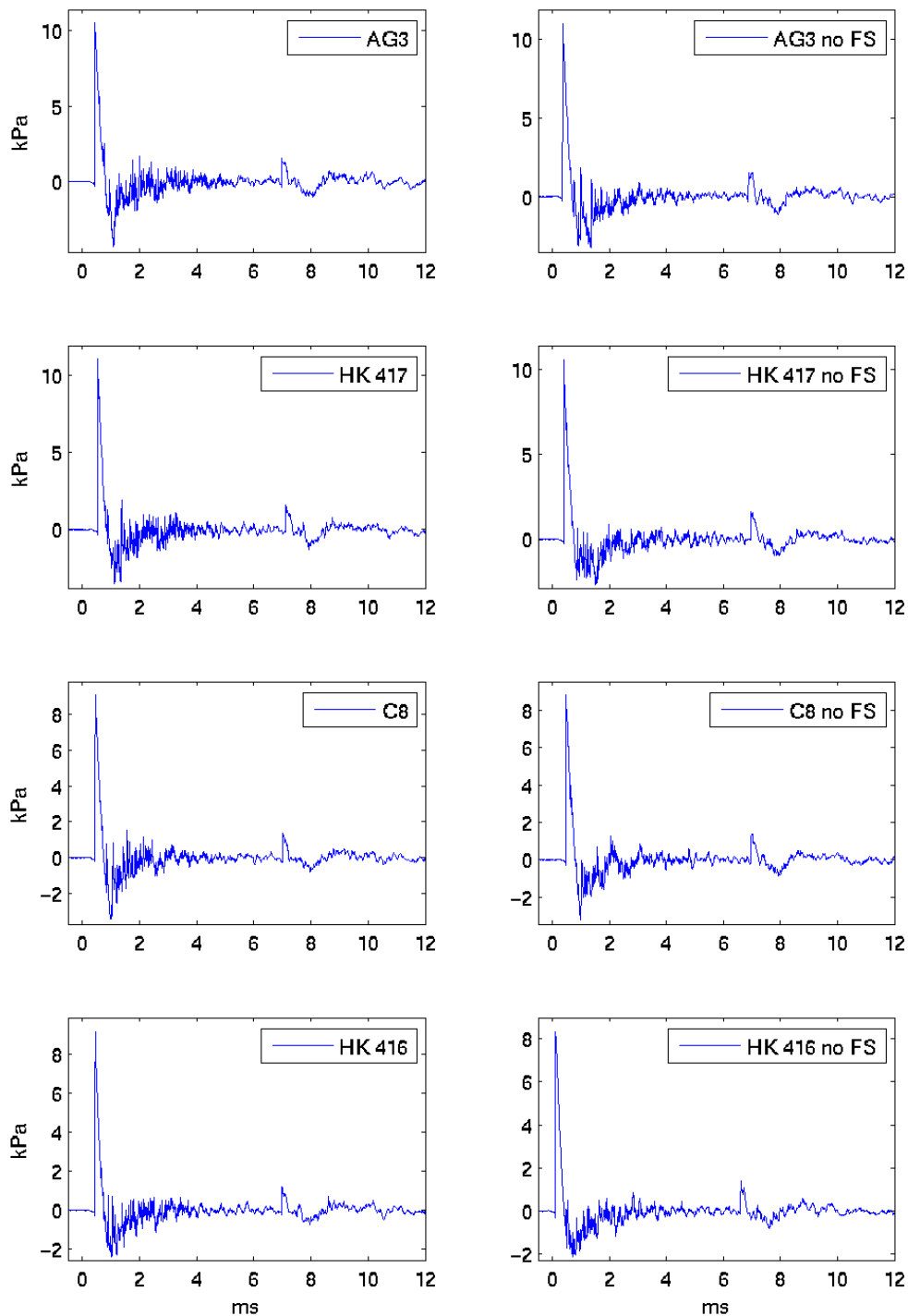
71 degrees



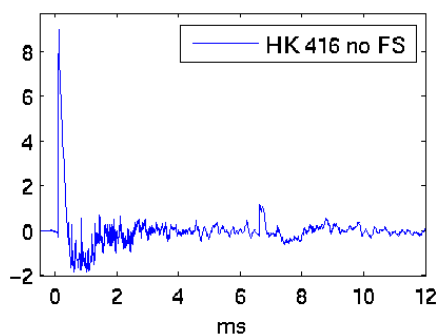
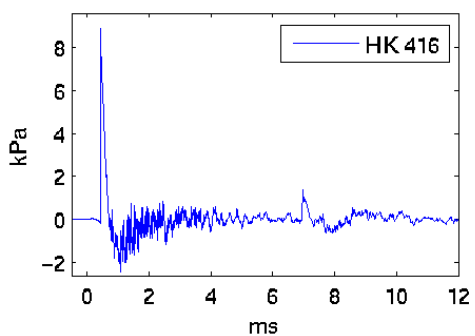
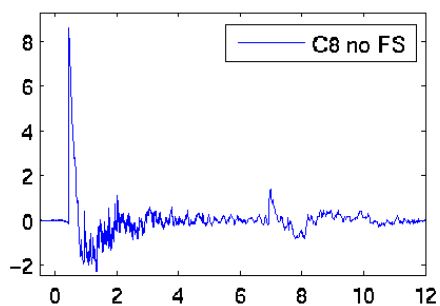
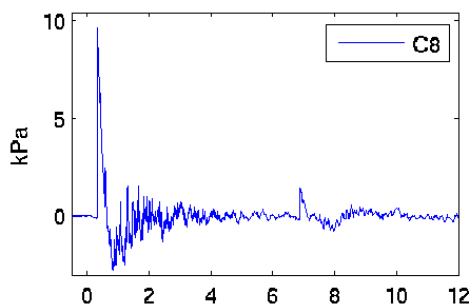
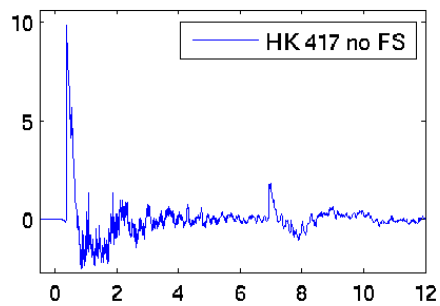
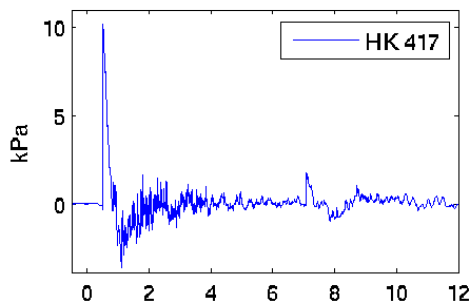
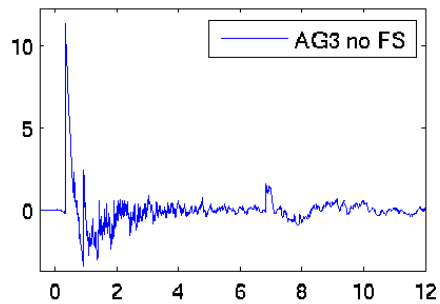
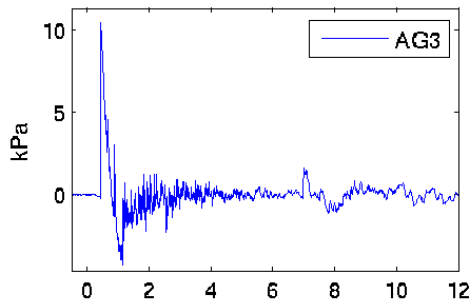
72 degrees



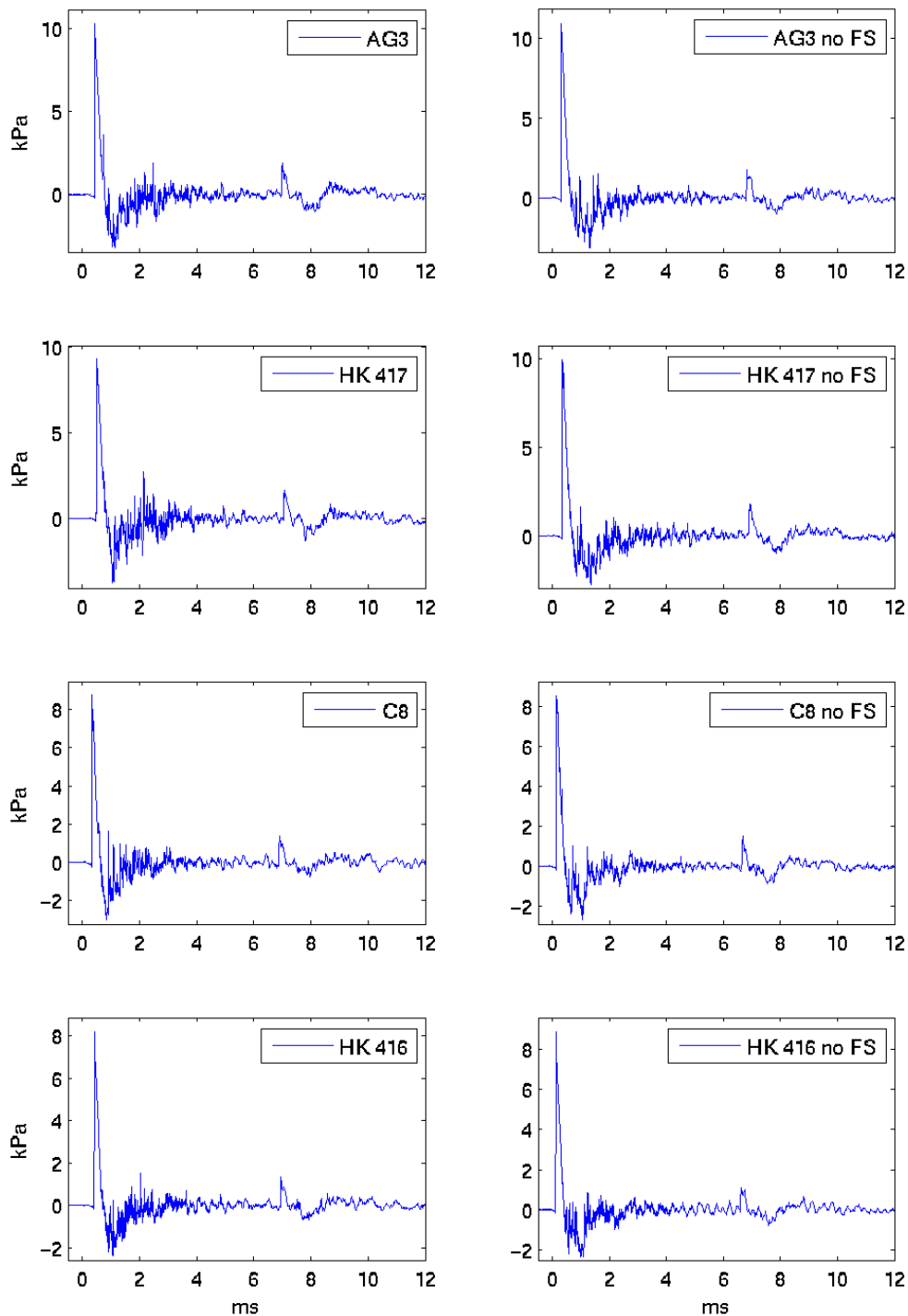
73 degrees



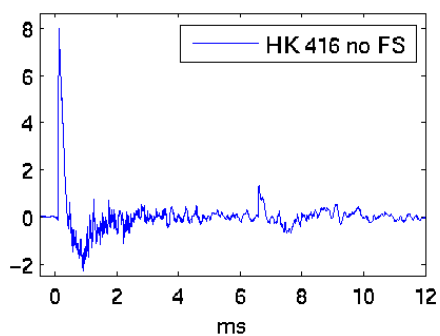
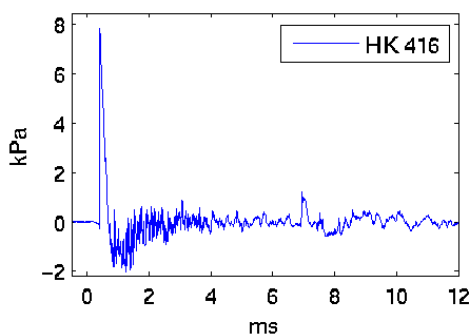
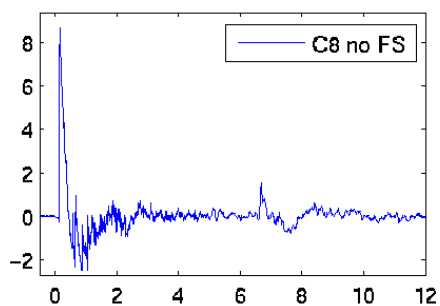
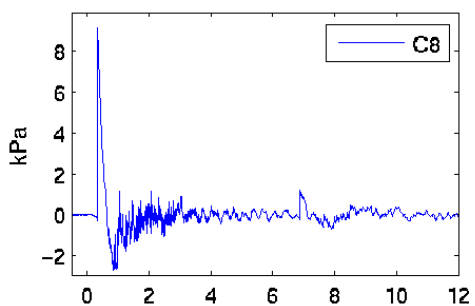
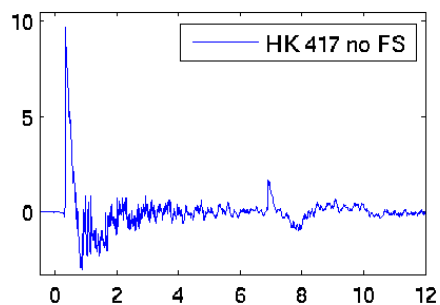
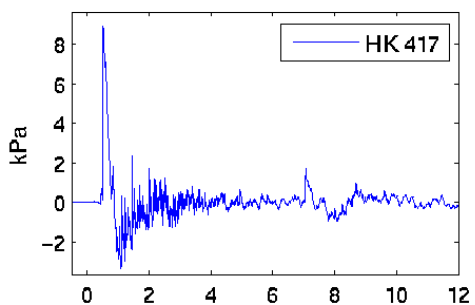
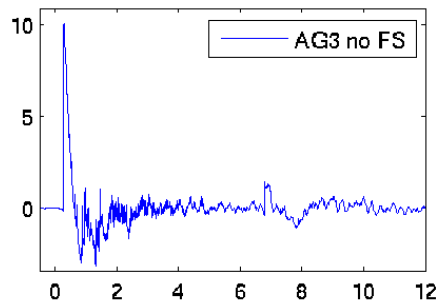
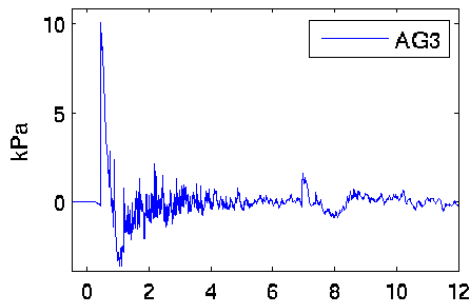
74 degrees

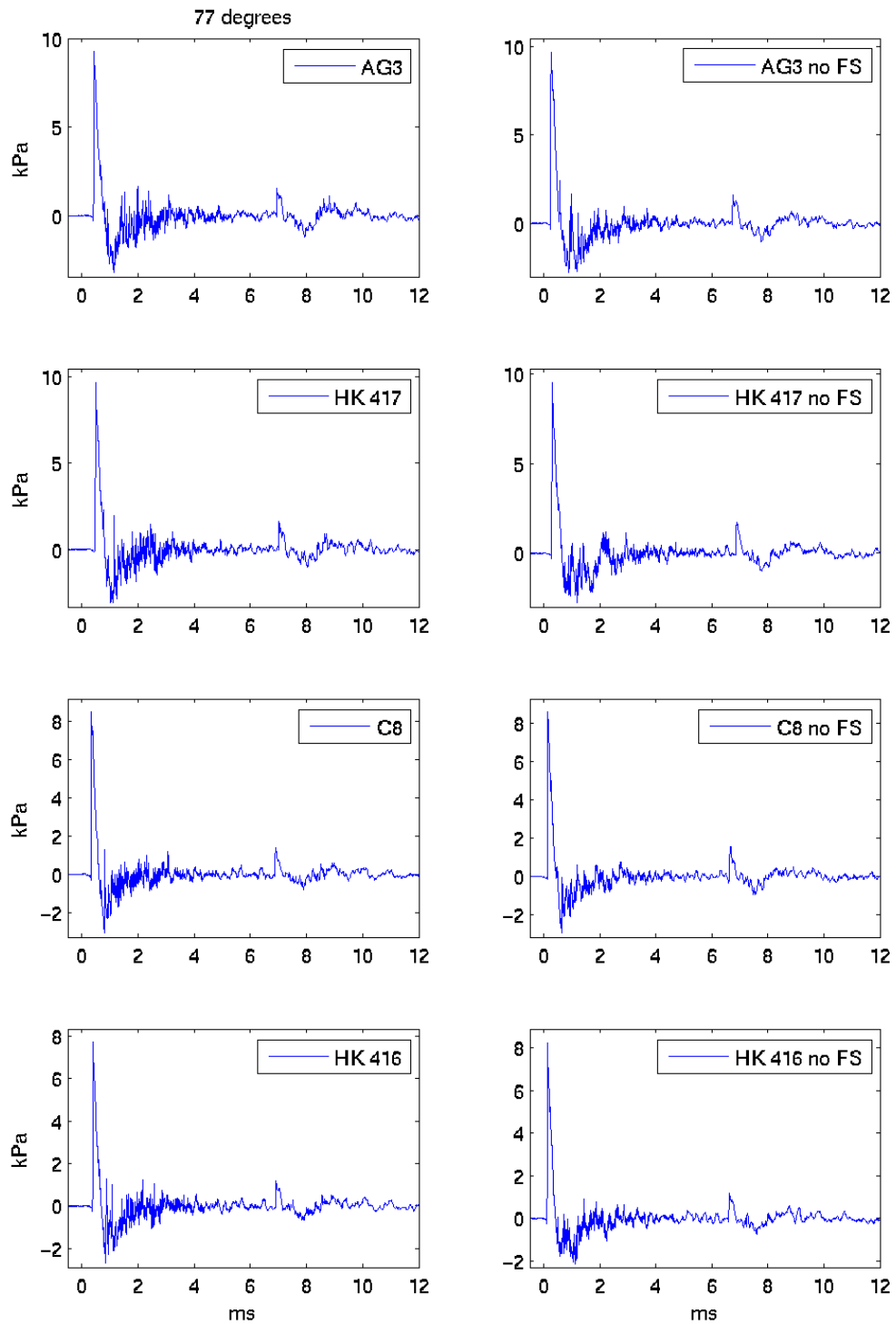


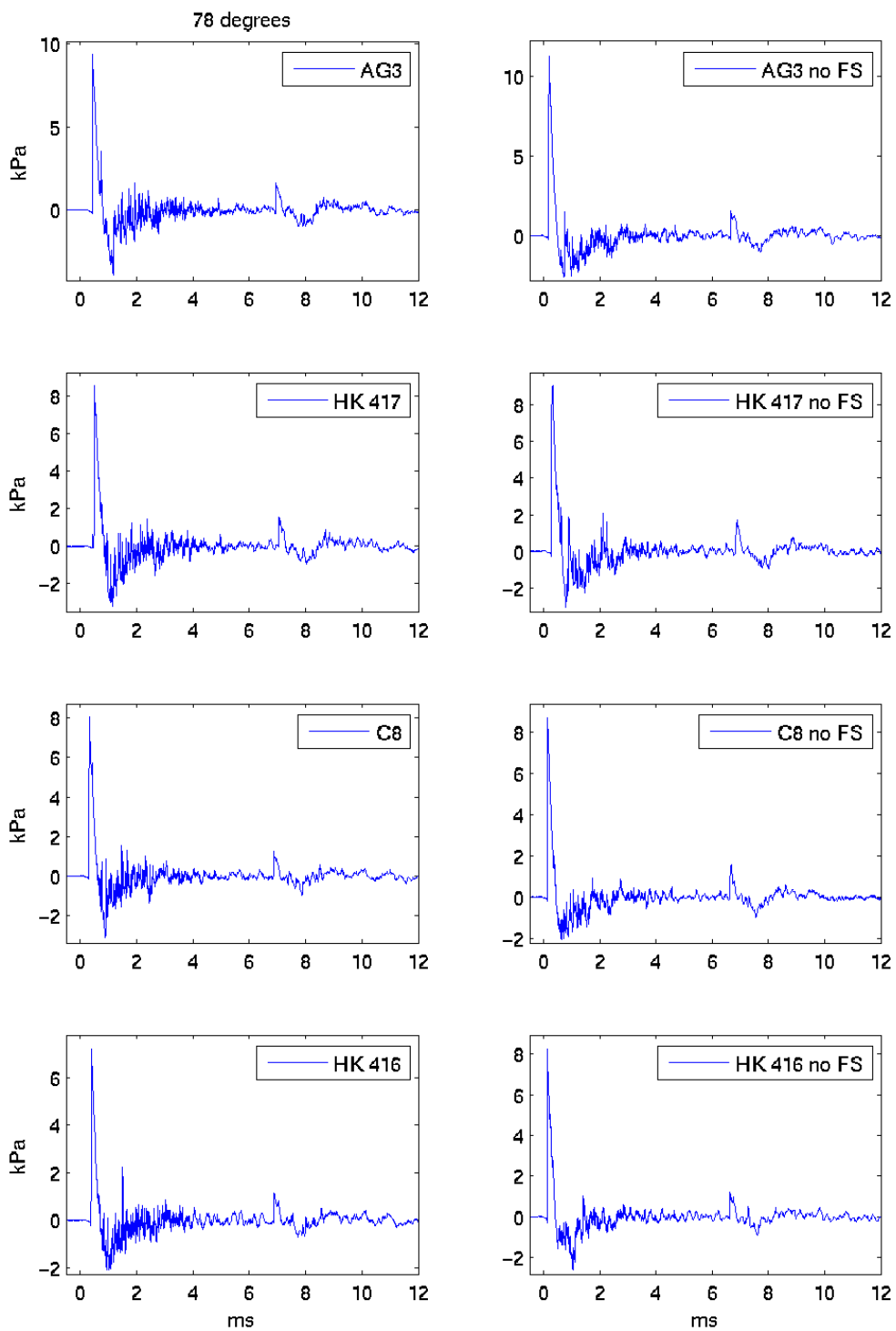
75 degrees



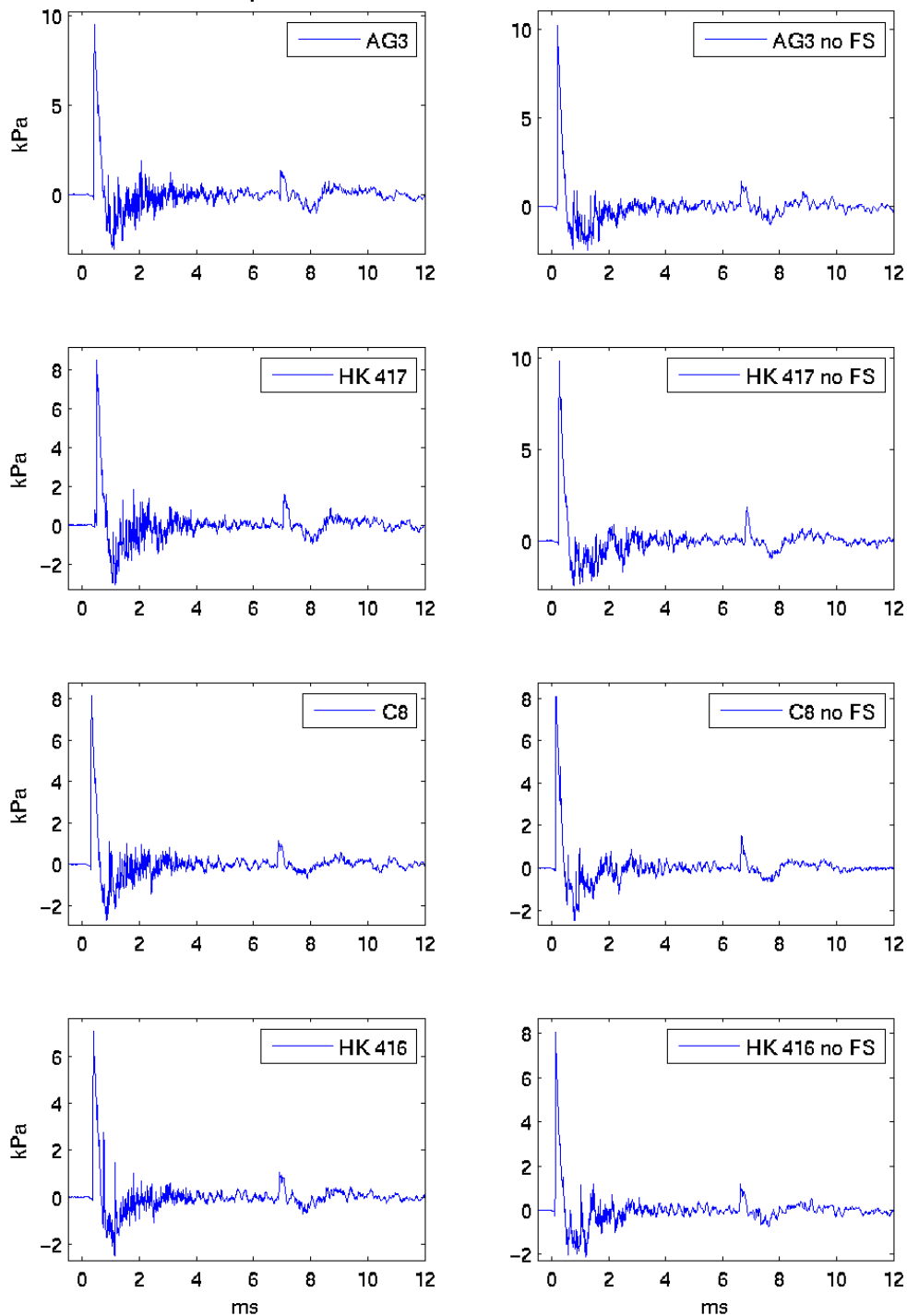
76 degrees



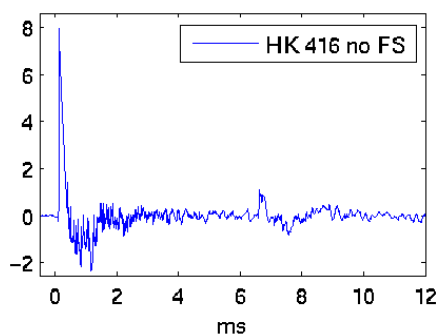
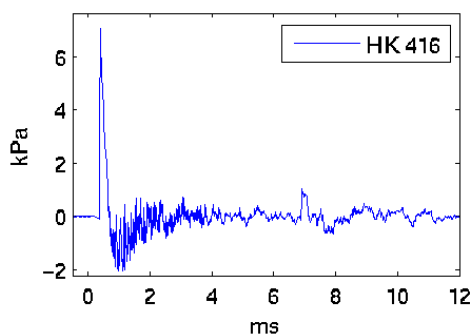
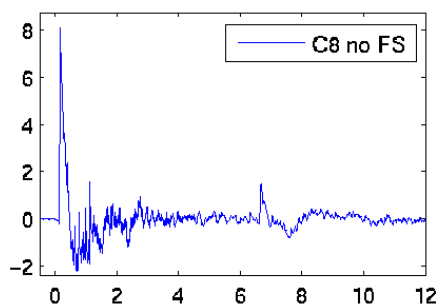
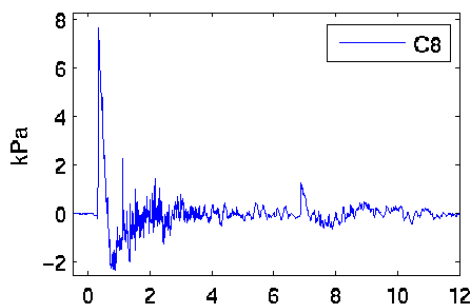
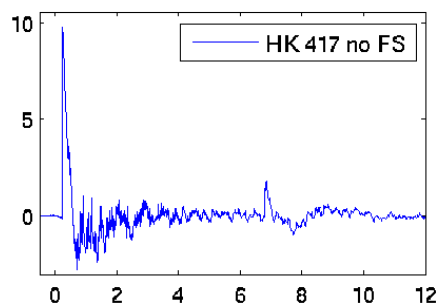
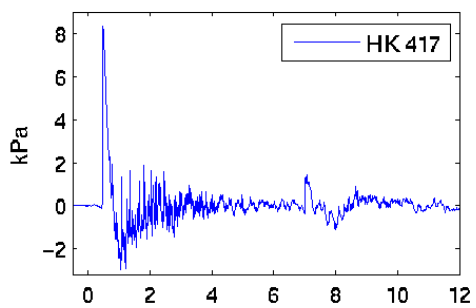
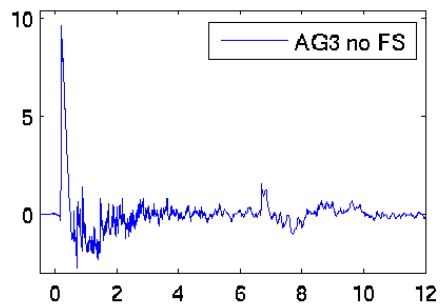
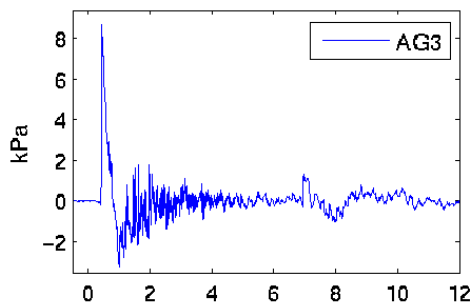




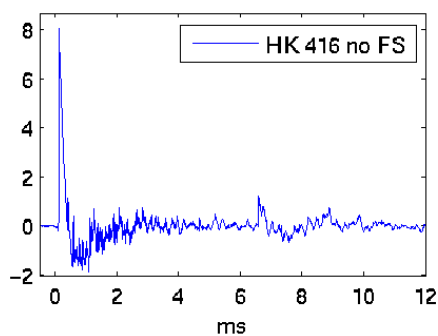
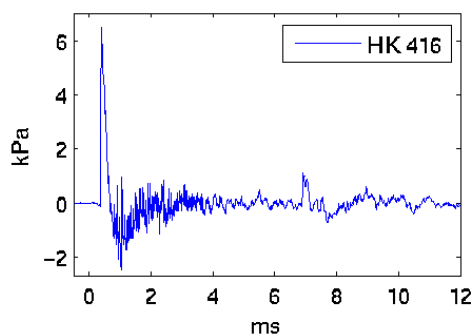
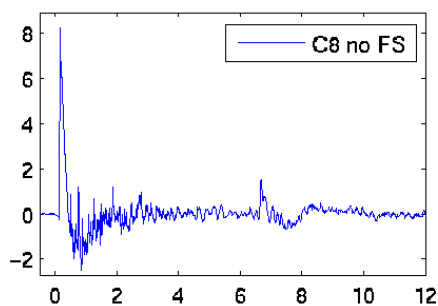
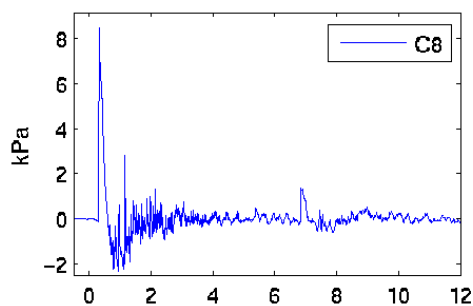
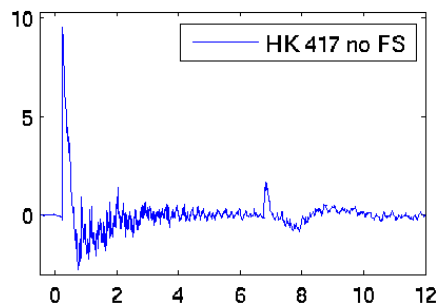
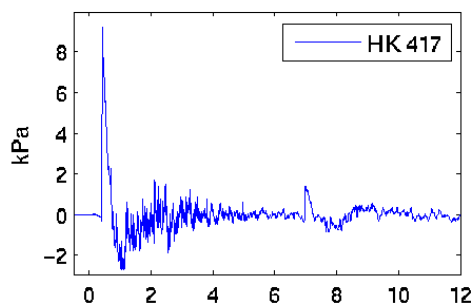
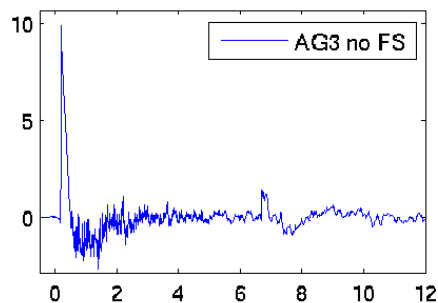
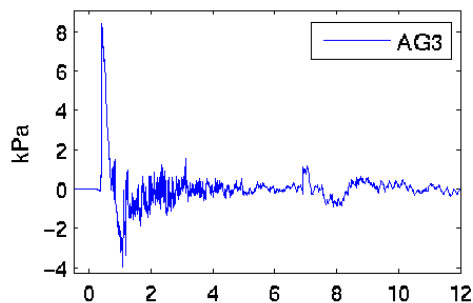
79 degrees



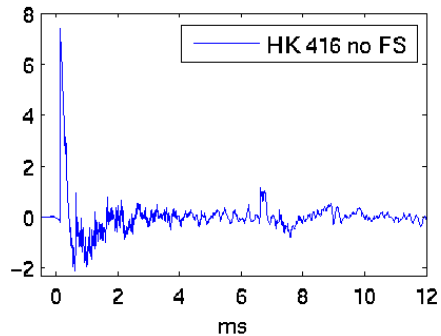
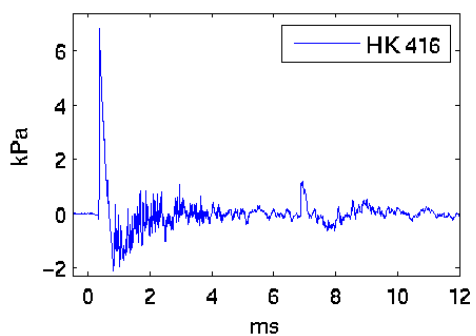
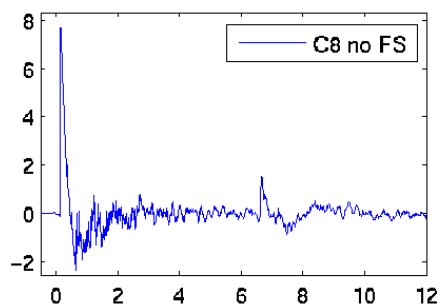
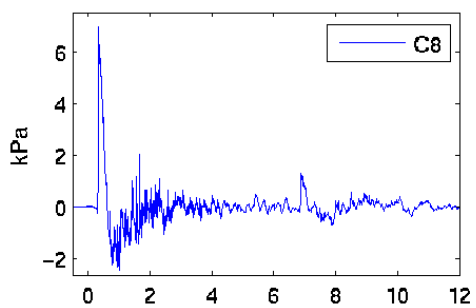
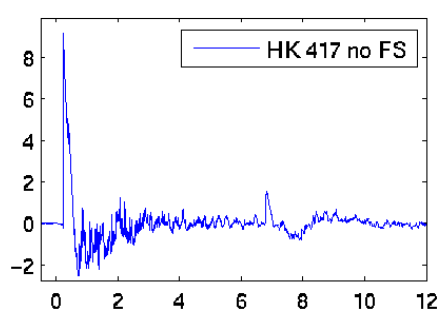
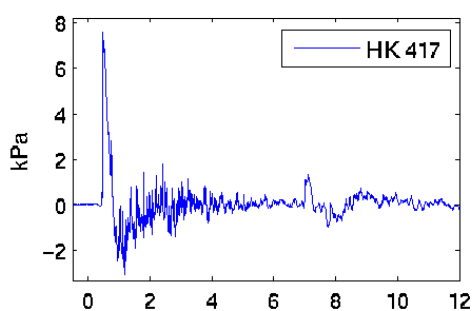
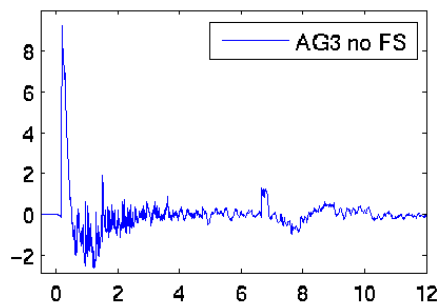
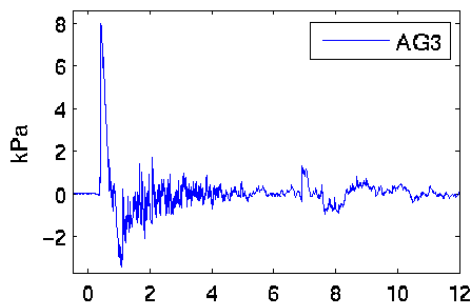
80 degrees



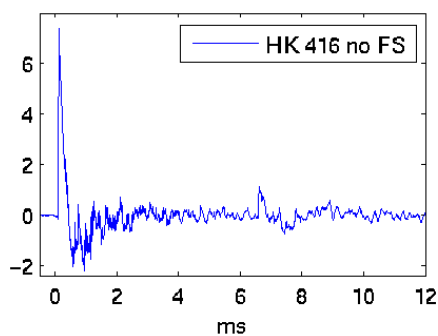
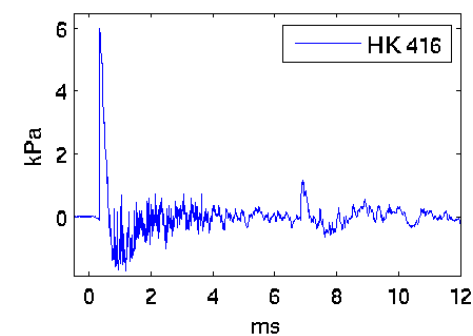
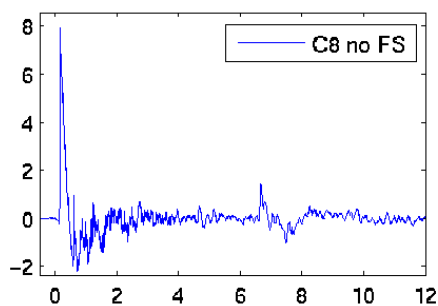
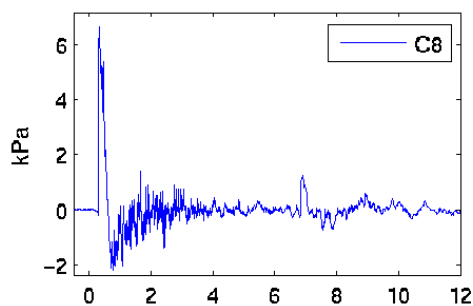
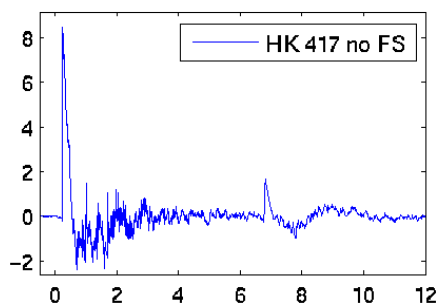
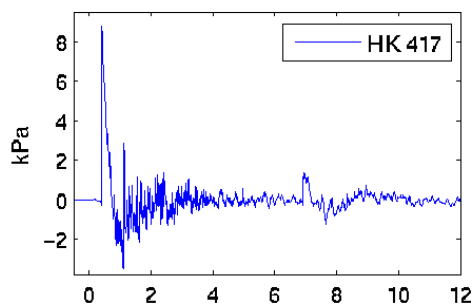
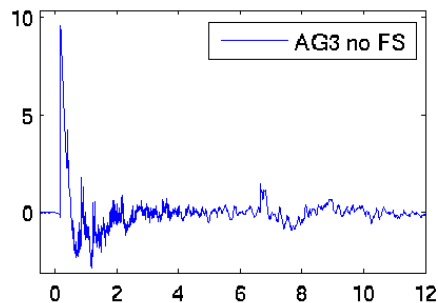
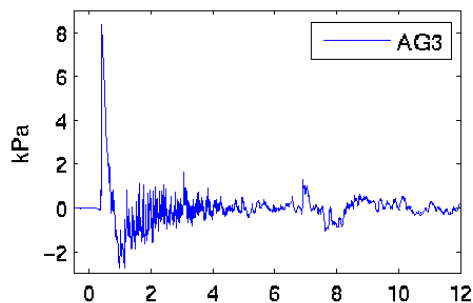
81 degrees



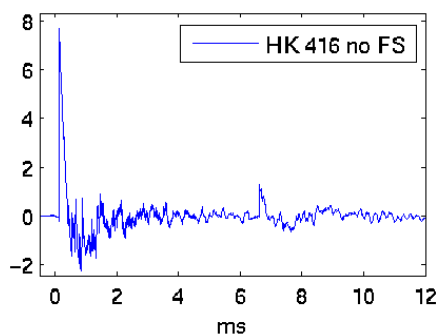
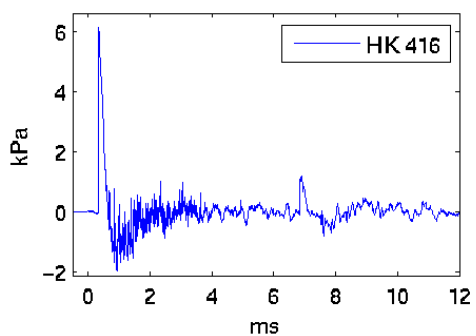
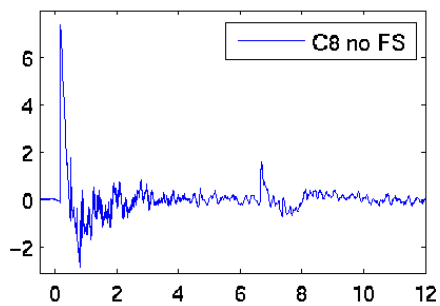
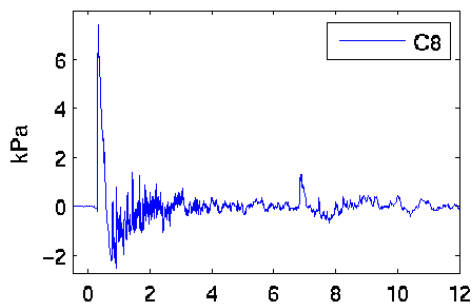
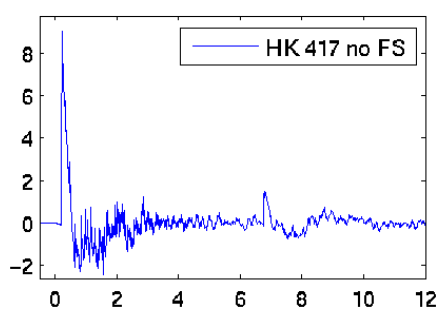
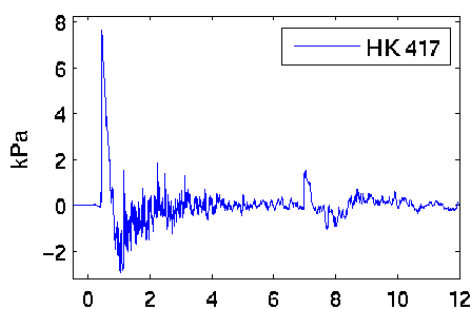
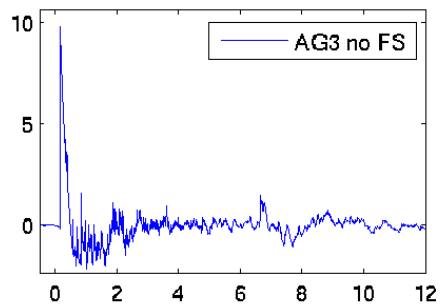
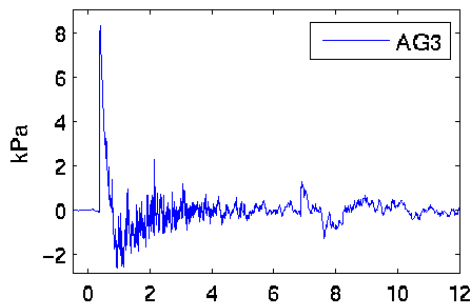
82 degrees



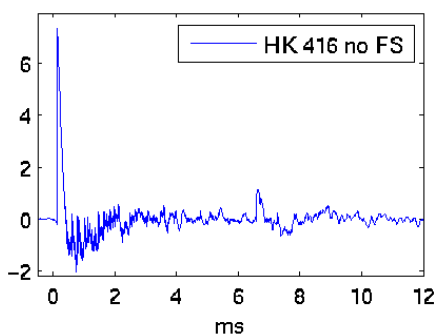
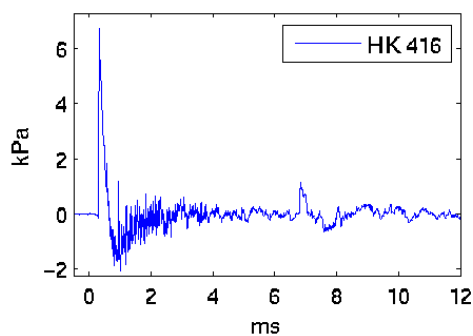
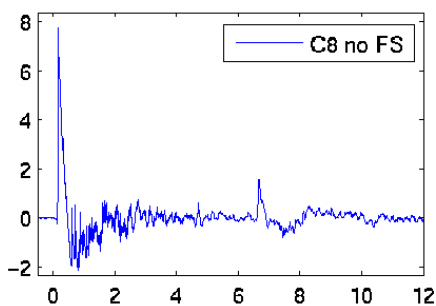
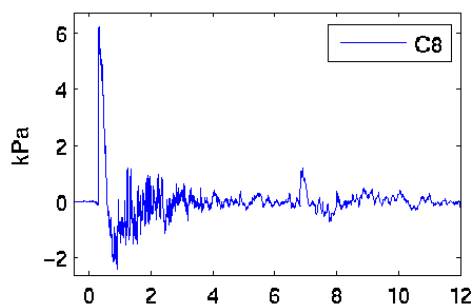
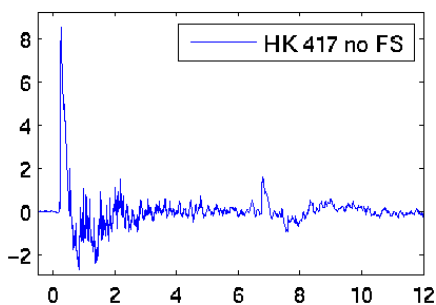
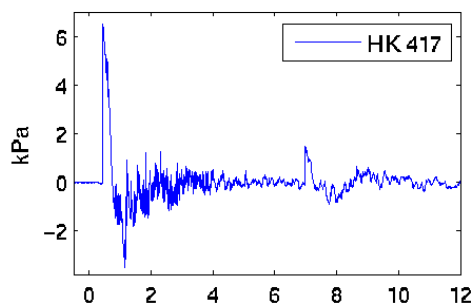
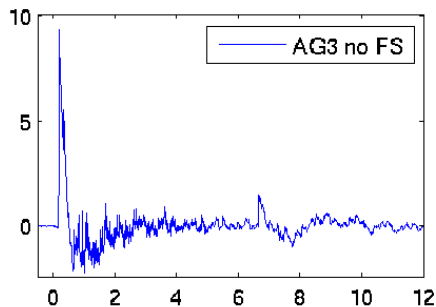
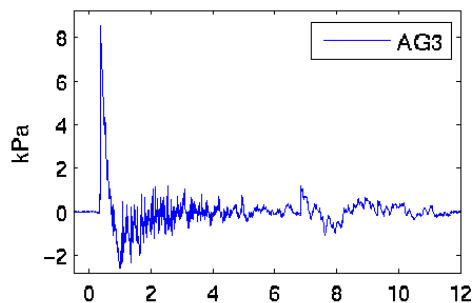
83 degrees



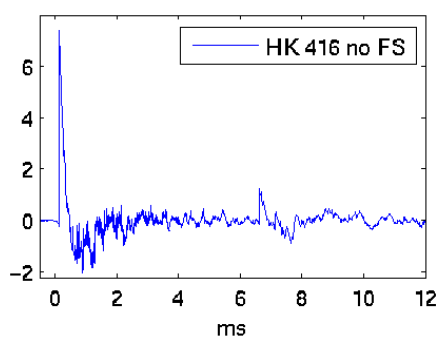
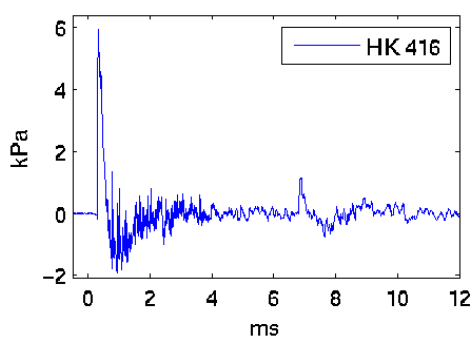
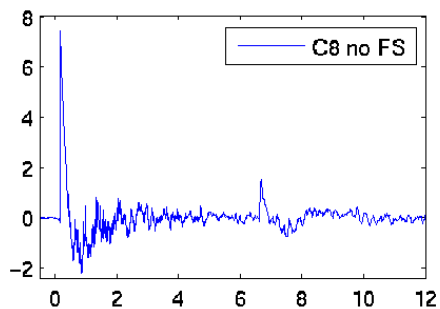
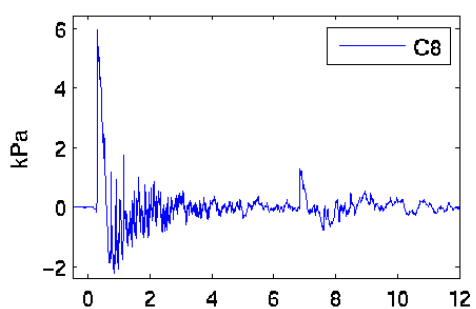
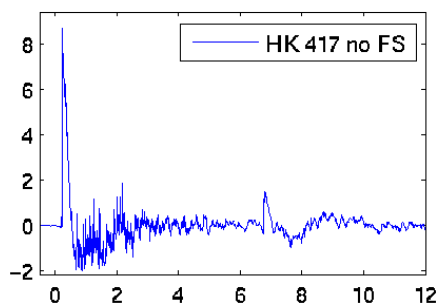
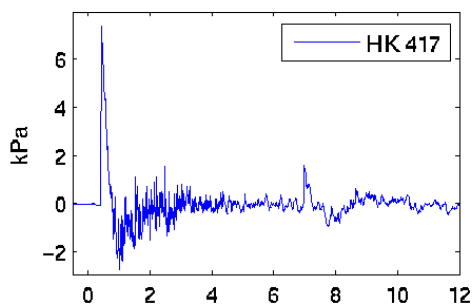
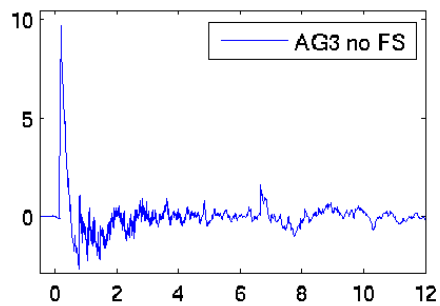
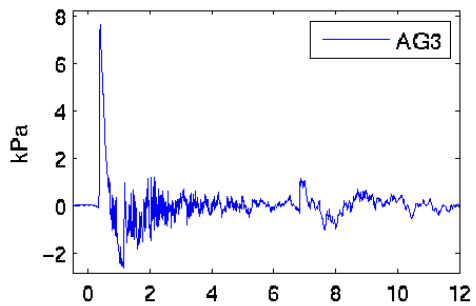
84 degrees



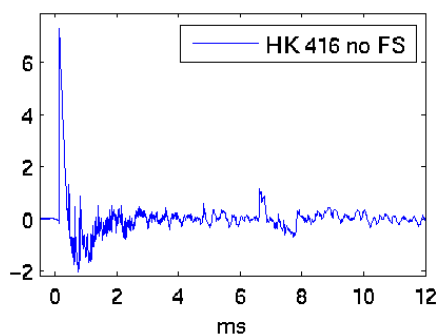
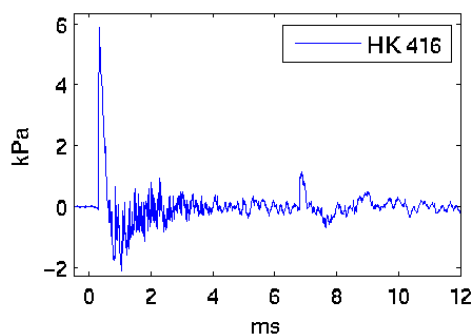
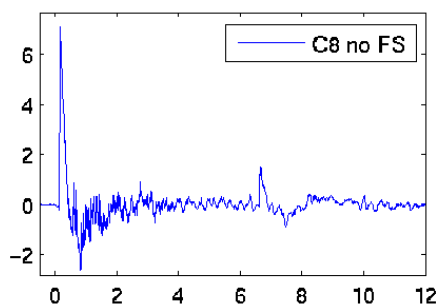
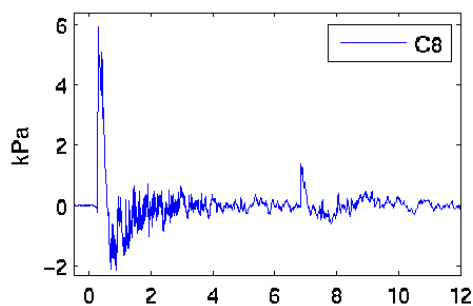
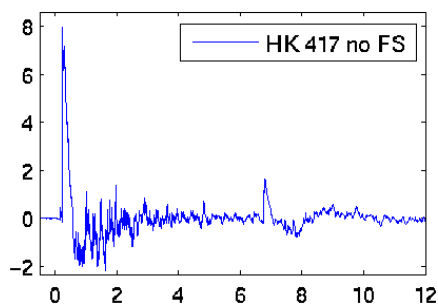
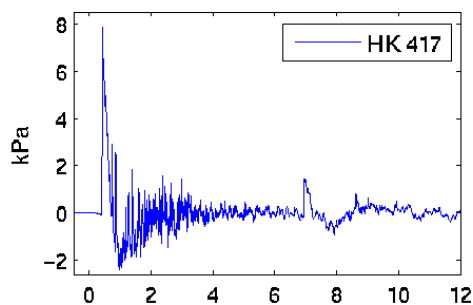
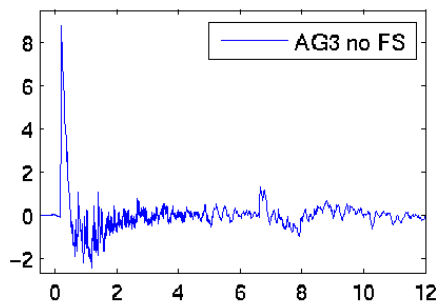
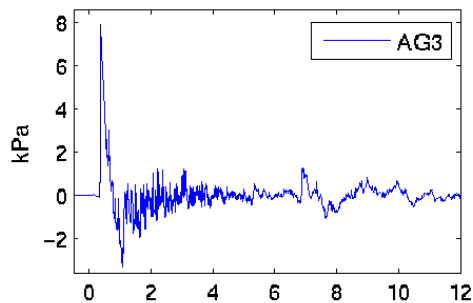
85 degrees



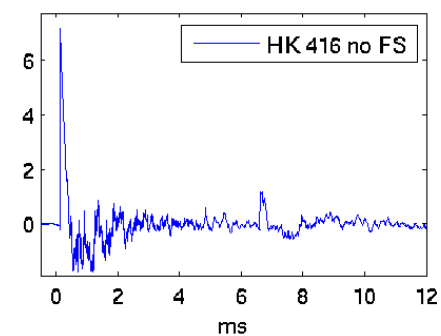
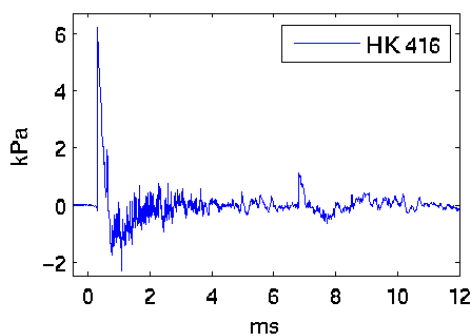
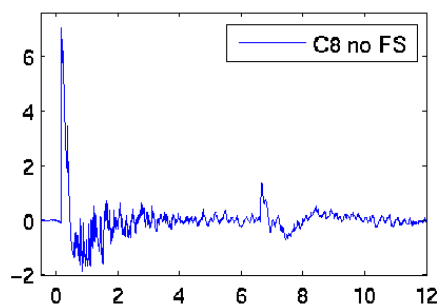
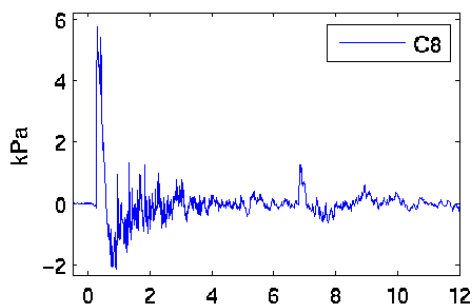
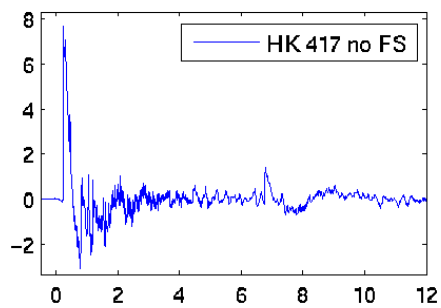
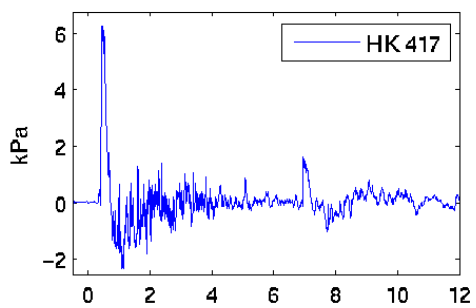
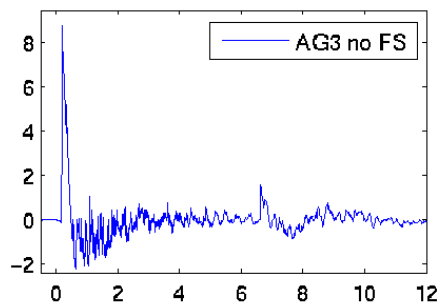
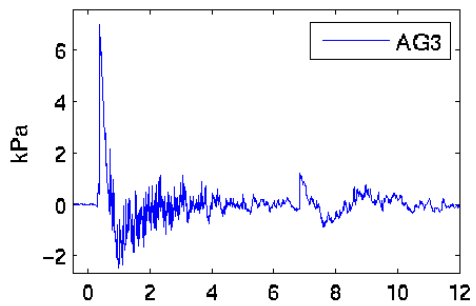
86 degrees



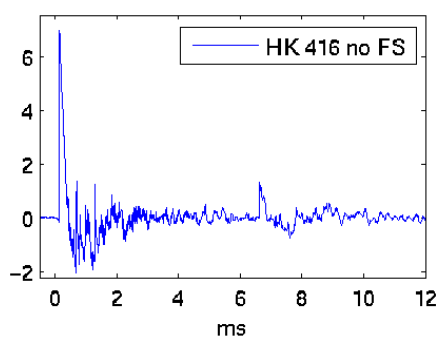
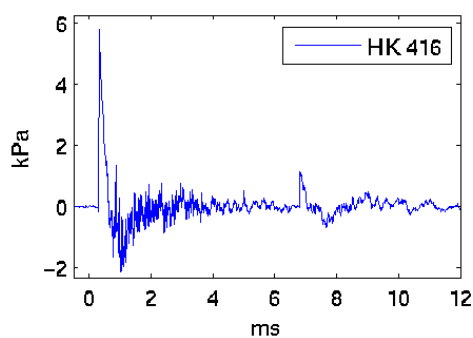
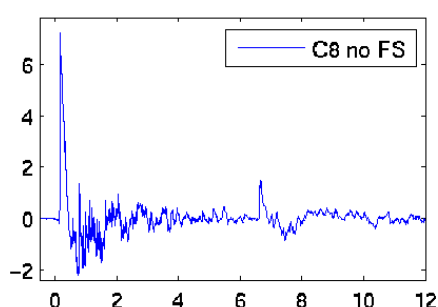
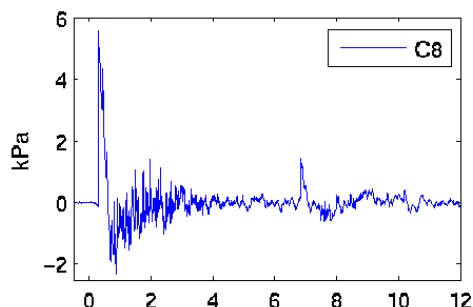
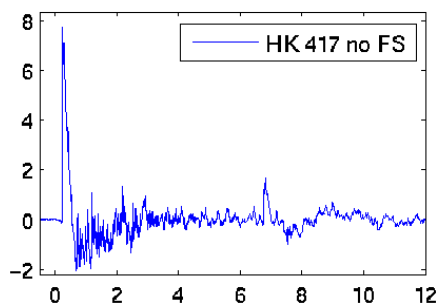
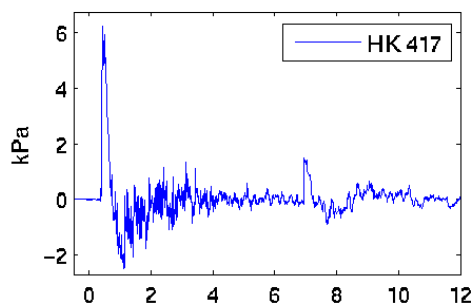
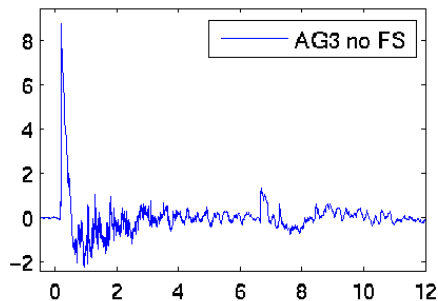
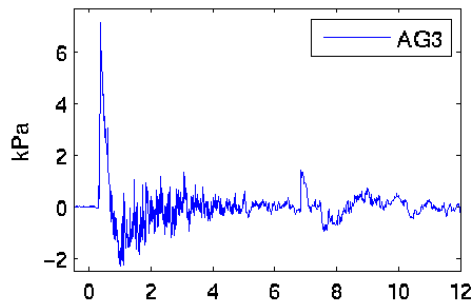
87 degrees



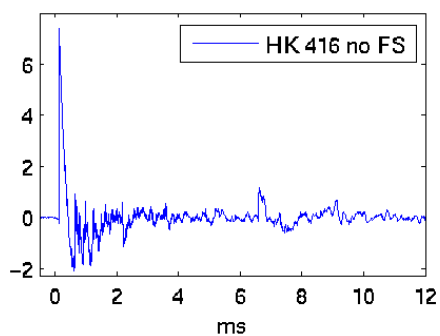
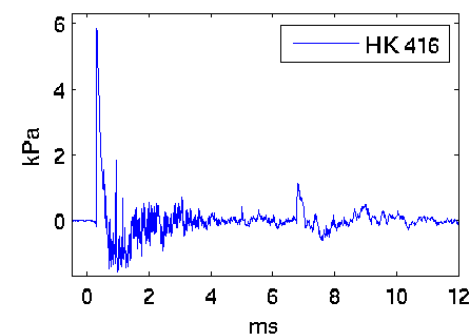
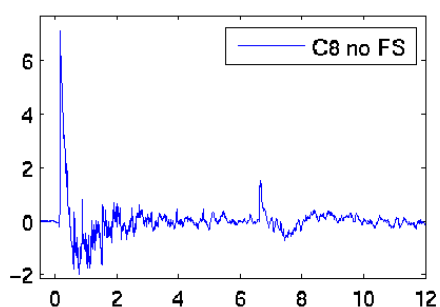
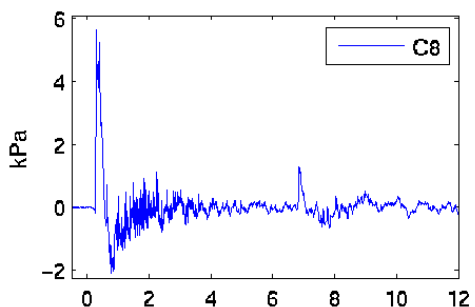
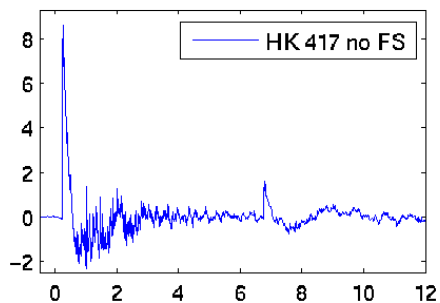
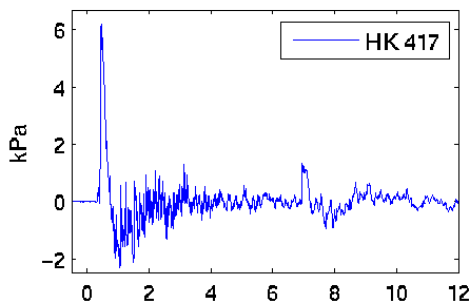
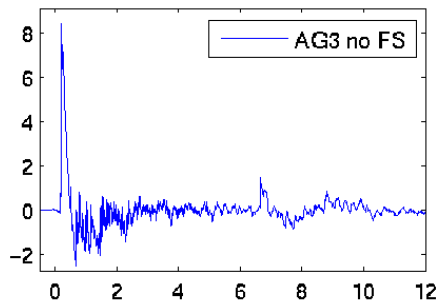
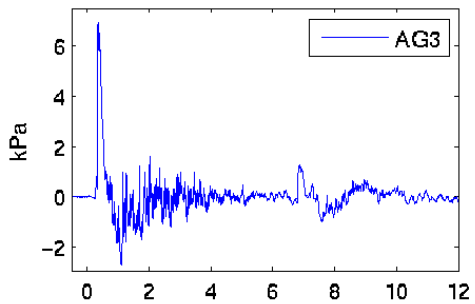
88 degrees



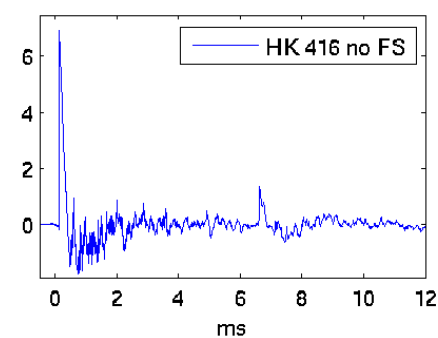
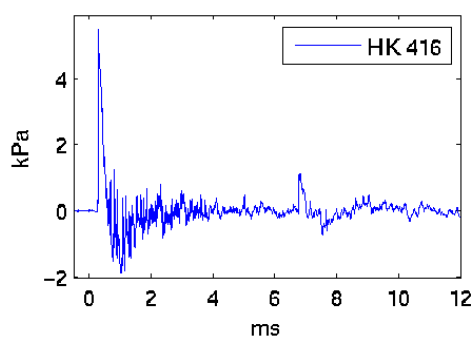
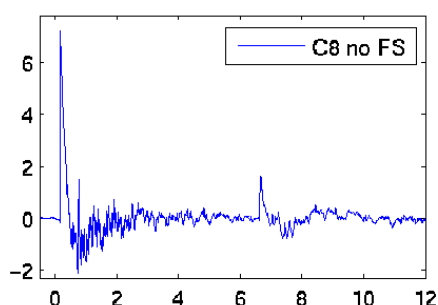
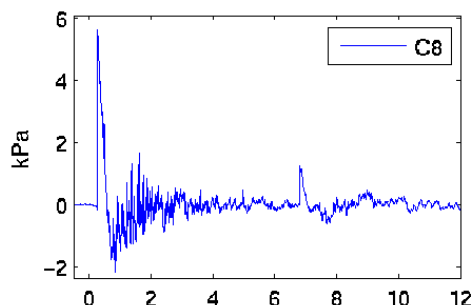
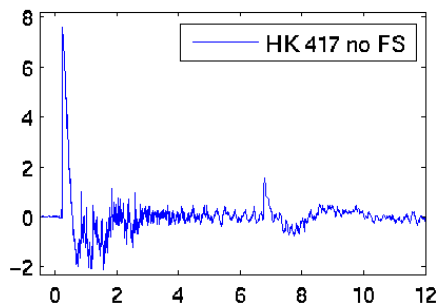
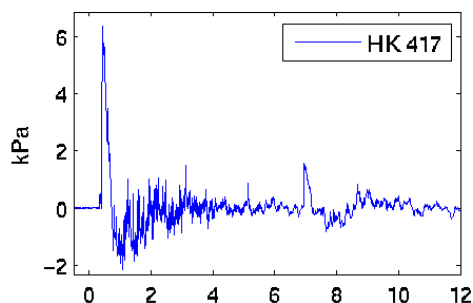
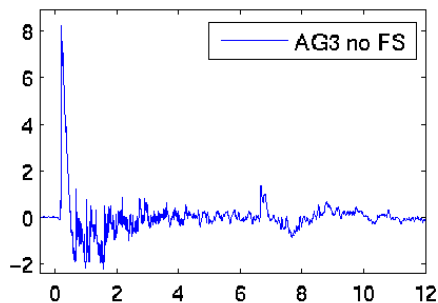
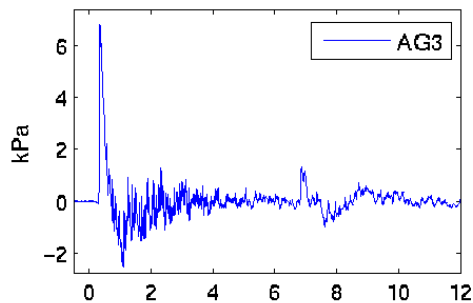
89 degrees



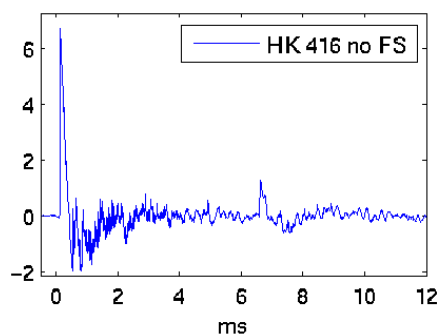
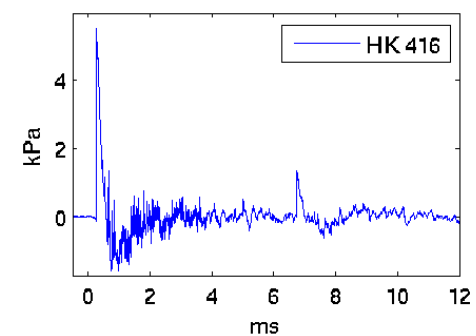
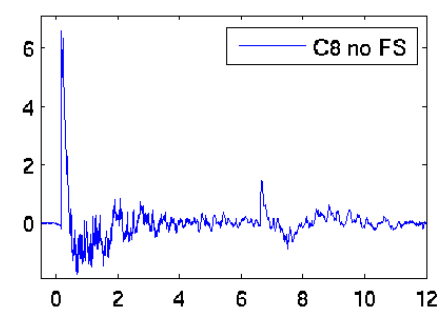
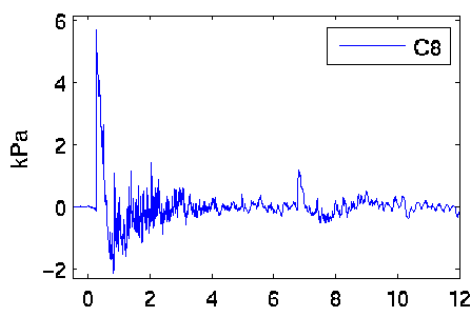
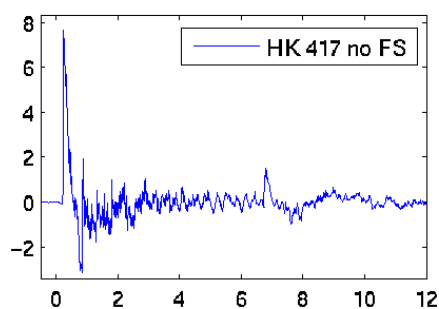
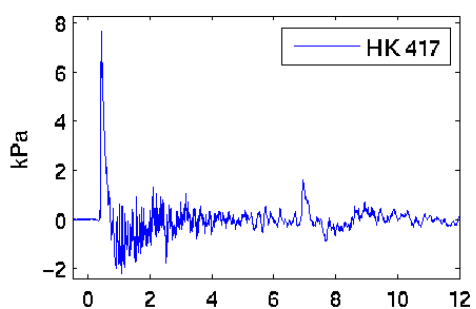
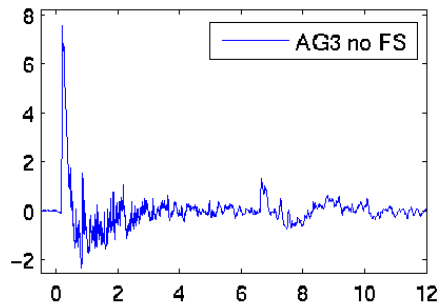
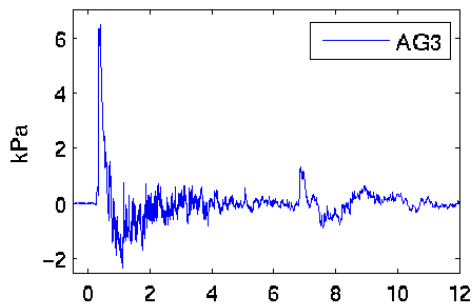
90 degrees



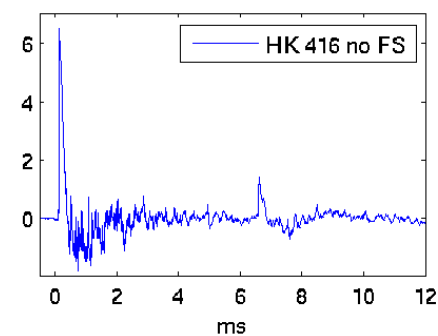
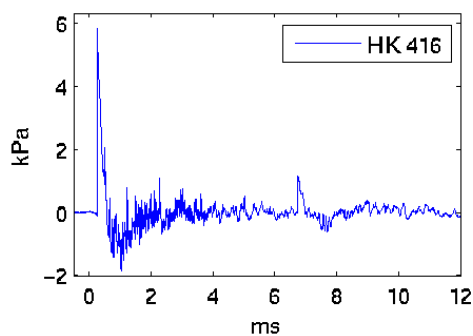
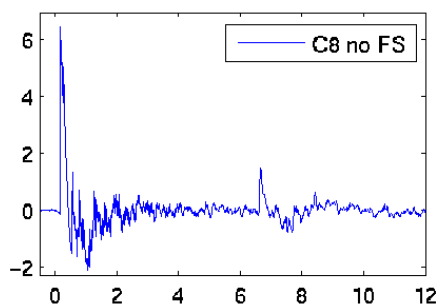
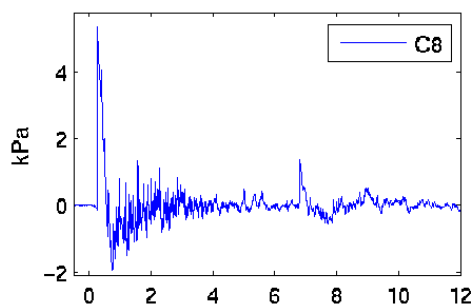
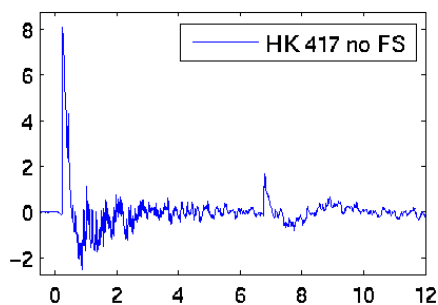
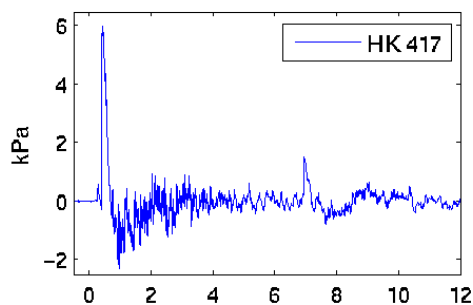
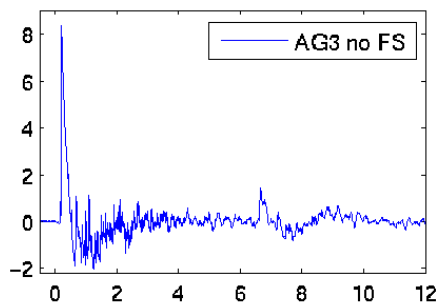
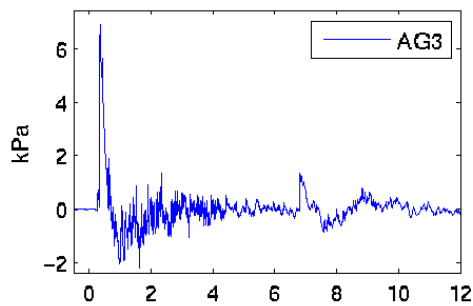
91 degrees



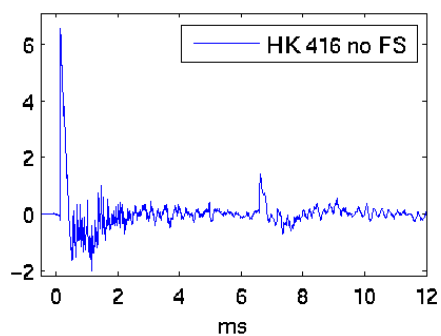
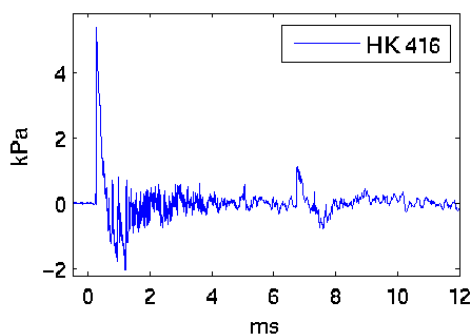
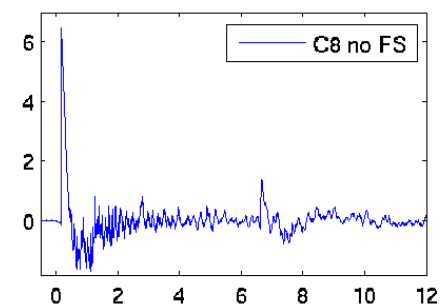
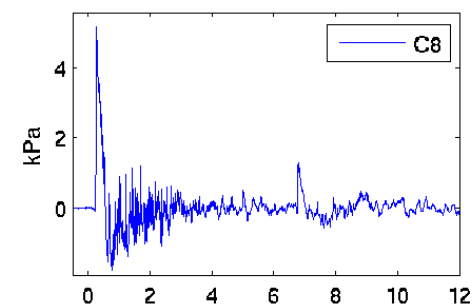
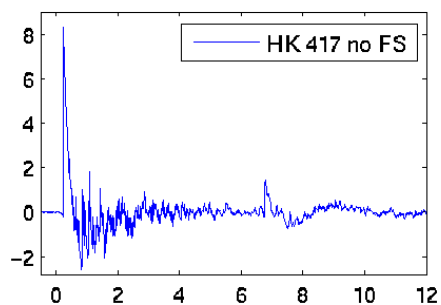
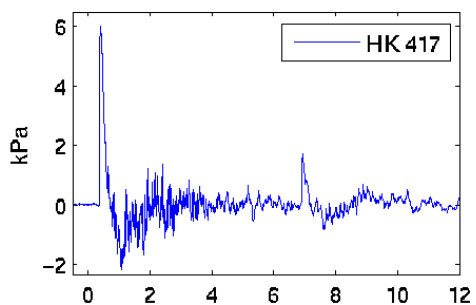
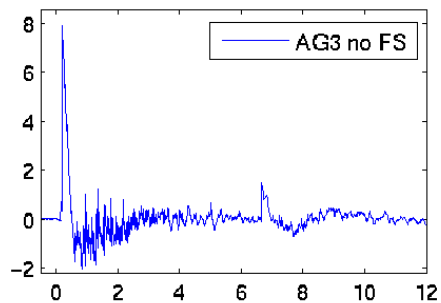
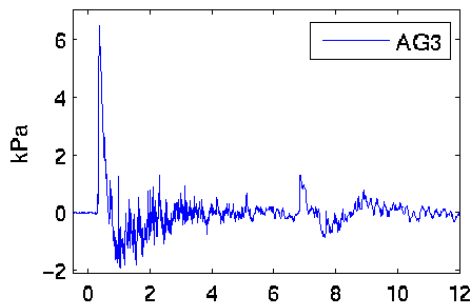
92 degrees

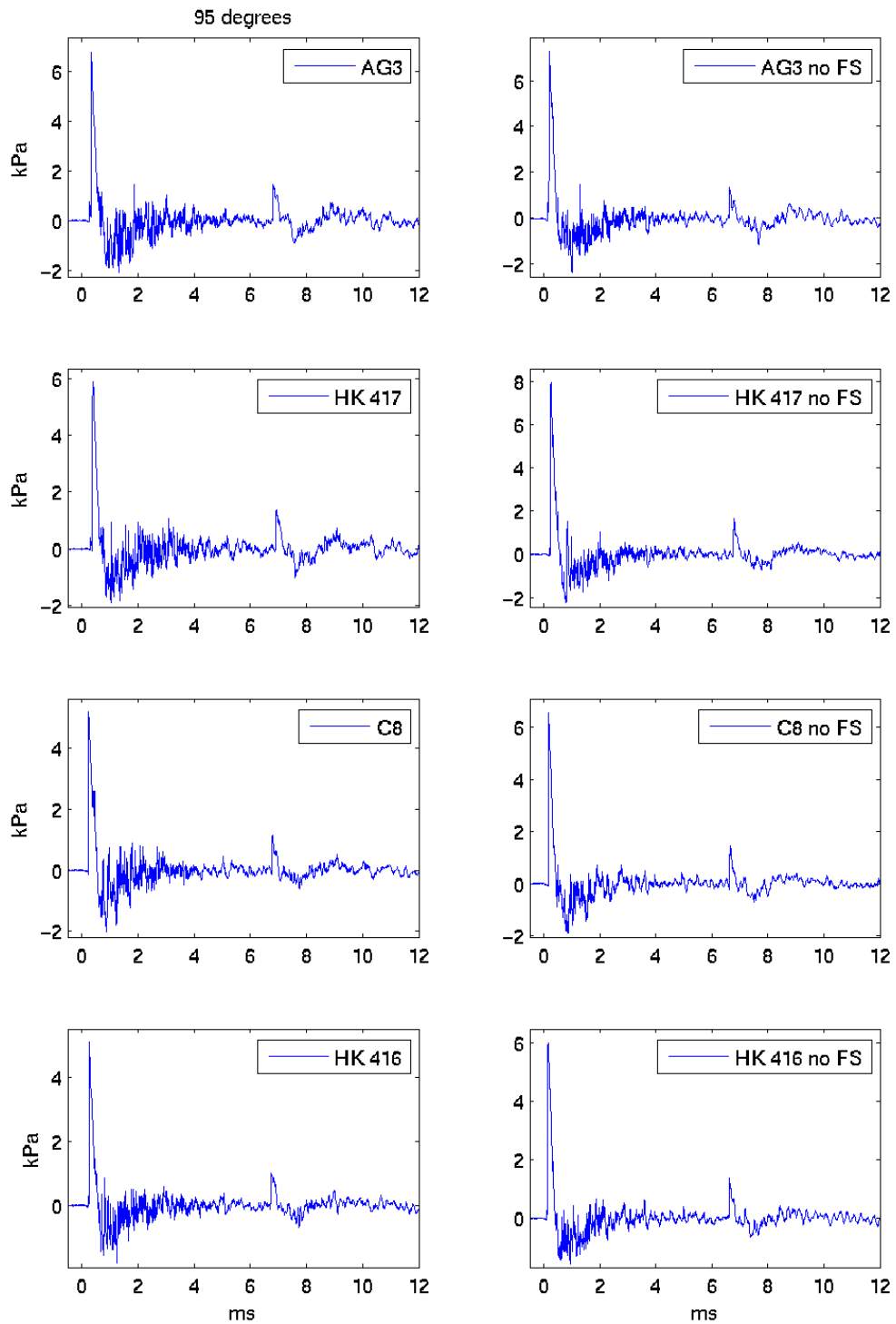


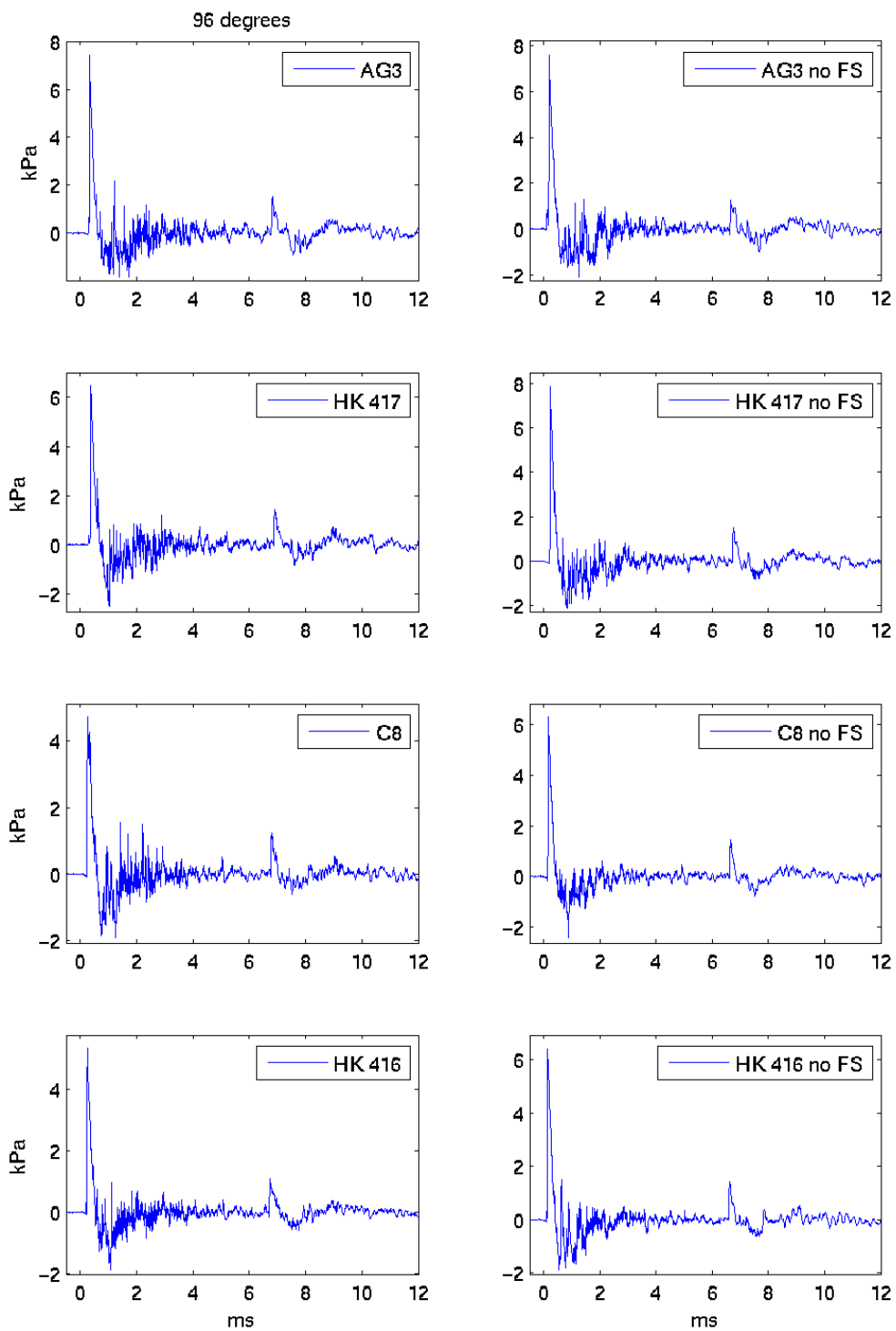
93 degrees



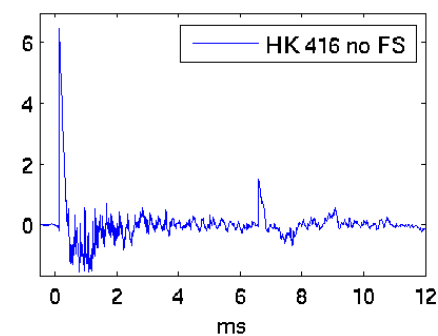
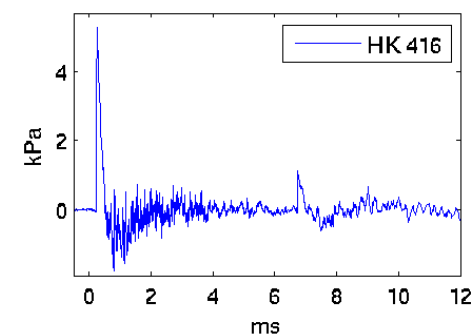
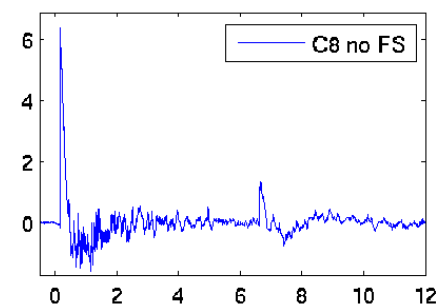
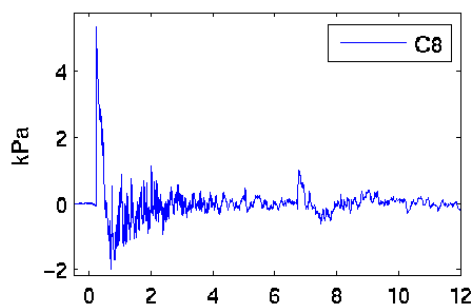
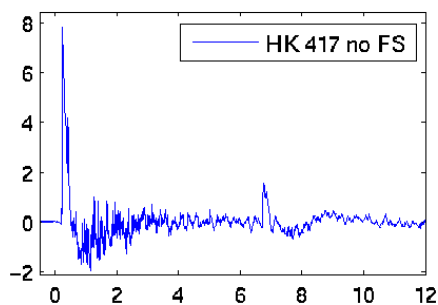
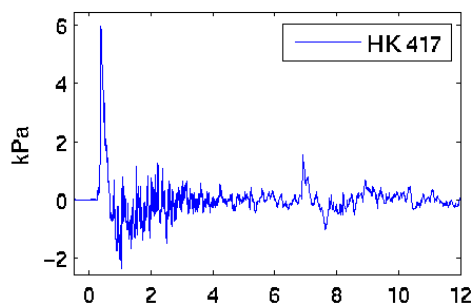
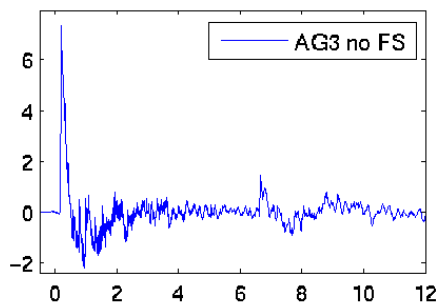
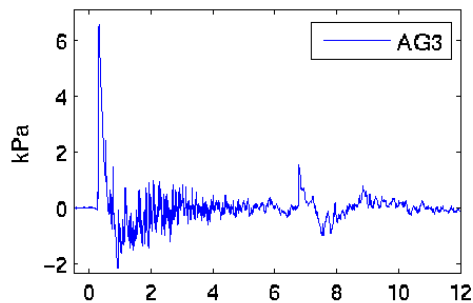
94 degrees



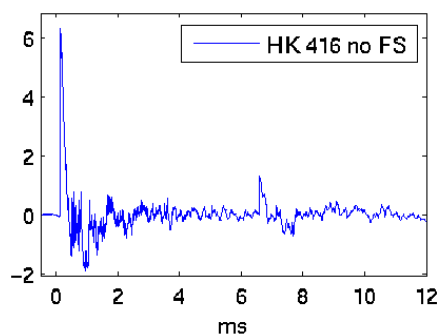
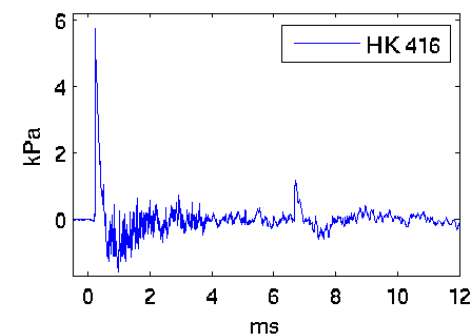
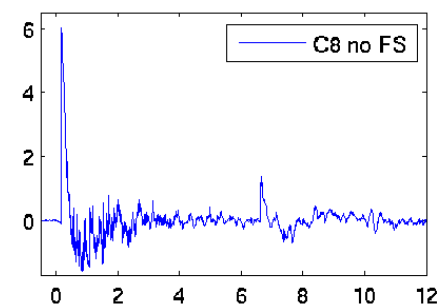
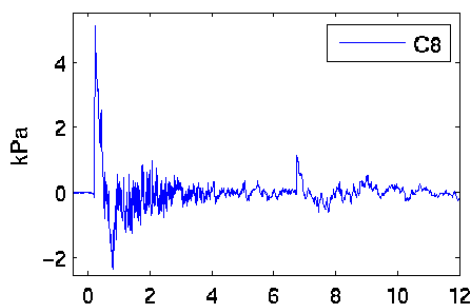
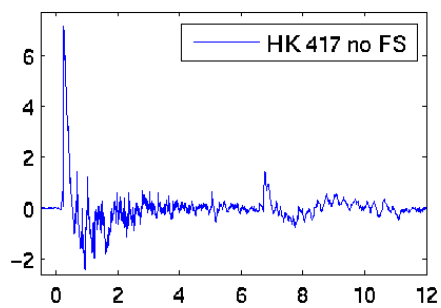
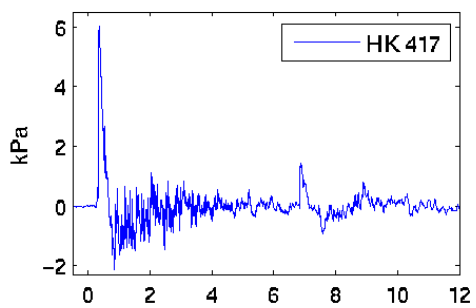
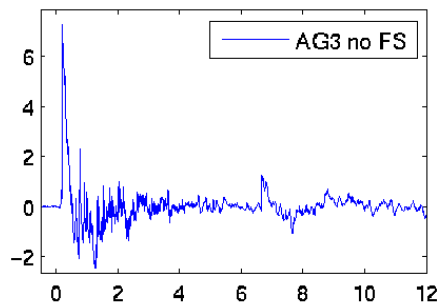
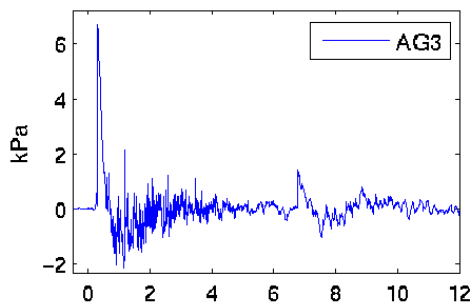




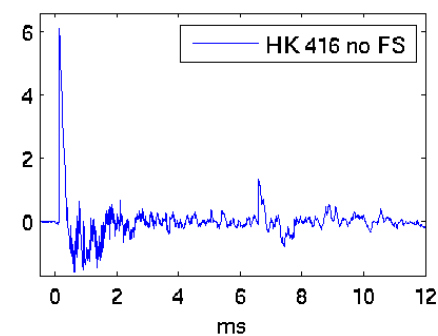
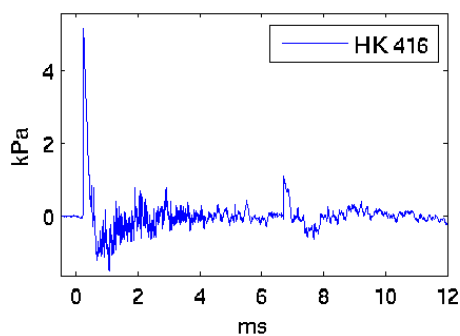
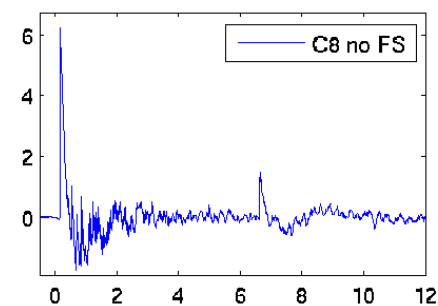
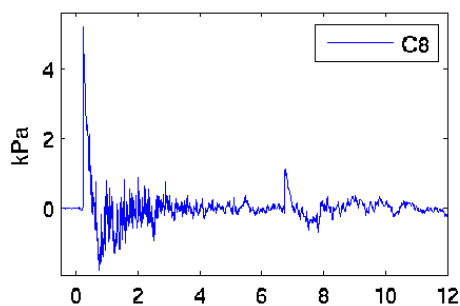
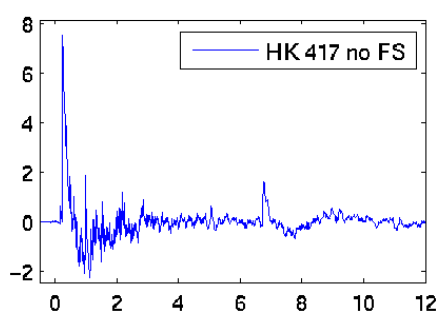
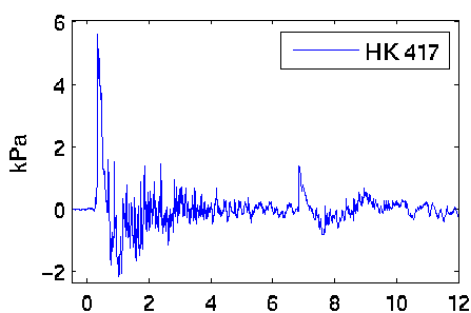
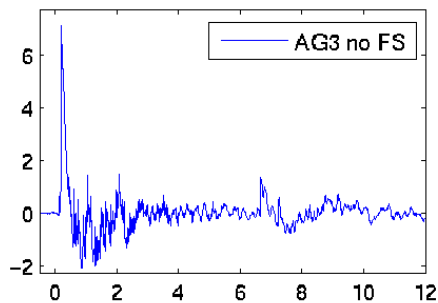
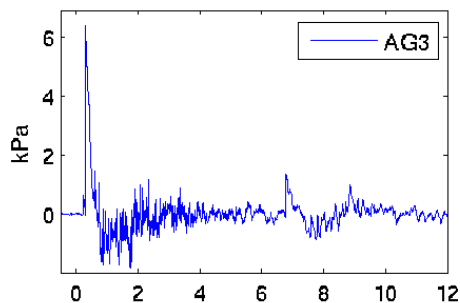
97 degrees

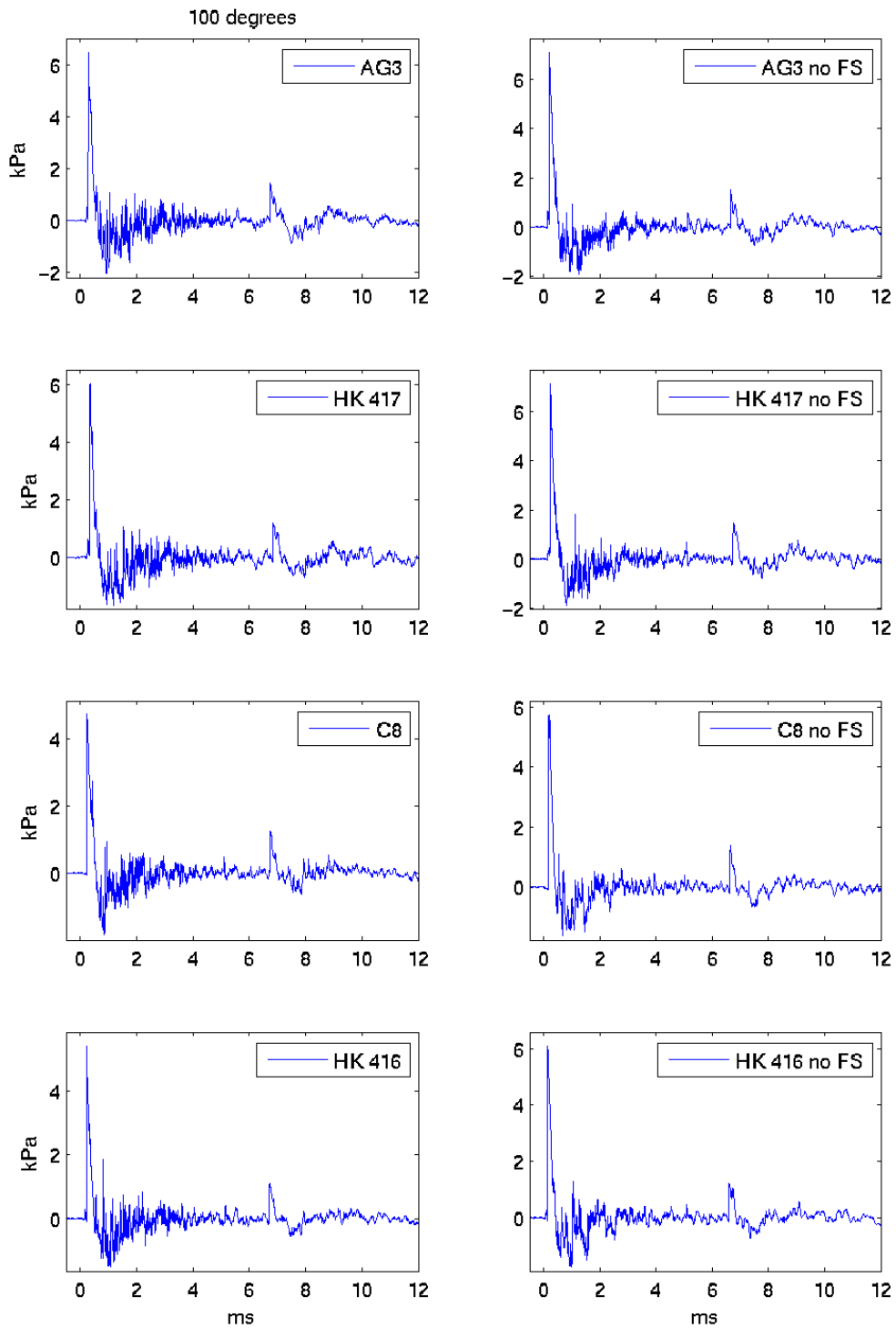


98 degrees

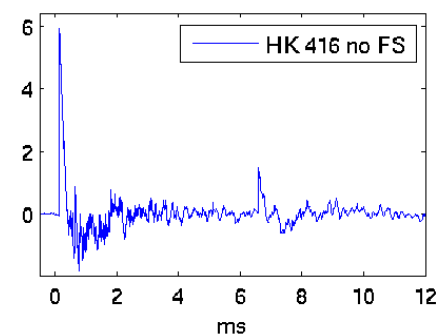
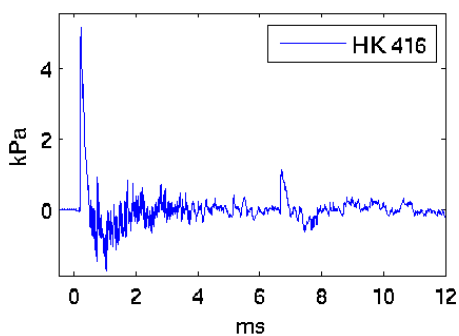
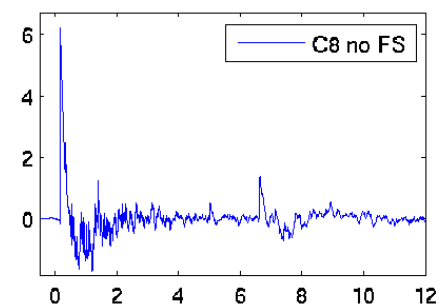
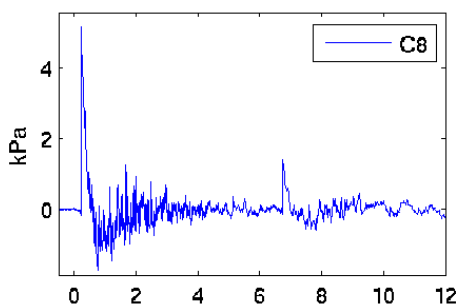
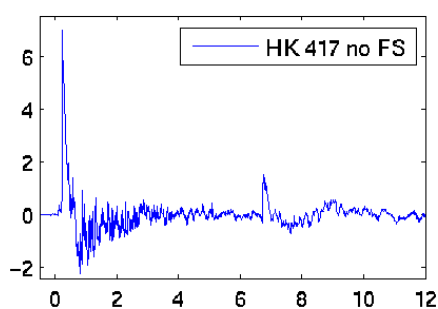
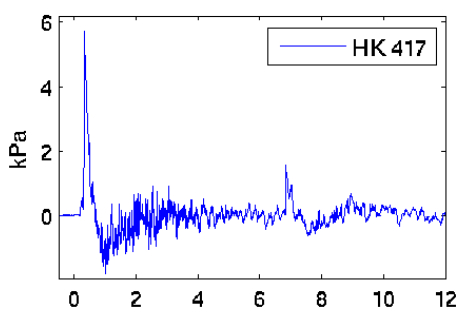
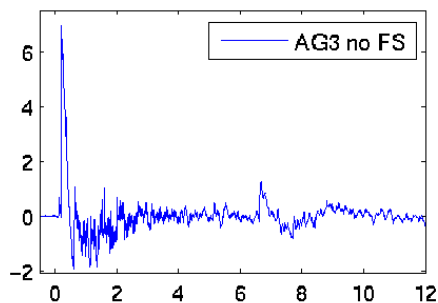
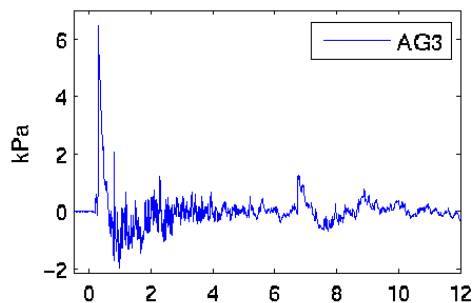


99 degrees

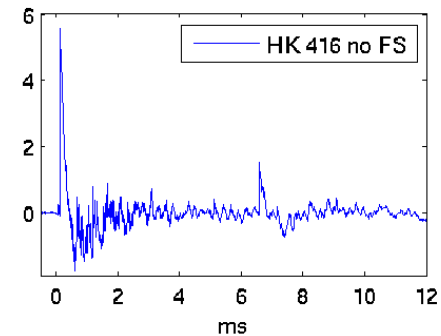
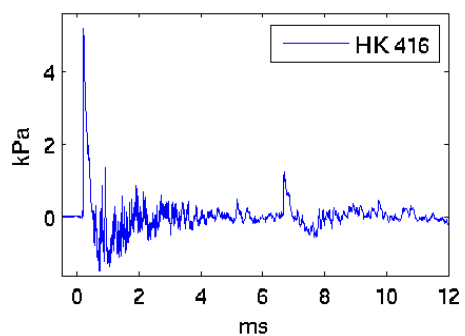
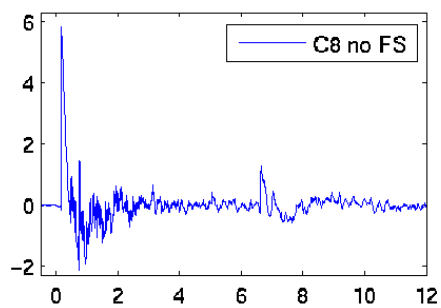
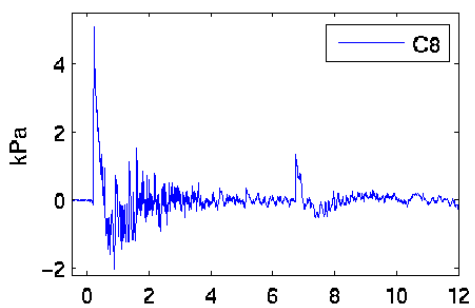
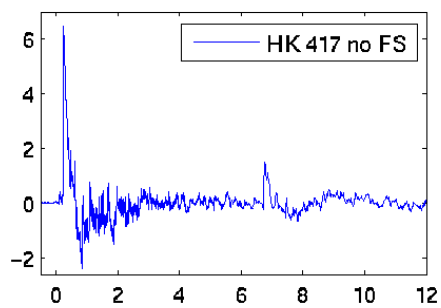
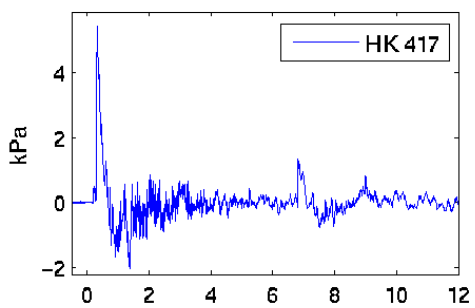
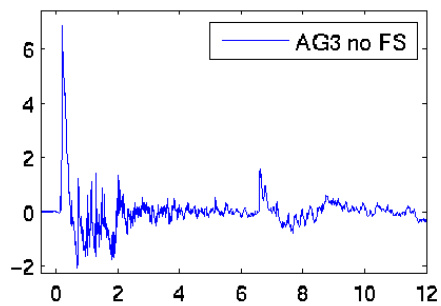
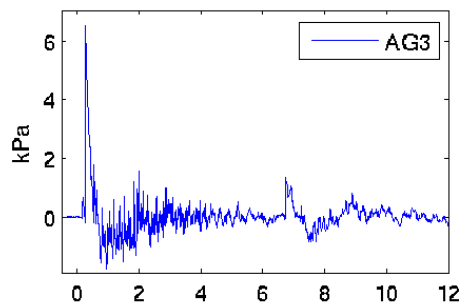




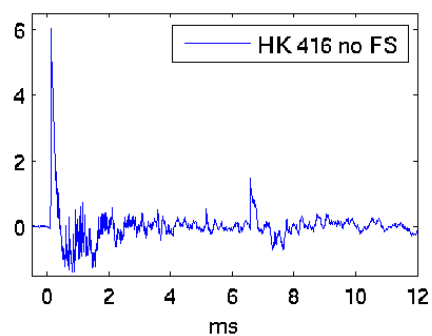
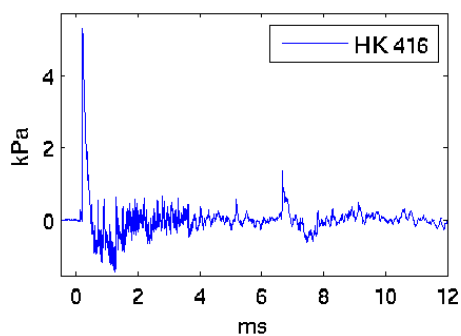
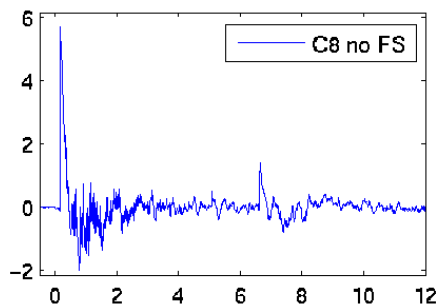
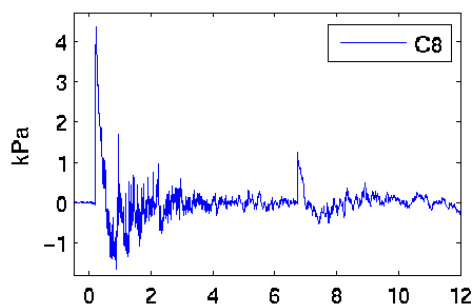
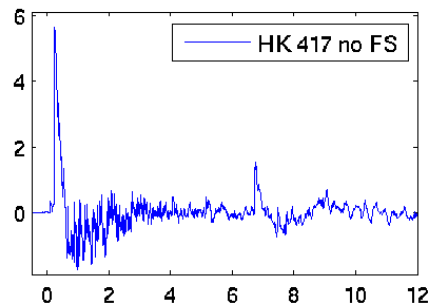
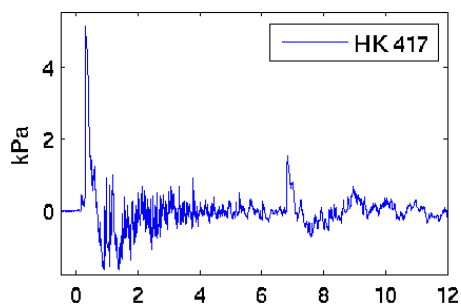
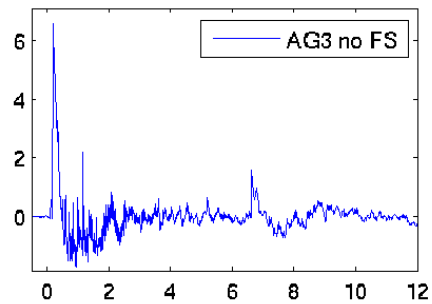
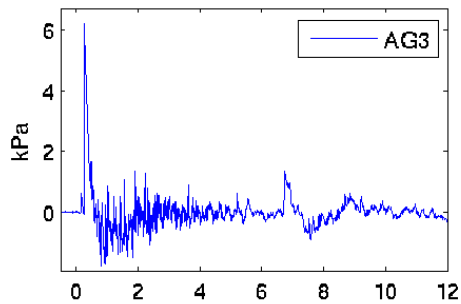
101 degrees



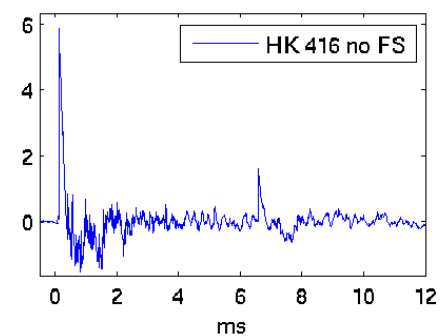
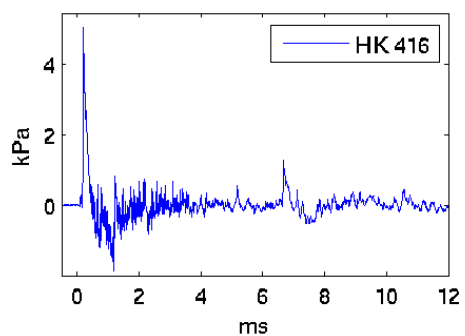
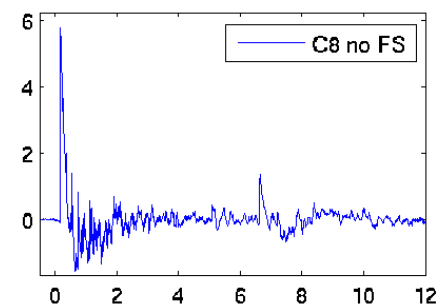
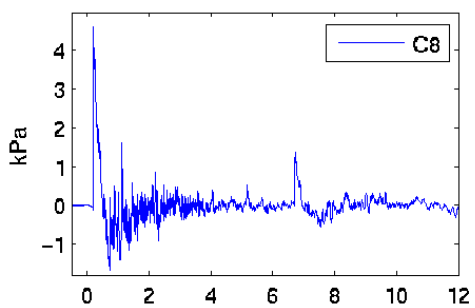
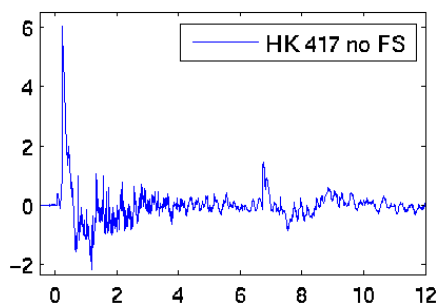
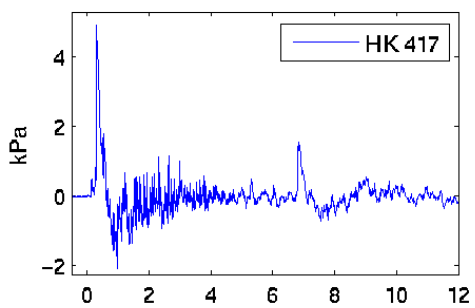
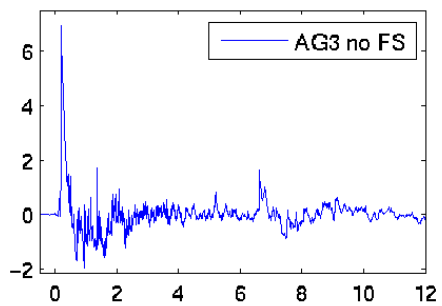
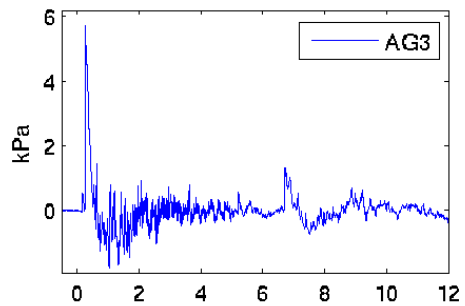
102 degrees



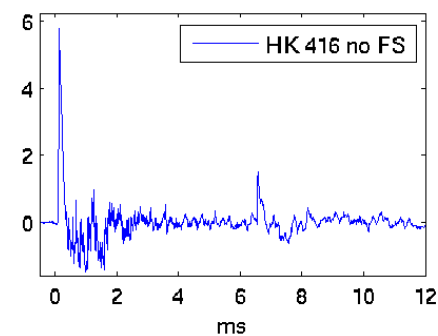
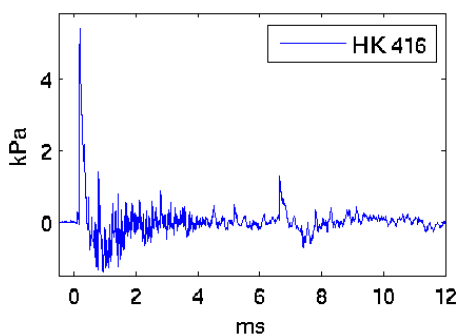
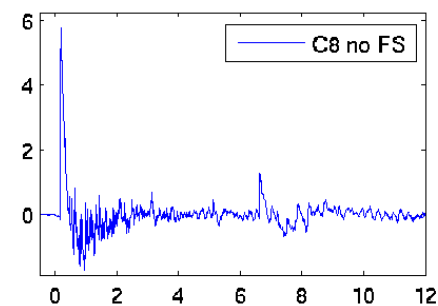
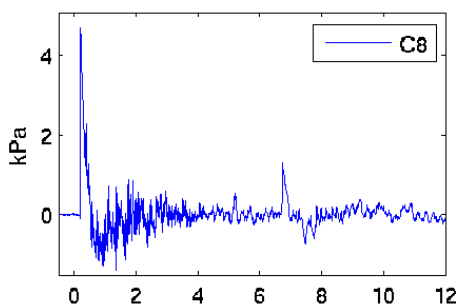
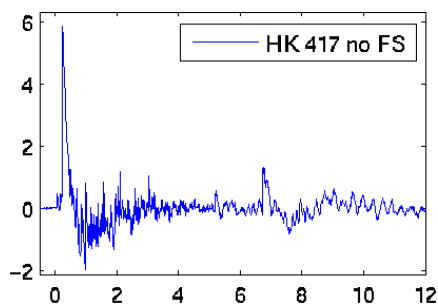
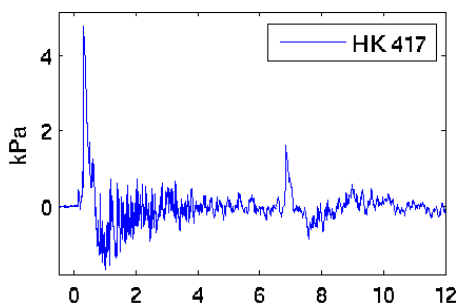
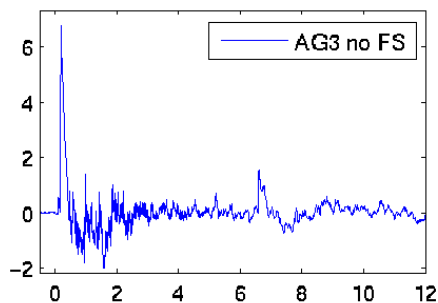
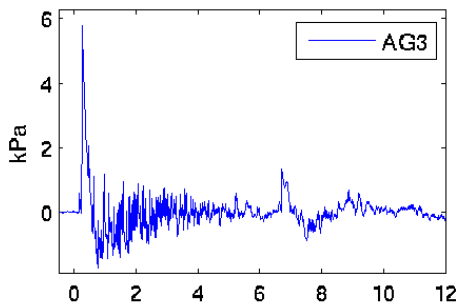
103 degrees



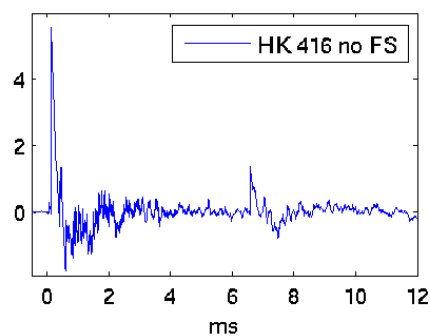
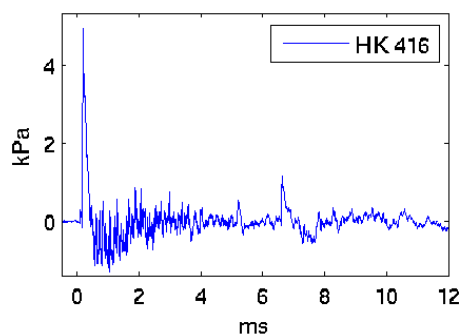
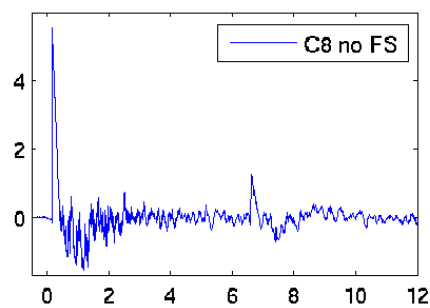
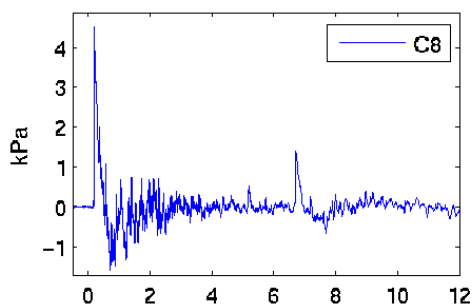
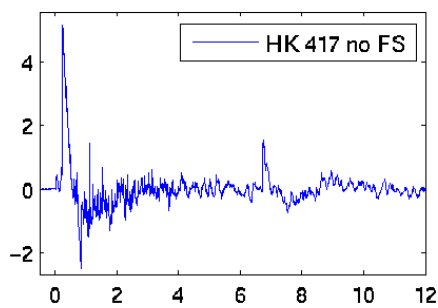
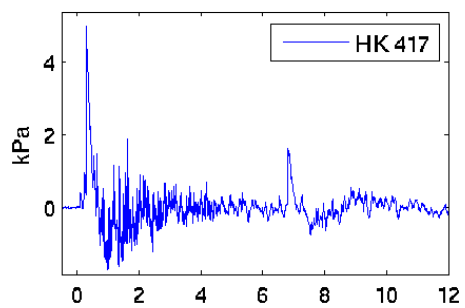
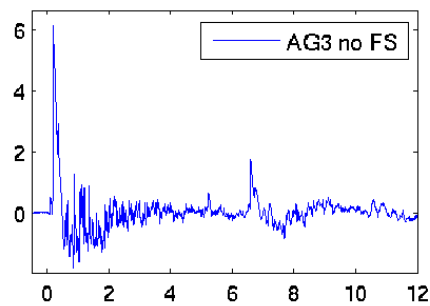
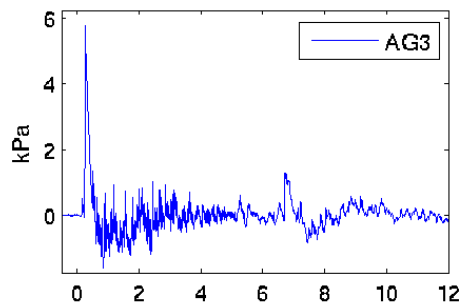
104 degrees



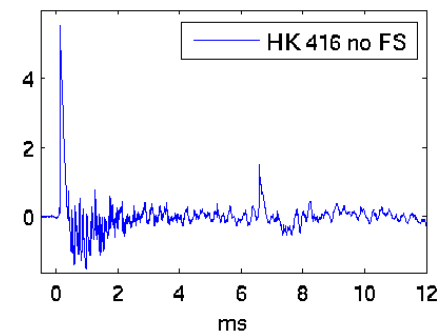
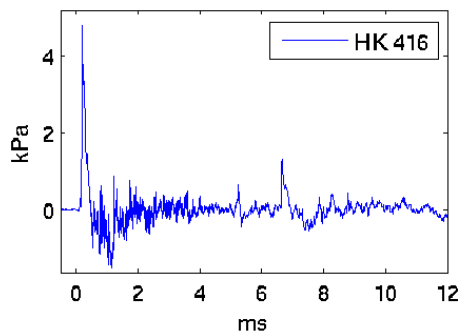
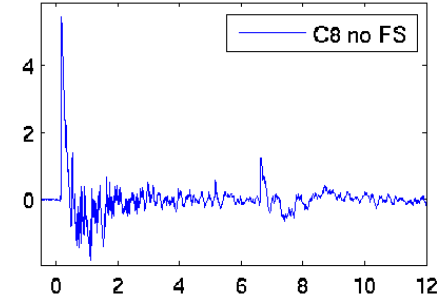
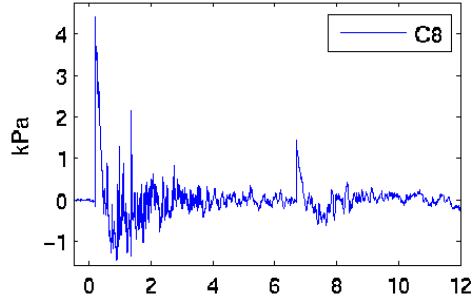
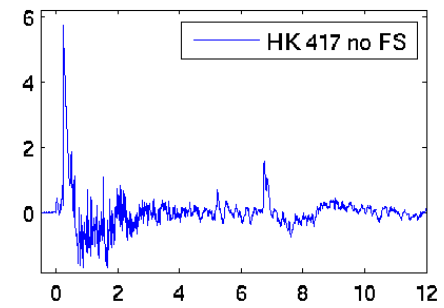
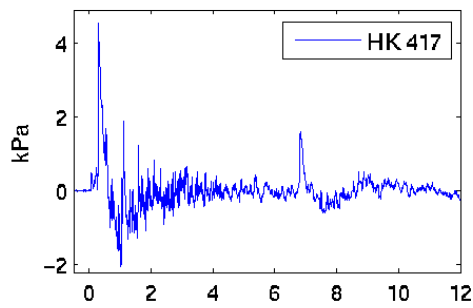
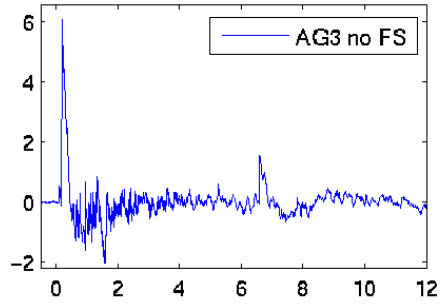
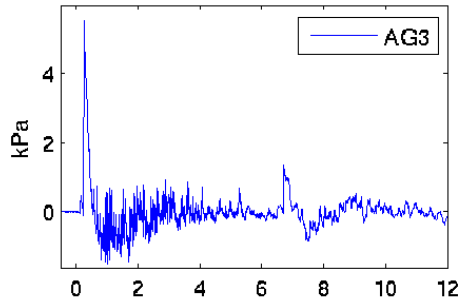
105 degrees



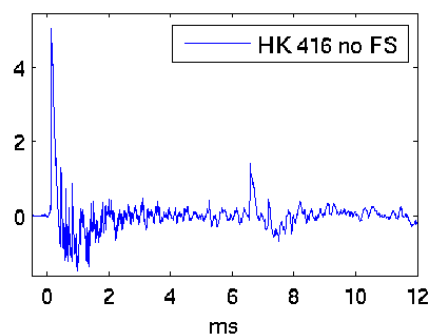
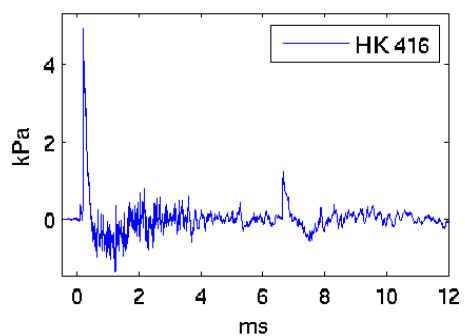
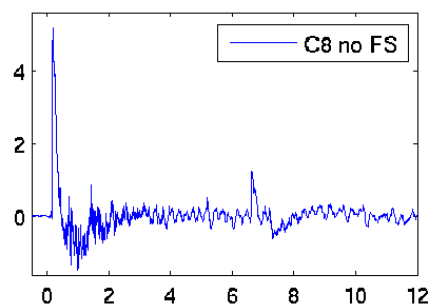
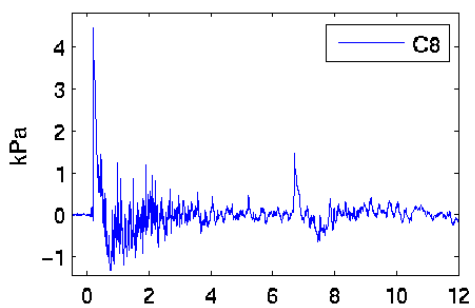
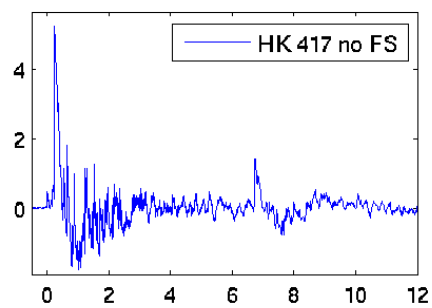
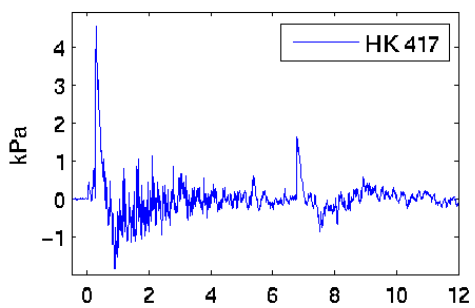
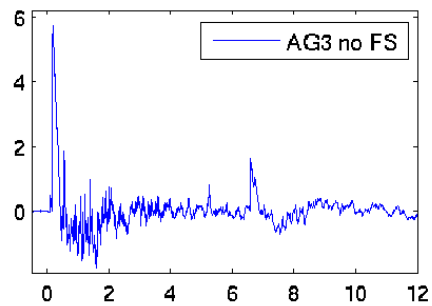
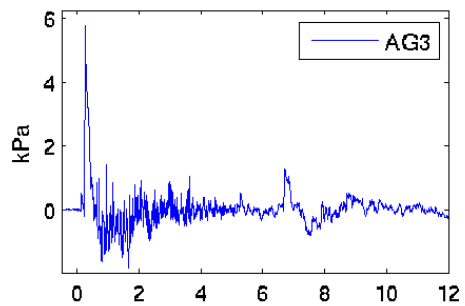
106 degrees



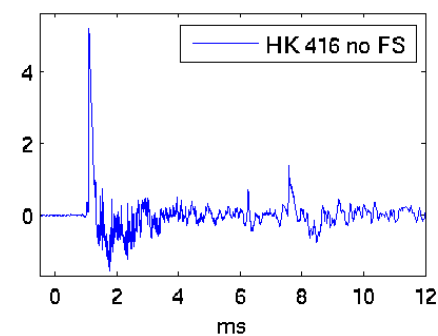
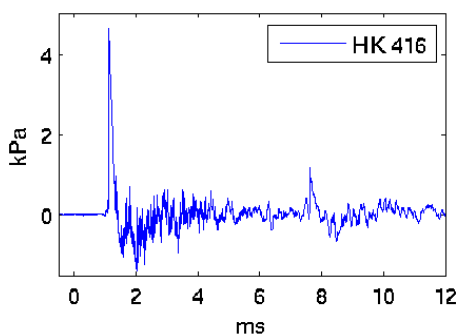
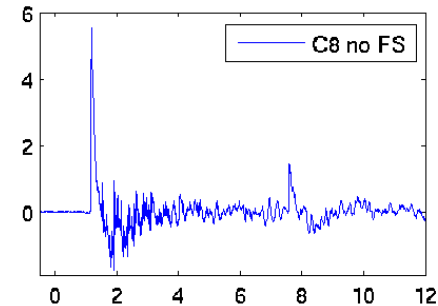
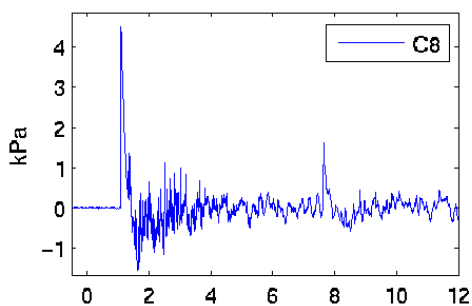
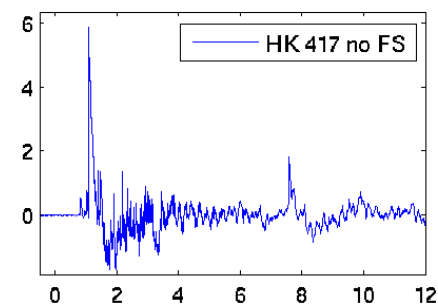
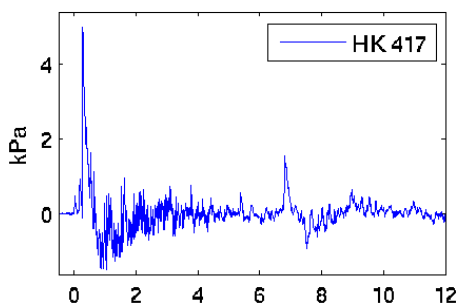
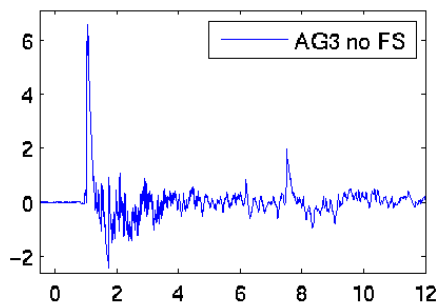
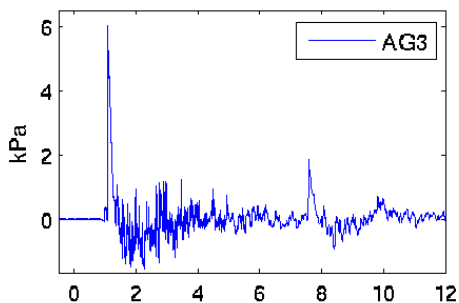
107 degrees



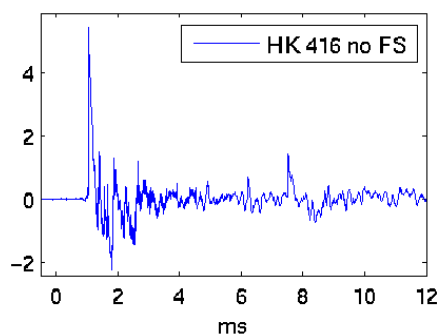
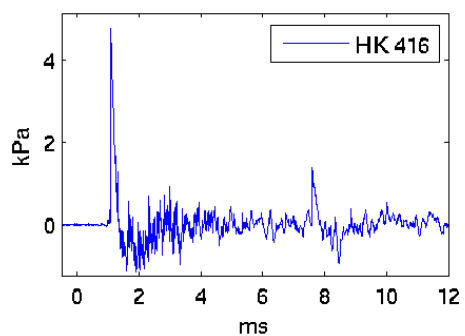
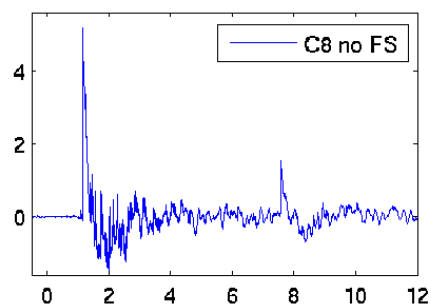
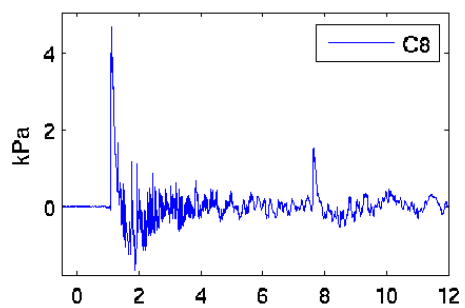
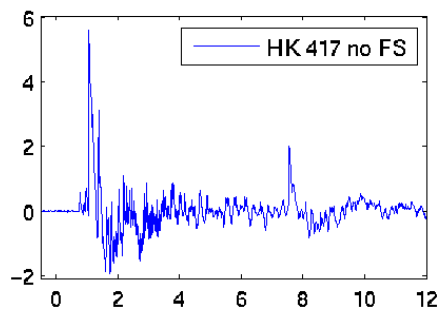
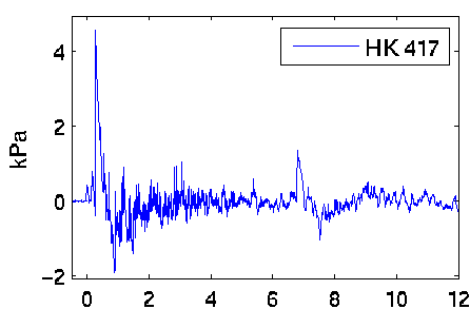
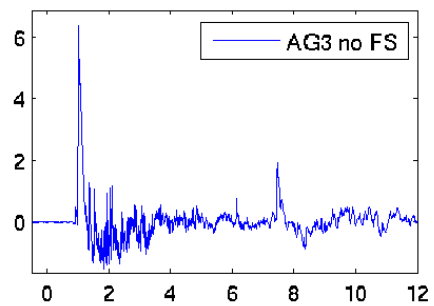
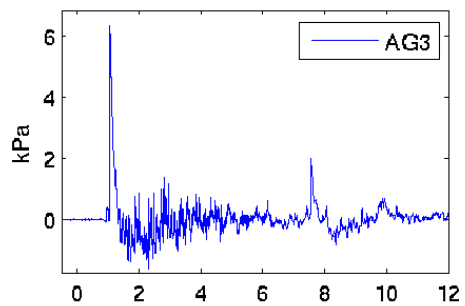
108 degrees



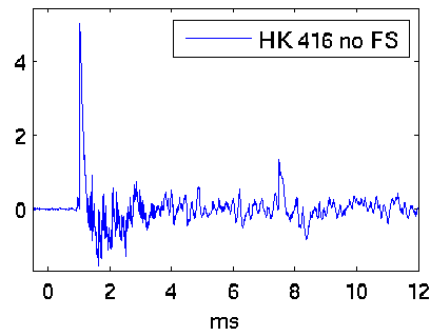
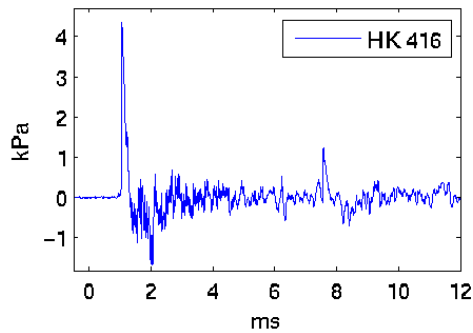
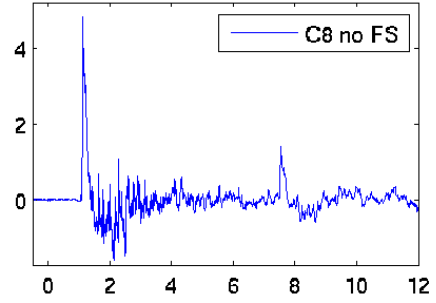
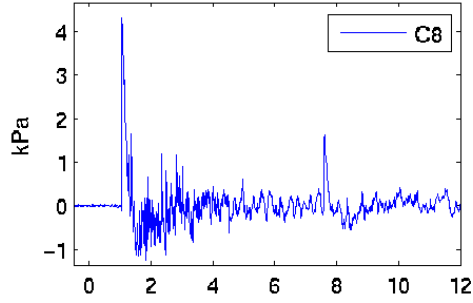
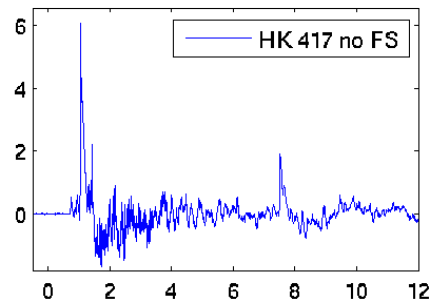
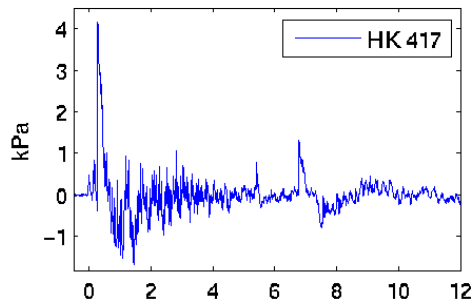
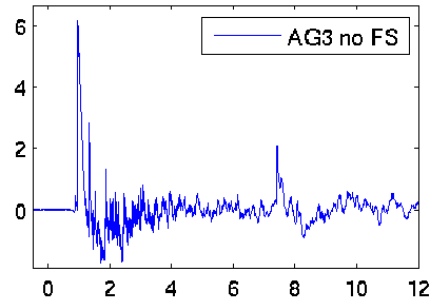
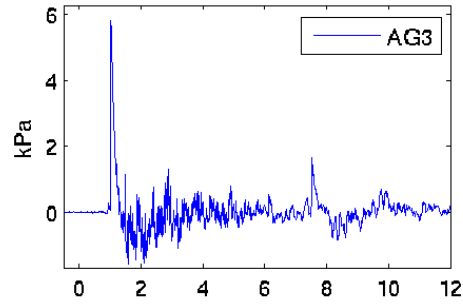
109 degrees



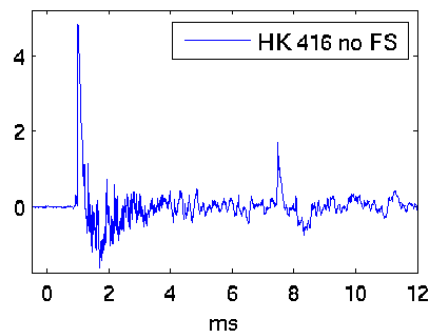
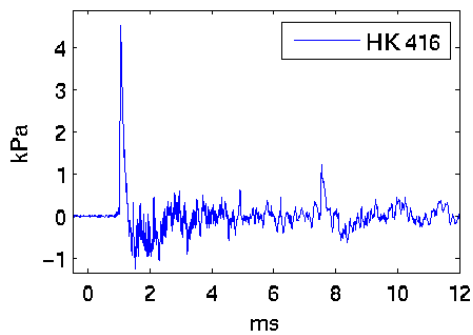
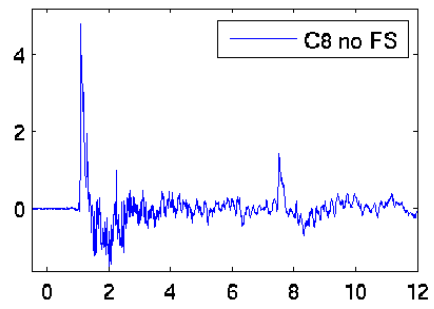
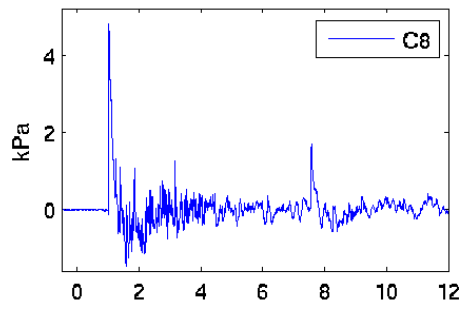
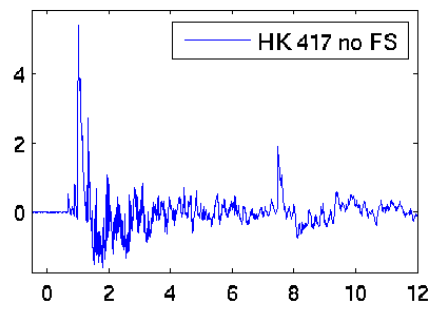
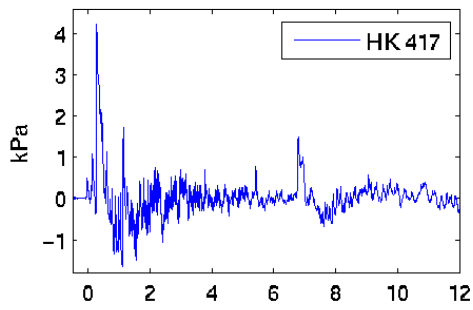
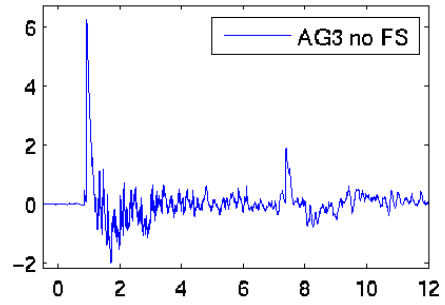
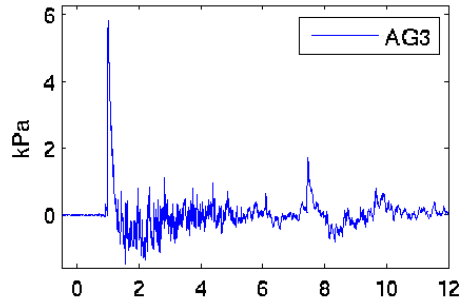
110 degrees



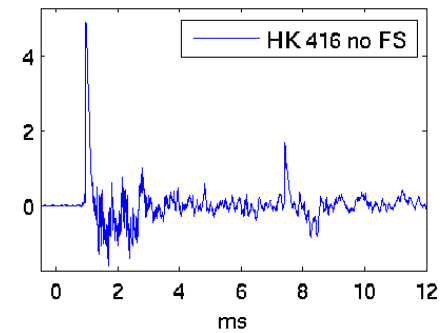
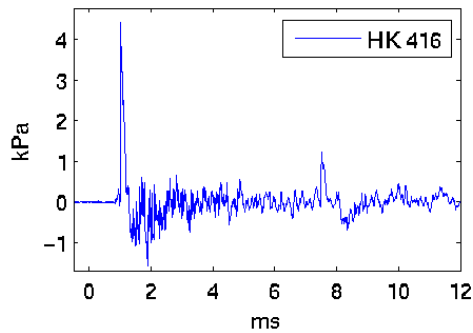
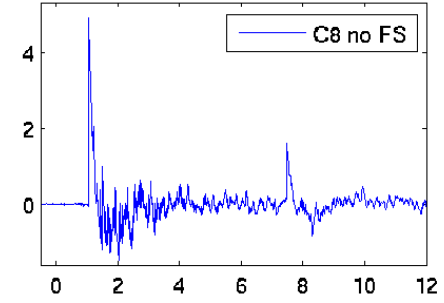
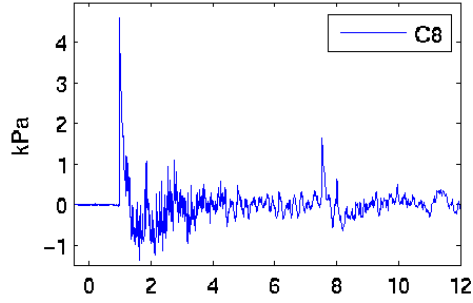
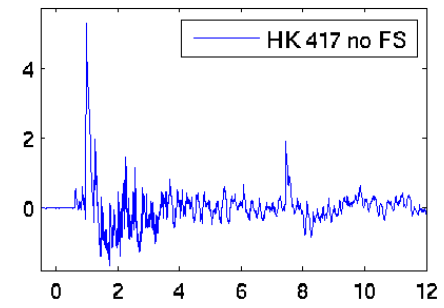
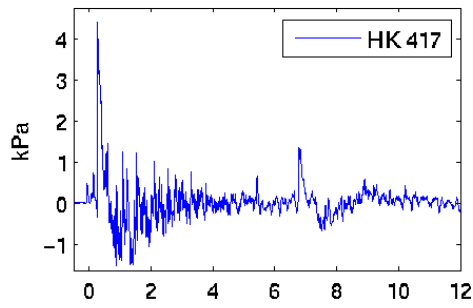
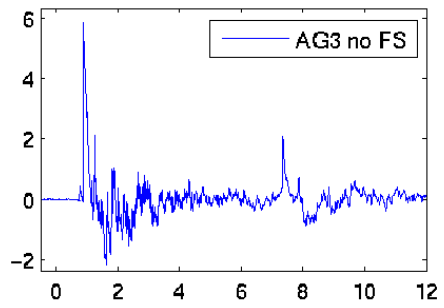
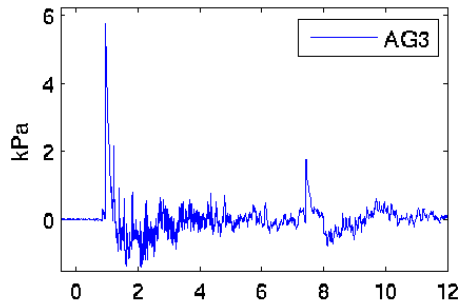
111 degrees



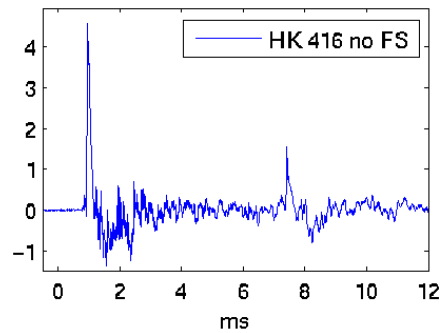
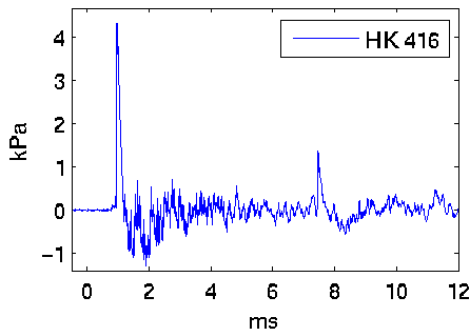
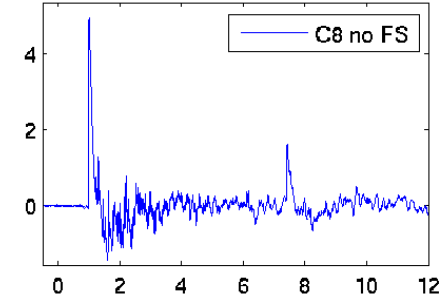
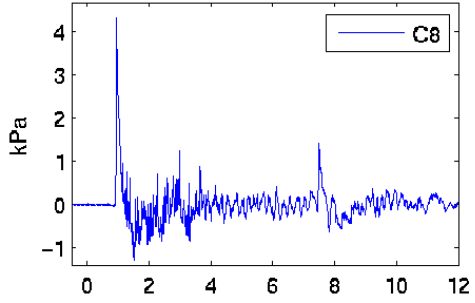
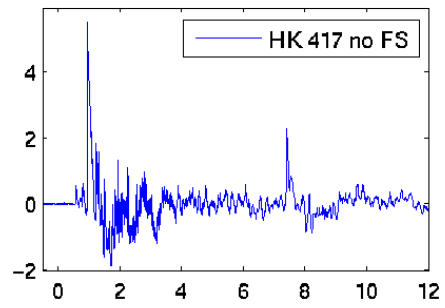
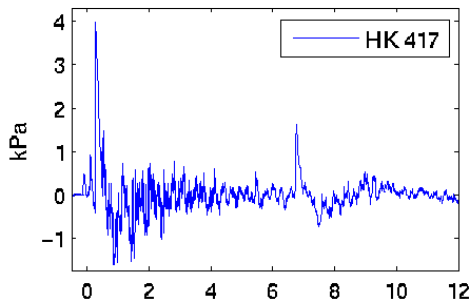
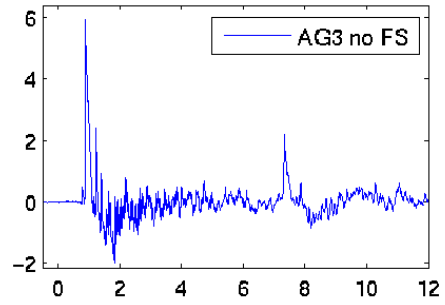
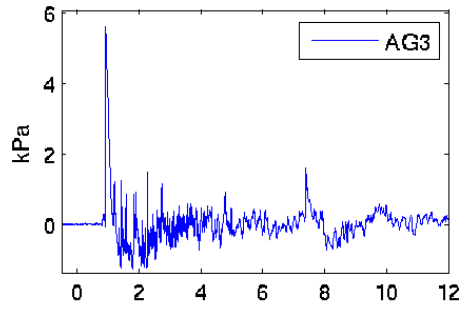
112 degrees



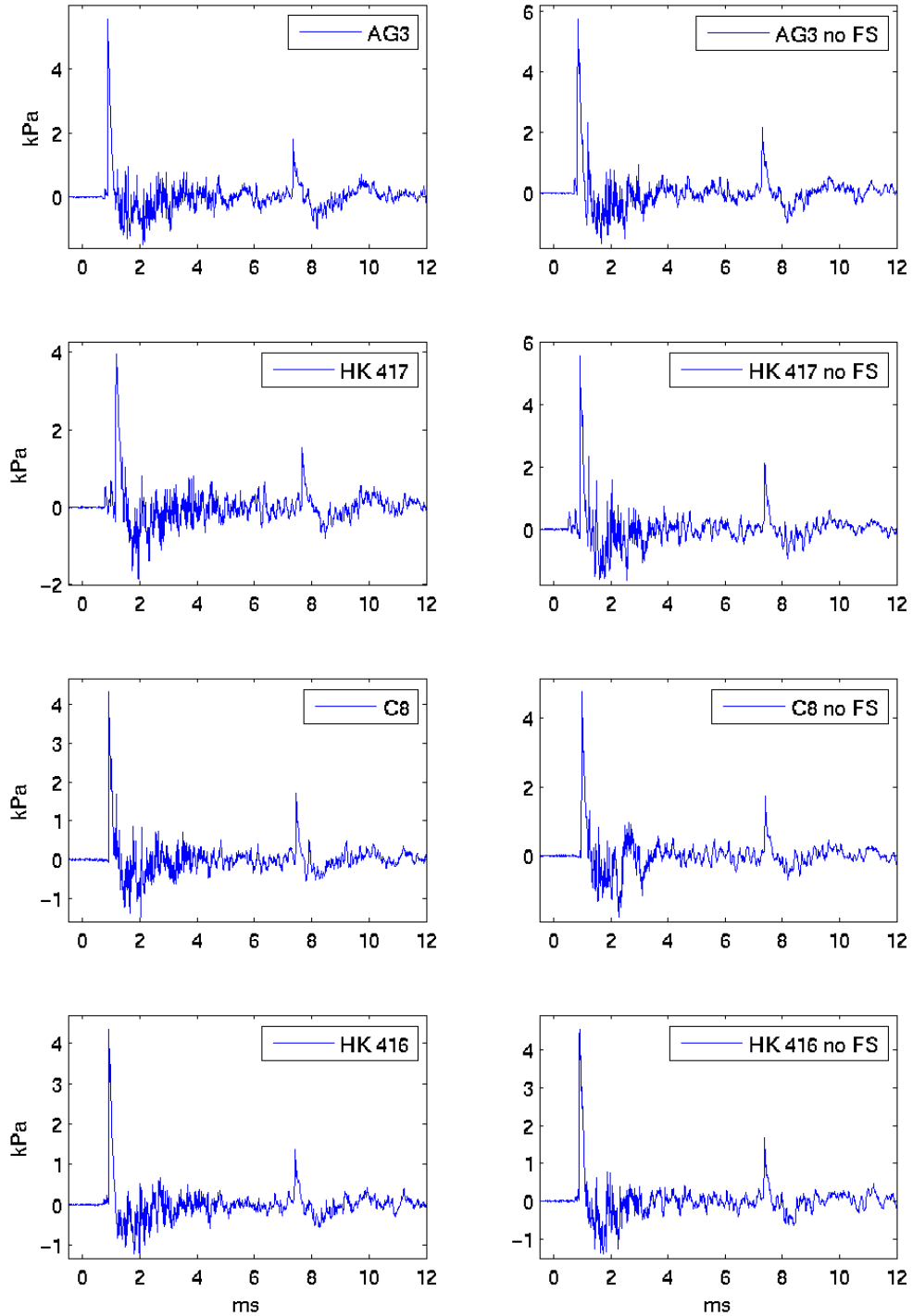
113 degrees



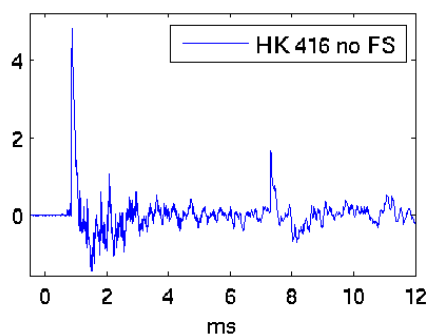
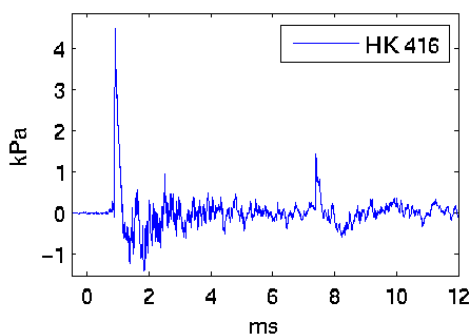
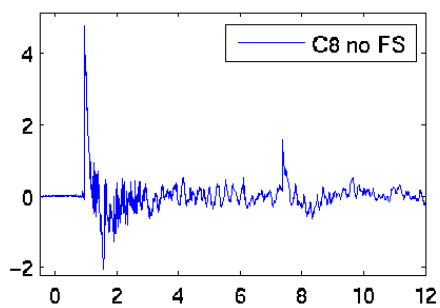
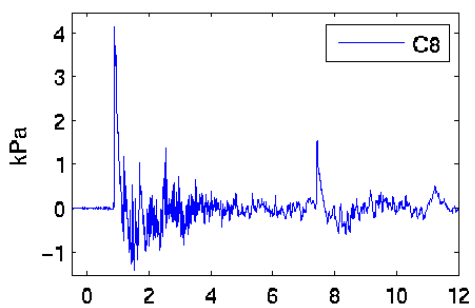
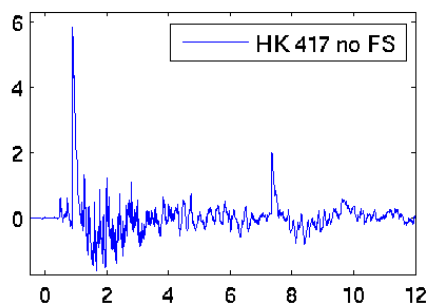
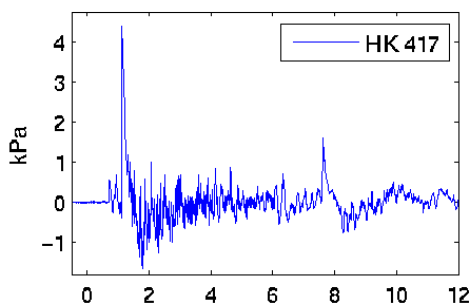
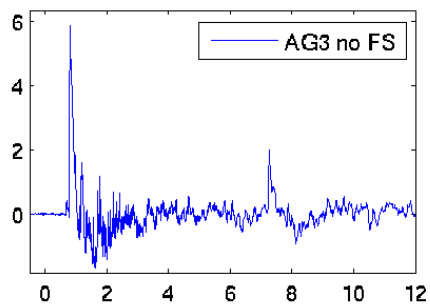
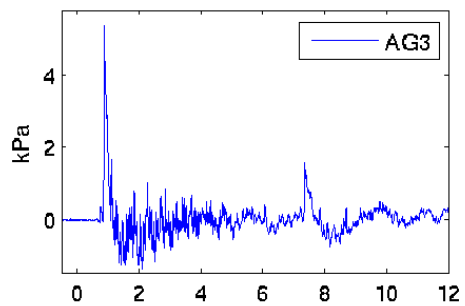
114 degrees



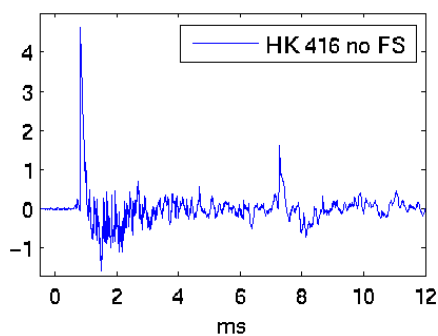
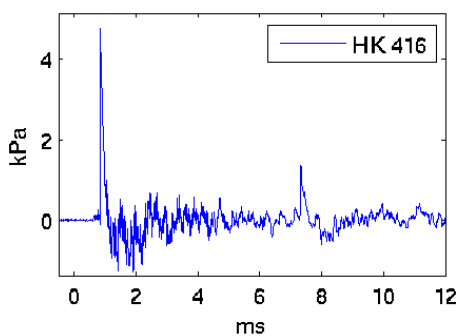
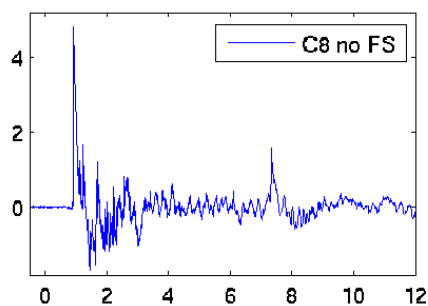
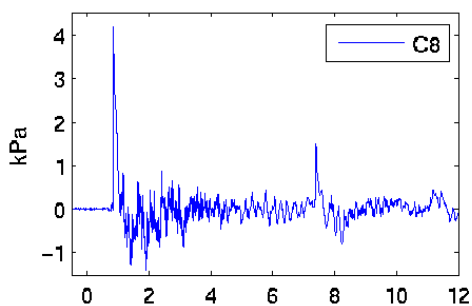
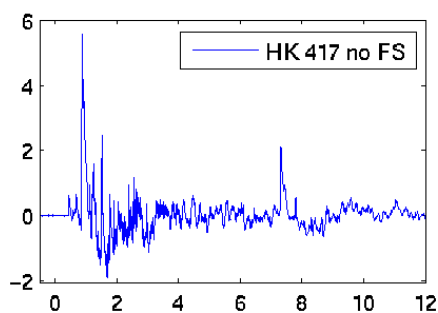
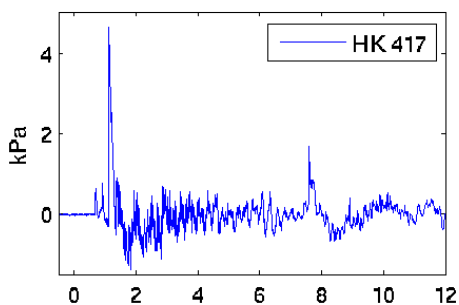
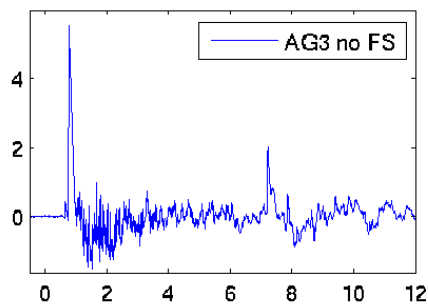
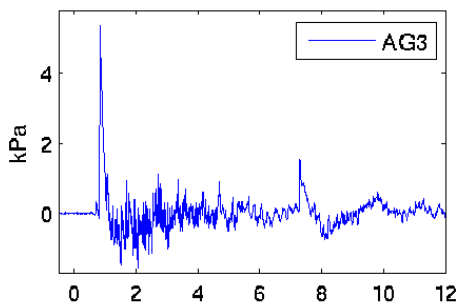
115 degrees



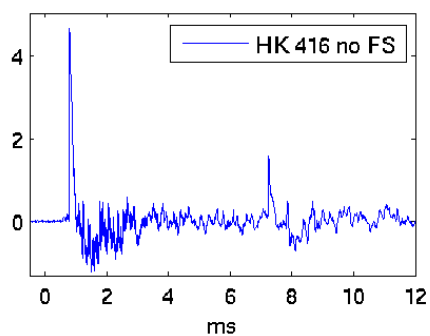
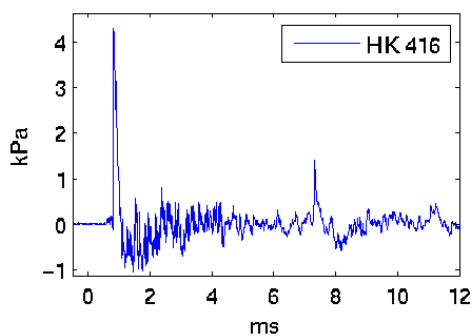
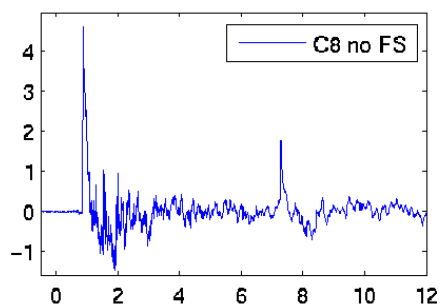
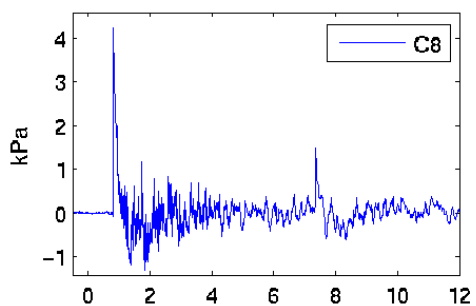
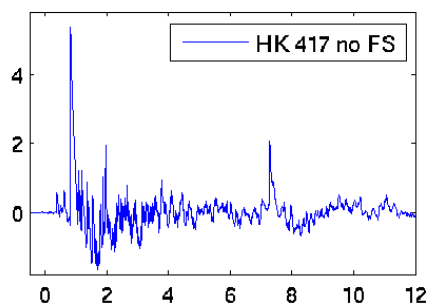
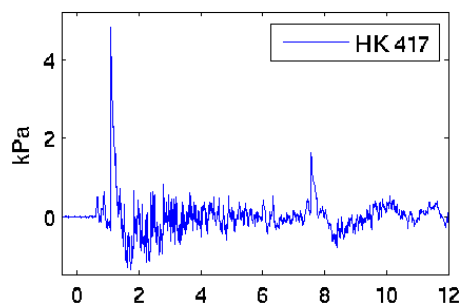
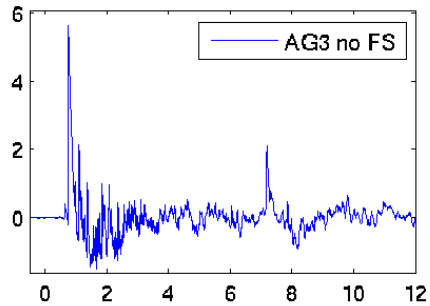
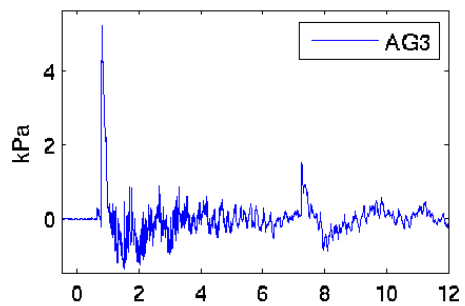
116 degrees



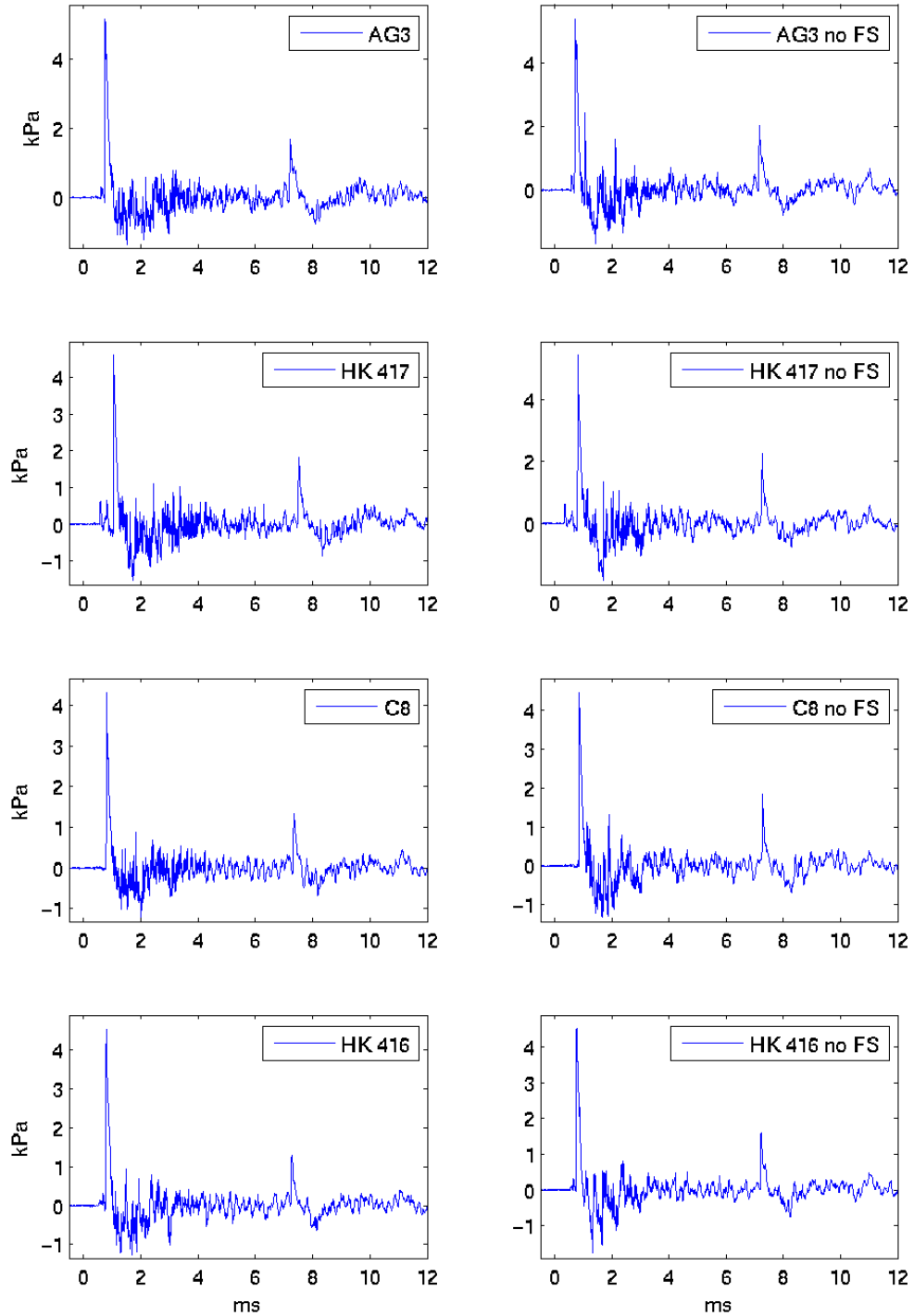
117 degrees



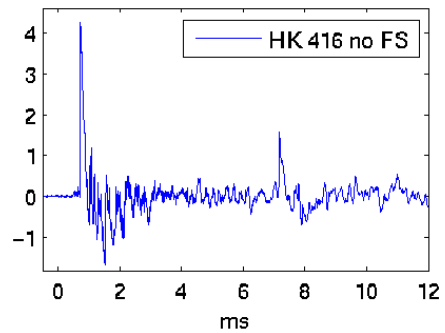
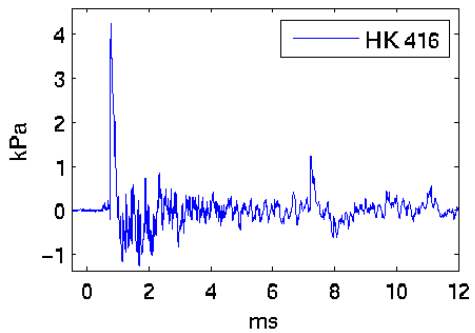
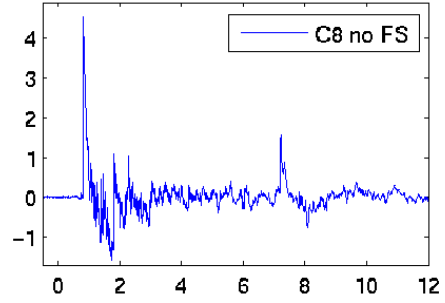
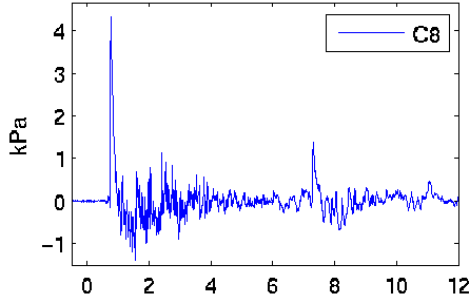
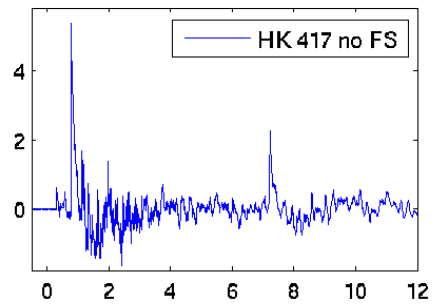
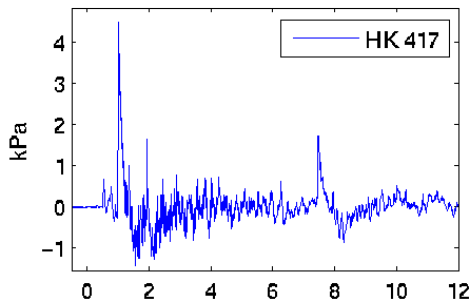
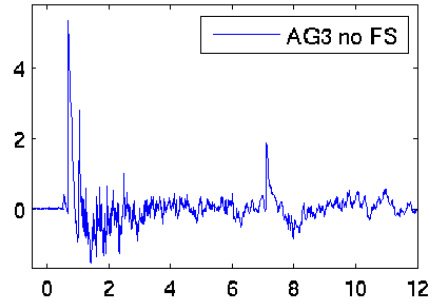
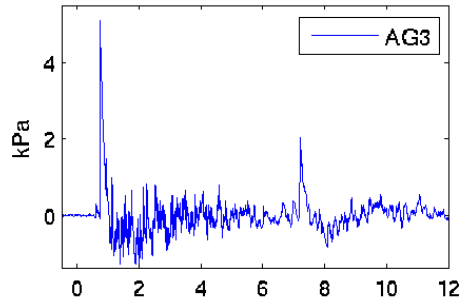
118 degrees



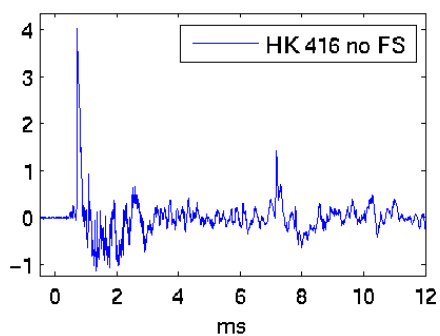
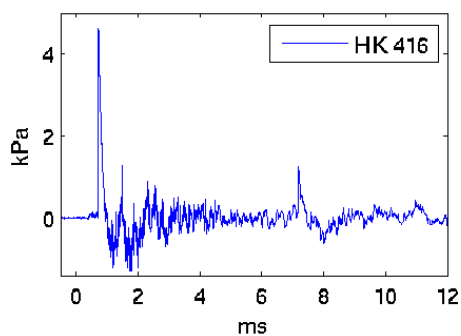
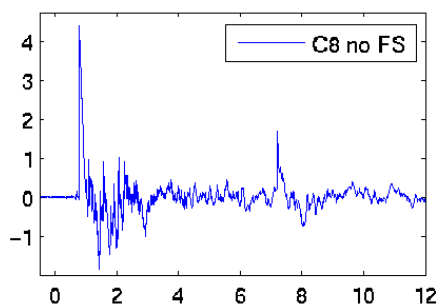
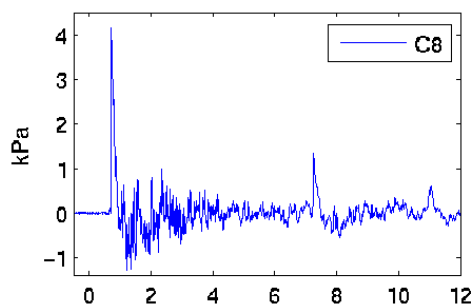
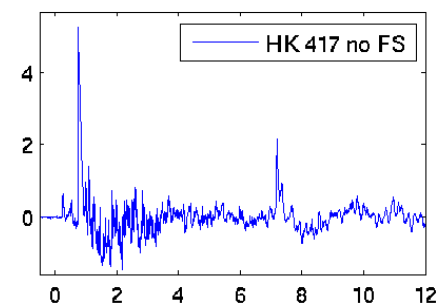
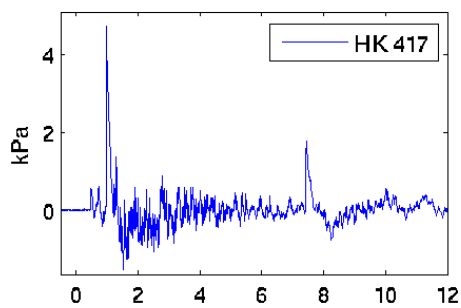
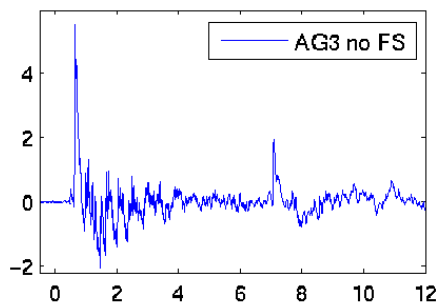
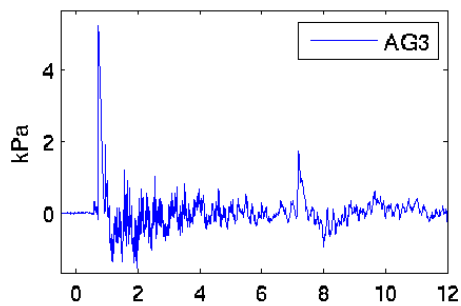
119 degrees



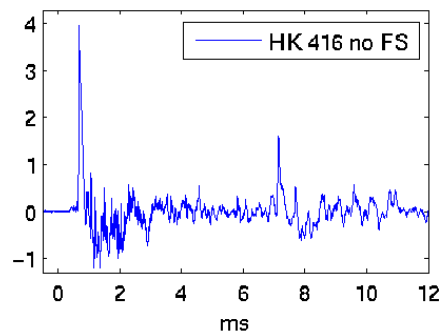
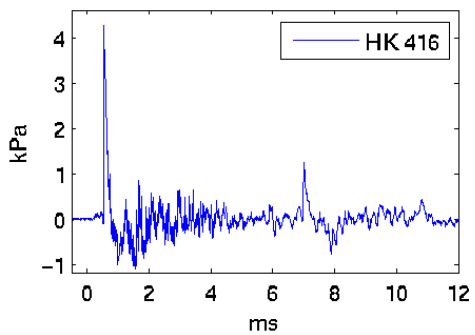
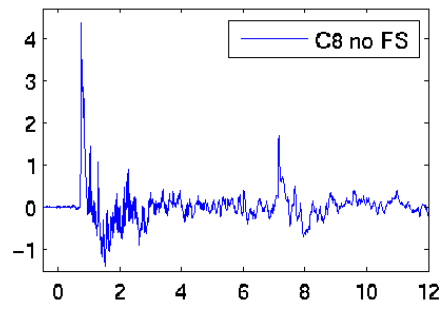
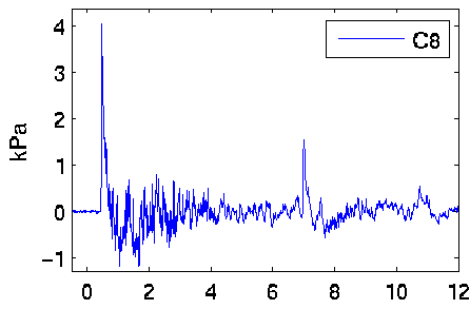
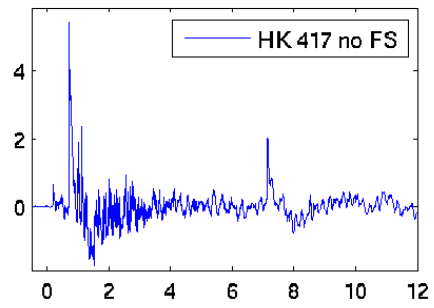
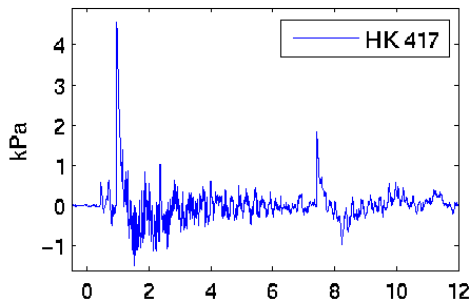
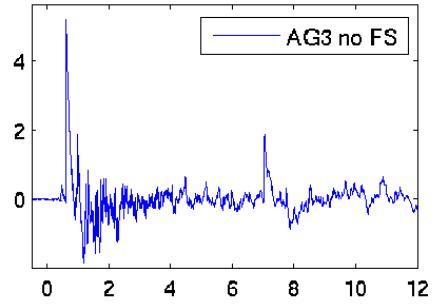
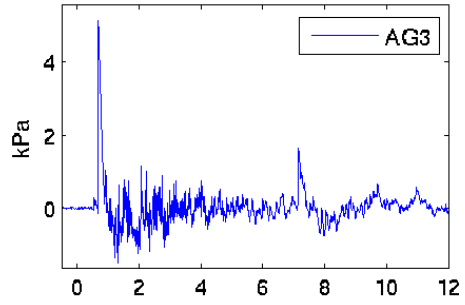
120 degrees



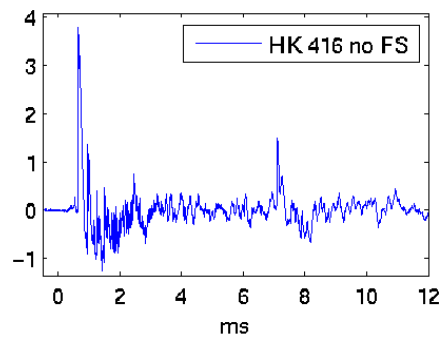
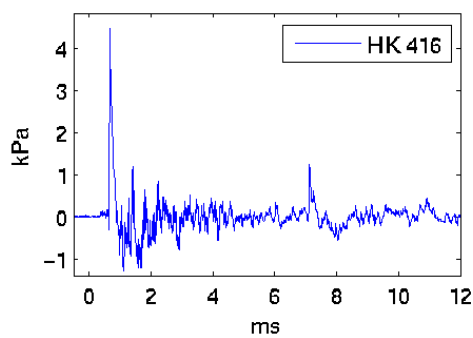
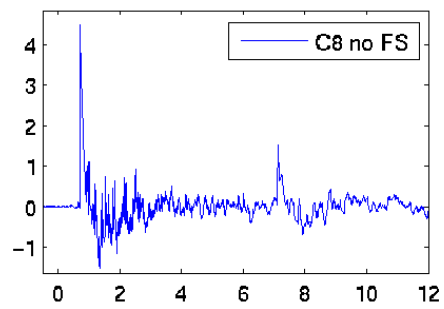
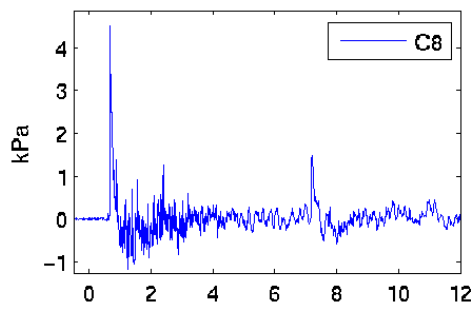
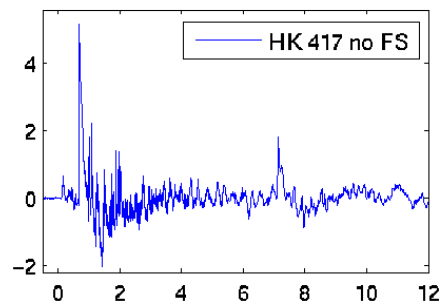
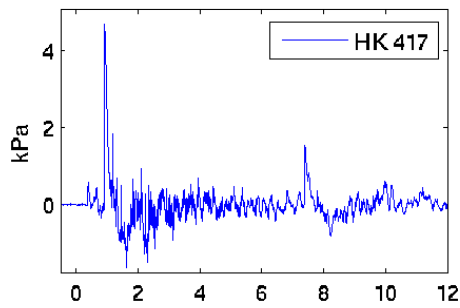
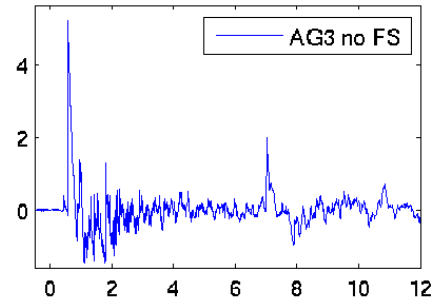
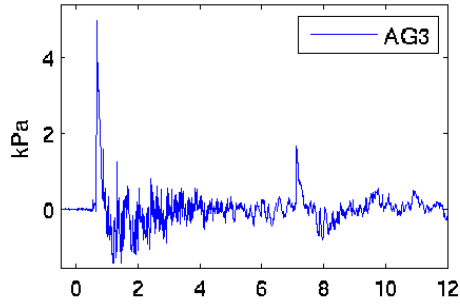
121 degrees



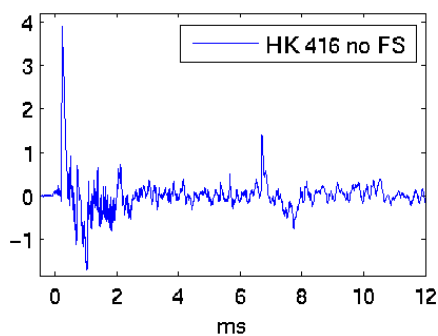
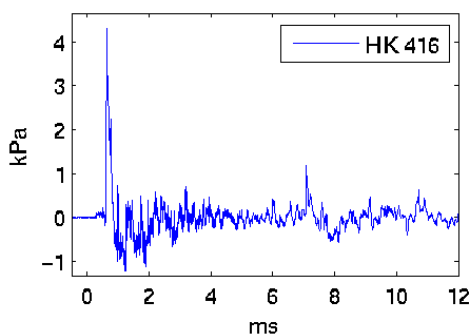
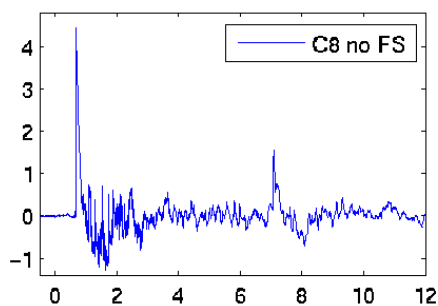
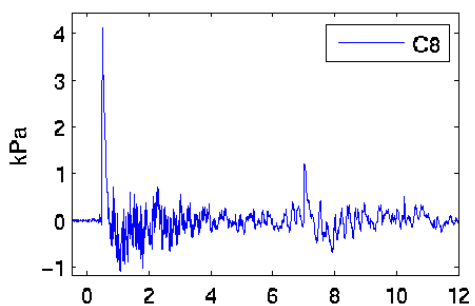
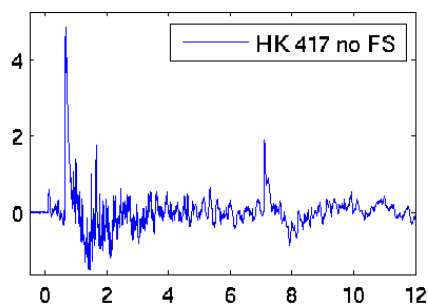
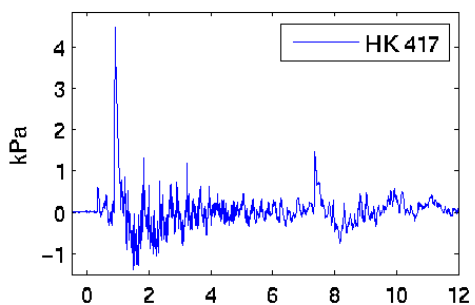
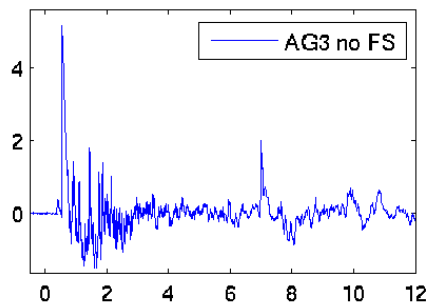
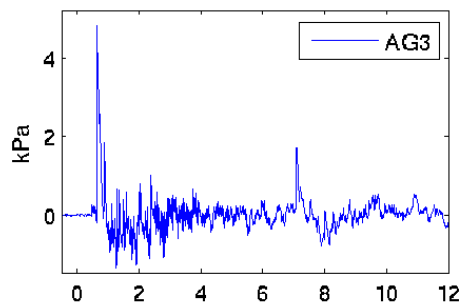
122 degrees



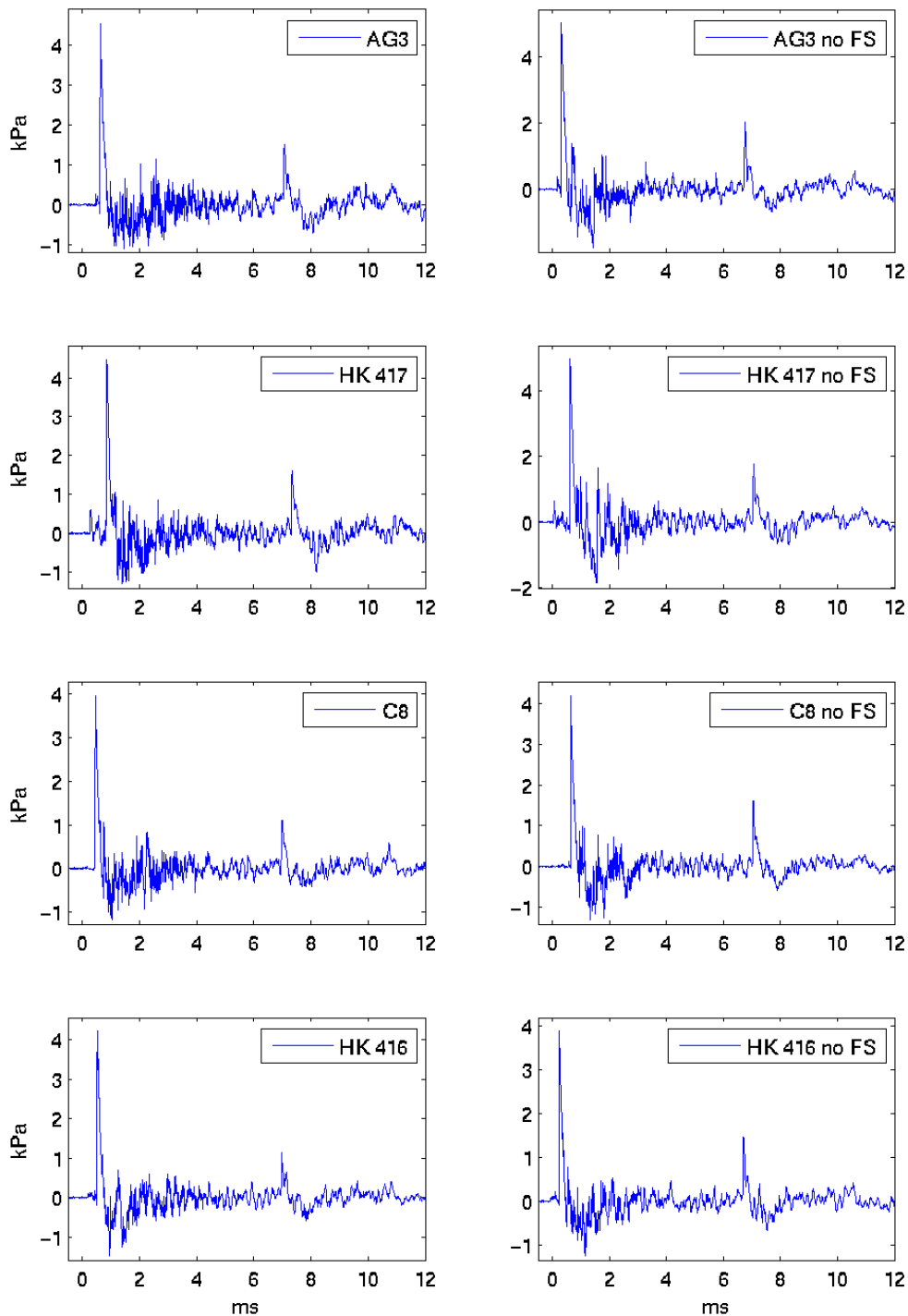
123 degrees



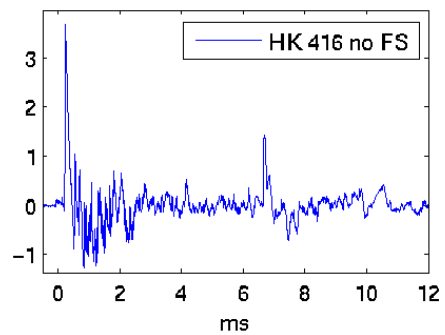
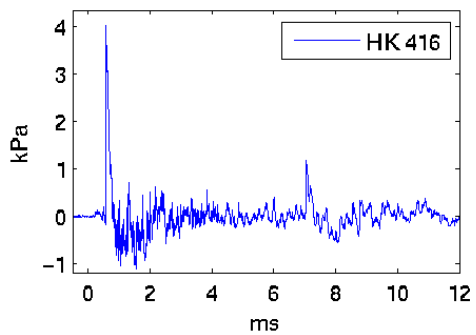
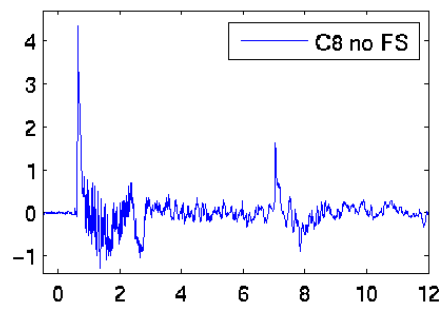
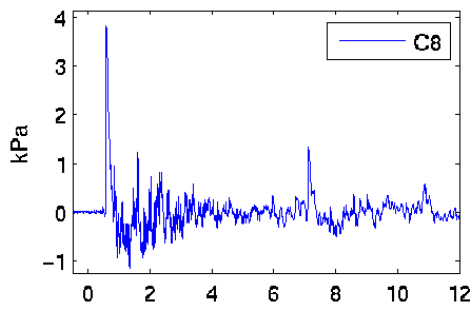
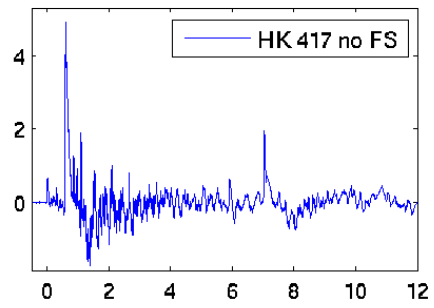
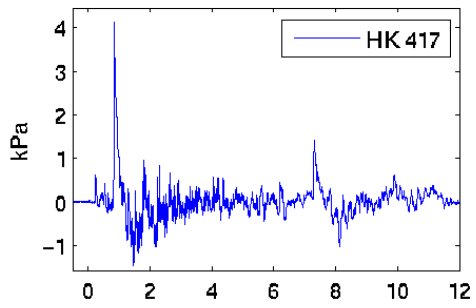
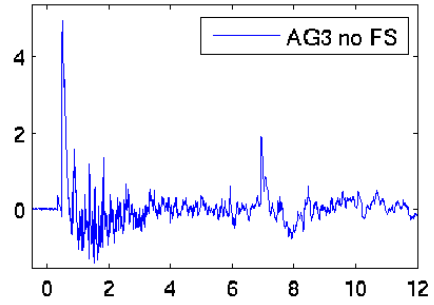
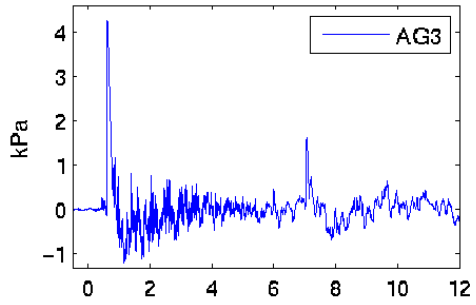
124 degrees



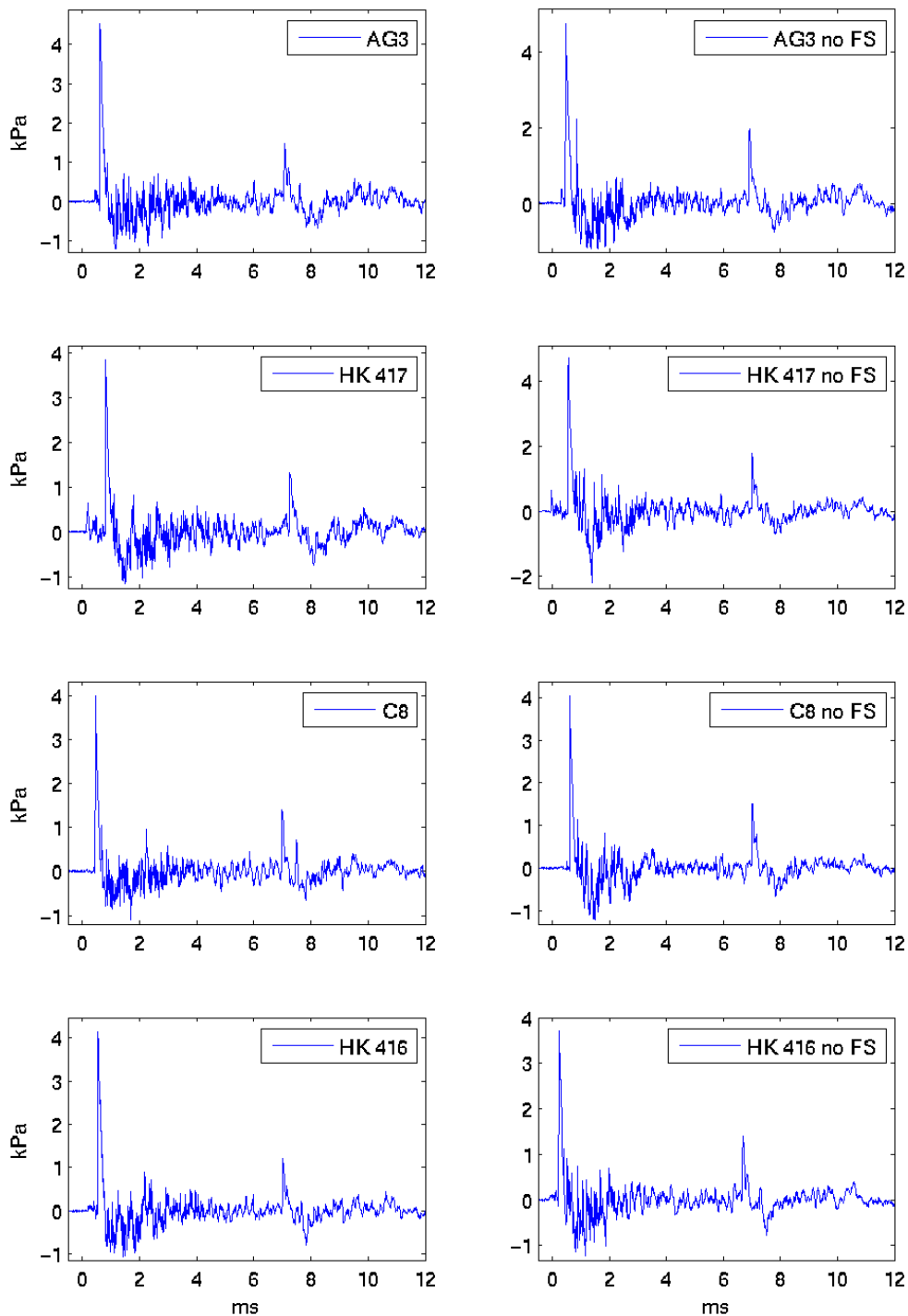
125 degrees



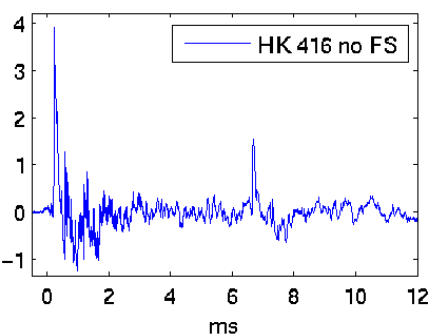
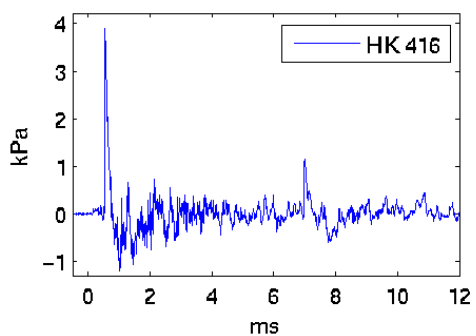
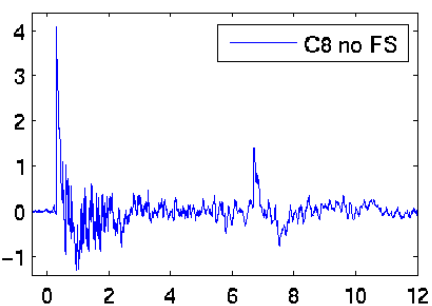
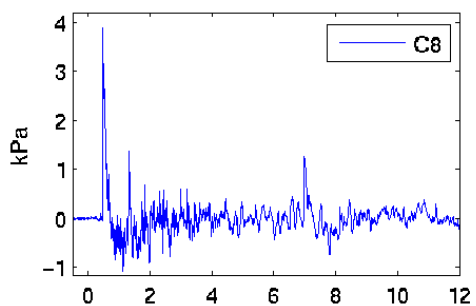
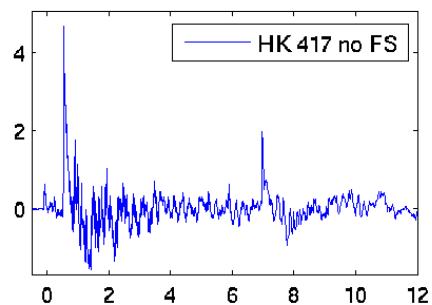
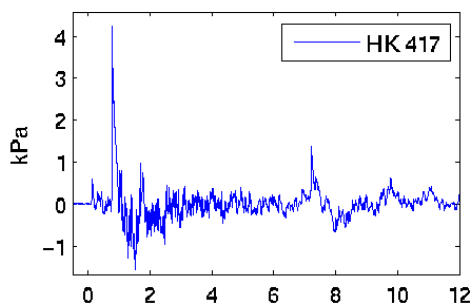
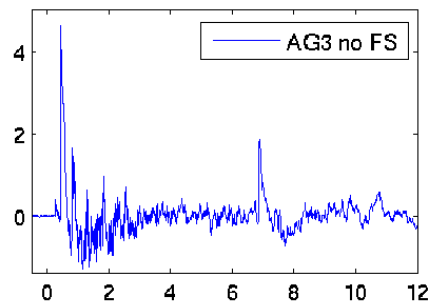
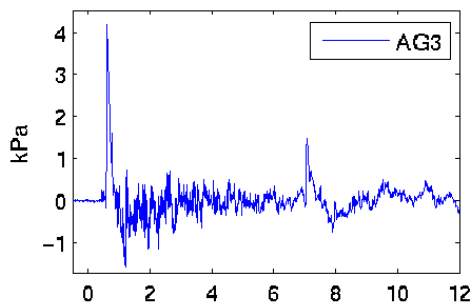
126 degrees

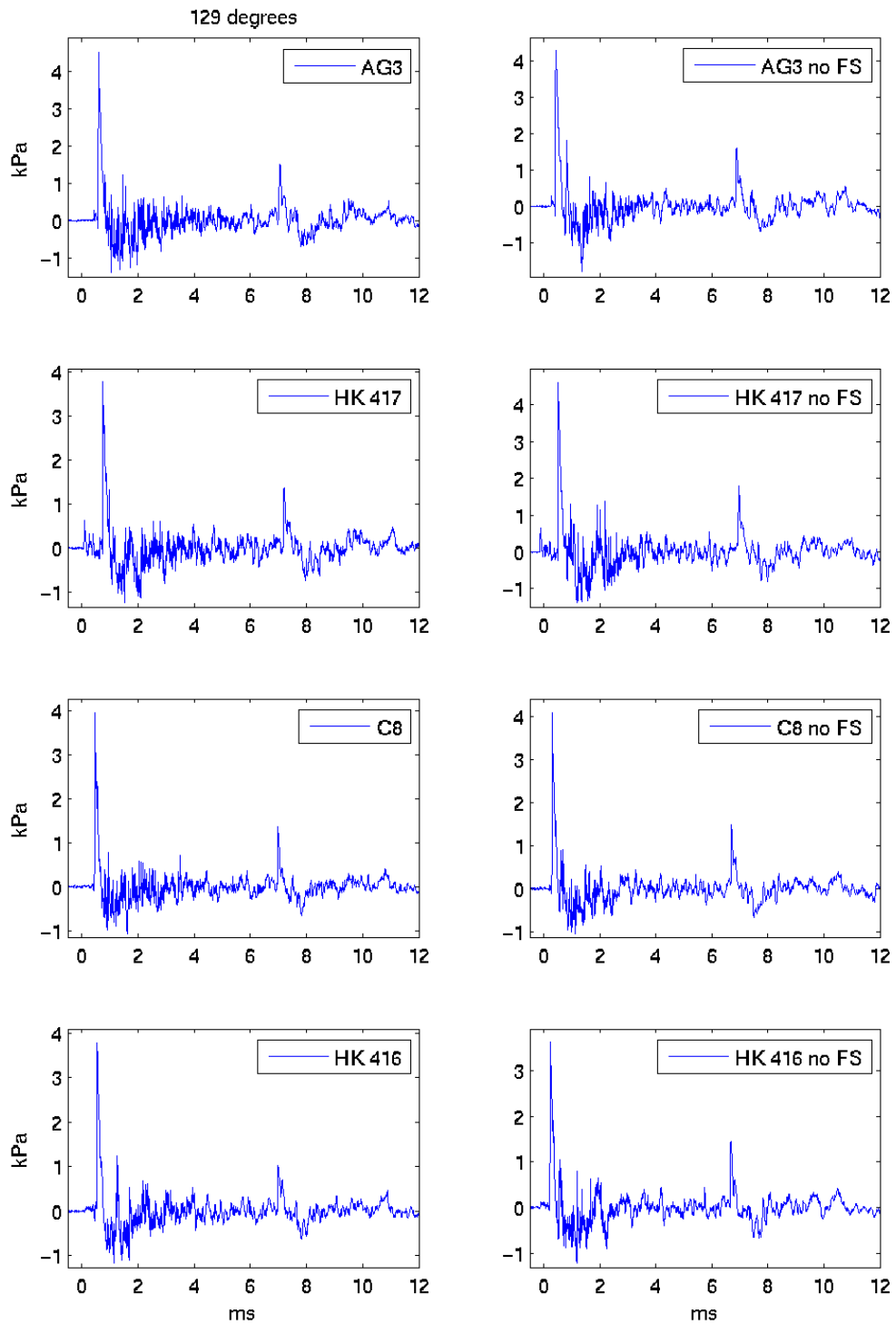


127 degrees

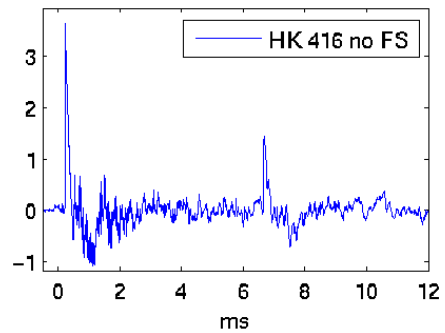
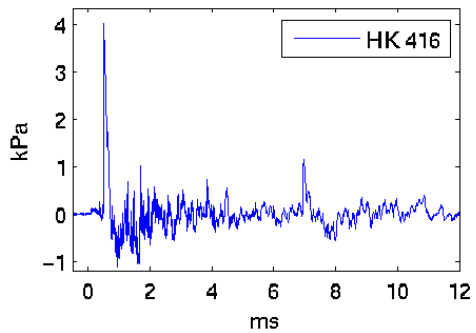
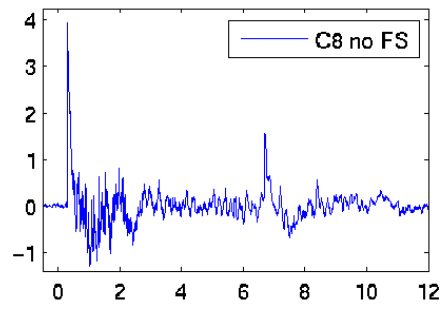
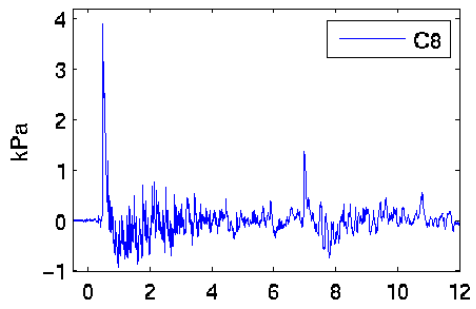
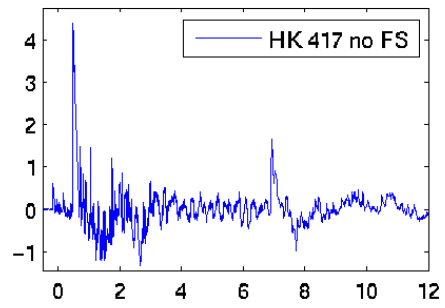
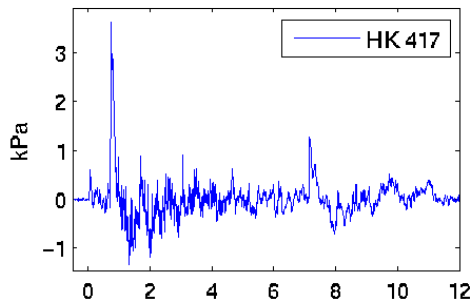
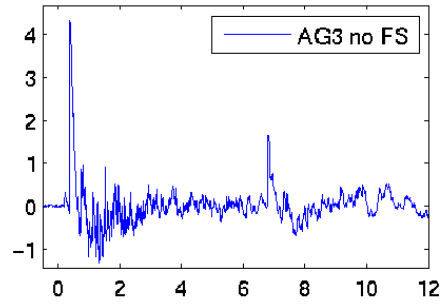
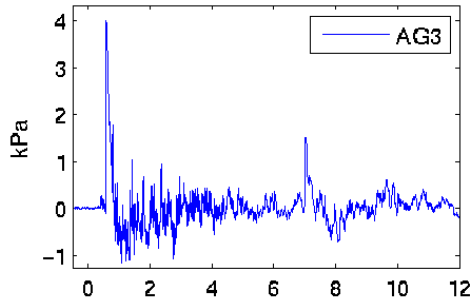


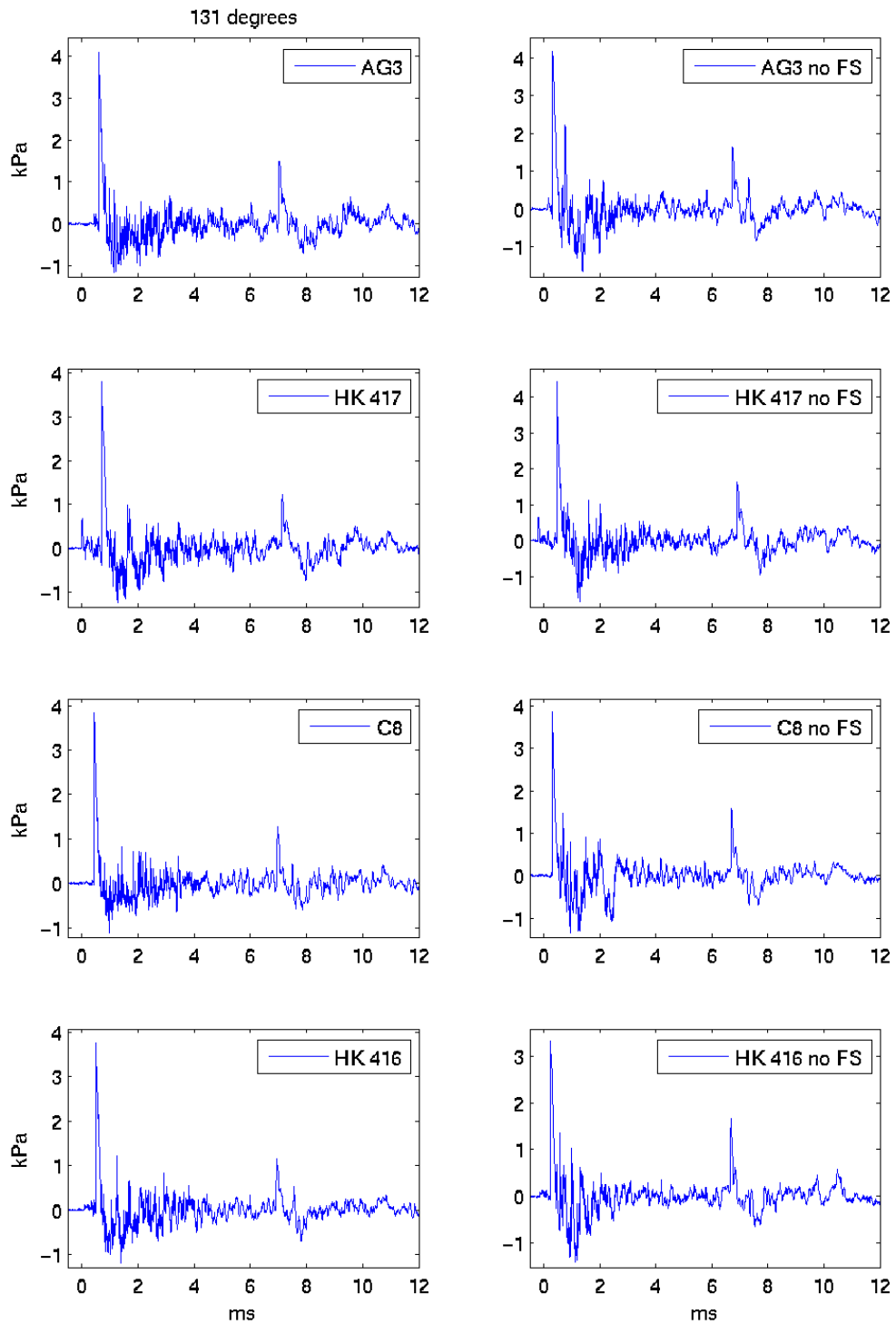
128 degrees

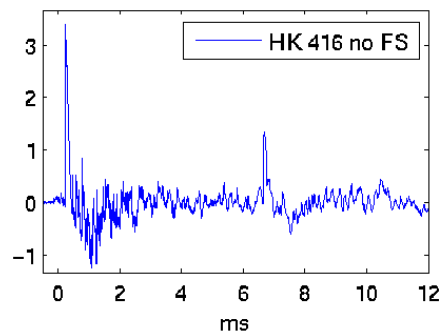
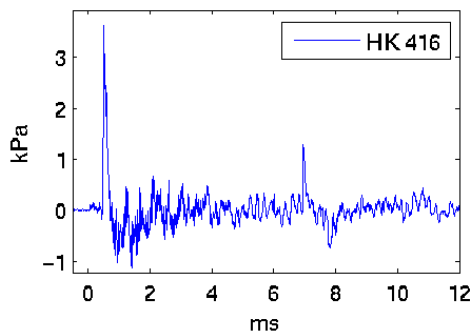
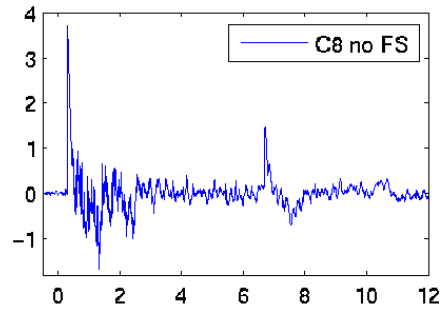
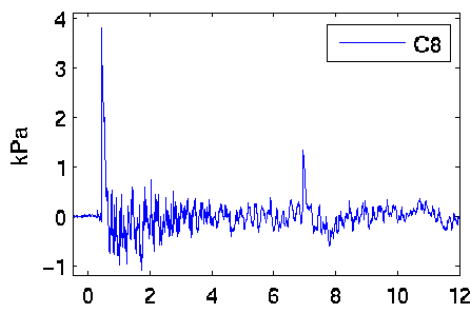
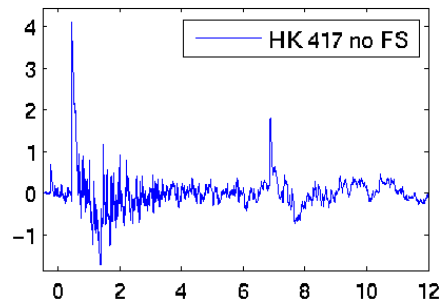
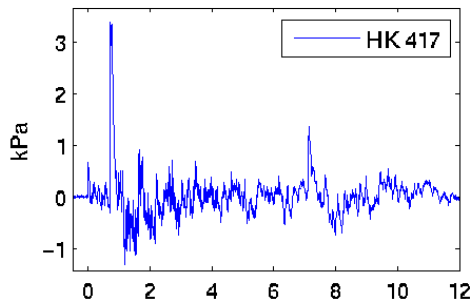
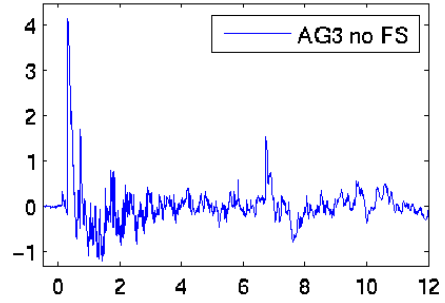
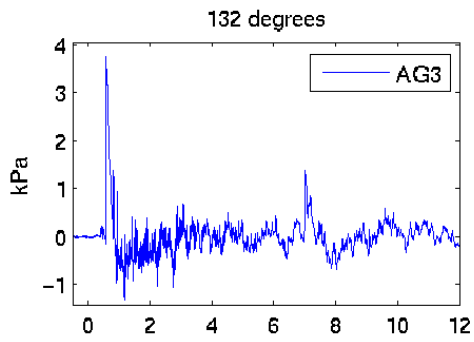


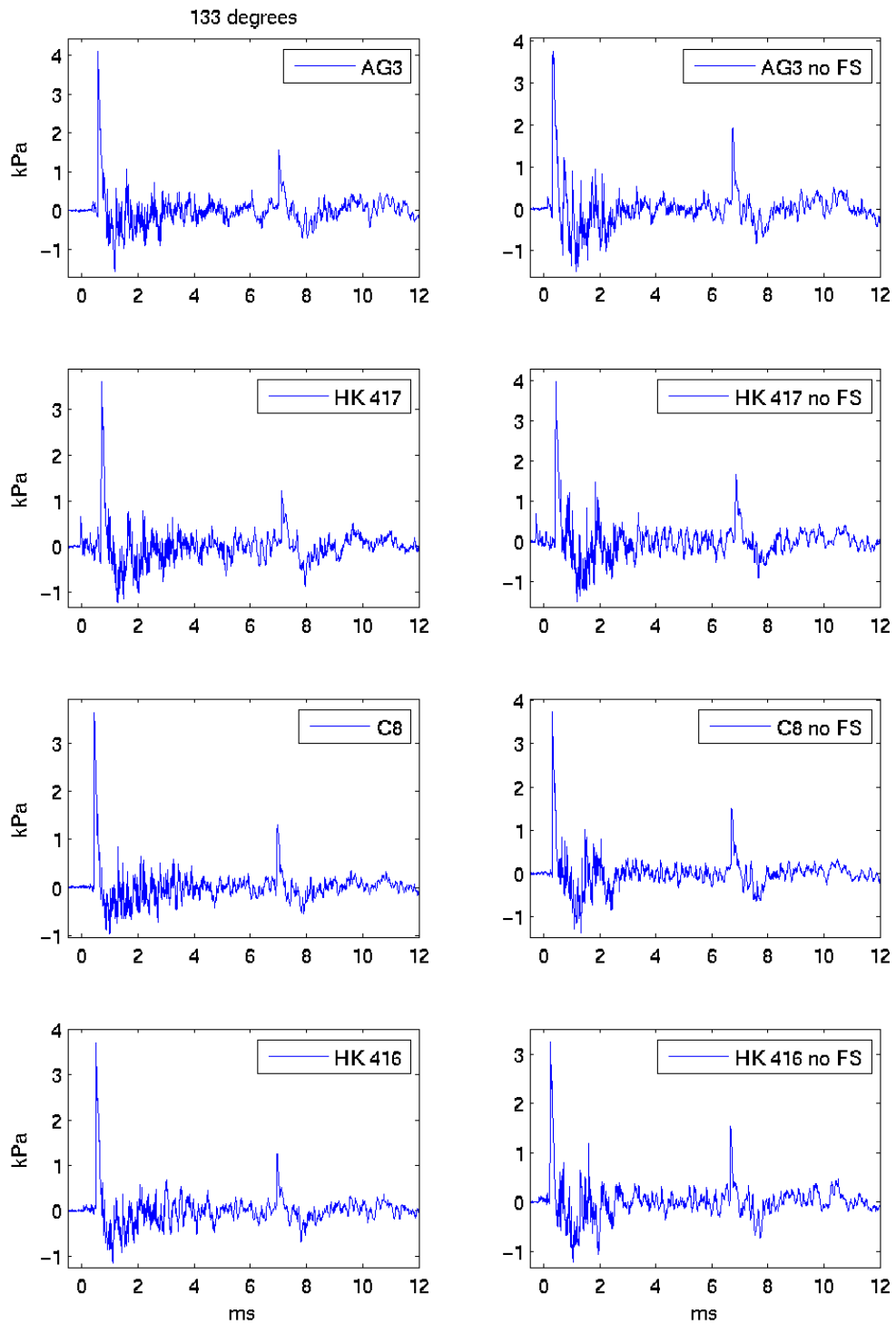


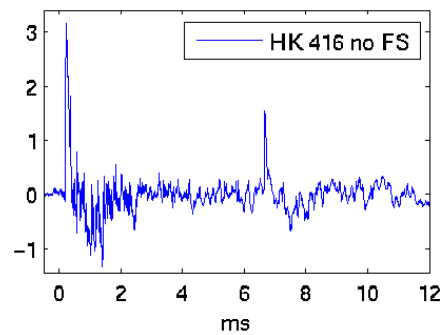
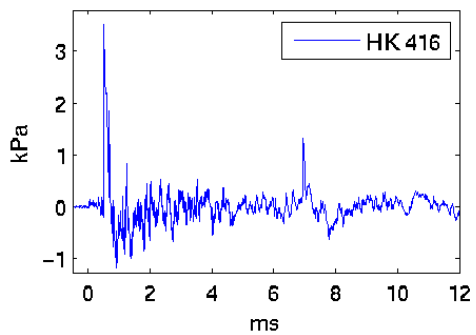
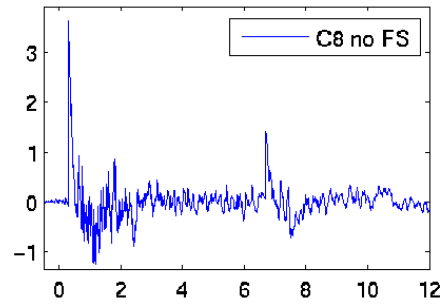
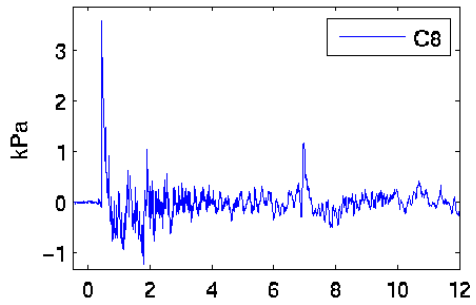
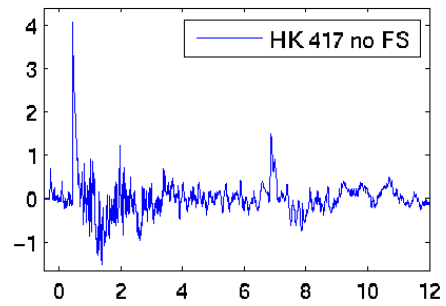
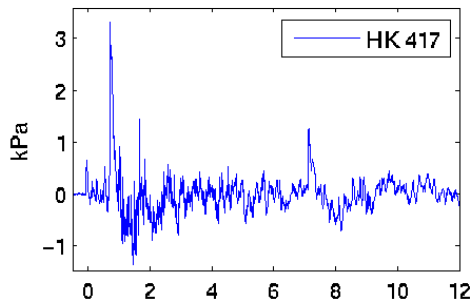
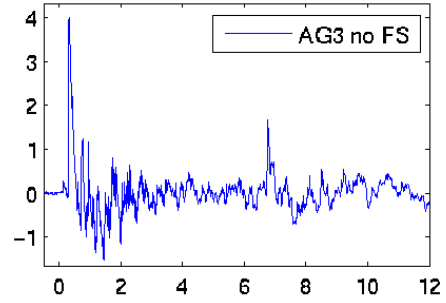
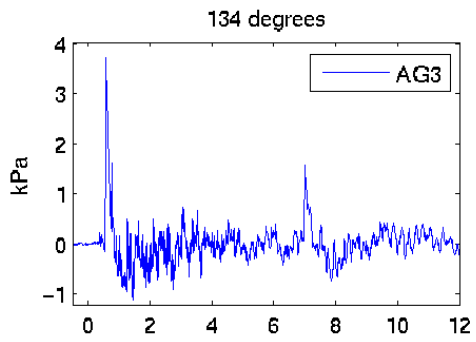
130 degrees



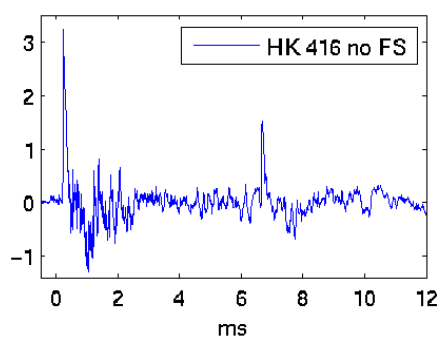
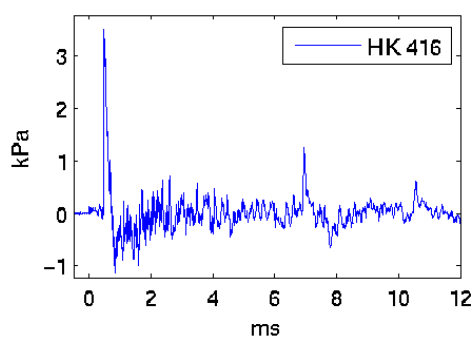
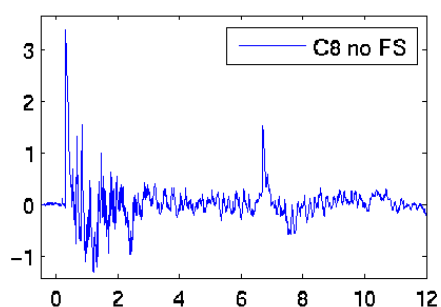
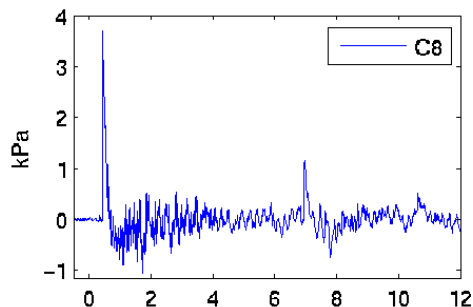
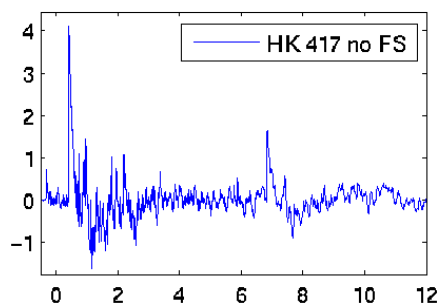
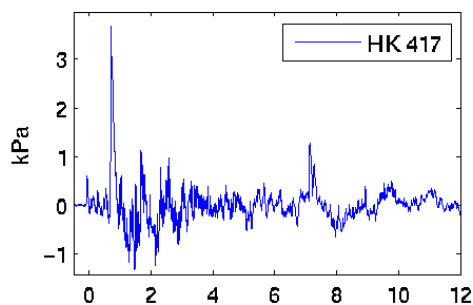
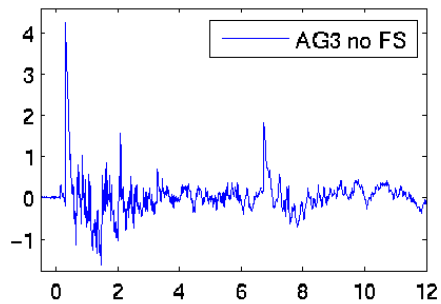
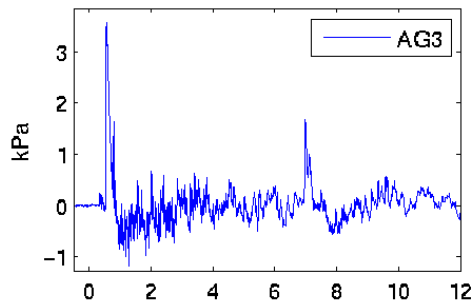




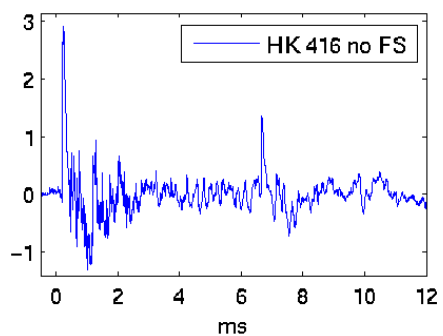
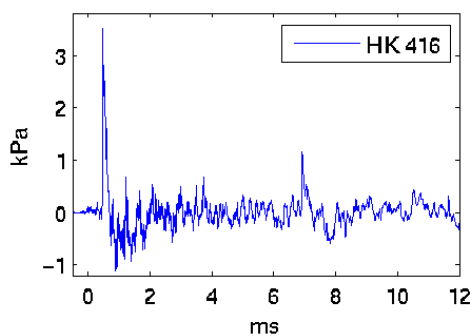
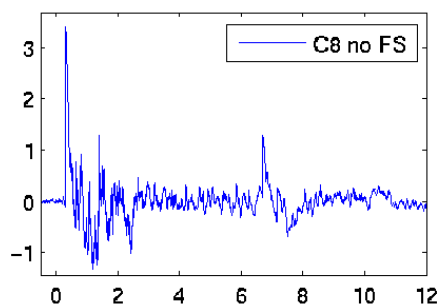
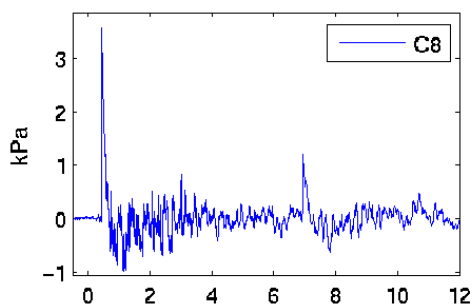
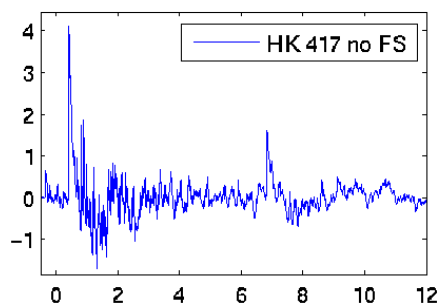
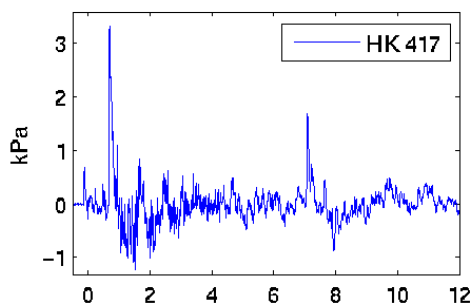
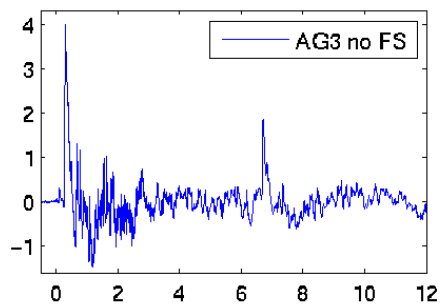
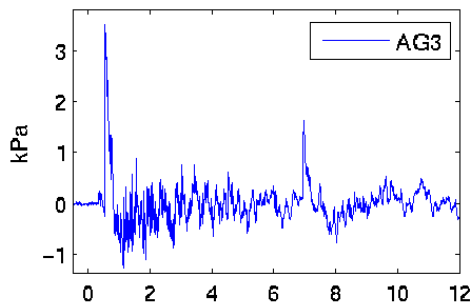


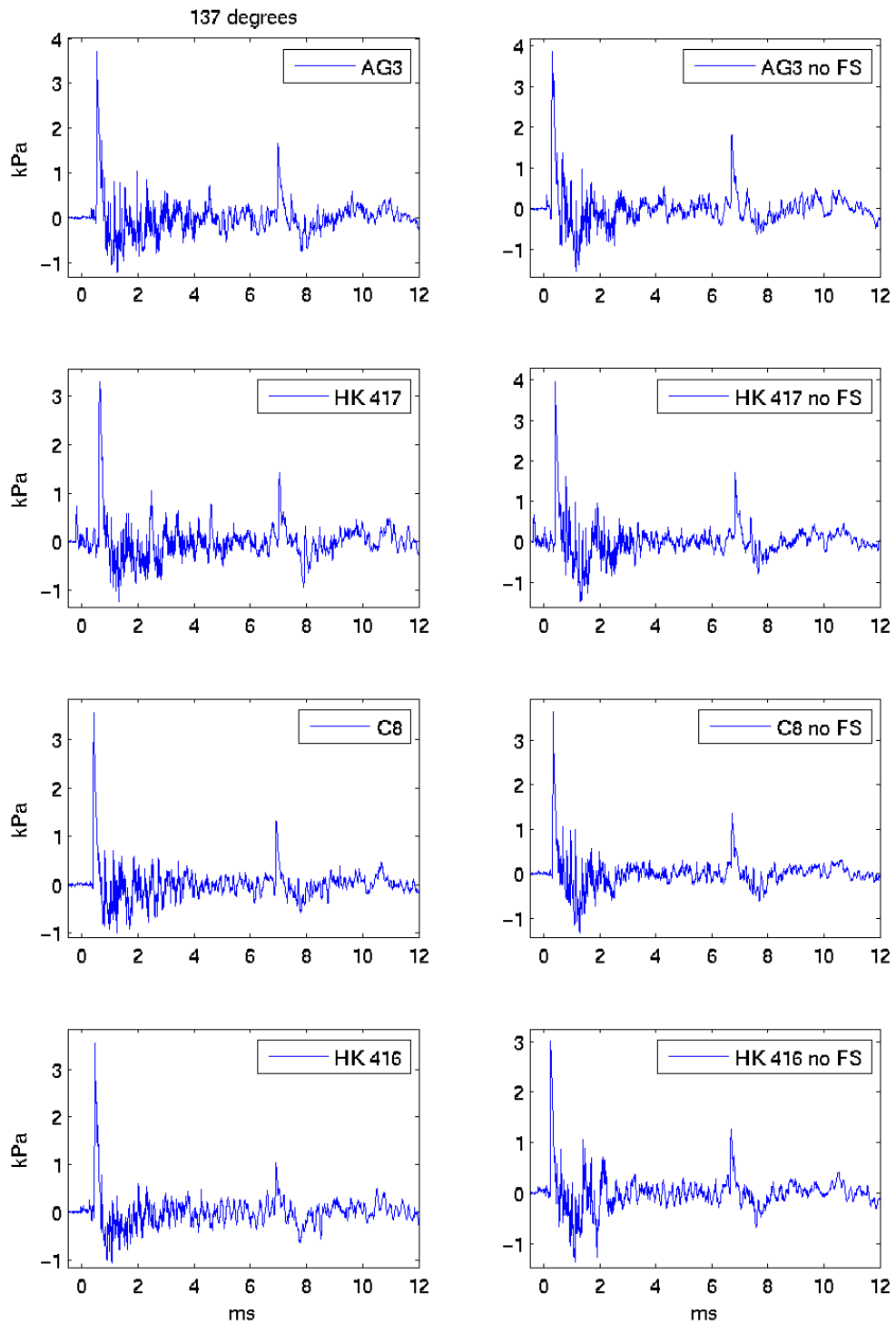


135 degrees

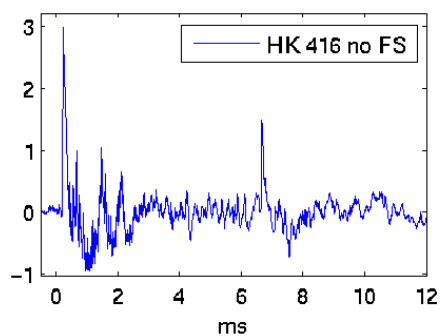
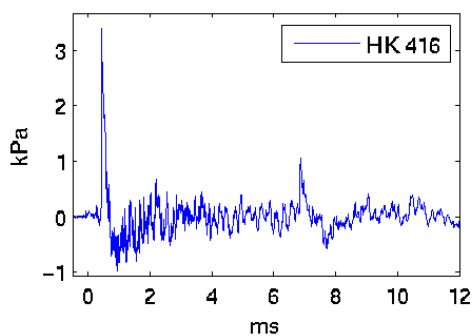
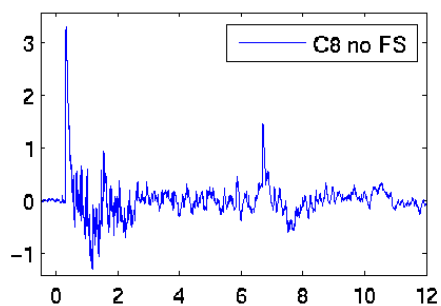
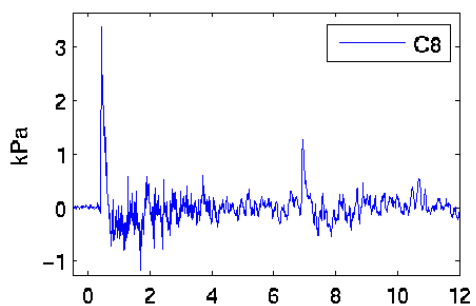
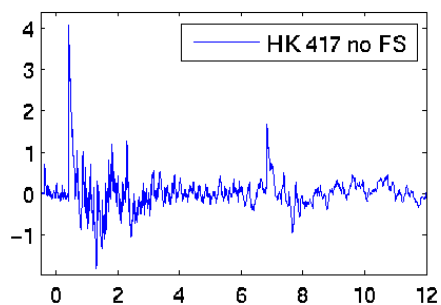
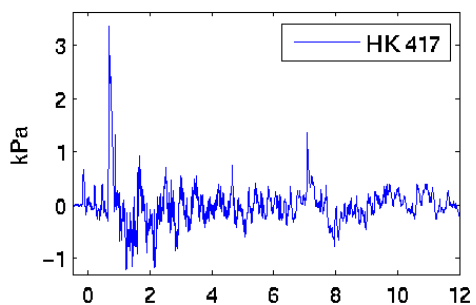
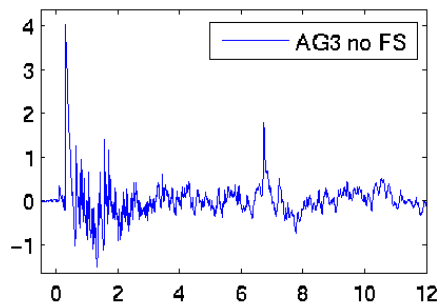
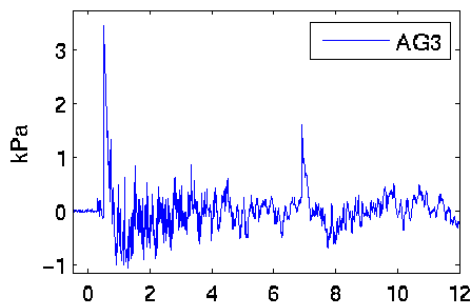


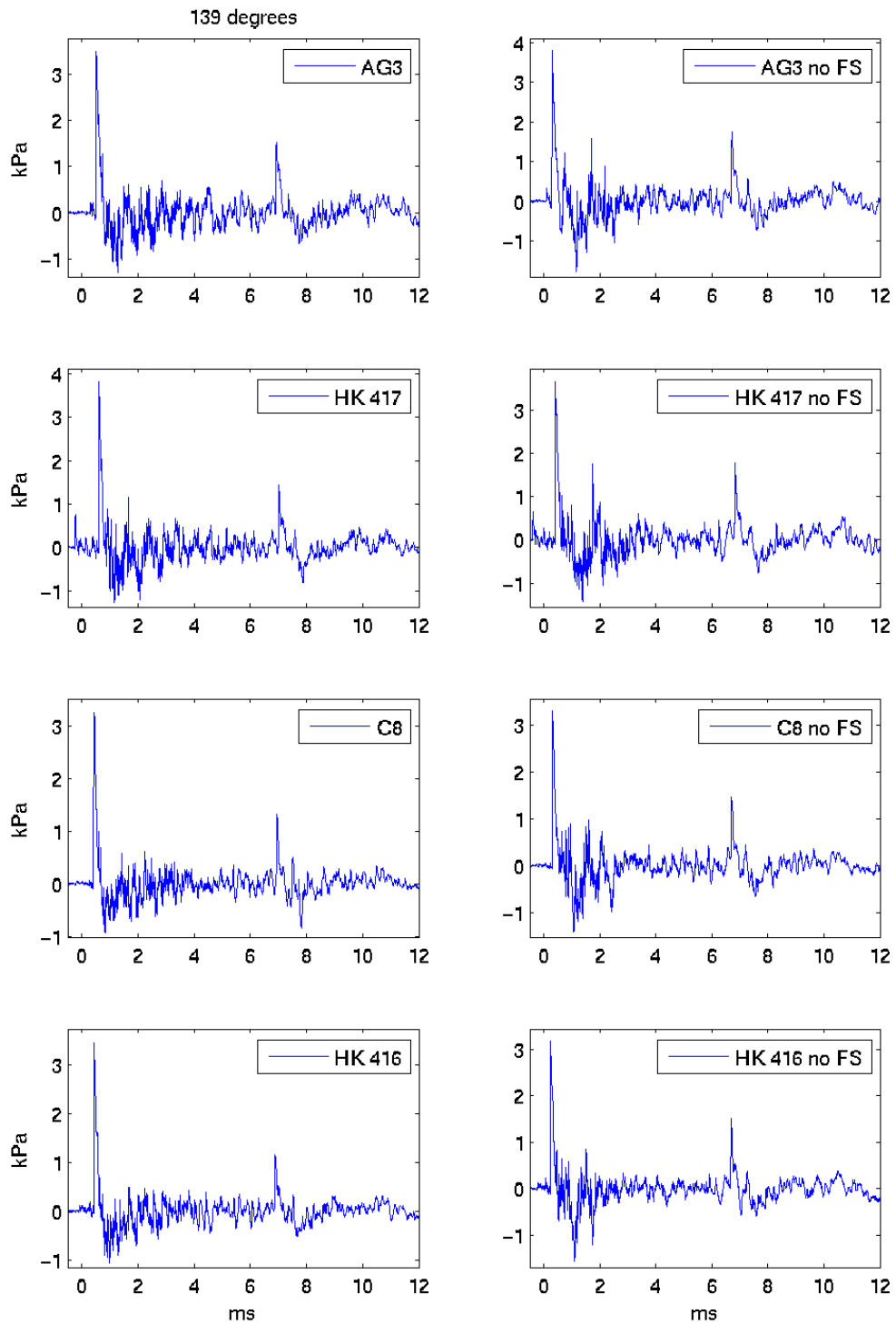
136 degrees

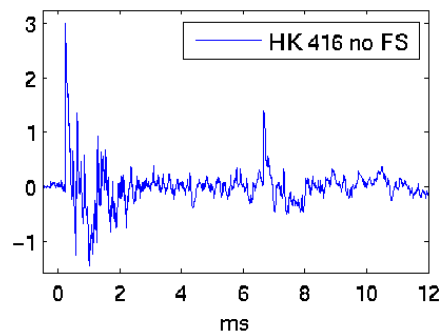
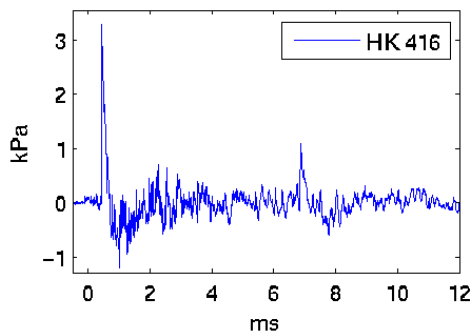
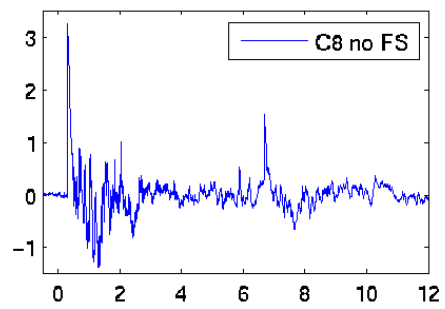
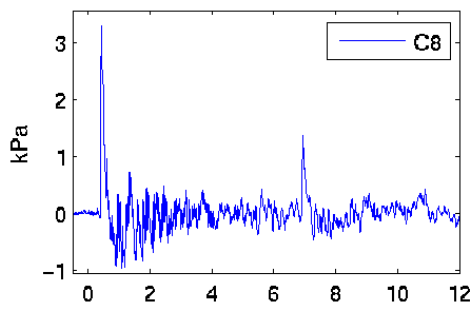
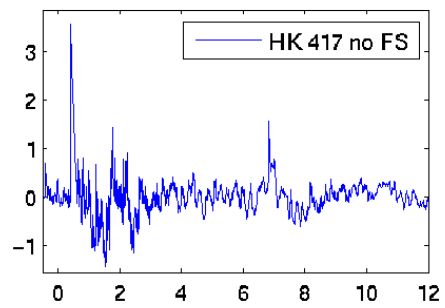
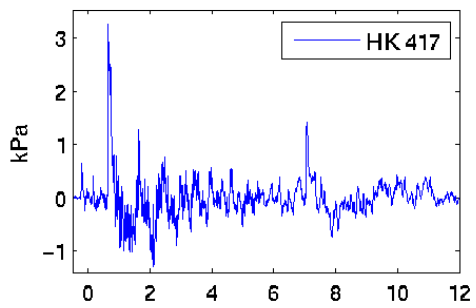
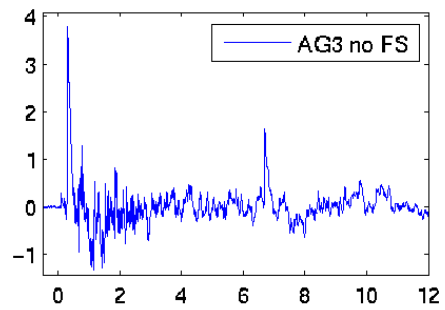
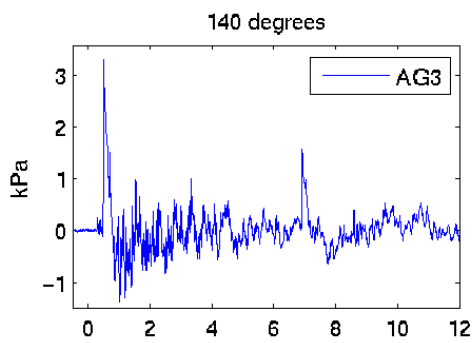




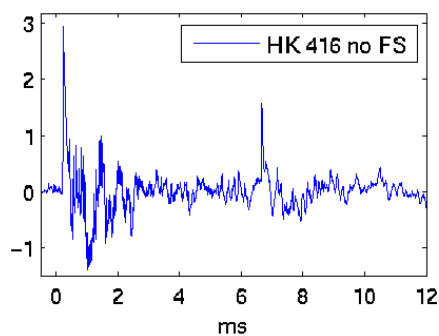
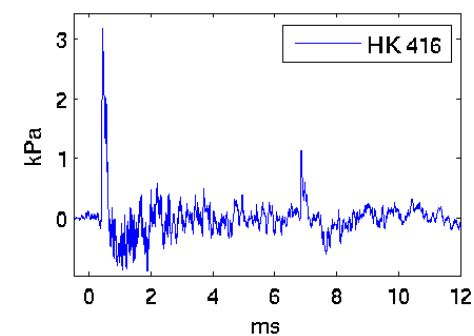
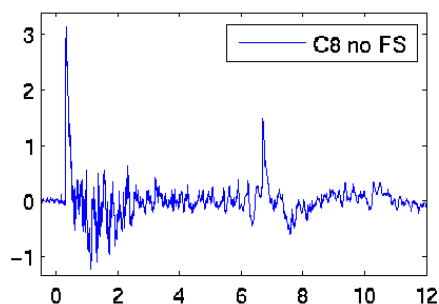
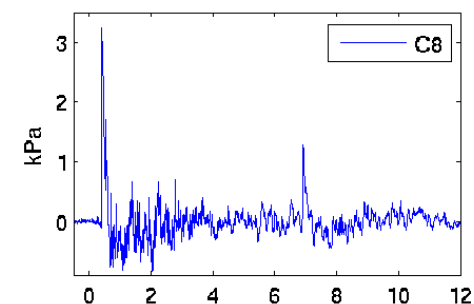
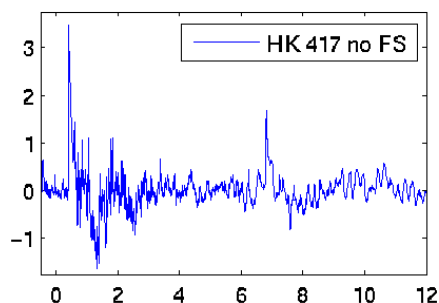
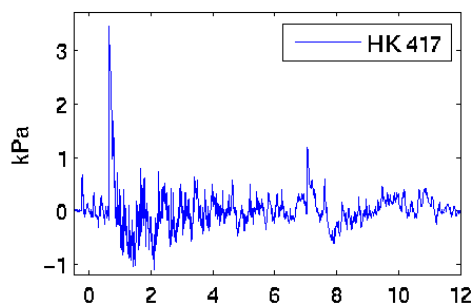
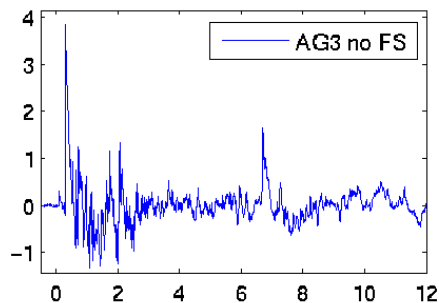
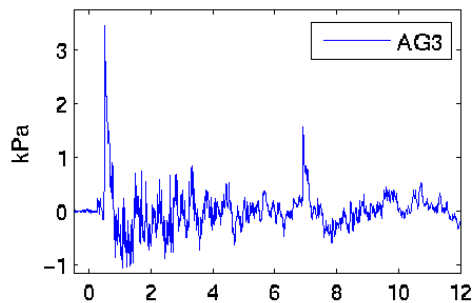
138 degrees



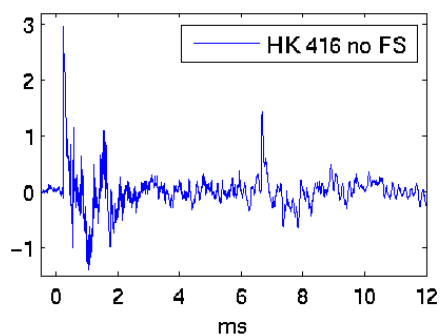
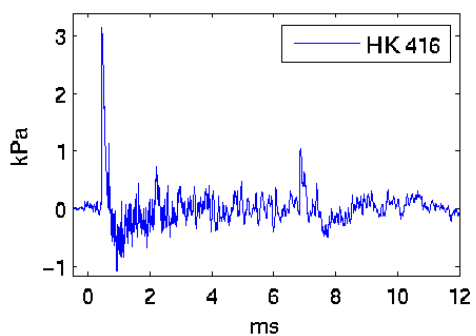
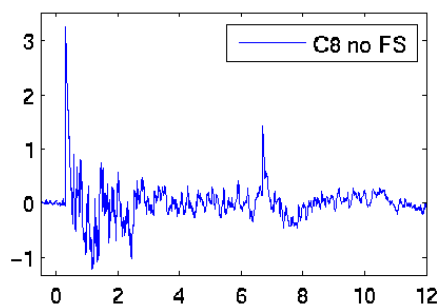
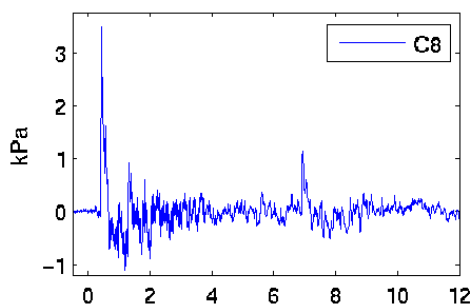
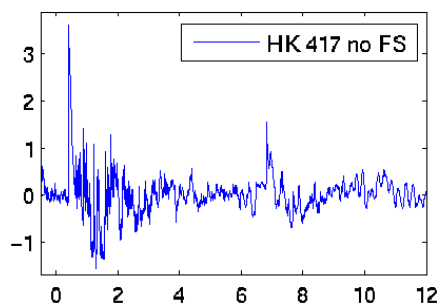
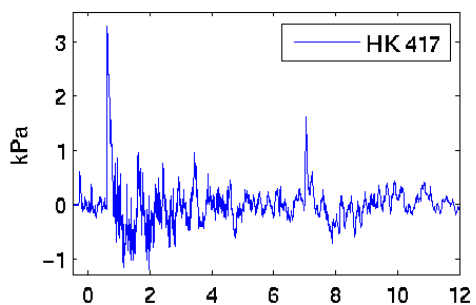
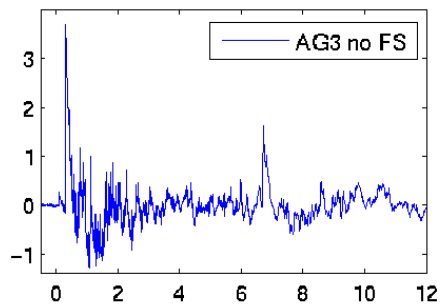
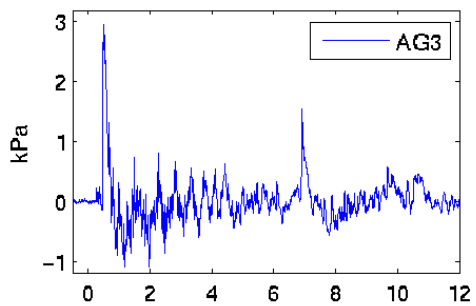


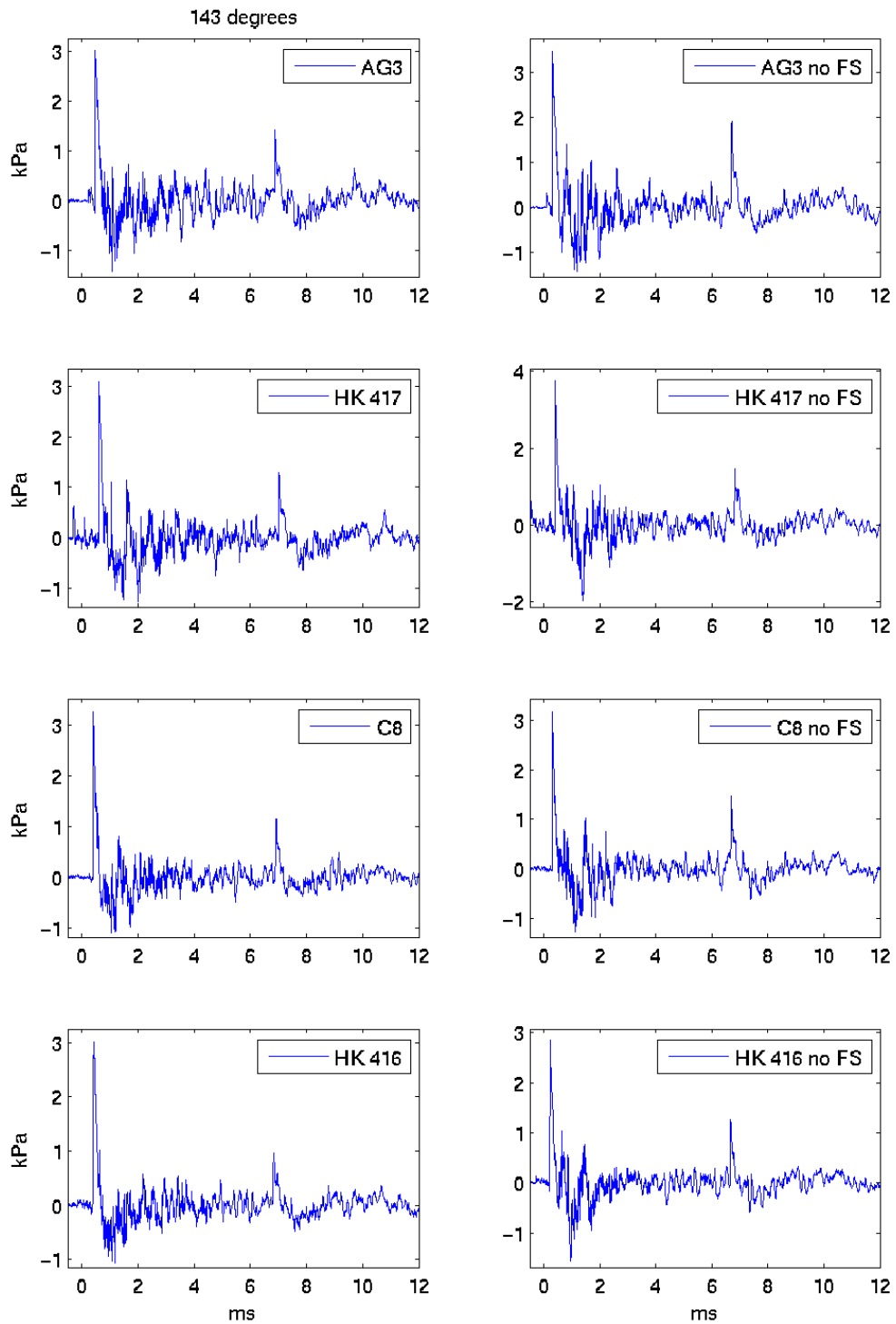


141 degrees

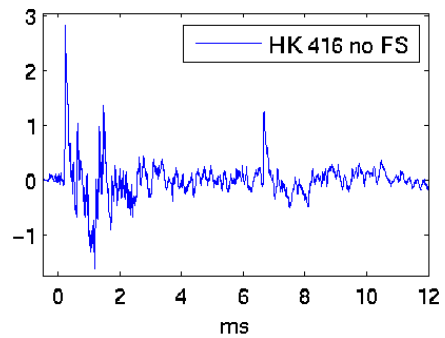
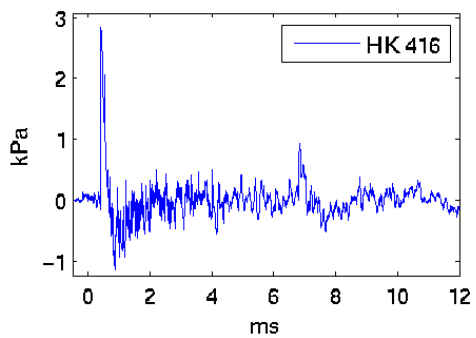
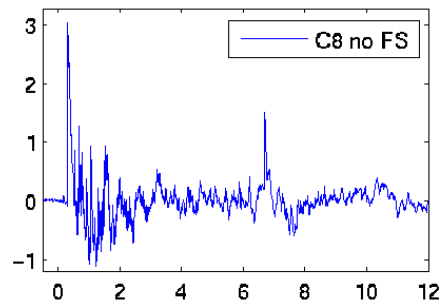
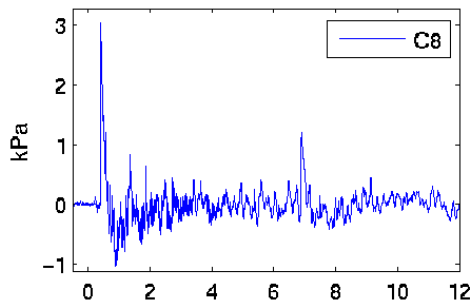
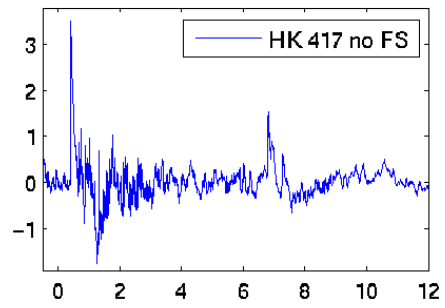
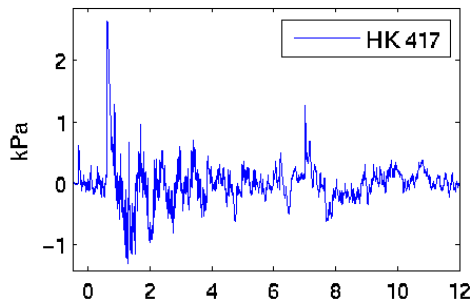
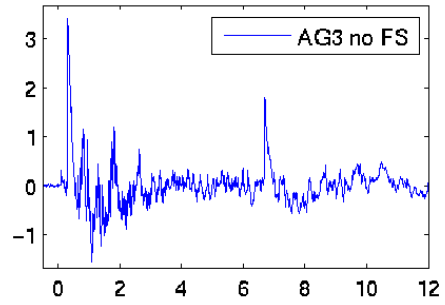
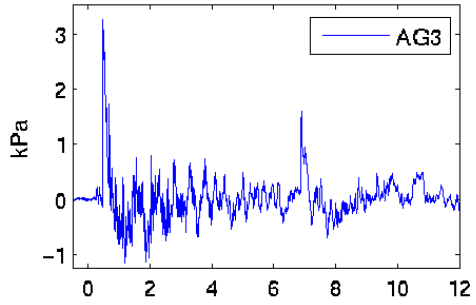


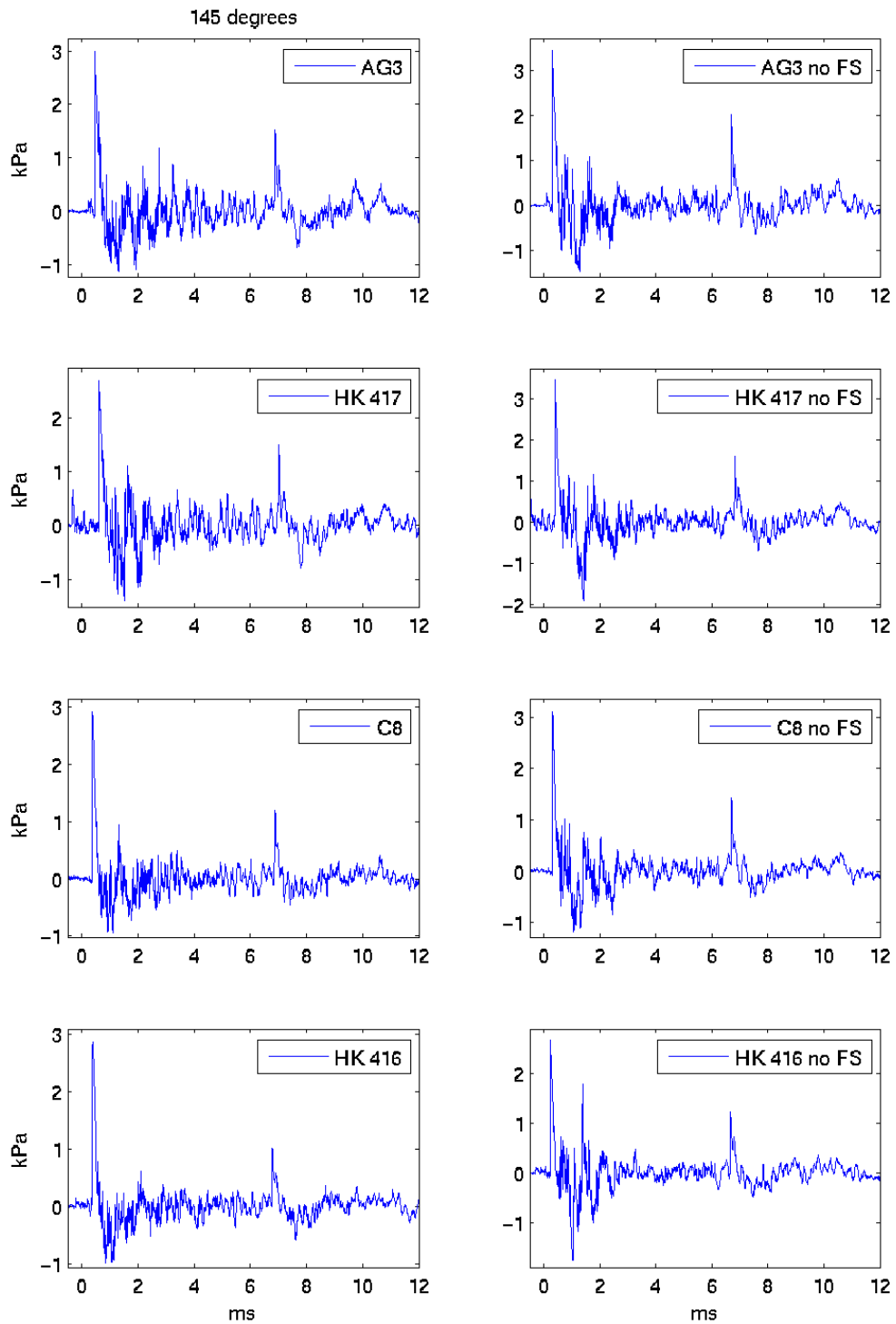
142 degrees



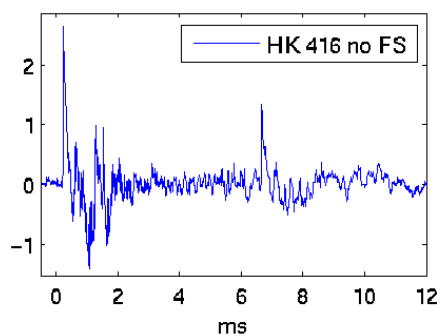
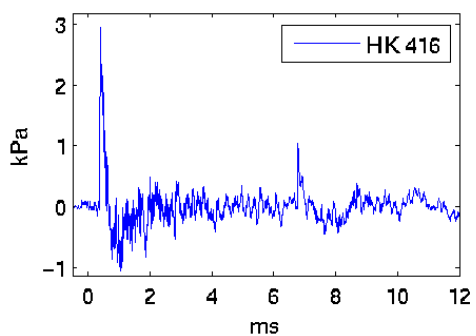
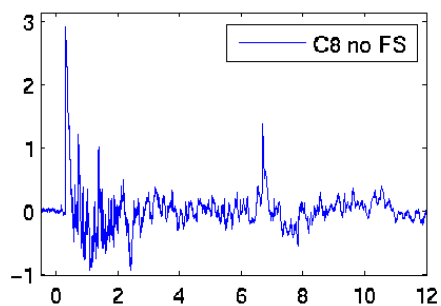
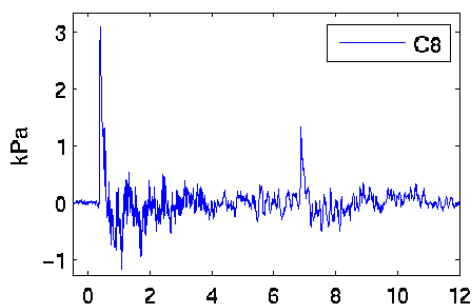
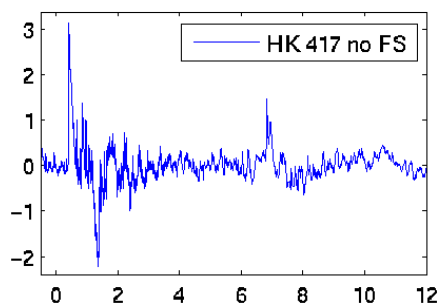
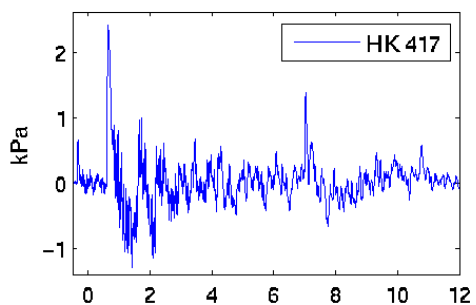
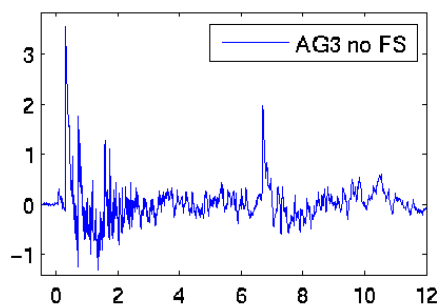
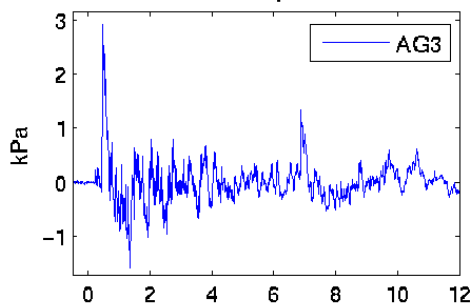


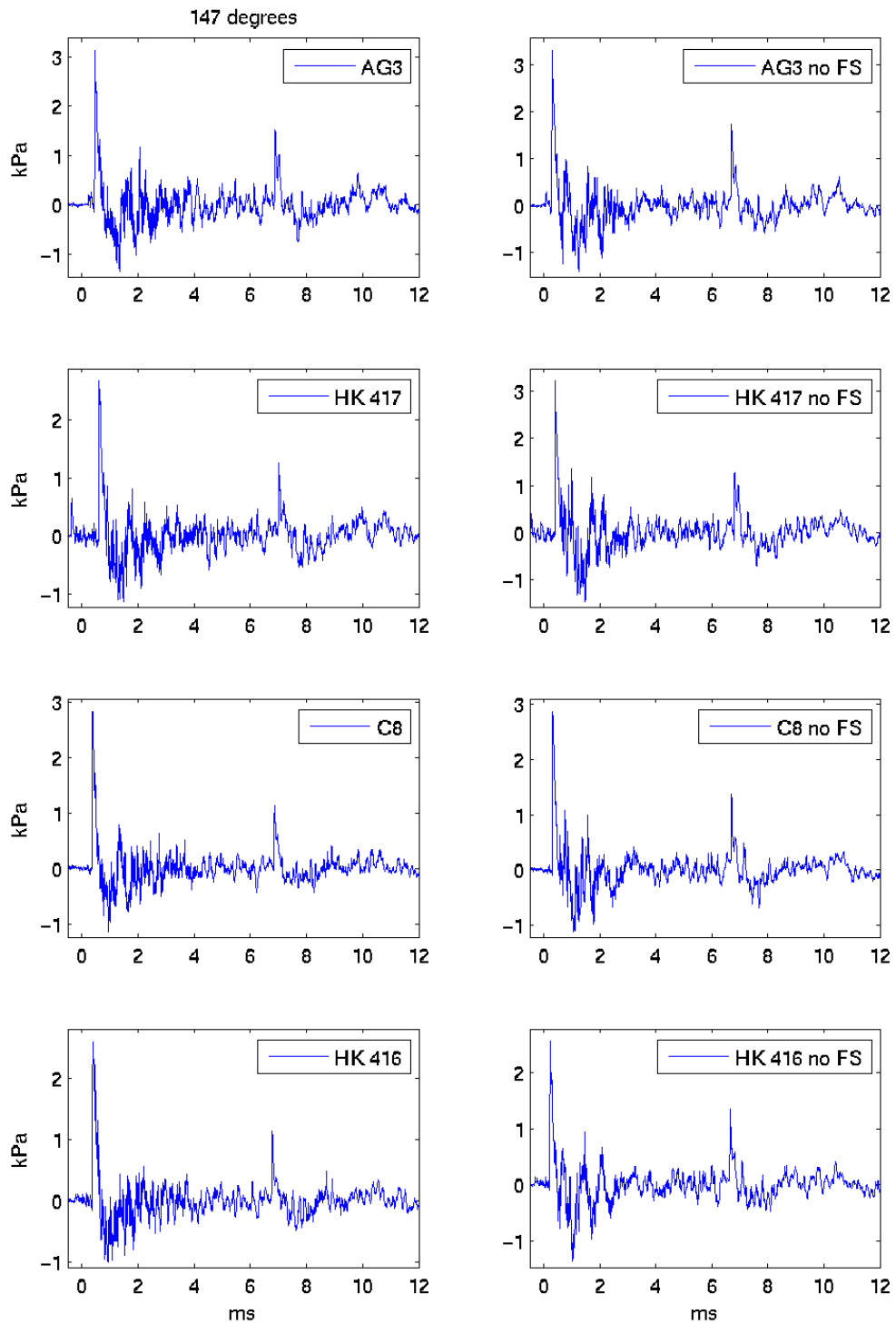
144 degrees



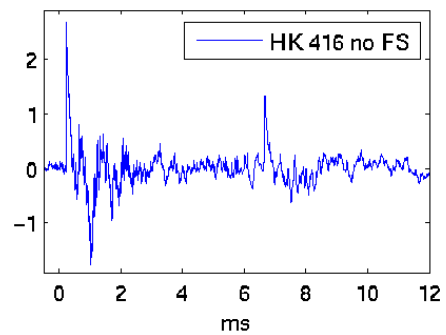
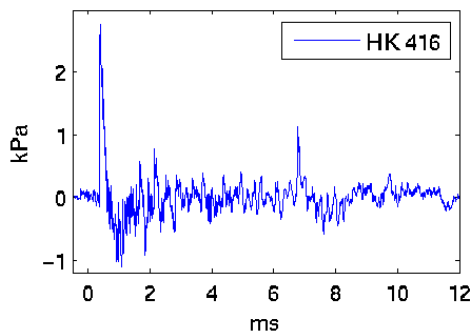
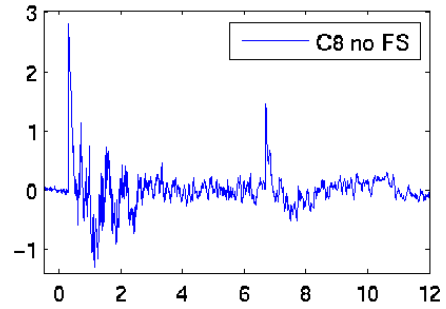
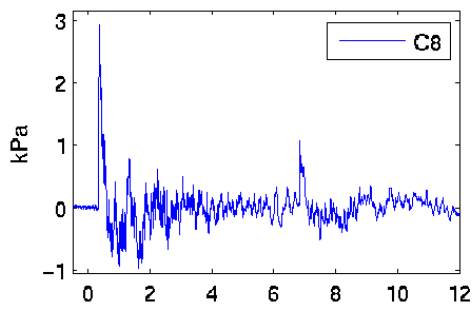
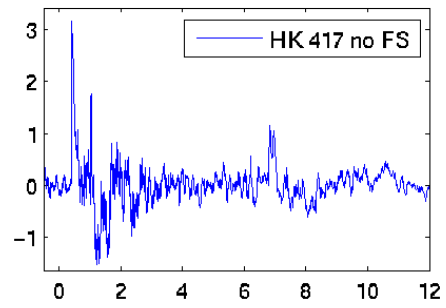
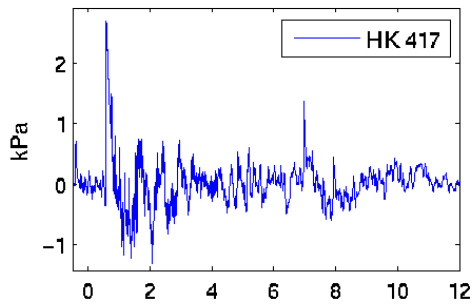
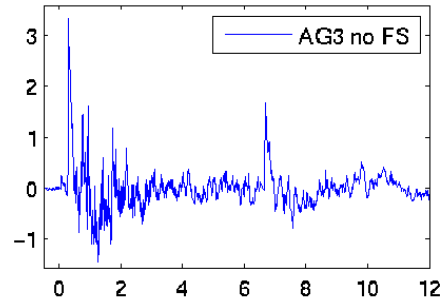
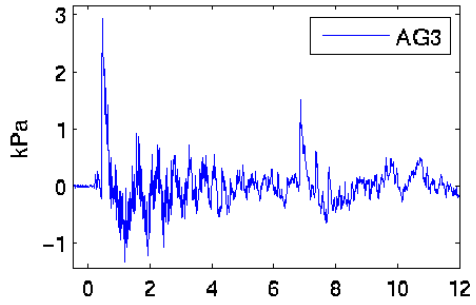


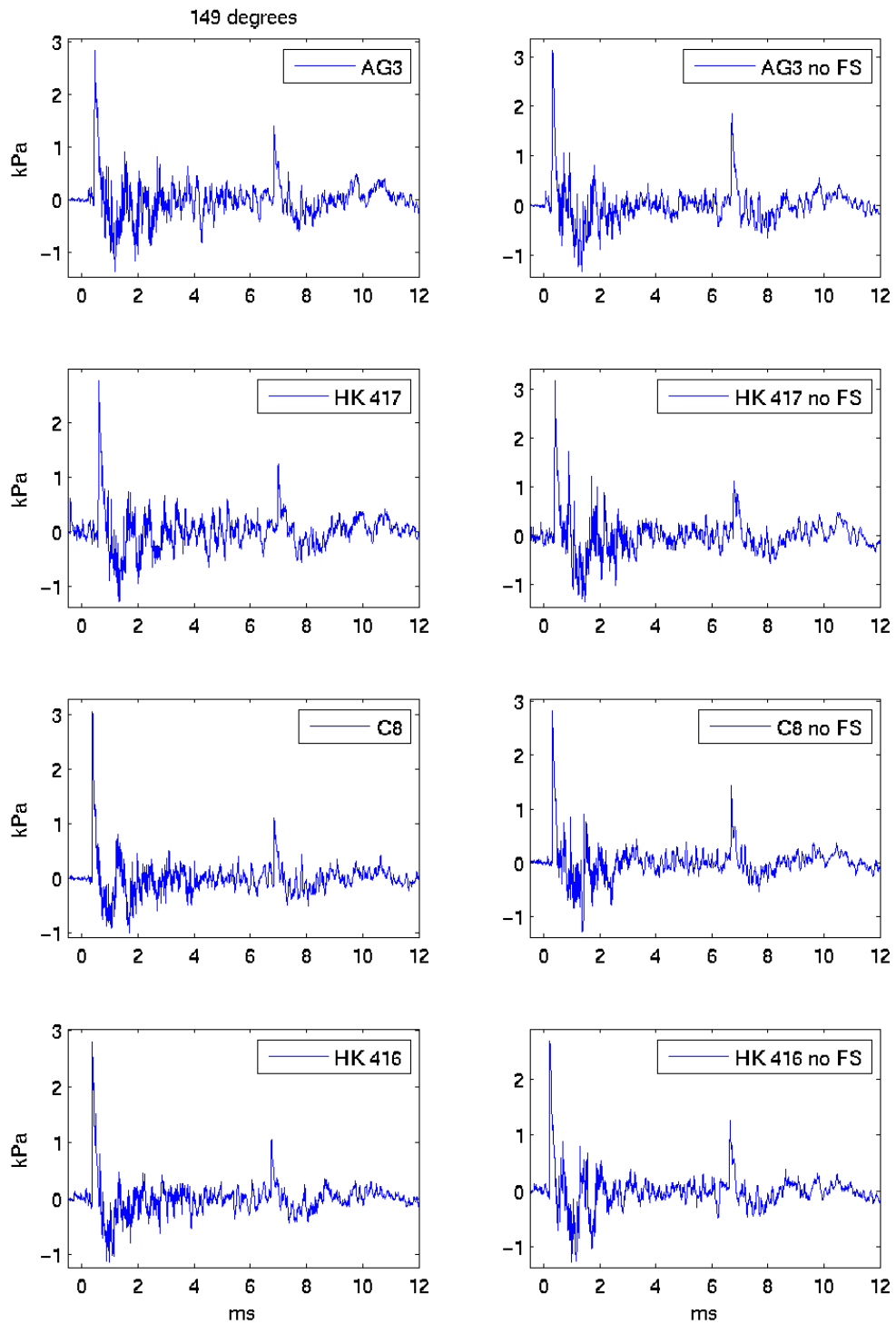
146 degrees

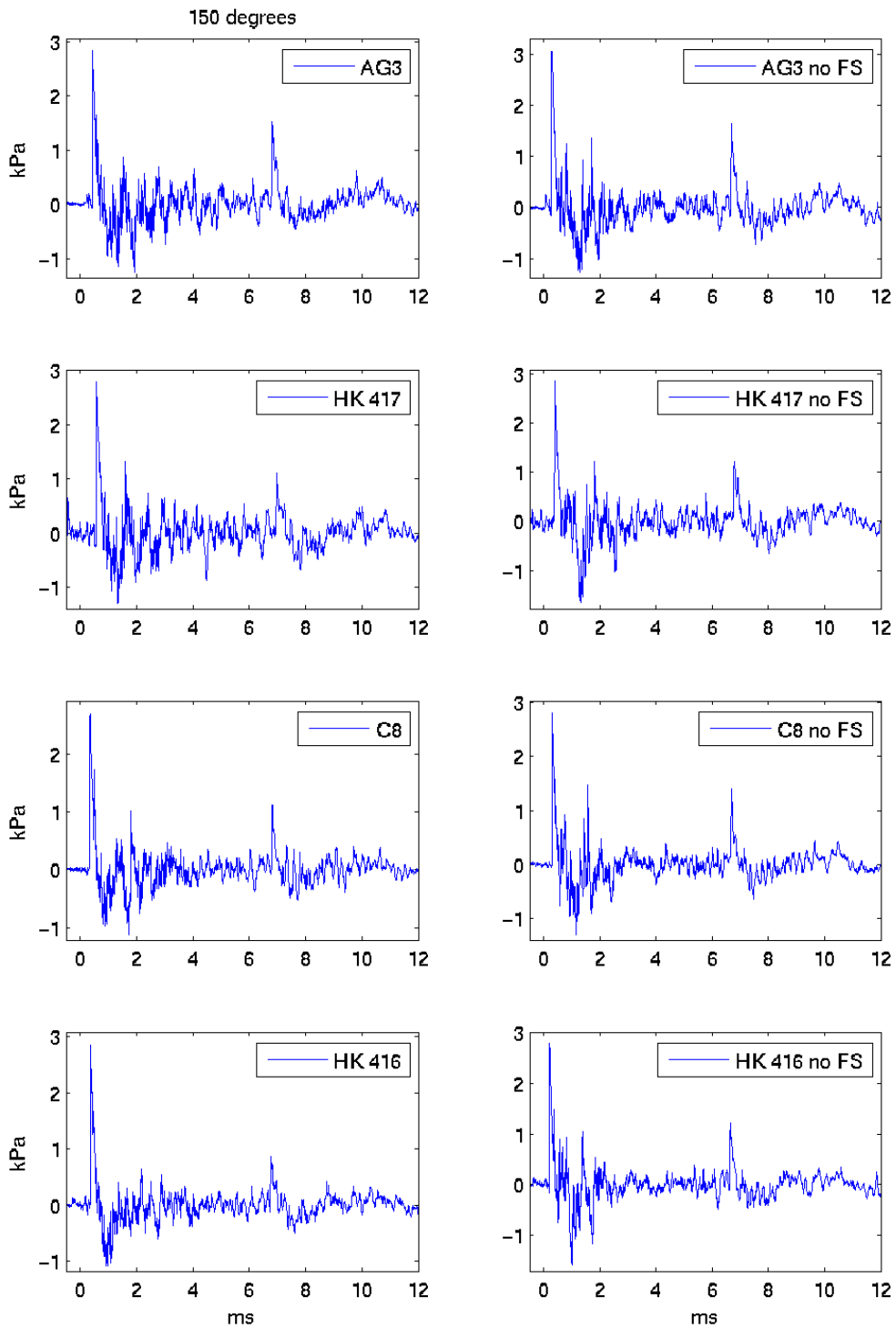




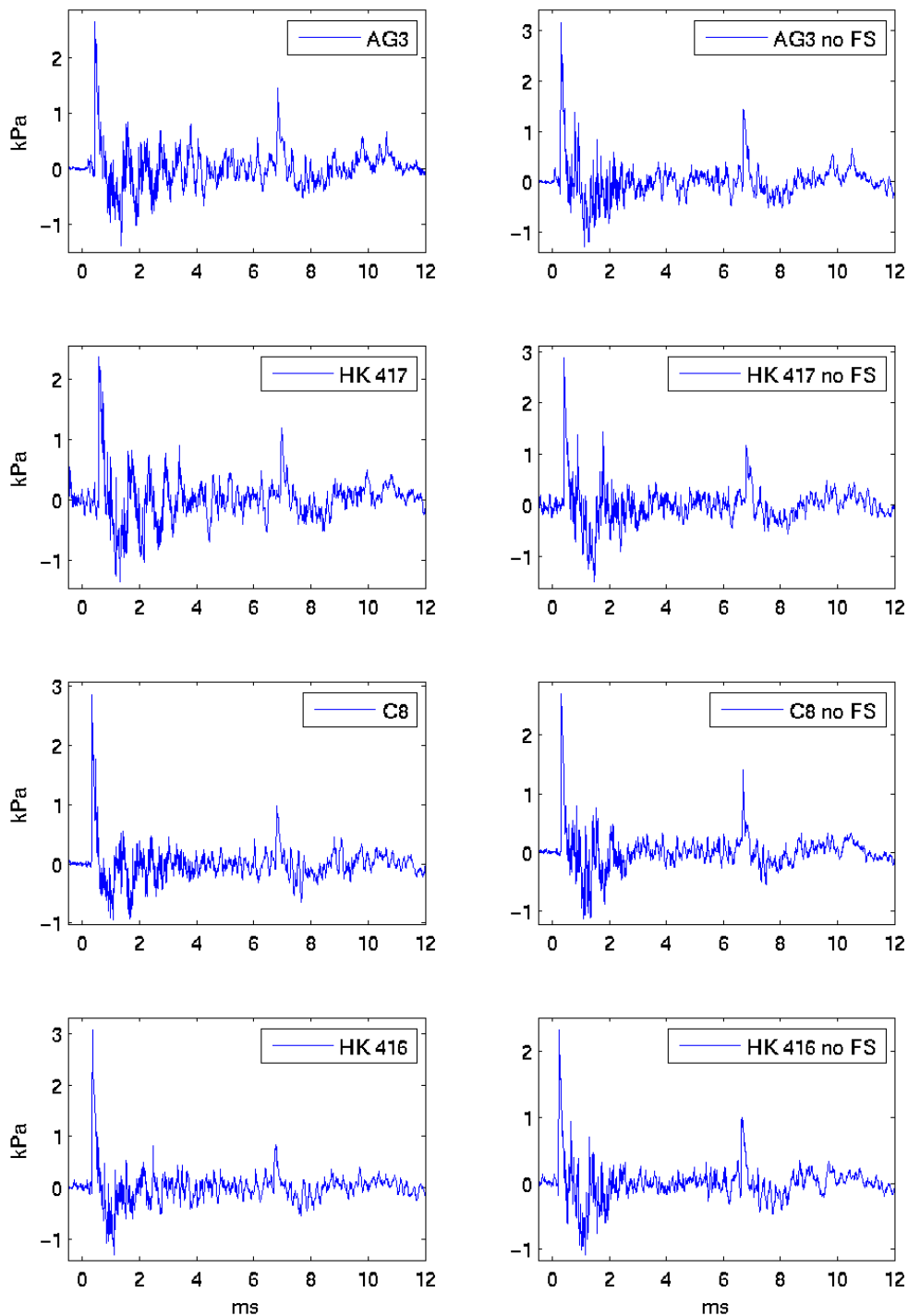
148 degrees



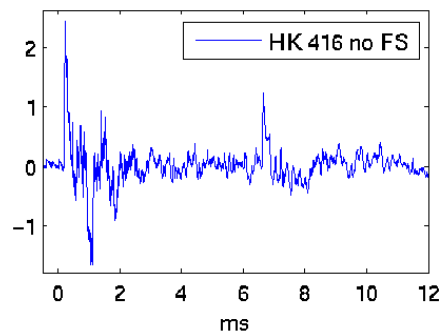
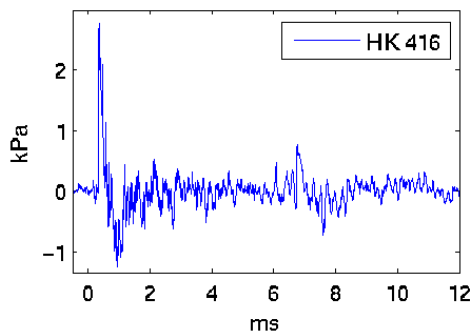
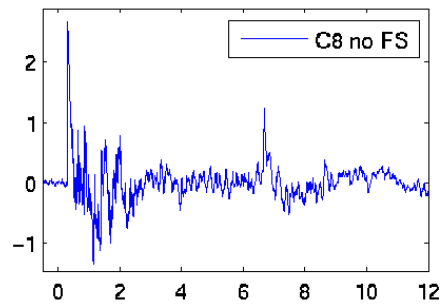
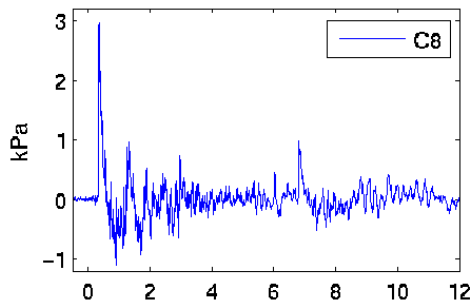
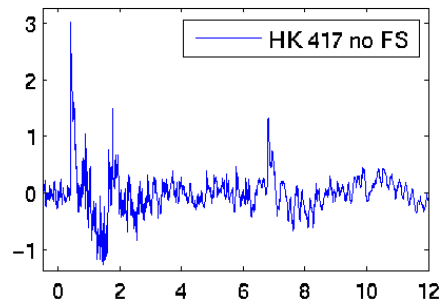
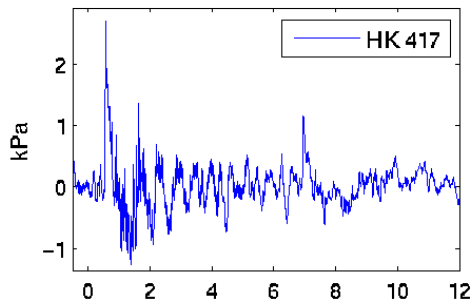
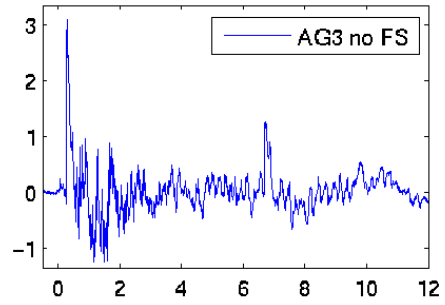
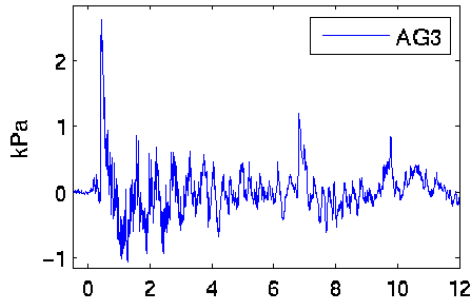




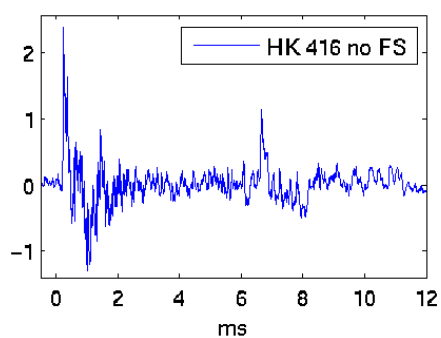
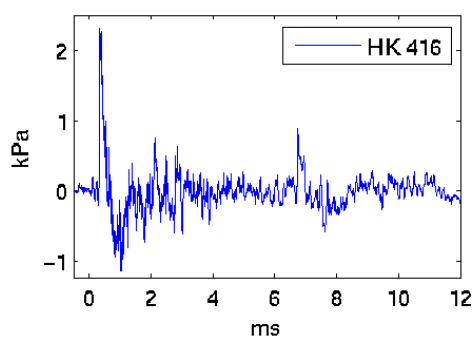
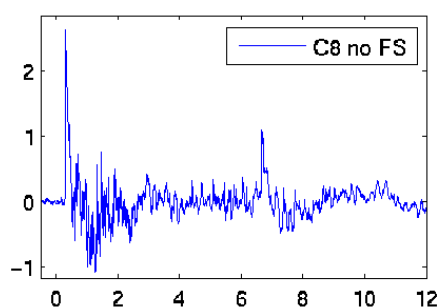
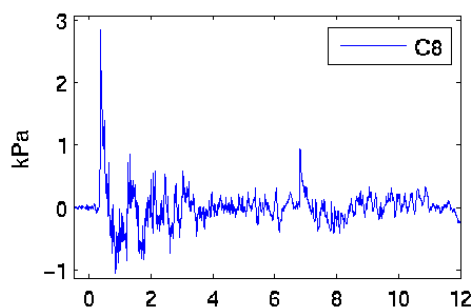
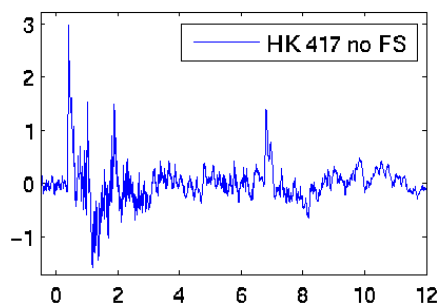
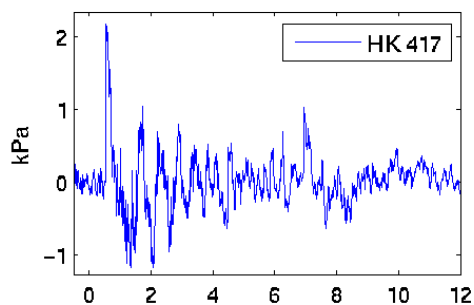
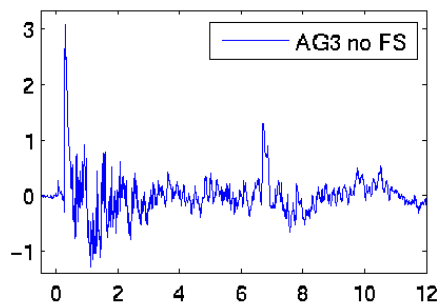
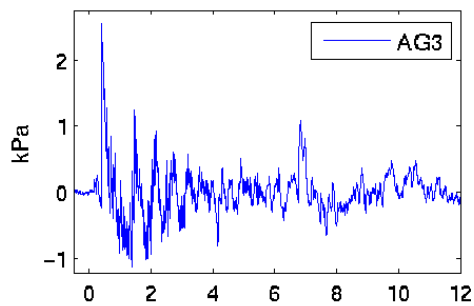
151 degrees



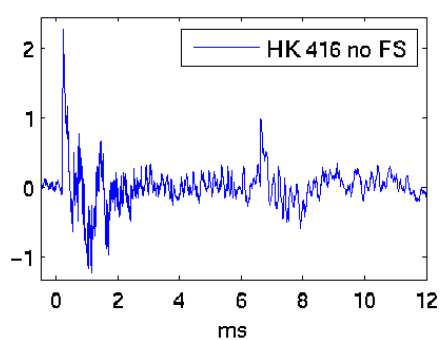
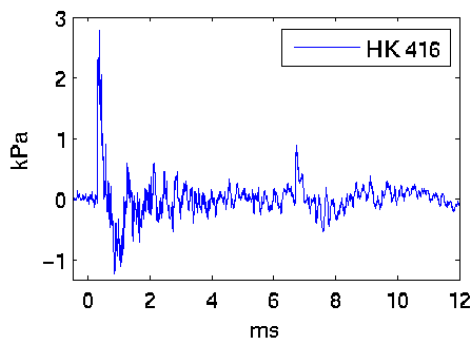
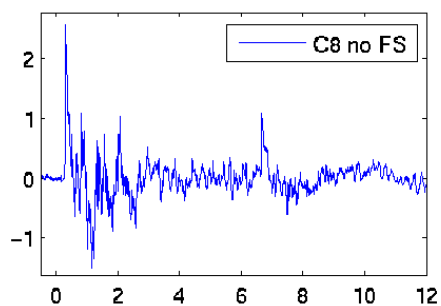
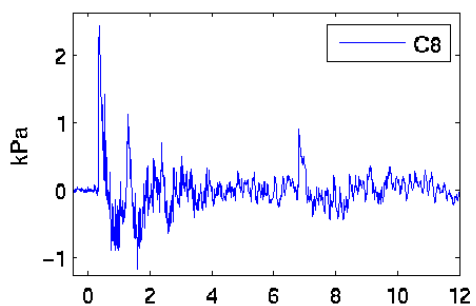
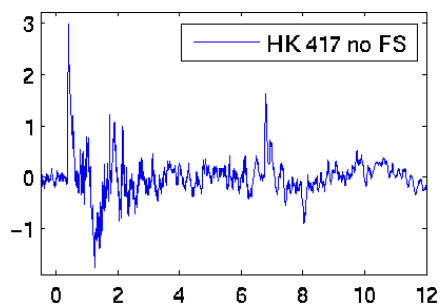
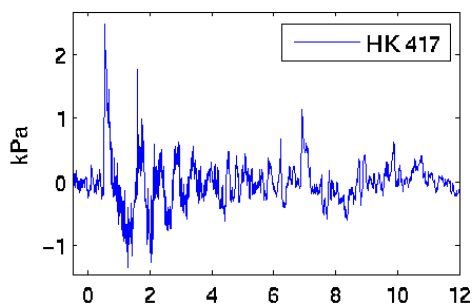
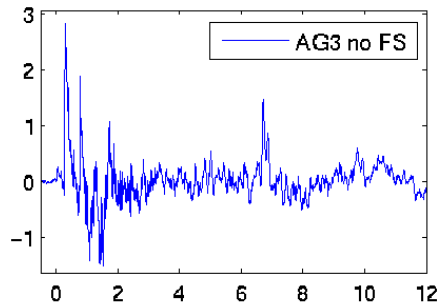
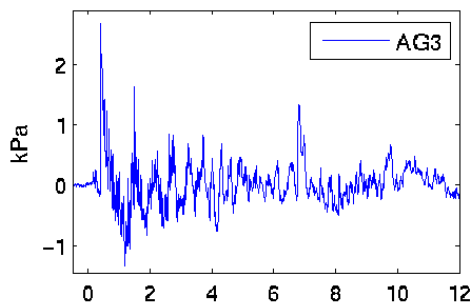
152 degrees



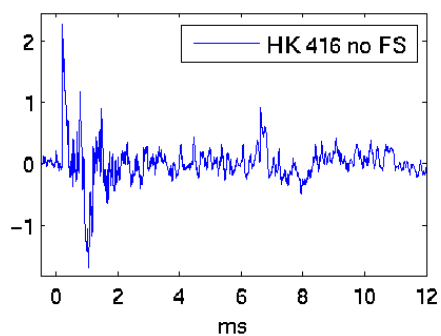
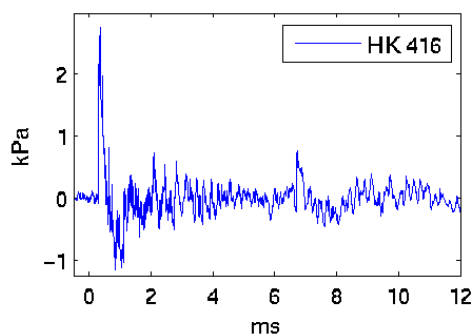
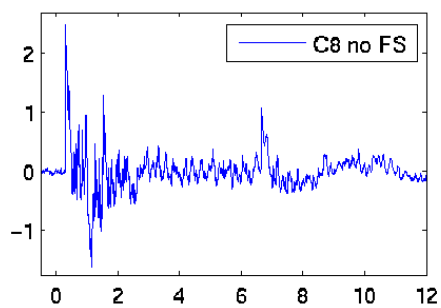
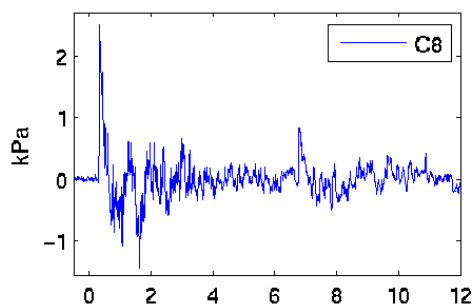
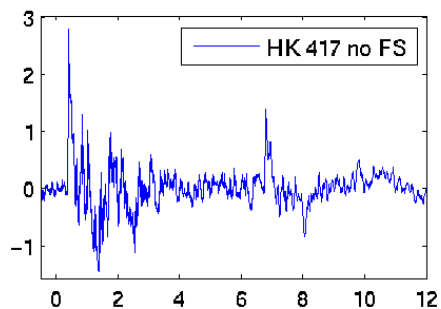
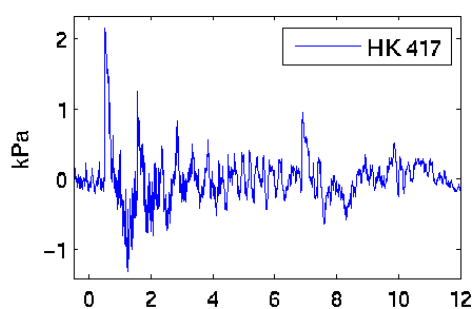
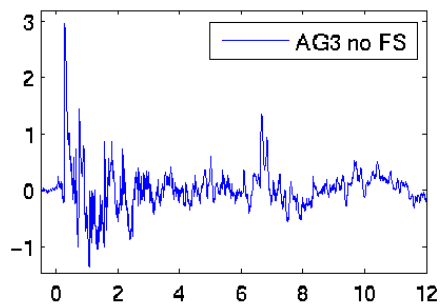
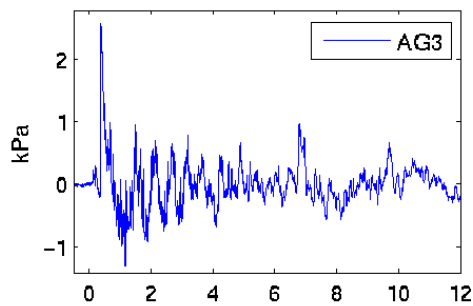
153 degrees



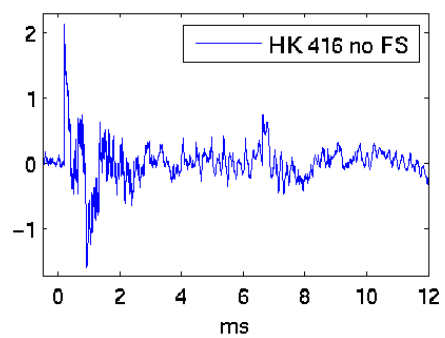
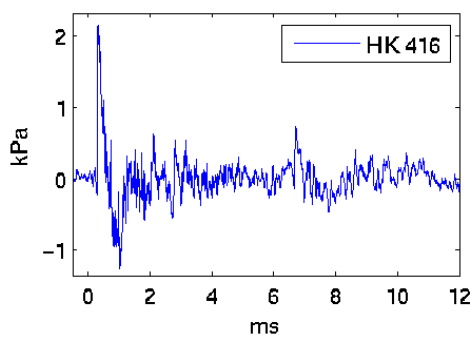
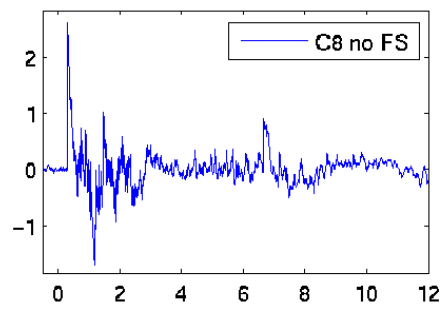
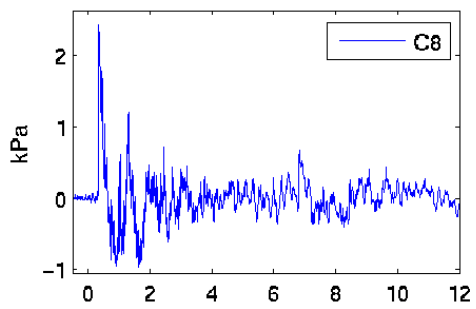
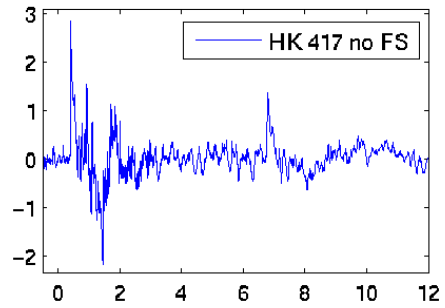
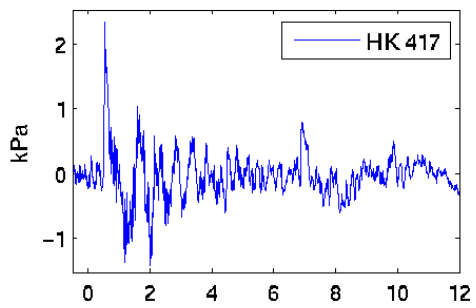
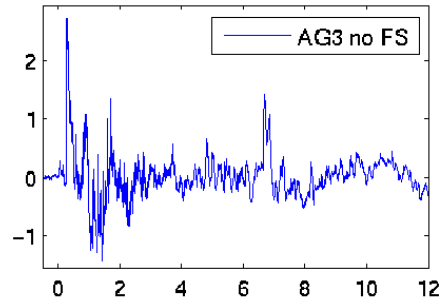
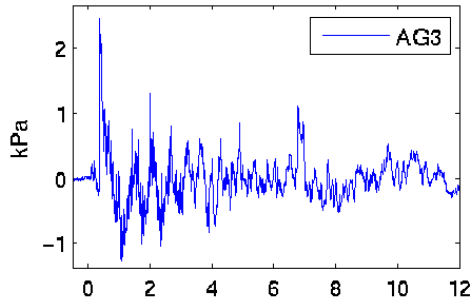
154 degrees

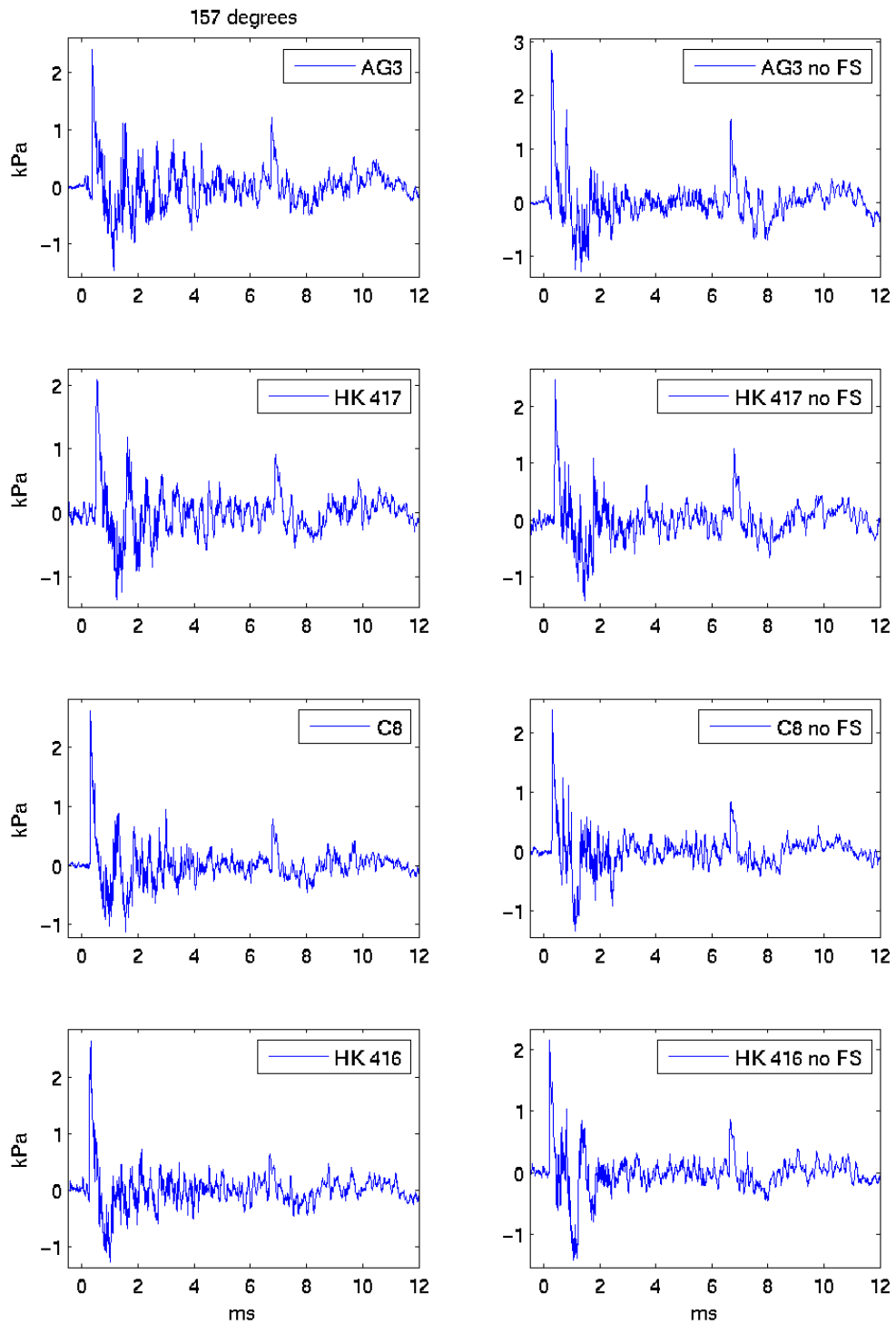


155 degrees

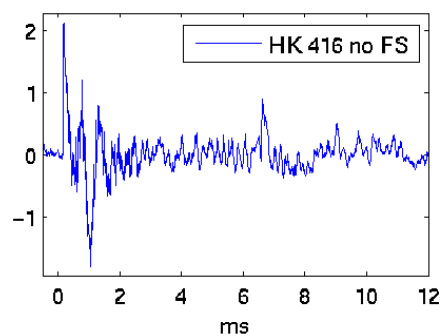
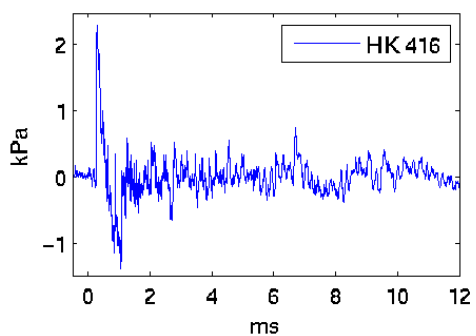
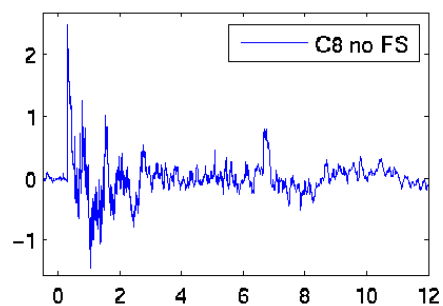
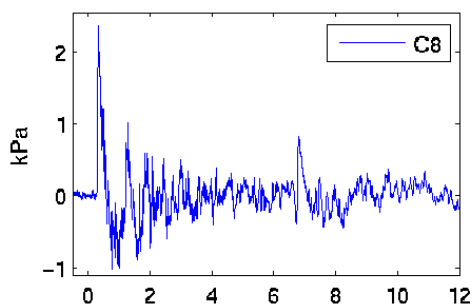
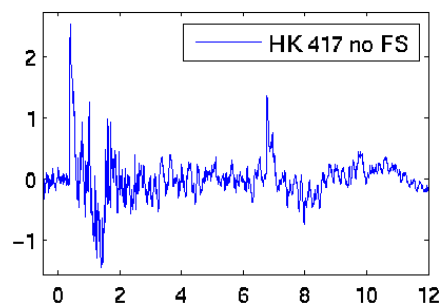
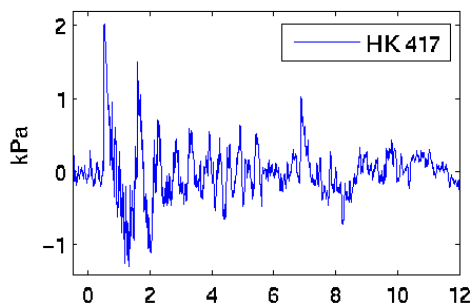
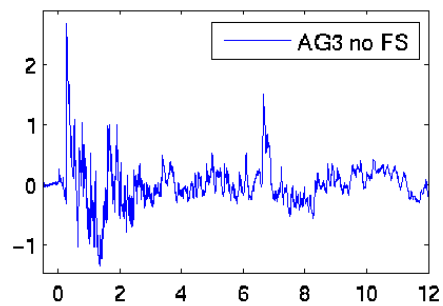
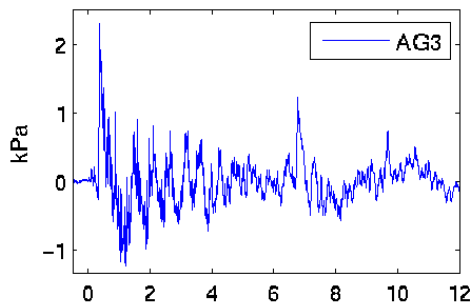


156 degrees

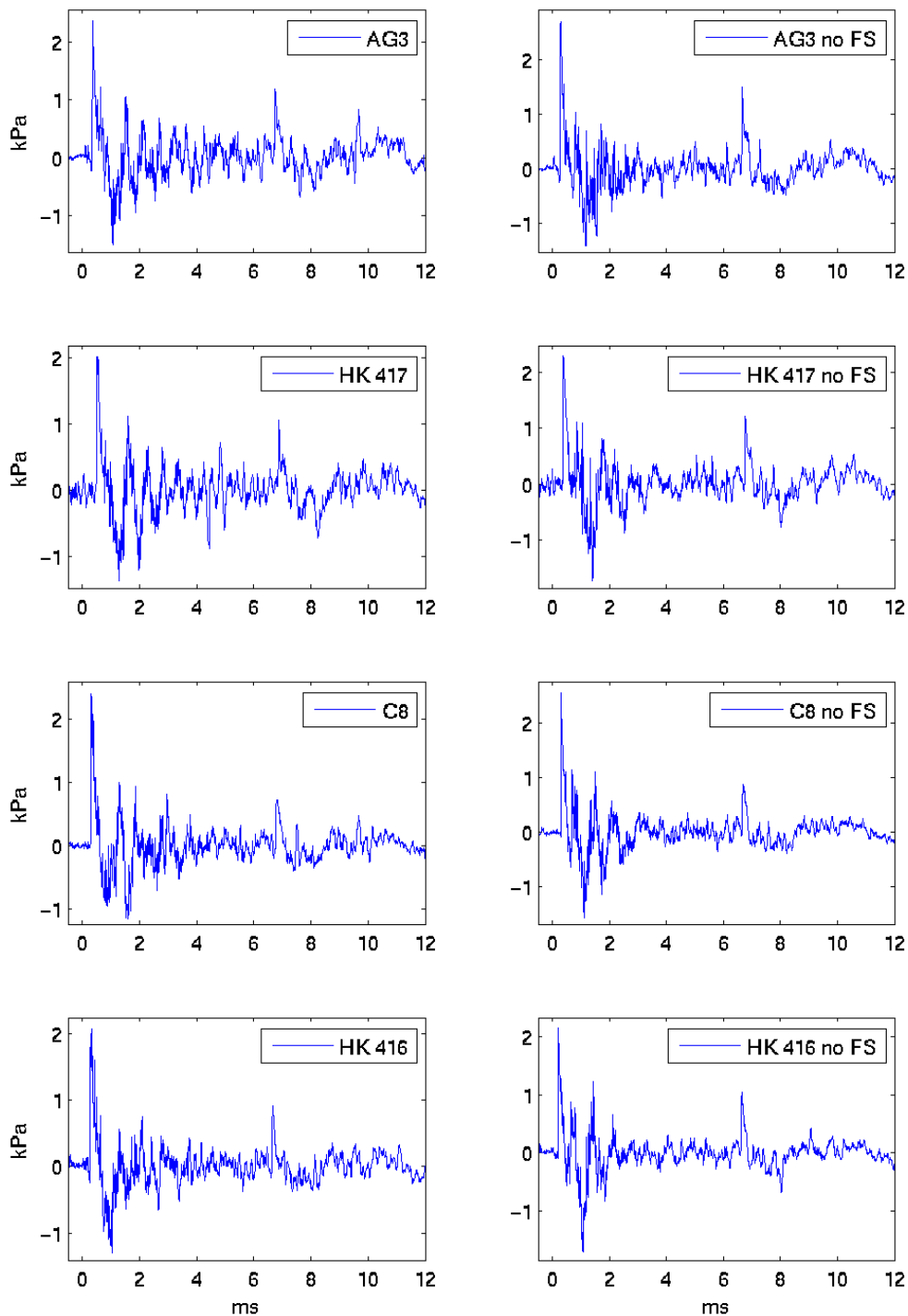


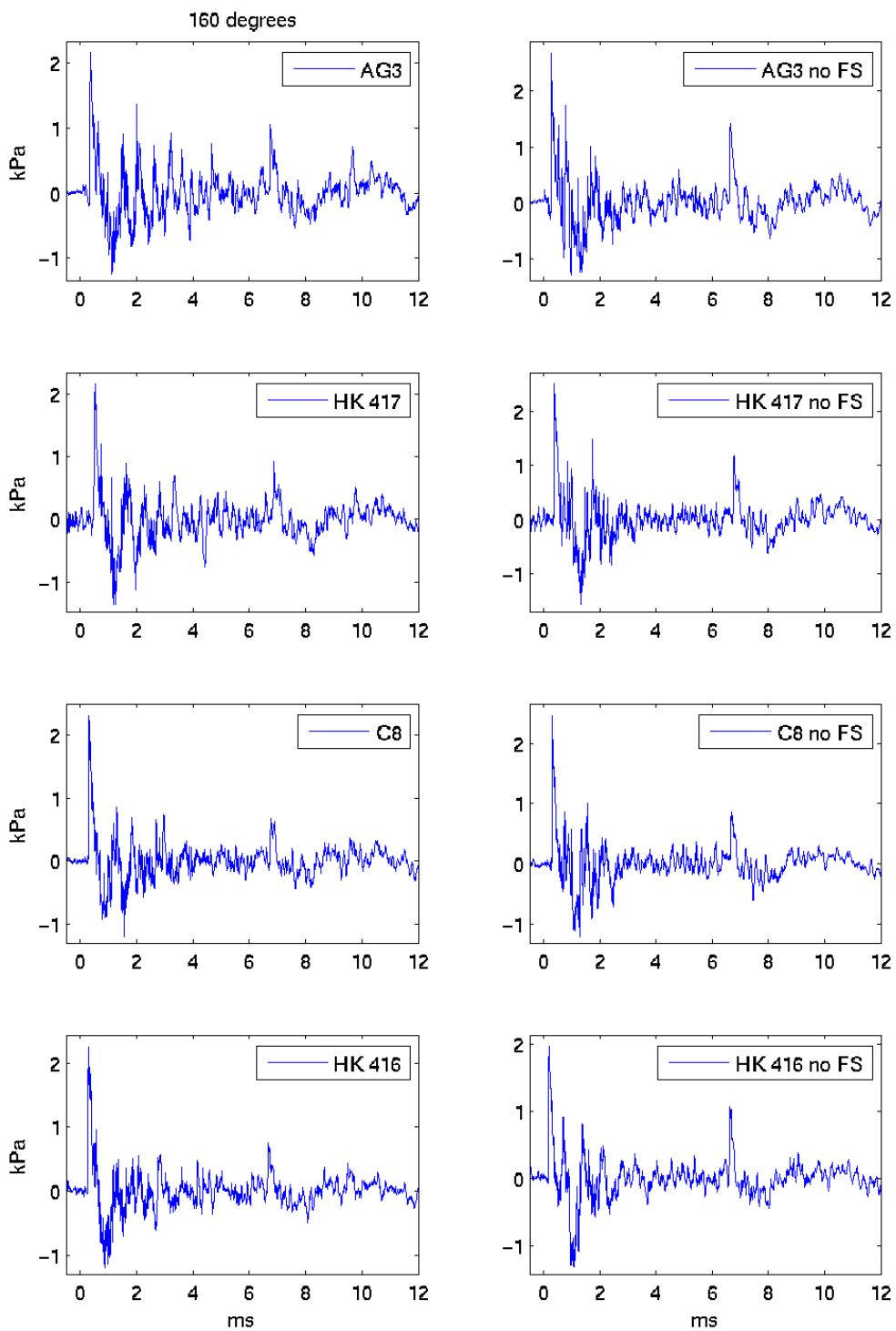


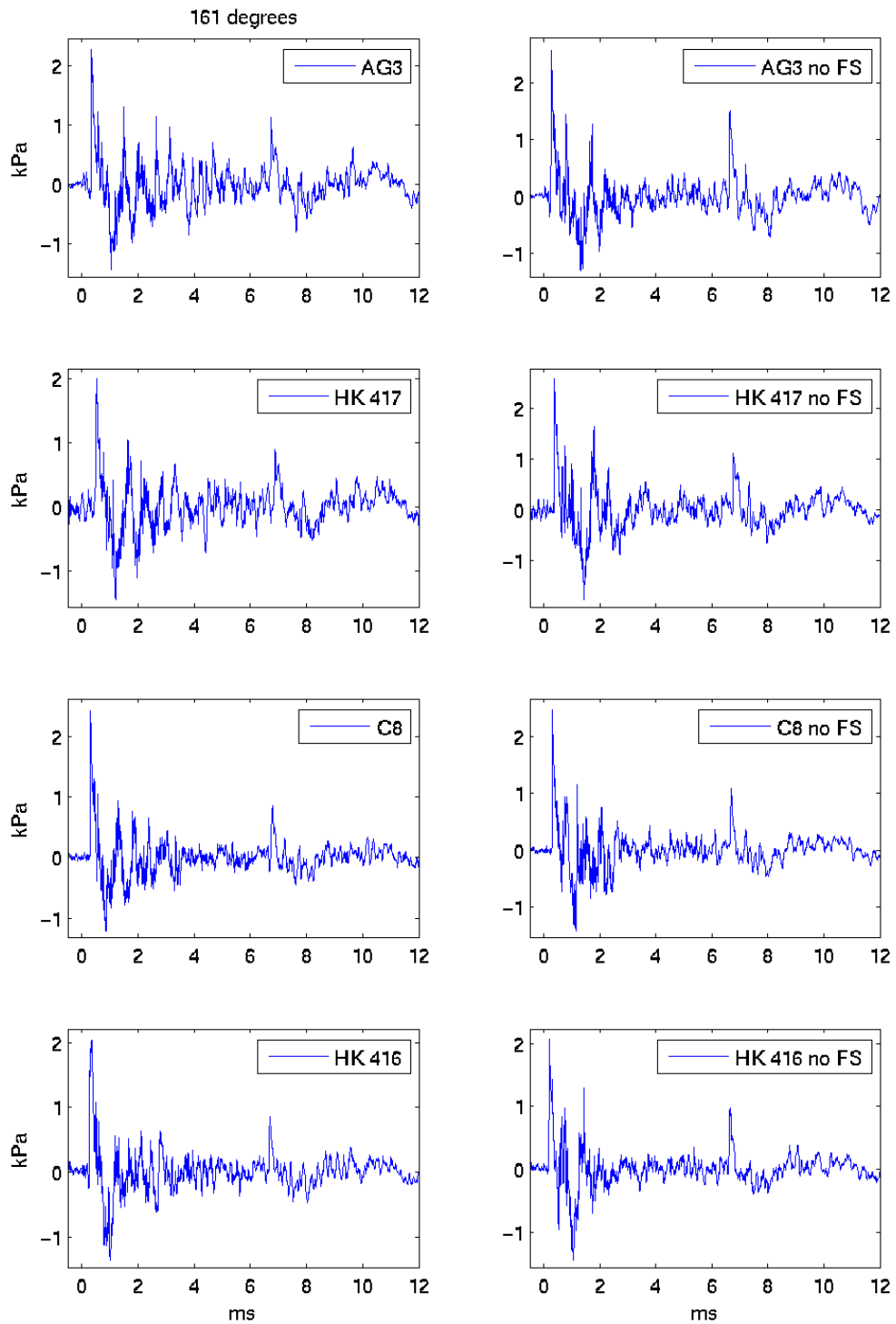
158 degrees



159 degrees



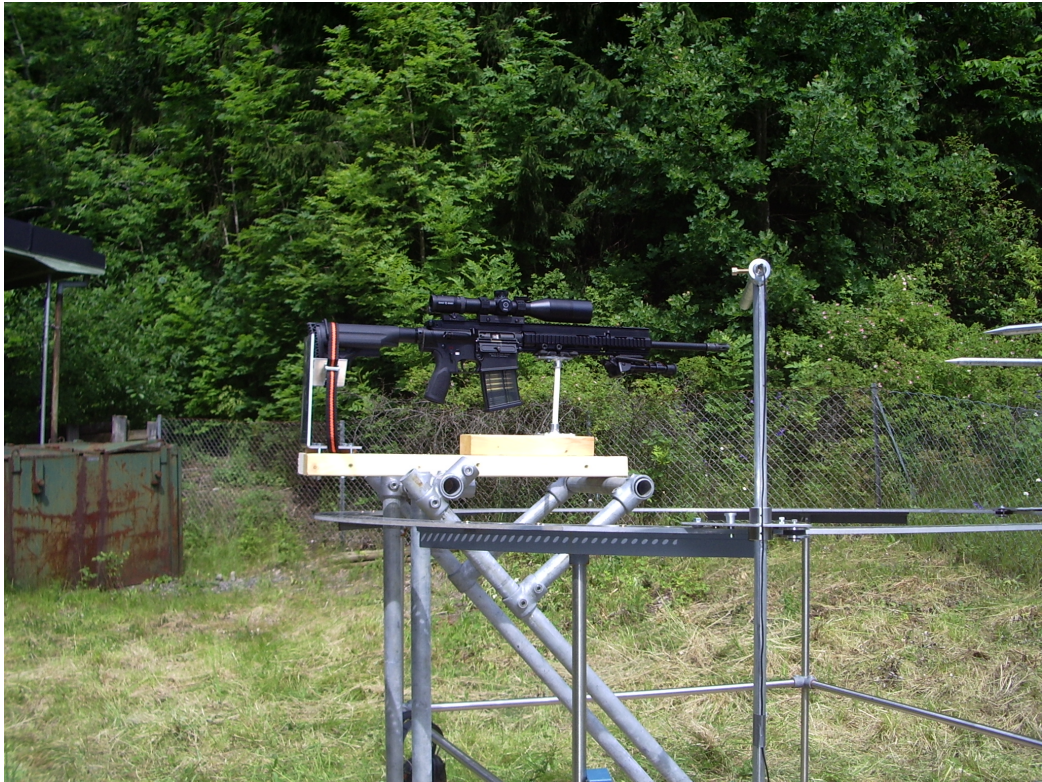


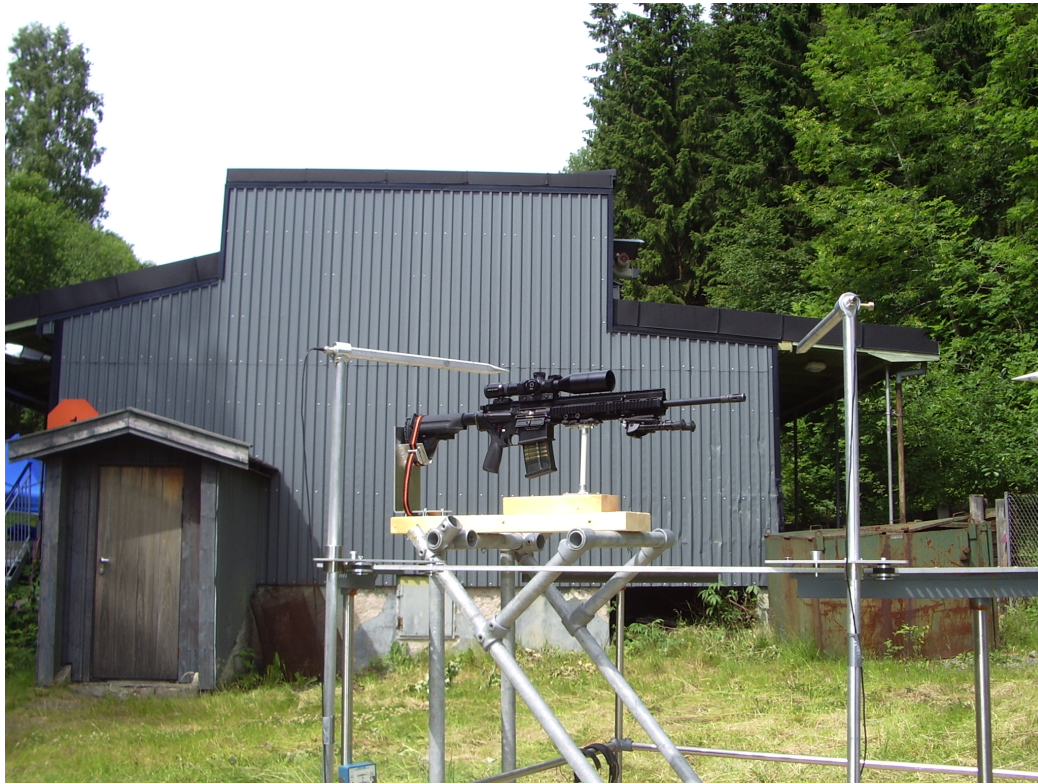


Appendix A Pictures of the measurement setup



















Appendix B Pictures of flas suppressors

In all the pictures the flash suppressor of the HK 416 N is to the left and the C8 to the right.







References

- [1] M. Huseby. Directivity of military noise sources used as input to long-range noise propagation codes. In *Proceedings Inter-Noise 2011*, pages 1–6, Osaka, Japan, 4–7 September, 2011. ISSN 0105-175x.
- [2] M. Huseby, H. Fykse, and R. Rahimi. Midertidige emisjonsdata for støy fra HK416 og HK417. FFI-rapport 2008/02125, Norwegian Defence Research Establishment, 2008.
- [3] M. Huseby, P. K. Opstad, and E. Svinsås. Forprosjekt: Faren for hjerneskrader hos personell som benytter forsvarrets våpen og eksplosiver. FFI-notat 2009/01062, Norwegian Defence Research Establishment, 2009.
- [4] M. Huseby and H. Fykse. Emisjonsdata for støy fra HK416 og HK417. FFI-rapport 2009/00354, Norwegian Defence Research Establishment, 2009.
- [5] G. Ling, F. Bandak, R. Armonda, G. Grant, and J. Ecklund. Explosive blast neuro-trauma. *J. Neurotrauma*, 26(6):815–825, June 2009.
- [6] P. M. Kochanek, R. A. Bauman, J. B. Long, C. E. Dixon, and L. W. Jenkins. Introduction to special issue on blast-induced traumatic brain injury and polytrauma: A critical problem begging for new insight and new therapies. *J. Neurotrauma*, 26(6):813–814, June 2009.
- [7] J. A. Teland, A. Hamberger, M. Huseby, A. Säljö, and E. Svinsås. Numerical simulation of mechanisms of blast-induced traumatic brain injury. *Proceedings of Meetings on Acoustics (POMA)*, 9(020004):1–14, 2010.
- [8] J. A. Teland, A. Hamberger, M. Huseby, and A. Säljö. Numerical simulation of blast induced mild traumatic brain injury. In *6th World Congress on Bio Mechanics*, pages 1–4, Singapore, 1–6 August, 2010.
- [9] A. Säljö, F. Arrhén, H. Bolouri, M. Mayorga, and A. Hamberger. Neuropathology and pressure in the pig brain resulting from low-impulse noise exposure. *J. Neurotrauma*, 25(12):1397–1406, December 2008.
- [10] A. Säljö, B. Svensson, M. Mayorga, A. Hamberger, and H. Bolouri. Low-level blasts raise intracranial pressure and impair cognitive function in rats. *J. Neurotrauma*, 26(8):1345–1352, August 2009.
- [11] M. Huseby, R. Rahimi, J. A. Teland, I Dyrdal, H. Fykse, B. Hugsted, C. E. Wasberg, E. Aker, R. Cleave, F. Løvholt, C. Madshus, K. Rothschild, H. Olsen, S. Storeheier,

and G. Taraldsen. Final report: Improvement of the computational methods of the Norwegian Defence Estates Agency for computing noise from the Norwegian defence training ranges. FFI-rapport 2007/02602, Joint report by: Norwegian Defence Research Establishment (FFI), Norwegian Geotechnical Institute (NGI) and SINTEF ICT, 2008.

- [12] M. E. Swearingen, M. Huseby, and M. J. White. Variation in measured sound level as a function of propagation environment and distance. *Proceedings of Meetings on Acoustics (POMA)*, 4(045016):869–874, 2008.
- [13] M. Huseby, K. O. Hauge, E. Andreassen, and N. I. Nilsen. Målinger av lydtrykket nær M109, 155 mm felthaubits. FFI-rapport 2007/01450, Norwegian Defence Research Establishment, 2007.
- [14] M. Huseby and H. P. Langtangen. A finite element model for propagation of noise from weapons over realistic terrain. In *Proceedings Internoise 2006*, pages 1–8, paper 513, Honolulu, Hawaii, USA, 3–6 December, 2006.
- [15] M. Huseby, R. Rahimi, J. A. Teland, and C. E. Wasberg. En sammenligning av beregnet og målt lydtrykk nær lette våpen. FFI/RAPPORT - 2006/00261, Norwegian Defence Research Establishment, 2006.
- [16] J. A. Teland, R. Rahimi, and M. Huseby. Numerical simulation of sound emission from weapons. *Noise Control Eng. J.*, 55(4), 2007.
- [17] J. A. Teland, R. Rahimi, and M. Huseby. Computation of sound emitted from firearms. In *Proceedings Internoise 2008*, pages 1–10, paper 0587, Shanghai, China, 26–29 October, 2008.
- [18] M. Huseby, B. Hugsted, I. Dyrdal, H. Fykse, and A. Jordet. Målinger av lydtrykket nær lette våpen, Terningmoen, revidert utgave. FFI/RAPPORT - 2006/00260, Norwegian Defence Research Establishment, 2006.
- [19] M. Huseby, B. Hugsted, and A. C. Wiencke. Målinger av lydtrykket nær CV90, AGL og 12.7, Rena. FFI-rapport 2006/01657, Norwegian Defence Research Establishment, 2007.
- [20] M. Huseby. Noise emission data for M109, 155 mm field howitzer. FFI-rapport 2007/02530, Norwegian Defence Research Establishment, 2007.
- [21] M. Huseby, R. Rahimi, and J. A. Teland. Noise from firing ranges. In R. Korneliussen, editor, *Proceedings 29th Scandinavian Symposium on Physical Acoustics*, Ustaoset, Norway, 29 Jan–1 Feb, 2006. ISBN 82-8123-001-0.

[22] IEC 61672-1. Electroacoustics – sound level meters – part 1: Specifications, 2002.